DISSERTATION

MODELING BIOENERGY AGROECOSYSTEMS FOR CLIMATE CHANGE MITIGATION AND VULNERABILITY ASSESSMENT

Submitted by

Jeffrey Kent

Graduate Degree Program in Ecology

In partial fulfillment of the requirements

For the Degree of Doctor of Philosophy

Colorado State University

Fort Collins, Colorado

Spring 2017

Doctoral Committee:

Advisor: Keith Paustian

Stephen Ogle
Greg McMaster
Joe von Fischer

ABSTRACT

MODELING BIOENERGY AGROECOSYSTEMS FOR CLIMATE CHANGE MITIGATION AND VULNERABILITY ASSESSMENT

Agriculture is a major driver of anthropogenic climate change while also directly bearing its impacts. In addition to emissions related to farm operations and inputs, substantial greenhouse gases are released from cropland soils. These include carbon dioxide (CO_2) fluxes due to long-term changes in soil organic carbon pools, and nitrous oxide (N_2O) produced by soil microbes primarily from excess nitrogen (N) fertilizer not assimilated by crops.

Agricultural bioenergy systems are expected to produce liquid fuels with lower life-cycle emissions than gasoline. Current US policy specifies several emissions reduction tiers for biomass-derived liquid fuels, ranging from 20% lower than gasoline for corn grain ethanol to 60% lower for ethanol made from perennial grasses or agricultural residues. While these tiers are based on detailed life-cycle assessments of "average" production conditions, they fail to convey the potentially large variability in emissions arising from farm management and biophysical factors.

The first half of this dissertation uses a survey of management practices from suppliers of corn grain to a biorefinery in the US Midwest to explore the magnitude and sources of this variability. The first phase of that study finds that feedstock from most of the farms would achieve the statutory threshold of 20%, but that best-performing farms may be producing grain that would

lead to fuel with 50% lower life-cycle emissions than gasoline. Key management practices identified are tillage intensity, efficient N fertilizer use and application of livestock manure.

Crop residues, such as corn stover, can also be converted to ethanol. The second part of this study explore the sustainability of corn stover collection for ethanol production by a hypothetical dual-feedstock biorefinery. Stover collection presents a tradeoff: when used to produce ethanol, it displaces emissions from gasoline, but at the cost of less soil organic carbon (SOC) accumulation. Still, soils on these farms could sustain relatively high stover collection rates without net SOC losses or erosion, especially in the context of manure application and reduced tillage intensity.

Climate change entails two major phenomena – increasing atmospheric [CO_2] and increasing extreme high temperatures – likely to have opposing impacts on agricultural productivity, and these impacts will tend to increase over the course of the 21st Century. Chapter 4 of this work reviews the current understanding of crop responses to elevated atmospheric [CO_2] and extreme heat as determined from agronomic studies and analyses of historical climate-yield data. It summarizes consensus findings and presents emerging topics in need of further research, and compares the state of knowledge with the simulation approaches employed by several major crop models.

The increasing atmospheric [CO_2] that largely drives climate change supports increased rates of photosynthesis in C_3 plants and improved water use efficiency in all plant types. The magnitude of this fertilization effect is uncertain, however, and recent free atmospheric CO_2 enrichment (FACE) experiments appear to show reduced gains relative to earlier enclosure experiments.

Chapter 5 tests the hypothesis that the algorithm designed to simulate the CO_2 effect in the DayCent ecosystem model overestimates crop responses to elevated [CO_2] as observed under FACE conditions.

ACKNOWLEDGEMENTS

Thanks to Keith Paustian for taking in a reformed “gene jockey” who wasn’t sure what to think about all this “pools and fluxes” business at first. Likewise to Joe von Fischer, whose thought-provoking and convivial Ecosystems class helped me (along with Alan Knapp’s similarly excellent Foundations class) to feel a bit less like an imposter when calling myself an Ecologist. I am grateful to Steve Williams, Ernie Marx and Mark Easter for teaching me the art of DayCent, and assuring me that all those runtime error messages mean things are working as expected. I owe a debt to Barb Gibson, Ken Reardon, and the rest of the IGERT crew for introducing me to the fascinating nuances of bioenergy research and giving me a pretext to be perhaps a bit wider and shallower than the average PhD student.

John Field provided indispensable feedback and moral support in the preparation of these chapters. John Sheehan was instrumental in building the life-cycle inventories upon which Chapters 2 and 3 are based. Stephen Ogle provided important guidance on shaping Chapters 4 and 5. Greg McMaster has been relentlessly generous with his time and expertise, and his enthusiastic engagement made the tedious parts of this work seem like less of a slog.

Of course, family and friends make possible any accomplishment of worth.

And finally, I’d like to thank the people who protect and maintain the Pacific Crest Trail, as well as my peripatetic companions: Cinch, French Fry, and Huck.

DEDICATION

To Mom and Dad,

Who let me play in the dirt.

TABLE OF CONTENTS

CHAPTER 1. OVERVIEW

Agriculture and Climate Change

Earth's climate is changing

Anthropogenic climate change is underway. Global mean air temperature has risen roughly 0.85°C since the late 19th Century, with varying regional trends in extreme events such as heat waves and droughts (Hartmann *et al.*, 2013). Projections for the next several decades include a mean temperature between 1 and 1.5°C warmer than the late 19th Century average (Kirtman *et al.*, 2013). When extended to the end of the 21st Century, mean warming estimates range from 1.6 to 4.3°C for the lowest- and highest-emission Representative Concentration Pathways (RCPs), respectively (Collins *et al.*, 2013).

These changes are driven by increases in solar forcing primarily mediated by increasing atmospheric concentrations of greenhouse gases (GHGs). Carbon dioxide (CO_2) is the most important of these, accounting for roughly 58% of anthropogenic radiative forcing (Collins *et al.*, 2013).

Agriculture is a significant contributor

Agricultural activities account for 10-12% of CO_2-equivalent anthropogenic GHG emissions, with agricultural soil management amounting to almost half of that total (Smith *et al.*, 2014). Notably, that figure assumes that agricultural soil carbon (C) stocks are net neutral in aggregate, while in reality newly-cultivated soils are major emitters of decomposed C as CO_2, and C can be sequestered in depleted soils through improvements in productivity and management. The other major GHGs emitted from agricultural activities are nitrous oxide (N_2O) and methane (CH_4),

with both gases emitted from manure handling and use and N_2O is also emitted in large quantities from the use of synthetic nitrogen (N) fertilizer and N-fixing crops.

Agriculture is directly dependent on climate

While agriculture contributes to climate change, it is also directly vulnerable to climate change impacts. Studies of yield and weather records indicate that historical climate change has already negatively affected yields of maize and wheat, with less impact on rice and soybean (Porter *et al.*, 2014). Projected future impacts vary widely based on region, crop, climate scenario and study methodology, but estimates become overwhelmingly negative by the closing decades of the 21st Century (Porter *et al.*, 2014).

Agricultural bioenergy magnifies these linkages

Crop-based bioenergy systems are promoted as a means to mitigate climate change, premised on the production of liquid fuels with lower life-cycle emissions than energy-equivalent fossil fuels. As a set of agricultural systems explicitly oriented toward climate mitigation, bioenergy cropping rightly bears particular scrutiny in its GHG impacts. The most prevalent US bioenergy pathway, corn grain ethanol, draws still greater attention due to its relatively modest mitigation benefits and direct competition with food and feed markets. It is conceivable, and even plausible, that ethanol made from poorly-managed corn could represent an increase in emissions relative to gasoline while marginally increasing food prices: a lose-lose outcome. By contrast, ethanol derived from corn stover may achieve large mitigation benefits with negligible impacts on food and feed markets. In the context of bioenergy, anything that affects feedstock productivity – including management choices and climate change – affects overall mitigation benefits, which feed back on the climate system. Figure 1.1 depicts some of the key causal pathways by which

bioenergy influences climate change, and climate change influences the productivity of bioenergy systems.

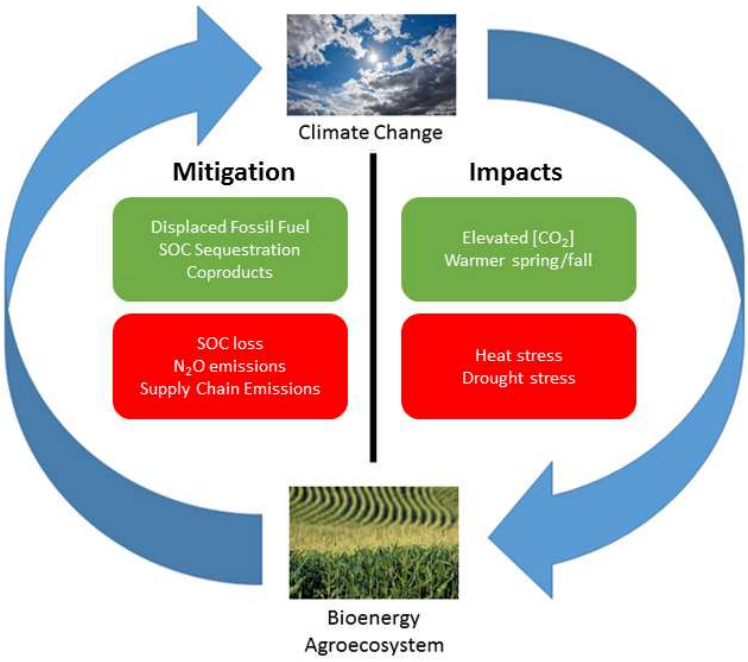

Figure 1.1. Major linkages between bioenergy systems and climate change. Processes on the left either mitigate (green box) or exacerbate (red box) climate change. Processes on the right either improve (green box) or impair (red box) the yields and functioning of bioenergy agroecosystems.

This dissertation examines the complex causal relationships between climate change and bioenergy cropping systems. The first half (Chapters 2 and 3) explores the magnitude and variability of feedstock life-cycle emissions as they relate to differences in farm management practices. The goal of these chapters is to understand how bioenergy production systems can be managed to maximize climate mitigation and minimize aggravating processes as depicted on the left side of Figure 1.1. The second half (Chapters 4 and 5) examines our understanding of major crop responses to historically-unprecedented levels of atmospheric CO_2 and increasing mean and extreme temperatures (right side of Figure 1.1). These chapters highlight areas of consensus and

identify areas of controversy that merit further study, as a clear understanding of these phenomena is fundamental to forecasting agricultural production, whether for food or bioenergy.

Chapter Synopses

Chapter 2 estimates bioenergy emissions variability based on a survey of farm management practices

Federal policy mandates increasing use of several distinct classes of biomass-derived liquid fuels (described in Table 1.1). Corn grain ethanol is likely to remain the largest contributor to this mandate, despite its status as the lowest-grade Renewable Fuel, with nominal GHG emissions reductions of 20% relative to gasoline (Schnepf & Yacobucci, 2011). Studies of corn grain ethanol emissions have found significant variability related to farm management (Adler *et al.*, 2004; Wang *et al.*, 2012), indirect effects on land-use (Searchinger *et al.*, 2008; Fargione *et al.*, 2010), and advances in conversion technologies and coproduct utilization (Liska *et al.*, 2009). Chapter 2 advances understanding of this variability by estimating emissions budgets using actual farm management data from 35 feedstock producers in the US Midwest. Management practices on this relatively homogeneous group of farms result in a large range of emissions, with best practices achieving reductions nominally equivalent to those from Advanced Biofuels or even (for one farm) Cellulosic Biofuels.

Table 1.1. Biofuel categories established by the Renewable Fuel Standard 2, their associated emissions reductions relative to gasoline and major qualifying pathways. Note that the categories qualify in a nested manner, so that (for example) any Advanced Biofuel may alternatively qualify as a Renewable Fuel for the purposes of fulfilling volume mandates.

Biofuel Category	Assumed Emissions Reduction	Qualifying pathway(s)
Renewable Fuel	20%	Corn grain ethanol
Advanced Biofuel	50%	Sugarcane ethanol
Biomass-based Diesel	50%	Soybean diesel Algae-derived diesel Diesel from waste oils
Cellulosic Biofuel	60%	Perennial-grass derived ethanol Residue- or waste-derived ethanol

Chapter 3 explores tradeoffs between management, emissions and production costs

As next-generation cellulosic biorefineries come into operation, crop residues such as corn stover comprise a large, readily-available feedstock. Such "agricultural wastes" can be critical for controlling erosion and supporting soil fertility and C stocks, however (Sheehan *et al.*, 2003; Graham *et al.*, 2007; Turhollow *et al.*, 2014). These sustainability constraints may be partially alleviated through compensatory management practices such as reduced tillage intensity, cover crops and organic matter amendments (Wilhelm *et al.*, 2004; Thelen *et al.*, 2010). Farm profits from stover harvest will also be a key factor in dictating the viability of these systems, with unit costs likely to fall with increasing collection rates (Graham *et al.*, 2007). Chapter 3 returns to the farms studied in Chapter 2, but replaces the present corn grain ethanol system with a hypothetical dual-feedstock (i.e., grain and stover) system and models a wide range of farm management scenarios to explore these emissions and profitability tradeoffs. Scenario emissions range from 10-100% of those from energy-equivalent gasoline, with reduced tillage intensity and moderate manure inputs supporting soil C stocks at high levels of residue removal. Stover removal

marginally increases farmer profits per unit area under current market conditions, but provides a considerable premium under C pricing scenarios.

Chapter 4 distills current understanding of crop responses to warming and [CO_2]

Climate change impacts on agriculture stem from two robustly-supported phenomena: CO_2 fertilization and increasing high temperature exposures. While experimental studies of each of these factors have been conducted for decades, the increasing focus on understanding ecosystem-scale effects has prompted a paradigm shift to sophisticated open-air designs (Hendrey *et al.*, 1993; Nijs & Kockelbergh, 1996; Kimball, 2005). No experiment can integrate the full range of exposures to extreme heat that will occur at very large spatial and temporal scales, however, and so statistical analyses of historical yield and weather data provide a vital independent source of corroboration.

Chapter 4 reviews the state of knowledge of crop responses to elevated atmospheric [CO_2] (eCO_2) and elevated temperatures and compares findings from experiments with related response signals identified using historical records. Experiments clearly align with theoretical predictions of increased photosynthesis and yield for C_3 crops (e.g., wheat, soybean, rice), and reduced stomatal conductance for both C_3 and C_4 crops (e.g., corn, sorghum; reviewed by Kimball, 2016). Several important interactions have been highlighted by recent work, however. A growing body of work suggests that eCO_2 reduces the ability of C_3 crops to assimilate soil nitrate (Bloom *et al.*, 2010), for instance, while a series of recent free-atmospheric CO_2 enrichment (FACE) experiments with wheat under water-limitation have found yield enhancements as high as 70% under eCO_2 Fitzgerald *et al.* (2016), greatly exceeding any previous agricultural FACE results.

Agronomic field studies have established that heat stress impacts on major crops are greatest during the late-season reproductive phases of flowering and grain-filling (Rezaei *et al.*, 2014), and statistical studies of historical yields are beginning to detect this signal (Butler & Huybers, 2015). The confounding role of water limitation is another developing topic in studies of heat stress, and new empirical analyses are going beyond coarse temperature and precipitation data to include mechanistic variables such as vapor pressure deficit and soil water content (Roberts *et al.*, 2012; Anderson *et al.*, 2015).

The interactions between eCO_2, extreme heat and other factors are just beginning to be elucidated at the field scale. Recent FACE studies of soybean using rain exclusion treatments found that the yield increase under eCO_2 could be attenuated or nearly abolished through interactions between eCO_2, leaf area development, canopy temperature, stress timing, and even altered leaf responses to stress signaling (Gray *et al.*, 2016). Complex interactions like these must be synthesized and rapidly incorporated into the dynamic crop models that form the basis of comprehensive climate change assessments, many of which were created for narrow, specialized applications and are updated only sporadically (Rötter *et al.*, 2011).

Chapter 5 tests a crop model's ability to simulate crop responses to eCO_2

Increasing atmospheric [CO_2] directly accelerates photosynthesis in C_3 crops, and indirectly promotes yields by reducing stomatal conductance and associated water losses in C_3 and C_4 crops (Leakey *et al.*, 2009). Several decades of experiments have exposed crops to eCO_2 in greenhouses and other enclosures and observed yield increases on the order of 33% (Kimball, 1983; Cure & Acock, 1986). FACE systems were developed in the early 1990s to better replicate open-field growing conditions (Hendrey *et al.*, 1993). Some authors contend that

FACE results indicate lower crop yield responses than enclosure studies (Long *et al.*, 2006; Ainsworth *et al.*, 2008a), while others maintain no significant difference (Tubiello *et al.*, 2007) or attribute differences to various methodological factors (Ziska & Bunce, 2007; Bunce, 2012). The crop CO_2 response processes in many crop models were developed using results from enclosure experiments (Tubiello *et al.*, 2007).

Chapter 5 tests the ability of one such model, DayCent, to reproduce crop responses to CO_2 enrichment from several FACE experiments. DayCent performed well at simulating yield and transpiration responses in C_4 crops, but significantly overestimated yield responses in C_3 crops. After adjustment of parameter values, DayCent was able to reproduce crop-specific FACE results, as well as some broader trends of CO_2-by-stress interactions.

CHAPTER 2. MODELING REAL-WORLD VARIABILITY OF ON-FARM GREENHOUSE GAS EMISSIONS FOR BIOENERGY FEEDSTOCK PRODUCTION

Introduction

Policy background

The US Renewable Fuel Standard 2 (RFS2) provides specific life-cycle greenhouse-gas (GHG) emissions reduction thresholds that must be met for different classes of biofuels to qualify as "renewable." These renewable fuel categories are defined in terms of feedstock type and end product. For instance, ethanol produced from corn grain would be credited with a 20% reduction in emissions relative to gasoline, regardless of farm management practices (Schnepf & Yacobucci, 2011). However, a large portion of the emissions budgets of crop-derived biofuels can be traced to biological soil processes and other materials and energy directly related to farm management (Kim & Dale, 2005; Smith *et al.*, 2008; Davis *et al.*, 2013). Major biogenic fluxes include soil emission of nitrous oxide (N_2O), uptake of methane (CH_4), and emissions (or removals) of CO_2 associated with net changes in soil organic carbon (SOC). Management also determines emissions from on-farm fuel use, chemicals and capital depreciation (Kendall & Chang, 2009).

Several authors have studied the emissions implications of bioenergy farm management using hypothetical scenarios. Adler *et al.* (2007) estimated emissions of fuels derived from corn-corn-soybean cropping under conventional and no-till management. They found that no-till management increased C sequestration by about 0.15 Mg C ha^{-1} yr^{-1}, corresponding to an additional 12% reduction in life-cycle emissions relative to displaced fossil fuels. Kim & Dale (2005) compared several corn-based bioenergy systems and found that continuous corn with

70% stover removal and a winter cover crop had the most favorable emissions profile. The cover crop compensated for C losses incurred from residue removal while reducing levels of soil N available for emission as N_2O. Wang *et al.* (2012) performed a sensitivity analysis of corn grain ethanol emissions to a range of life-cycle parameters and found that the single most sensitive parameter was the rate of conversion of applied N to N_2O, which in turn is influenced by a wide range of site and management factors (Robertson & Vitousek, 2009). While each of these studies explores the potential importance of variable management in bioenergy emissions, none accounts for the actual practices of feedstock producers. This work addresses that gap by assessing current emissions impacts and potential areas for improvement based on a detailed survey of management practices from a group of corn-soybean producers in the US Midwest.

Nitrous oxide

EPA estimates that N_2O is the single greatest source of GHG forcing from the U.S. agricultural sector, accounting for 263.7 Tg CO_2e in 2012 (EPA, 2015). Nitrous oxide is produced by soil microbes as a byproduct of nitrification and denitrification, with levels influenced by available nitrogen (N) and soil texture and moisture, among other variables (Del Grosso *et al.*, 2010). In addition to on-site production and emission of N_2O, cropping systems contribute to so-called indirect N_2O emissions. One instance of such indirect N_2O emissions occurs when nitrate (NO_3^-) is leached out of the soil profile into aquatic systems, where a portion may be denitrified and returned to the atmosphere as N_2O. A second mechanism for indirect N_2O emissions involves volatilization of ammonia (NH_3) and non-N_2O nitrogen-oxide (NO_x) species, off-site deposition, and subsequent emission as N_2O as a result of soil microbial transformations (Del Grosso *et al.*, 2009).

A common approach to estimating N_2O emissions from agricultural soils is via the emissions factor methodologies described by the IPCC Guidelines for National Greenhouse Gas Inventories (de Klein *et al.*, 2006). As part of their GREET-based LCA for corn-grain ethanol, for example, Wang *et al.* (2012) estimated N_2O emissions from farm soils by assuming that 1.53% of applied synthetic N is transformed to N_2O. While emissions factor methodologies based on N inputs are appropriate for estimating emissions in broad analyses and data-poor scenarios, dynamic process-based models such as DayCent allow for more detailed estimation of N_2O emissions by tracking several important drivers such as soil texture, soil water status, plant N uptake, temperature, and tillage effects. The DayCent model has been compared with emissions factor methodologies at global (Del Grosso *et al.*, 2009), national (Del Grosso *et al.*, 2005; Ogle *et al.*, 2010), and site (Del Grosso *et al.*, 2008) scales, and is currently used as part of the U.S. Tier 3 methodology for estimating N_2O emissions from agricultural soils for reporting to the United Nations Framework Convention on Climate Change (UNFCCC; Lokupitiya & Paustian, 2006).

Methane

Well-drained agricultural soils are typically net sinks for methane (CH_4) due to the action of methanotrophic bacteria (Ogle *et al.*, 2014). Cultivation reduces soil CH_4 oxidation capacity relative to non-agricultural (e.g. native grassland) soils (Mosier *et al.*, 1991), and recent evidence suggests that long-term adoption of reduced tillage may gradually restore soil properties that support this capacity (Abdalla *et al.*, 2013; Jacinthe *et al.*, 2014; Zhao *et al.*, 2016). DayCent simulates CH_4 oxidation as a function of land cover history and various soil properties according to relations developed by del Grosso *et al.* (2000).

SOC change

Yearly changes in SOC reflect the difference between carbon (C) inputs (plant production, manure addition) and losses (decomposition to the atmosphere, harvested biomass) (Conant *et al.*, 2011). Most soils under natural vegetation lose substantial amounts of SOC in the decades following conversion to cultivated agriculture. These historic losses have been estimated at more than 50 Pg C globally (Paustian *et al.*, 1998; 1 Pg = 10^{15} g). Various management practices, when tailored to local conditions, have been demonstrated to restore some of these losses (Lal, 2004a). While many agricultural soils have the potential to sequester C from the atmosphere, the total potential for sequestration is finite and depends on a variety of climatic and soil properties (Six *et al.*, 2002; Stewart *et al.*, 2009).

Significant research has examined the role of reduced tillage practices in promoting SOC sequestration. West and Post (2002) reviewed field data from 67 long-term agricultural experiments for a total of 276 paired treatments to determine rates of C sequestration and uncertainties for changes from CT to NT. They found that soils sequestered 0.44+/-0.27, 0.25+/-0.26, 0.61+/-0.46, and 0.90+/-0.59 Mg C ha^{-1} yr^{-1} under continuous corn, continuous wheat, continuous soybean, and corn-soybean, respectively. Baker and colleagues (2007) have suggested that these apparent SOC increases may be an artifact of shallow soil sampling protocols, which detect SOC increases at shallow depths under no-till but neglect increases that may occur deeper in the profile under conventional tillage. However, recent research examining SOC by depth in plots with varying levels of tillage intensity found increases in the surface soil increment (0-30 cm) under no-till, while SOC levels in the 30-60 cm increment were highly-variable *within* tillage treatments but showed no consistent differences *between* treatments (Syswerda *et al.*, 2011). DayCent has been tested and validated for tracking SOC stock changes

in a variety of cultivated (Del Grosso *et al.*, 2002; Chamberlain *et al.*, 2011; Chang *et al.*, 2013) and natural (Pepper *et al.*, 2005; Li *et al.*, 2006) ecosystems.

Energy and materials

The SimaPro™ life-cycle software and database package (Pre Consultants, 2012) was used to account for life-cycle flows associated with the supply chains for material inputs as well as energy consumed during farm operations. These "supply chain emissions" included flows such as emissions embodied in N fertilizer and other farm chemicals, emissions due to liming of fields, on-farm fuel combustion, and emissions embodied in depreciation of farm equipment. According to Wang et al. (2012), emissions from the production and distribution of N fertilizer alone account for about 13% of the FTW emissions of corn grain ethanol.

Study rationale

The fuel classifications in the RFS2 ignore differences in farm site conditions and management practices that may have a large influence on the actual life-cycle GHG emissions of a biofuel. Even the California Low Carbon Fuel Standard, which allows for market credits for C savings, relies on generic farm level estimates of emissions (Sperling & Yeh, 2007). The focus of this study was on understanding the variability in FTP emissions attributable to differences in farm management practices within a relatively small, homogeneous agricultural region. Since biogenic emissions are highly sensitive to specific management practices and supply chain emissions are a direct consequence of management practices, we hypothesized that the FTP emissions of corn grain from farms using best management practices would be substantially lower than those of their peers.

Methods

Survey description

Farmers located near the site of a proposed corn-grain-to-butanol biorefinery near Luverne, Minnesota were surveyed on a range of management practices, including fertilization levels, tillage, and manure application, as well as annual crop yields. Farmers submitted data for three years of operation (2008 through 2010). A total of 291 farmers were surveyed, and responses were received from 52. Of the 52 responses received, 35 were found to include data sufficient to create the required DayCent model input files. These 35 farms were located in 13 counties and three states in the vicinity of Luverne, MN (Table 2.1). Table 2.2 summarizes the overall and annual synthetic N fertilizer use reported by the survey respondents. The type and amount of fertilizer used varied some from year to year. Average rates were calculated on an area-weighted basis.

Greenhouse gas (GHG) emissions associated with processing and transport of manure use were ignored in our estimate of life-cycle fossil C emissions—with the implication that manure was available nearby, and was applied with little or no water removal. These assumptions were consistent with survey data indicating that the majority of manure was in liquid form (no drying) and came from regional swine and dairy operations. We did, however, estimate the C and N contributions made by the manure within the DayCent simulations. Assumptions for N, phosphate and potassium content of the different manure types are shown in Table A2 and are based on data from the University of Minnesota Extension (Blanchet & Schmitt, 2007).

Discussion of other farm inputs including fuel use, on-farm chemicals and lime application can be found in the Appendix.

Table 2.1. States and counties of respondents to the Gevo, Inc. feedstock supplier survey.

State	County	Number of Responses
Minnesota	Rock	32
	Yellow Medicine	1
	Nobles	6
	Lincoln	1
	Pipestone	2
	Martin	1
	Jackson	1
Iowa	Lyon	2
	Sioux	1
	Emmet	1
South Dakota	Turner	1
	Minnehaha	2
	Moody	1
Total		52

DayCent inputs

Daily weather data, including high and low temperatures and precipitation running from January 1, 1979 through December 31, 2009 were obtained from the NCEP North American Regional Reanalysis database (Mesinger *et al.*, 2006). A single set of weather inputs was obtained for the county centroid of counties in which surveyed farms were located.

DayCent soil input files were created using soil physical and chemical characteristics of specific soil series from the USDA Soil Data Mart database (NRCS, 2004). Where soil series were not identified by name in survey responses, the field was assigned the soil series most frequently identified for surveyed farm fields in the same county.

DayCent schedule files, which describe farm management, were created for every farm field (most farmers described multiple fields) reported by the 35 included farmers, resulting in 94

unique management schedules. Since all farms were simulated with a corn-soybean crop rotation, we created alternate files for each management schedule, with one file for planting corn on even years and soybean on odd years, and the other vice-versa. This alternate rotation phasing was done to avoid possible bias due to interactions between crop type and anomalous weather events. Results from these alternately-phased rotations were averaged to produce reported values, unless otherwise noted. Farm-specific management practices from survey responses used in DayCent schedule files included cultivation events (timing and intensity), synthetic N fertilizer (timing and amount), and manure application (timing, amount and type). Some survey respondents reported the use of manure additions on a portion of their acreages. Manure C:N ratios were estimated by manure source type (summarized in Table A2).

DayCent historic land use

Each DayCent model run was initialized using a 3000-year 'equilibrium' simulation designed to mimic pre-agricultural land cover and to allow the soil organic matter pools in the model to reach a steady state (Basso *et al.*, 2011). For all runs in this study, the sites were modeled as a mixed warm- and cool-season grassland with regular grazing and periodic fire. From the pre-cultivation conditions, the model was then run for a spinup period or 'base history' simulating changes following initial plowout (1861) and conversion to annual cropland, through to the simulated start of current management (i.e., farmer-reported management, here starting in 1979). Over this 119-year base history, 4 distinct management periods were simulated to reproduce major agronomic changes, in part based on historical NASS cropping data for the counties in the study. Period 1 (1861-1908) included a complex rotation designed to support livestock and draft animals including grazing, hay production, and relatively low-productivity oats and corn with significant residue removals (75% of corn stover, 50% of oat straw). Period 2 (1909-1954)

included grazing and hay in rotation with crops, but the oats and corn during this period were medium-productivity varieties with continuing residue removals (50% of corn stover, 50% of oat straw). Period 3 (1955-1964) was designed to reflect the addition of significant synthetic N fertilizer and reduced reliance on forage (i.e., no hay cropping or residue removals) due to replacement of draft animals with tractors, and included high-productivity corn, oats, and soybeans. Period 4 (1965-1978) included high-productivity corn, oats, and soybeans and higher levels of synthetic N application. The current corn-soybean management (based on survey responses) was initiated in 1979 and continued for 31 years through 2010. In order to avoid high short-term rates of change in state variables (e.g., soil C) due to this transition in management, results discussed below are based on the final 12 simulation years (1999-2010) unless otherwise noted.

NASS-based C input estimates

To provide a rough check on the simulated SOC changes, we developed independent estimates of historic C inputs using historical statewide Minnesota NASS yield data in conjunction with IPCC reference values (de Klein *et al.*, 2006) for harvest-index and aboveground-belowground biomass ratio. We first used the reference harvest index and the NASS yield to calculate total aboveground biomass for each crop (corn, soybean, oats, hay) and each year of the base history period (1866-1978). The reference aboveground-belowground biomass ratios were then used to calculate total crop biomass. To calculate the NASS-based estimated C input, we subtracted the NASS grain yield and the assumed fraction of aboveground residue removal (i.e. same fraction of removal simulated in DayCent schedule) from the total biomass.

DayCent was calibrated by adjusting the radiation use efficiency parameter for corn and soybean crops to reproduce the area-weighted average survey-reported yields across included farms for 2008-2010, the years covered by the survey. DayCent model runs simulated farmer-reported applications of N from synthetic fertilizer on the day of planting of corn years, and manure application 30 days after harvest on soybean years. Since synthetic N was applied to corn but not soybean, the rotation-averaged N input rates given in the text (unless noted otherwise) are half of the amounts farmers used for their corn crops. Survey responses detailing cultivation practices were translated into DayCent cultivation events that simulated both the timing and intensity of soil disturbance, based on the tillage equipment reported. Scores were developed to reflect the increase in decomposition rate (Tillage Decomposition Effect score, TDE) based on these cultivation schedules as described in the Appendix.

Field-level emissions calculations

DayCent simulates processes that account only for soil-based GHG emissions and not emissions from the use of farm machinery and related embodied emissions for fuels and chemicals consumed. The latter are estimated in the life-cycle inventories discussed below. The biogenic emissions budget generated from DayCent outputs can be divided into four components: net change in SOC stocks, direct emissions of N_2O from soil, indirect emissions of N_2O from N transported off-site by leaching and ammonia volatilization from crop biomass, and oxidation of CH_4 by methanotrophic soil bacteria. Unless otherwise noted, each of these components was calculated as a 12-year average and converted to carbon-dioxide equivalents (CO_2e) based on 100-year global warming potential (de Klein *et al.*, 2006).

Calculation of emissions due to indirect nitrous oxide emission used a formulation described by del Grosso et al. (2006), which assumes that 2.5% of leached N as NO_3^- and 1% of N emitted as NH_3 or nitric oxide (NO) are ultimately transformed to N_2O and emitted.

Life-cycle inventories for supply chain emissions

Life-cycle inventories were obtained for each raw material consumed on the farm from the SimaPro™ life-cycle software and database package (Pré 2012). The inventory includes direct and embodied emissions associated with the use of all raw materials reported in the farmer survey or estimated post-survey for which data was available in SimaPro™. Post-survey estimates included detailed calculations of fuel consumed for reported planting and tillage practices, as well as application methods used for fertilizers, chemicals and manure. Direct emissions in the inventory consist of non-soil mediated emissions primarily from on-farm combustion of fossil fuels (CO_2, SO_x, NO_x, volatile organics and particulate matter). Direct emissions also included stoichiometric calculations of the release of CO_2 from lime and urea applied in the field.

Embodied emissions include those associated with the extraction, processing and distribution of all raw materials used upstream (up to delivery at the plant gate) of each raw material. For example, N fertilizer production generally involves the use of natural gas. Its embodied emissions are included, as well as release of CO_2 during conversion of natural gas to N fertilizer, fuel related emissions for process energy and the embodied emissions of any other raw material inputs. A significant effort was made in this study to estimate herbicide and pesticide embodied emissions. Because farmers reported many of these chemicals as commercial product names, it was necessary to obtain detailed formulation data, and link each chemical ingredient to its

specific life-cycle inventory in the SimaPro™ database. Table A1 lists all raw materials tracked in the life-cycle inventory for each farm.

Results

Summary of survey results

The responding farms averaged 327 ha (807 acres) in size, which is almost twice the US average of 178 ha (441 acres). Corn accounted for 55% of managed land area, with soy on 40%, Conservation Reserve Program on 3%, and 2% in other uses. Corn yields on the surveyed farms averaged over 11.9 Mg ha^{-1} (190 bushels $acre^{-1}$) in 2008-2010 growing seasons.

An estimated 22% of all corn area received some amount of manure. A small number of farmers appeared to apply manure to all of their corn acreage, while most farmers relied primarily on synthetic N fertilizer. Table 2.2 summarizes the types and amounts of N fertilizer used by the surveyed farms on an area-weighted basis. More than half of all synthetic N applied was urea, and about one-third of the total was ammonia.

Table 2.2. Area-weighted average N fertilizer usage among survey respondents in kg N ha^{-1} (lb N $acre^{-1}$).

Fertilizer	2008	2009	2010	Avg
Ammonia, anhydrous	77.0 (68.6)	73.2 (65.2)	46.6 (41.5)	64.2 (57.2)
Ammonium polyphosphate	0.8 (0.7)	0.6 (0.5)	0.6 (0.6)	0.7 (0.6)
Ammonium thiosulfate	0.0 (0.0)	0.0 (0.0)	0.0 (0.0)	0.0 (0.0)
Diammonium phosphate	16.6 (14.8)	14.6 (13.0)	14.5 (13.0)	15.2 (13.5)
Monoammonium phosphate	4.7 (4.2)	4.0 (3.5)	5.4 (4.8)	4.7 (4.2)
Urea	88.3 (78.7)	87.2 (77.7)	114.4 (101.9)	98.0 (87.2)
Ammonium sulfate	1.6 (1.4)	2.0 (1.8)	2.0 (1.8)	1.9 (1.7)
Total synthetic N	189.0 (168.4)	181.5 (161.7)	183.7 (163.7)	184.5 (164.4)

DayCent yield calibration

DayCent was calibrated to match the average of the farmer-reported yields for the years included in the survey: 2008, 2009 and 2010. Small adjustments in the crop radiation use efficiency parameters resulted in 3-year simulated, average yields of 10.7 Mg ha-1 for corn and 3.2 Mg ha-1 for soybean compared with reported averages of 10.8 Mg ha-1 for corn and 3.3 Mg ha-1 for soybean. Per-farm yields for 2008-2010 based on DayCent model results and survey data are shown in Figure 2.2 and Figure 2.3.

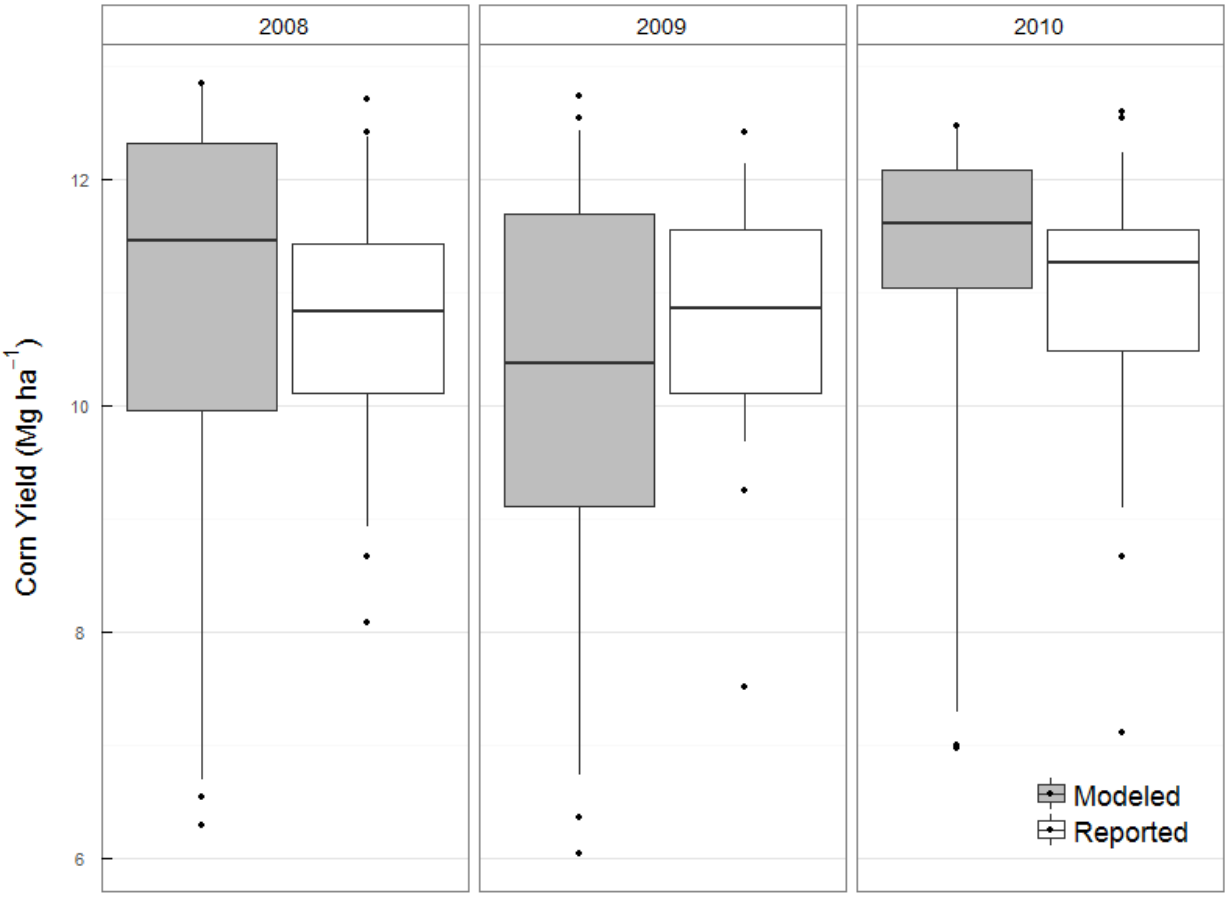

Figure 2.2. Per-farm corn yields for 2008-2010. Center lines indicate average, hinges indicate 1st and 3rd quartiles, whiskers encompass 95% confidence intervals, and remaining outliers appear as points.

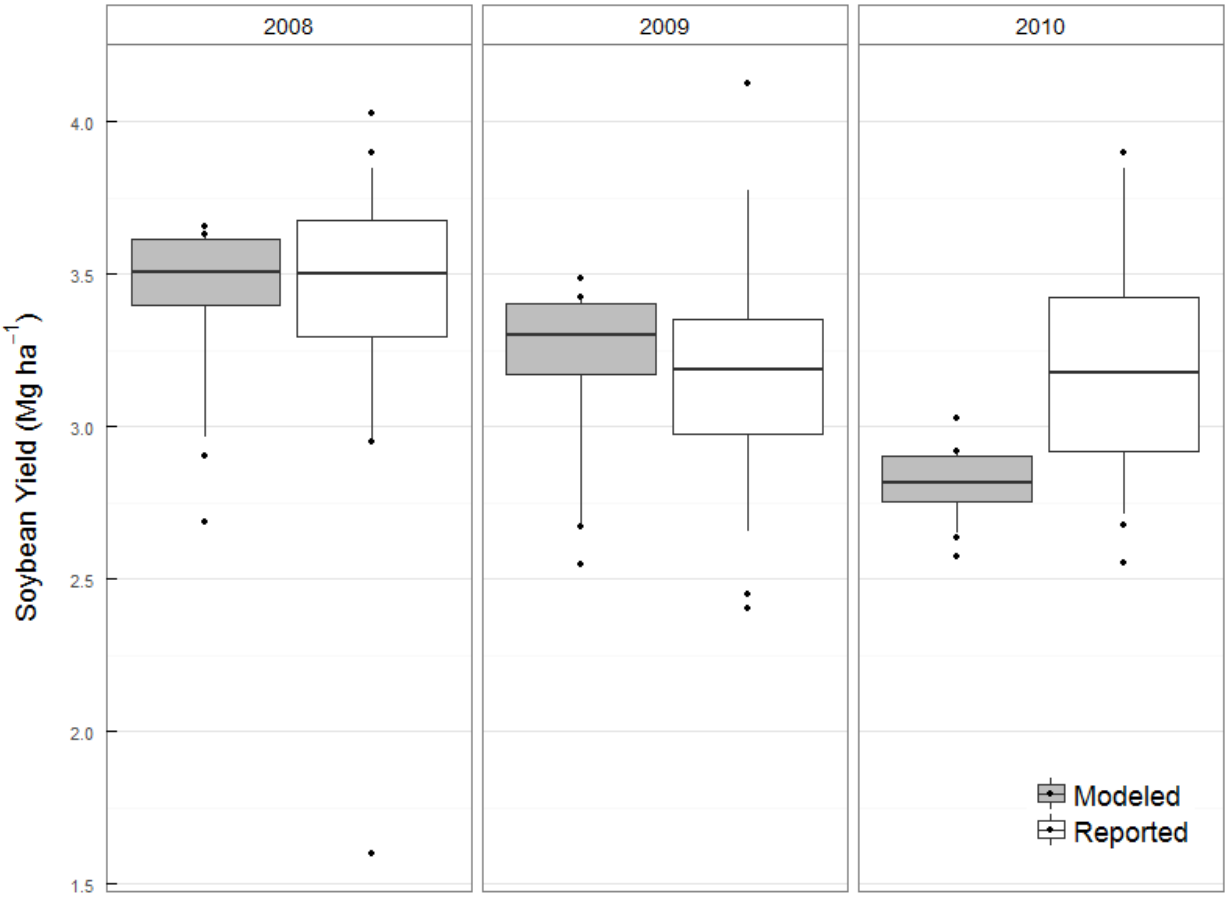

Figure 2.3. Per-farm soybean yields for 2008-2010. Center lines indicate average, hinges indicate 1st and 3rd quartiles, whiskers encompass 95% confidence intervals, and remaining outliers appear as points.

Field-to-plant-gate emissions budgets

Biogenic emissions calculations were made using averaged data from the last 12 years (1998-2010) of the simulation period to smooth out effects of interannual variability of weather and changes in management practices (Figure 2.4). The results in Figure 2.4 show each emission source by farm, sorted horizontally based on average per-farm total net FTP emissions, indicated by large black dots. All of the 35 farms surveyed showed average net increases in SOC over the final 12 simulation years (Figure 2.4). The spread in FTP emissions between the lowest- and highest-emitting farms was 4.16 Mg CO_2e ha^{-1} yr^{-1}. These results suggest that, while many

farmers already achieve C sequestration in the field, success in C sequestration varies substantially across farms as a result of both differences in soil conditions and, importantly, management practices adopted.

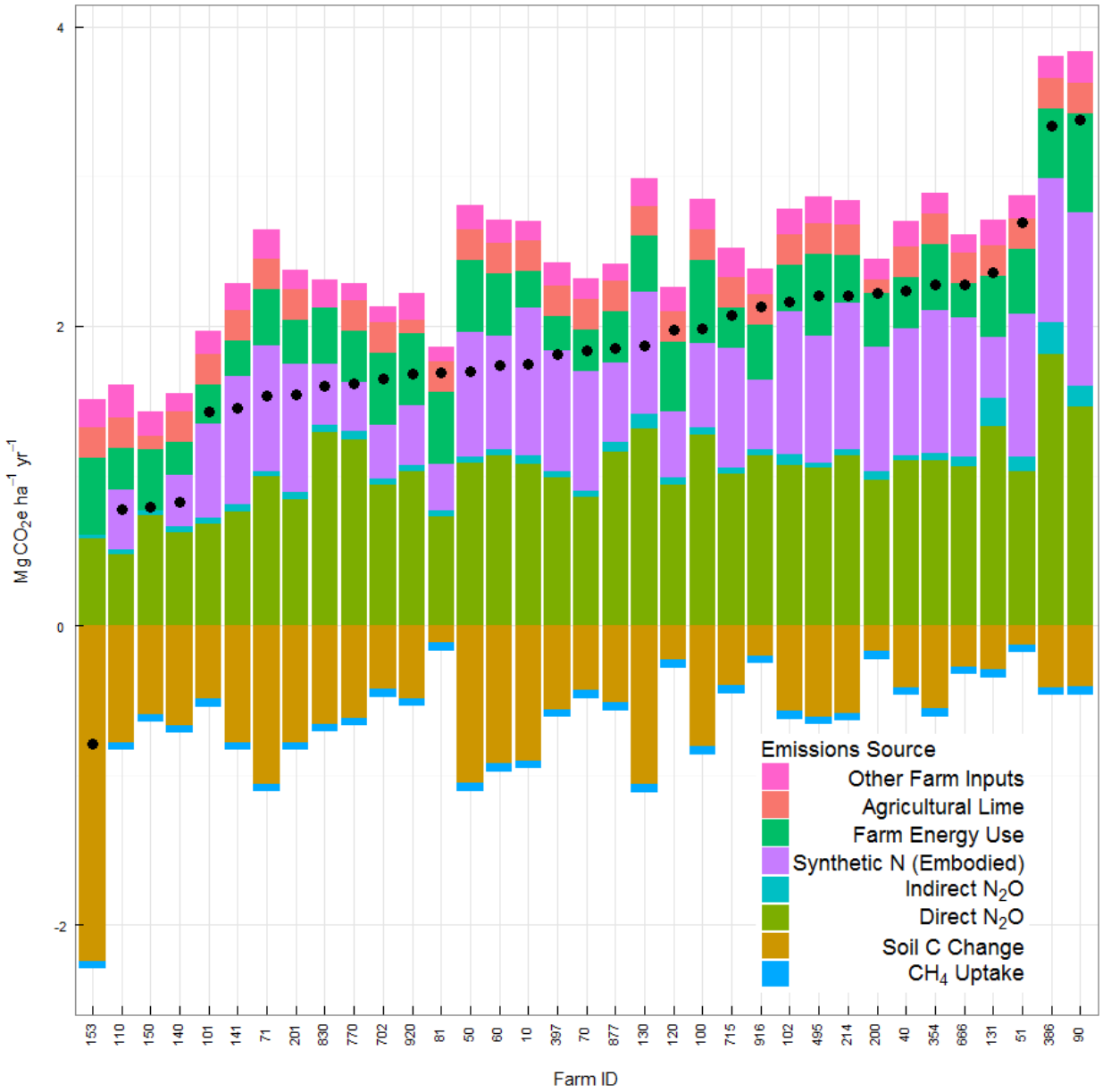

Figure 2.4. Per-farm, 12-year average field-to-plant-gate emissions components based on DayCent and SimaPro modeling. Total net emissions after accounting for CH_4 uptake and SOC increases (negative emissions) are indicated by black dots.

Direct N_2O emissions varied nearly fourfold, with a low of 0.47 Mg CO_2e ha^{-1} $yr^{-1}$and a high of 1.81 Mg CO_2e ha^{-1} yr^{-1}. Indirect N_2O emissions from leaching and other off-site transport of N generally amounted to a small fraction of total emissions, with a mean value of 0.060 Mg CO_2e ha^{-1} yr^{-1}. Simulated uptake of CH_4 was minimally variable between farms and amounted to an average emission of -0.053 Mg CO_2e ha^{-1} yr^{-1}. The total simulated biogenic emissions ranged from a low of -1.69 Mg CO_2e ha^{-1} yr^{-1} to a high of 1.56 Mg CO_2e ha^{-1} yr^{-1}, with a median value of 0.51 Mg CO_2e ha^{-1} yr^{-1}.

Supply chain emissions (i.e. those not modeled by DayCent) ranged from 0.67 Mg CO_2e ha^{-1} yr^{-1} to 2.23 Mg CO_2e ha^{-1} yr^{-1}. Finally, the total FTP emissions (black dots in Figure 2.4) ranged from -0.79 Mg CO_2e ha^{-1} yr^{-1} to 3.38 Mg CO_2e ha^{-1} yr^{-1}.

Soil C dynamics

Closer inspection of the lowest-emitting, median-emitting, and highest-emitting farm simulations illustrated the behavior of the dominant emissions components over time. SOC increased at an average annual rate of 0.61 Mg C ha^{-1} in the lowest-emitting farm, 0.16 and 0.12 Mg C ha^{-1} in the two median-emitting farms and 0.11 Mg C ha^{-1} in the highest-emitting farm.

Manure application constituted a major input of organic C on many of the surveyed farms. These manure additions could increase SOC levels relative to a baseline of no addition, depending on the amount of manure C that was sequestered over the time interval of interest. The lowest-emitting farm in this study applied manure equivalent to 2.67 Mg C ha^{-1} in the fall after soybean harvest, or 1.33 Mg C ha^{-1} yr^{-1} on an annualized basis. Twenty-one of the 35 farms simulated applied no manure, including the median-emitting and highest-emitting farms.

Tillage in the fall after corn harvest is likely to be a particularly important driver of immediate SOC loss, since it entails mechanical disturbance and mixing of large amounts of residue C with mineral soil horizons. Among the surveyed farmers simulated for this study, 26 practiced some kind of fall tillage following corn harvest, while 10 did not. The mean rate of SOC increase among those practicing tillage after corn harvest was 0.15 Mg C ha^{-1} yr^{-1}, while among farmers who left corn residues undisturbed it was 0.21 Mg C ha^{-1} yr^{-1}. These two groups of farmers differed on other management practices as well, however, confounding the relationship between fall tillage and rates of SOC change. In fact, tillage in the fall after corn turned out to be a simple criterion for dividing the surveyed farms between those practicing generally more-intensive management, versus those practicing less-intensive management. On average, the farmers who reported tilling in the fall after corn (n=26, "Conventional") also applied more synthetic N fertilizer (184 vs. 120 kg N ha^{-1} on corn years) and less manure (340 vs 778 kg manure C ha^{-1} on corn years) than those who did not (n=9, "Low-impact"). Thus, fall tillage after corn provided a useful indicator variable for grouping the surveyed farms on a broader set of management practices.

Since SOC dynamics are strongly linked to historic land use, we compared simulated historic C inputs with estimates derived from corresponding NASS crop yields (see Methods for details). The NASS-based estimated C inputs, DayCent simulated C inputs, and DayCent simulated SOC content are compared in Figure 2.5. The rolling-average NASS-based C input estimates (Figure 2.5c) begin to increase around 1954 from roughly 1 Mg C ha^{-1} to just over 4 Mg C ha^{-1} due to a combination of increasing biomass productivity and reduced reliance on crop residues for forage. While there is clearly large uncertainty surrounding these estimates, their general agreement with

the simulated C inputs (Figure 2.5b) corroborates the simulated "rebound" in SOC stocks (Figure 2.5a) that undergirds the C stock increases (Figure 2.5a) simulated for these farms.

Soil N dynamics

Simulated direct emissions of N_2O for the lowest-, median-, and highest-emitting farms were 0.58, 1.07 and 1.81 Mg CO_2e ha^{-1} yr^{-1}, respectively. Since N_2O emissions are directly related to the amount and duration of mineral N in the soil profile, which in turn is heavily influenced by the difference between N fertilizer application and crop uptake, we calculated an indicator variable called N uptake ratio (NUR). This was calculated by taking the ratio of N in aboveground crop biomass at harvest (based on reported yields and literature values for N content of crop components; see Appendix for details) to the total N applied from both manure and synthetic sources between soybean harvest and corn planting. Since none of the simulated farms applied N from any source between corn harvest and soybean planting, we assessed NUR only for corn years. Figure 2.6a shows NUR as a function of N application rate for all 35 farms. As might be expected, there was a discernible trend toward lower NUR among farms applying above-average amounts of total N, reflecting the limited capacity for additional crop uptake at high application rates. Since large fractions of N were left in the soil at low NUR, these same farms also displayed the highest levels of simulated direct N_2O emissions (Figure 2.6b).

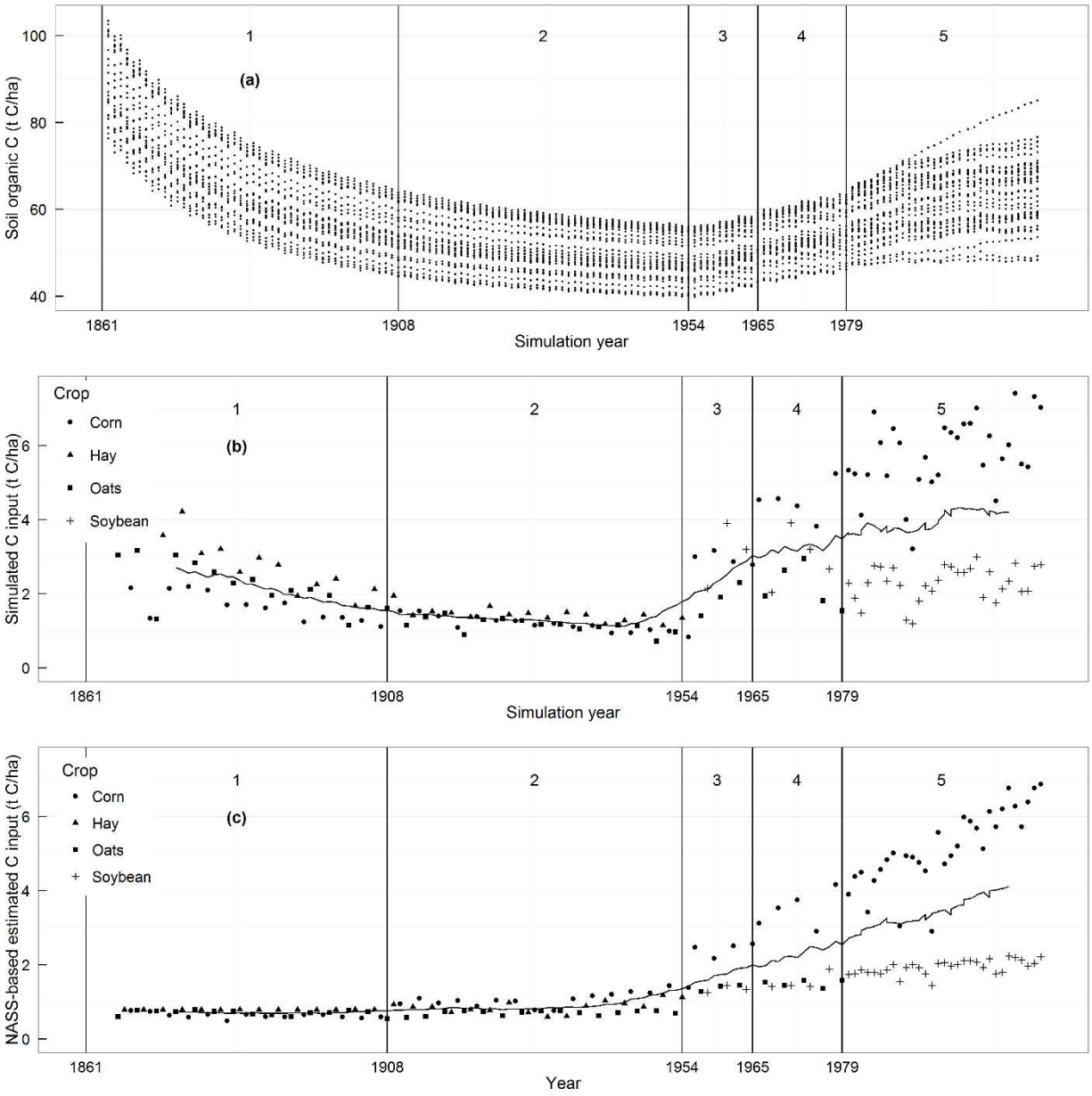

Figure 2.5. Simulated SOC of farms in this study (a), as compared with annual C inputs to soil as simulated by DayCent (b) and estimated from historical NASS yield data (c). Increases in crop yield and reductions in residue removal for forage since the mid-1900s have increased C inputs to intensively-managed cropland soils. Simulated transitions in management practice are marked by vertical lines. Lines for panels (b) and (c) reflect 20-year moving average C inputs. Specific assumptions for each numerically-labeled historical management period are described in Methods.

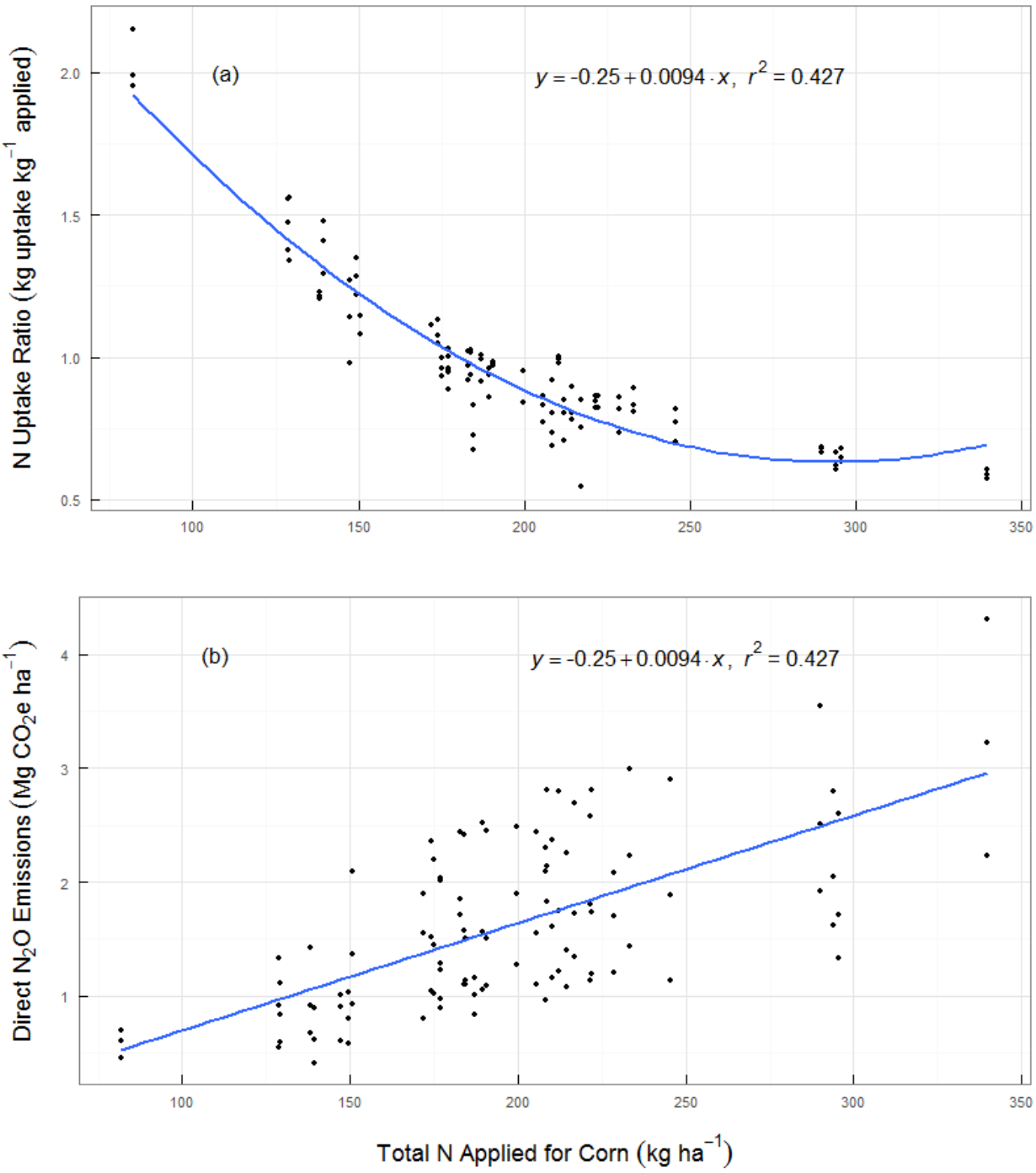

Figure 2.6. N Uptake Ratio (6a) for the 35 simulated farms, estimated from survey-reported grain yields and fertilization schedules and literature-derived values for N content of biomass components, and corresponding DayCent-simulated direct N_2O emissions (6b). Note that both panels share the same x-axis units.

We compared DayCent's simulated N_2O emissions values with those calculated using methodologies recommended by the USDA (Ogle et al. 2014) and IPCC Tier 1 (de Klein *et al.*,

2006; additional details can be found in Appendix). Figure 2.7 shows the distributions of per-farm direct N_2O emissions for corn and soybean years as estimated using these three methods. As can be seen in Figure 2.7, the IPCC method predicted the lowest average emissions under both corn and soybean cropping, while the USDA method predicted the highest average emissions under corn and DayCent predicted the highest average emissions under soybean.

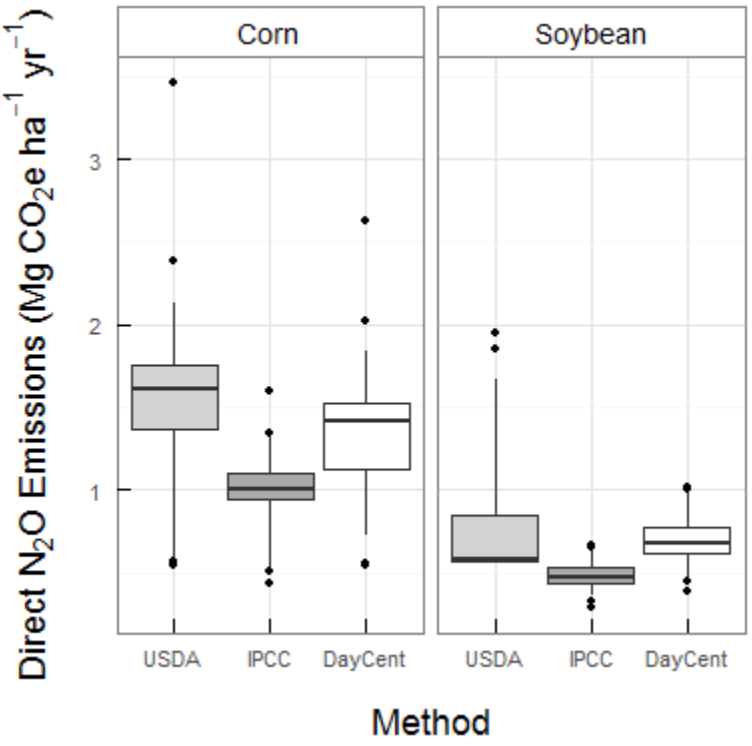

Figure 2.7. Direct N_2O emissions calculated using USDA methodology (Ogle et al., 2014), IPCC Tier 1 guidelines (de Klein et al., 2006), and DayCent simulations. Center lines indicate averages, hinges indicate 1st and 3rd quartiles, whiskers encompass 95% confidence intervals, and remaining outliers appear as points. Note that emissions attributed to each crop from DayCent simulations reflect fluxes that occur between planting of that crop (May) and planting of the alternate crop (next May).

Indirect N_2O emissions averaged 0.060 Mg CO_2e ha^{-1} yr^{-1}, or about 6% of the magnitude of direct N_2O emissions. Indirect emissions represented a weighted sum of three N-transport processes that result in off-site N_2O production: NO_3^- leaching, NO emission, and NH_3

volatilization. At the level of individual farms, leaching was highly variable and ranged from 0.6 to 45.8 kg N $ha^{-1}yr^{-1}$, with an average of 6.4 kg N $ha^{-1}yr^{-1}$. When compared with indirect N_2O emissions estimated using the IPCC Tier 1 method with the default value of 0.3 (uncertainty range: 0.1-0.8) for fraction of applied N that is leached (de Klein *et al.*, 2006), the DayCent outputs were noticeably low. The DayCent-calculated amounts of N leached corresponded to a leaching fraction of 0.07. If the higher IPCC leaching estimates were used in the emissions budgets of each farm, they would increase average emissions relative to DayCent by 0.16 Mg CO_2e $ha^{-1}yr^{-1}$ in corn years and 0.010 Mg CO_2e $ha^{-1}yr^{-1}$ in soybean years, or 0.085 Mg CO_2e $ha^{-1}yr^{-1}$ averaged across the full rotation.

Field-to-wheels emissions budgets

To get a better idea of the magnitude of variability observed here in FTP emissions relative to the full field-to-wheels (FTW) life-cycle emissions used in the provisions of the RFS2, we used a uniform literature value to estimate the full FTW emissions that might be expected from fuels derived from corn grain produced by the farms in this study. This value, 31 g CO_2e MJ^{-1}, was derived from Figure 5 of Wang et al. (2012) and was a sum of emissions due to ethanol production, land-use change, transportation and distribution, combustion, and a coproduct credit for distillers' grains and solubles (DGS). The resulting FTW estimates were plotted in Figure 2.8 as a fraction of the well-to-wheels emissions of gasoline, with specific emissions ranges shaded to correspond with the renewable fuel classifications defined by the RFS2. Figure 2.8a-c each include one point for each farm in this study, but plot them against different management variables to convey their potential for reducing feedstock emissions. In general, these FTW estimates suggest that ethanol derived from corn grain produced on these farms would fall within

the emissions range stipulated for Renewable Fuels under the RFS2 (i.e., no more than 80% of the emissions of gasoline).

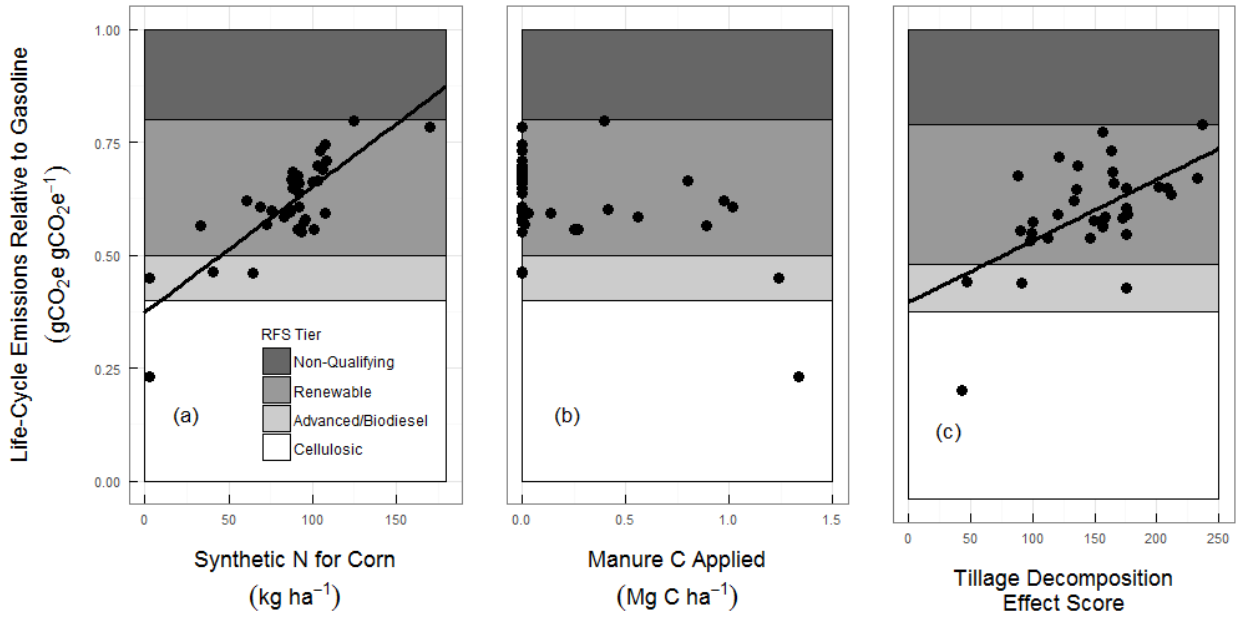

Figure 2.8. Per-farm field-to-wheels emissions as a function of synthetic N fertilization rate (9a), manure C application rate (9b), and DayCent Tillage Decomposition Effect score (9c; described in the Appendix). Plant-gate-to-wheels emissions sources were obtained from Wang et al. (2012) and combined with FTP budgets from this work to arrive at the FTW totals shown here. Background shading indicates the RFS2 emissions reduction tier achieved by the corresponding farms. Trend lines were included when statistically significant at $p<0.05$.

Discussion

Emissions totals and variability

We found that corn grain ethanol from all 35 farms modeled would meet the RFS2 requirement for "Renewable Fuels" of achieving a 20% reduction in FTW emissions relative to gasoline (Figure 2.8). In addition, four of the farms achieved 50% or greater reductions, a level set aside for "Advanced Biofuels" that specifically excludes corn starch ethanol. One unusual farm even exceeded the 60% reduction threshold set aside for next-generation "Cellulosic Biofuels", although his emissions are sensitive to our decision to credit C sequestered from manure as a

negative farm emission (discussed further below). The mean reduction across farms found in this study (39%) was similar to that found by Adler *et al.* (2007) for a corn-corn-soybean rotation (38%) under conventional tillage. In a more general LCA study tabulating emissions from various biomass-based fuels for U.S. consumption, Wang *et al.* (2012) found a similar reduction for corn grain ethanol of 34%. Since the PTW portion of their study (31 g CO_2e MJ^{-1}) was used as a generic estimate of PTW emissions for this work (see Results), we can directly compare the FTP values generated by our respective analyses.

Nitrous oxide estimation methods

Wang *et al.* (2012) employed a mean N_2O emissions factor of 1.53% of applied N based on their review of the experimental literature, with 10^{th}- and 90^{th}-percentile values of 0.413 and 2.96%, respectively. The combination of this broad uncertainty range and the large overall role of N_2O in the emissions budgets of corn ethanol led to their finding that the N_2O EF is the most sensitive parameter in the life-cycle emissions of corn ethanol. The distribution of N_2O per-farm EF values calculated from our DayCent modeling was significantly narrower, with 10^{th}-, 50^{th}, and 90^{th}-percentile values of 1.18, 1.42, and 1.57% of applied N, respectively. This is likely due to the fact that the field and management conditions in our study were homogeneous relative to the range of agronomic conditions under which the experimental data reviewed by Wang et al. (2012) were collected.

Soil C accounting issues

To our knowledge, Wang et al. (2012) did not consider SOC changes in their analysis. This is equivalent to assuming stable SOC stocks, which is a common and understandable simplification

with respect to US croplands as a whole, especially in view of the sensitivity of SOC changes to past and present management.

Our SOC results were sensitive to the assumption that manure C could be considered a "free" input to the farm soils and sequestered manure C being credited as a negative emission. This reflected a baseline scenario in which all manure C would otherwise be respired as CO_2, which may not be accurate. As noted in the Methods, consultation with a USDA manure management official in the area indicated a high concentration of confined animal feeding operations (CAFOs) in the study region (Doug Bos, personal communication), suggesting that transport emissions would be relatively low and alternative manure handling may lead to emission of more potent GHGs, including CH_4 and N_2O. The EPA (2015) indicates, for instance, that liquid manure management is increasingly common on U.S. CAFOs, leading to greater anaerobic production of CH_4. At the same time, concerns over air and water pollution from over-application to land have led to regulations restricting application rates, increasing on-site storage times (EPA, 2015). By increasing the land supply, the decision of a given farmer to utilize manure that is locally in surplus could be assumed to reduce those storage times. From the perspective of identifying emissions-reducing practices for corn-soybean cropping systems in this area, then, the treatment of manure C and N as "free" nutrients seems like a justifiable simplification, although a more detailed analysis would be valuable.

The SOC sequestration rates simulated for the farms in this study reflect a postulated "rebound" in SOC stocks from lows reached under historic low-productivity cropping. Typical historical agronomic practices and their impacts on SOC were described by Allmaras *et al.* (2000), who suggested that American tallgrass prairie soils lost as much as 60% of their initial SOC following

cultivation. Blocks 3 and 4 in Figure 2.5a illustrate the start of this rebound, supported by increasing C inputs from more-productive cropping practices. Block 5 (simulation years 1979-2010) shows its continuation and divergence as a function of the differing management practices reported in our farm survey. The area-weighted average of 0.16 Mg C ha^{-1} yr^{-1} was modest compared with the 25-year sequestration rate of 0.37 Mg C ha^{-1} yr^{-1} calculated by Clay *et al.* (2012) for corn croplands in South Dakota. Similarly, long-term monitoring of the Sanborn Field in Missouri found that SOC stocks fell sharply until around 1950, but have aggraded at rates ranging from 0.50-1.50 Mg C ha^{-1} yr^{-1} since then as a function of reduced tillage and increased C inputs (Buyanovsky & Wagner, 1998).

Conclusions

The results of this study supported our hypothesis that the GHG emissions associated with corn grain ethanol can vary widely based on differences in farm management and site characteristics. These results were based on actual management practices as reported by surveyed farmers within a relatively uniform geographic region. Specifically, we found a total range in FTW emissions of 21.2 to 72.8 g CO_2e MJ^{-1}, with a median value of 55.5 g CO_2e MJ^{-1}. The lowest-emitting farm was distinguished by its low-intensity tillage regime (including no-till following corn harvest) and reliance on large quantities of manure to the exclusion of synthetic N fertilizer. We also found that reported corn yields were not significantly correlated with synthetic N inputs in the survey data, suggesting that reduced N application may also be a feasible approach for reducing emissions from some farms. Further work should explore the agronomic practicality (and limits) of broader adoption of these practices in both the Luverne region and other areas of the U.S. Corn Belt as a means of maximizing the climate-mitigating impacts of corn grain ethanol.

CHAPTER 3. DUAL-FEEDSTOCK BIOENERGY FROM CORN: CONNECTING AGRONOMY, EMISSIONS AND PRODUCTION COSTS

Introduction

Policy background

The US Renewable Fuel Standard 2 (RFS2) mandates national use of an estimated 90.7 billion L of qualifying renewable fuels in 2017. Of that total, 20.8 billion L are slated to come from cellulosic feedstocks, with that amount increasing annually to 60.5 billion L by 2022 (Schnepf & Yacobucci, 2011).

Potential stover supply

Crop residues represent a large potential source of biomass-based energy. The 2011 update to the US Department of Energy's "Billion Ton Study" (BTS2) estimated that US annual production of residues from major grain crops is greater than 318 million dry Mg, with 70% of this resource consisting of corn stover (Perlack *et al.*, 2011). Using a bounding assumption of 100% collection and an estimated ethanol (EtOH) yield of 375 L Mg^{-1} dry matter (Wang *et al.*, 2012) gives a rough upper limit of 83.5 billion L EtOH available from corn stover, more than four times the 2017 cellulosic volume mandate. Increases in corn productivity and/or planted acreage could significantly increase this limit. Of course, leaving aside the enormous logistical and financial barriers to stover utilization on such a scale, there are a range of constraints on collection rates that are related to soil sustainability.

Sustainability constraints

Under conventional management, corn stover is left on fields after grain harvest, where it serves a number of agronomic functions. Stover serves to impede evaporation from the otherwise bare soil surface during fallow periods, and in some rainfed systems this water conservation is essential, precluding significant residue removal. It plays a similarly crucial role in other systems by reducing soil loss to wind and water erosion (Mann *et al.*, 2002). Much of the C content of retained stover is lost as CO_2 within a short time frame, but a fraction is incorporated into soil organic carbon (SOC) pools, where it improves water-holding capacity, cation exchange capacity and other soil fertility traits. Finally, stover is a valuable reservoir of nitrogen (N), phosphorous and potassium, some of which become available to subsequent crops as decomposition proceeds (Blanco-Canqui & Lal, 2009). This reduces the need for synthetic fertilizers to replace these nutrients.

Management complementarities

There are potentially important complementarities between stover removal and reduced- or no-till management. For instance, compared to conventional tillage, lower-intensity tillage increases rates of SOC and soil moisture retention, while reducing susceptibility to wind and water erosion (Mann *et al.*, 2002; West & Post, 2002). This is caused by the reduced mechanical degradation of stover structure and greater fraction of stover left on the soil surface, as opposed to being turned under the soil. Conversely, no-till management can be problematic in certain circumstances, as large amounts of intact stover left on fields can foster crop pests and diseases, and in colder regions delays soil warming and thus planting (Wilhelm *et al.*, 1986; Sims *et al.*, 1998). In contexts where these are barriers to no-till adoption, removal of a portion of the stover may facilitate adoption by reducing residue buildup.

Even as stover collection may facilitate reduced tillage in some contexts, application of livestock manure has the potential for replacing some of the benefits lost with stover removal. At the most basic level, manure represents an input of organic C to soils which tends to increase SOC stocks. Beyond providing organic C, most manures contain substantial amounts of N and P, both of which are lost during stover removal. National scale estimates suggest that recoverable livestock manure contains as much as 15% of all N and 42% of all phosphorous purchased as commercial fertilizer for crops each year (Risse *et al.*, 2006). In addition, manure application has been shown to improve soil physical properties such as porosity and water holding capacity, and to reduce water erosion (Risse *et al.*, 2006).

Other management considerations

The rate and timing of N application is a key determinant of both yield and N_2O emissions, a major greenhouse gas, while production of synthetic N fertilizer itself produces substantial emissions. Typically, crop yields display a saturating response to N application, with even small declines in yields at rates far above optimal. Maximum economic return occurs at rates lower than the rates needed to support maximum grain yield. Accounting for the increasing marginal damages from N production, leaching and biogenic emissions – which combined account for greater than a third of the field-to-wheels (FTW) emissions footprint of US corn EtOH production (Wang *et al.*, 2012) – would likely lower the "preferred" N application rate further.

Study rationale

Davis *et al.* (2013) coined a useful phrase for thinking about bioenergy system sustainability. Their phrase, "management swing potential," referred to the potential for farm management decisions to significantly improve or detract from the GHG savings achieved by a bioenergy

production pathway. These pathways are often defined in terms of a particular crop species in conjunction with the final fuel product (eg., "corn grain EtOH"). This is a convenient policy shorthand, but it masks variability stemming from farm management ("swing potential") that may in some cases be greater than mean emissions differences *between* two pathways, as defined by species and fuel type.

The primary objective of this work was to explore emissions impacts and management swing potential for the feedstock supply of a hypothetical integrated grain- and stover-bioenergy facility situated in Luverne, MN. The analysis was particularly focused on exploring complex tradeoffs between grain and stover utilization, emissions intensity, and farm production costs. This was accomplished through a combination of DayCent biogeochemical modeling, SimaPro and literature-based life-cycle assessment, and basic farm budget analysis.

Methods

This work extended the biogeochemical and life-cycle modeling described in Chapter 2 by attempting to map the multi-dimensional emissions space resulting from discrete levels of various farm management practices. The life-cycle emissions reported here were derived from a combination of DayCent dynamic modeling of farm biogenic emissions, and SimaPro (Pre Consultants, 2012) and literature-based estimates for supply chain emissions.

Farm management scenarios

The first step of this work was to determine a list of management practices and levels of each practice to be modeled. This was done in consultation with area stakeholders representing farm and environmental organizations and ultimately identified six farm management practices of

interest and discrete levels of each practice to be modeled (Table 3.1). These were combined in a full factorial analysis, leading to 1,920 unique management scenarios.

Table 3.1. Farm management practices and levels modeled for this work. All permutations of the various practice levels were modeled.

Practice	Description	Levels	Number of Levels
Tillage	Intensity of soil disturbance from cultivation	Conventional till Reduced till No-till	3
N Application Rate	Total N applied from synthetic fertilizer and/or manure (kg ha^{-1})	5 10 15 20 25	5
N Fraction from Manure	Fraction of N derived from manure	0 0.2 0.4 1.0	4
Stover Removal	Fraction of corn residue removed	0 0.25 0.5 0.75	4
Crop Rotation & N Fert Timing	Cropping and N application timing	Cont corn/N at planting Cont corn/N in fall Cont corn/split N Corn-soy/N at planting	4
N Inhibitor	Use of nitrification inhibitor	Yes No	2
Total Management Scenarios:			1,920

DayCent simulations

DayCent simulations were run using North American Regional Reanalysis (NARR) daily weather inputs (Mesinger *et al.*, 2006), with scenario management practices running from simulation years 1979 through 2009. Each of the 1,920 management scenarios was simulated for the same 65 fields included in a previous study (Kent et al., in submission), and results from these fields were aggregated to the level of 36 farms using area-weighted averaging. Biogenic emissions, including methane uptake, direct and indirect N_2O and average annual change in SOC, were calculated for the final 12 years of each simulation, in the same manner as in previous work (see Appendix for details). The DayCent modeling for this analysis used the same weather, site, and soil inputs as the previous work (Kent et al., in submission), but replaced farmer-reported management practices with the hypothetical management scenarios outlined in Table 3.2.

Supply chain emissions accounting

For life-cycle emissions not included in DayCent simulations, such as those from farm chemical manufacture and distribution, farm equipment manufacture and fuel use, and biomass drying and transport, a variety of sources were used. In order to preserve the survey-derived inter-farm variability developed for previous work (Kent et al., in submission), farm inputs not directly affected by management scenarios were reused from that analysis. For instance, farm chemicals and non-N fertilizers were not specified by the scenarios in Table 3.2, and so the farm survey input rates were used. In contrast, emissions due to manufacture and distribution of synthetic N fertilizer are directly linked to the N Application Rate used in a given scenario, and so the scenario-based input rate and corresponding emissions were used. The sources and emissions

values (where appropriate) for major life-cycle inputs and related parameters are summarized in Table 3.2.

Table 3.2. Major life-cycle emissions sources and related parameters not modeled by DayCent. Survey supply chain inputs are those not directly related to the management scenarios being investigated, and so per-area amounts are reused from the case study in Chapter 2. See text for further details on assumptions and how specific inputs were integrated into emissions budgets.

Input	Value	Unit	Source(s)
Crop Seeds	3.7	g CO_2e m^{-2}	SimaPro; Farm Surveys
Phosphorous & potash fertilizers	28.7	g CO_2e m^{-2}	SimaPro; Farm Surveys
Pesticides & herbicides	2.3	g CO_2e m^{-2}	SimaPro; Farm Surveys
Equipment depreciation	5.8	g CO_2e m^{-2}	SimaPro; Farm Surveys
Tillage, corn:		g CO_2e m^{-2}	(Lal, 2004b)
Conventional	9.46		
Reduced	5.50		
No-till	1.39		
Tillage, soy:			
Conventional	4.22		
Reduced	3.30		
No-till	1.39		
Synthetic N, embodied	4.77	g CO_2e g^{-1} N applied	(Lal, 2004b)
Synthetic N, application	2.79	g CO_2e m^{-2}, per application	(Lal, 2004b)
Manure, transport to field	845	g CO_2e Mg^{-1} mi^{-1}, wet manure	(Lal, 2004b; Qin *et al.*, 2015)
Manure, broadcast application	4.62	g CO_2e m^{-2}	(Lal, 2004b; Qin *et al.*, 2015)
Manure, phosphorous offset credit	-450	g CO_2e Mg^{-1} wet manure; max offset is 100% of P emissions	(Lal, 2004b; Qin *et al.*, 2015)
Stover, cutting, baling and stacking at field edge	0.0166	g CO_2e g^{-1} dry stover removed	(Qin *et al.*, 2015)
Stover, mass loss, uncovered at field edge	0.148	g lost g^{-1} dry stover collected	(Qin *et al.*, 2015)

Grain Drying	0.0198	g CO_2e g^{-1} dry grain	(Camargo *et al.*, 2013)
Grain Transport	5899	g CO_2e Mg^{-1} dry grain	(Wang *et al.*, 2013)
Stover Transport	5665	g CO_2e Mg^{-1} dry stover collected	“”
EtOH production: Grain Stover	 31 10	g CO_2e MJ^{-1} EtOH	(Wang *et al.*, 2012)
Land-use change: Grain Stover	 9 -1	g CO_2e MJ^{-1} EtOH	“”
Distillers’ grains and solubles credit	-14	g CO_2e MJ^{-1} grain EtOH	“”
Surplus electricity credit	-17	g CO_2e MJ^{-1} stover EtOH	“”
EtOH distribution and combustion Grain Stover	 5 4	g CO_2e MJ^{-1} EtOH	“”
EtOH yield Grain Stover	 425 375	L Mg^{-1} dry feedstock	“”
EtOH lower heating value	21.3	MJ L^{-1}	“”

Tillage is modeled in DayCent as a series of equipment passes representative of conventional, reduced, and no-till regimes. The primary effect of simulated tillage is to increase decomposition rate of organic matter pools and the mixing of residues into the soil, with more intensive regimes causing greater degrees of residue incorporation and stimulation of decomposition. The tillage emissions given in Table 3.2 account for fuel use and equipment manufacture for tillage operations. They were calculated by summing the mean emissions factors developed by Lal (2004) for passes by the specific tillage implements simulated for each tillage intensity level.

The application of N to fields likewise results in emissions that occur within the field and are modeled by DayCent (direct and indirect N_2O emissions) and substantial embodied emissions related to 'upstream' manufacture, distribution, and application, not simulated by DayCent, were estimated using the mean emissions factors given by Lal (2004).

Manure supply-adjustment procedure

Since manure application builds SOC stocks of cropland soils, a farm emissions analysis that credits farms with this sequestration leads to a trivial corner case where "best management" entails maximal manure utilization. We avoided this unrealistic conclusion by scaling the emissions benefits of each management scenario in proportion to the actual supply-demand dynamics that prevail within the Rock County, MN feedlot-cropping landscape (see Appendix for a full description). This approach assumed that all manure produced on feedlots within the county would be applied to cropland within the county. Thus, the aggregate benefits of application of the entire supply should be evenly distributed across cropping area in the county, and that rate used for crediting the particular area supplying feedstock for bioenergy production. Using this "supply-adjustment" procedure, maximal rates of application are no longer necessarily optimal since they exhaust the available manure on a small fraction of acres, whereas lower rates may sequester more manure C in aggregate by building SOC stocks more gradually.

The emissions from stover cutting, baling and stacking operations were estimated from values given by Wang *et al.* (2013). We also assumed stover kept at the field edge would be uncovered and lose 14.8% of its dry mass before transport to the biorefinery (Emery, 2013), effectively increasing the emissions intensity of the delivered feedstock by a factor of 1.17.

Post-farm emissions accounting

While the detailed modeling for this work concerned farm management variables, post-farm emissions components were included in the life-cycle budgets to facilitate comparison of farm management effects with other emissions drivers. These components were taken from mean values presented in Wang *et al.* (2012). The values for EtOH Production in Table 3.2 assumed that the lignin fraction of stover was used to supply heat and energy for the conversion process. Land use change accounted for the market-mediated impacts of each feedstock's allocation to EtOH production on cultivation of new land area elsewhere. The credits for distillers' grains and solubles and surplus electricity reflect emissions displaced by by-products of the conversion processes for grain and stover, respectively. The values for EtOH yield per Mg feedstock and lower heating value were used to convert emissions from an areal to energy basis (referred to here as emissions intensity), allowing direct comparison with life-cycle emissions from fossil energy sources such as gasoline.

Marginal vs. mass feedstock allocation

Since the RFS2 classifies biofuels in part by feedstock type, we explored the implications of alternative methods for allocating emissions between grain and stover produced on the same land area. We developed two alternate approaches, referred to as marginal allocation and mass allocation, which are described and discussed in the Appendix.

Net abatement vs. emissions intensity

We calculated two primary metrics for comparing the full life-cycle impacts of varying management scenarios (Table 3.3). The first, which we refer to as the scenario's "emissions intensity," was a measure of the FTW emissions generated per MJ of EtOH energy. The other

metric, “net abatement”, was calculated as the total CO_2-equivalent life-cycle emissions avoided – through displacement of gasoline – per unit cropland area.

Table 3.3. Metrics used to compare life-cycle emissions impacts between scenarios. Abatement was calculated relative to gasoline emissions of 94 g CO_2e MJ^{-1}, from Wang et al. (2012).

Name	Units	Description
Emissions intensity	g CO_2e MJ^{-1}	FTW emissions per unit of fuel energy yield
Net abatement	g CO_2e m^{-2}	Avoided emissions per unit of cropland area through displacement of gasoline

USD farm budgets

We developed monetary farm budgets using a methodology similar to that used for farm emissions. As with emissions, certain input costs were assessed based on survey information specific to each farm. Many other inputs were assessed based on rates dictated by management scenarios (e.g., synthetic N). Finally, some budget items were not clearly related to scenarios but could not be calculated from survey responses (eg., land rent), and these items were estimated using the default rates and costs from Iowa State University Extension cropping budgets (Plastina, 2015). Further details of the monetary accounting methods can be found in the Appendix.

Results

Analytical emissions classes

The life-cycle emissions budgets constructed for this work included three analytically-distinct classes of inputs: biogenic emissions (i.e., those modeled by DayCent), survey supply chain emissions (i.e., farm inputs based survey responses), and scenario supply chain emissions (i.e., farm inputs dictated by management scenarios). The means and distributions of emissions from

these source categories are depicted for all scenarios (Figure A1-Figure A3) and summarized in the Appendix.

Farm-gate emissions budgets

The field-to-farm-gate (FFG) emissions budgets summarized in Figure 3.1 were calculated for each scenario by adding together the scenario supply chain and soil-derived emissions, and the average of the farm supply chain emissions. Those budgets represent the emissions for all farm inputs and soil processes for feedstock harvested and ready for transport to the biorefinery. The FFG emissions averaged 141 g carbon-dioxide equivalent m^{-2} (g CO_2e m^{-2}) and ranged from -112 to 408 g CO_2e m^{-2}.

Field-to-wheels emissions budgets

Figure 3.2 displays the emissions intensities of EtOH from each management scenario, plotted against the net GHG abatement achieved by that management scenario. Each of the four panels shows the same mapping of all 1824 scenarios along with Scenario IDs from several best- and worst-performing scenarios (further detailed in Table 3.4). While emissions intensity and net abatement were generally negatively correlated ($r = -0.69$), these plots show that the correlation was far from perfect. In other words, the scenarios with the lowest emissions per unit of EtOH energy were not necessarily the most space-efficient ways to displace a given volume of gasoline.

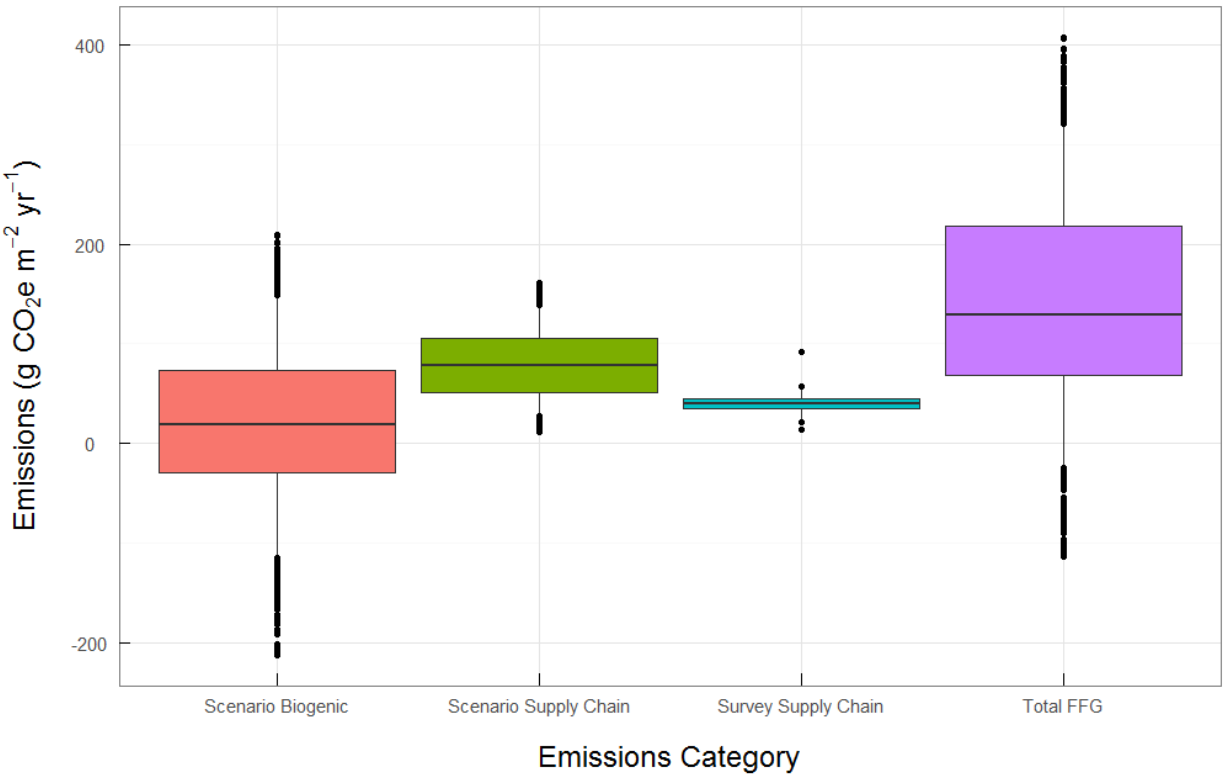

Figure 3.1. Means and distributions of the farm supply chain emissions, scenario supply chain emissions, scenario biogenic emissions, and total emissions (FFG, sum of other 3 categories). Center line indicates mean, box edges indicate 25th and 75th percentiles, whiskers extend to the 5th and 95th percentiles, and remaining values are plotted as points. Note that the survey supply chain emissions box represents 35 farm emissions budgets that are uniform across scenarios, while the other boxes represent 1824 scenario budgets that incorporate the same set of survey supply chain budgets.

The best-performing scenario for total emissions intensity was ID 565, with emissions of only 8.0 g CO_2e MJ^{-1} EtOH. Its net abatement of 416 g CO_2e m^{-2}, however, only placed it in the 66th percentile of all scenarios. Conversely, Scenario 640 had the highest net abatement at 639 g CO_2e m^{-2} and a total emission intensity of 26 g CO_2e MJ^{-1} EtOH (7th percentile; note that percentiles are ranked in ascending order, so that lower percentiles are "best" for emissions intensity while higher percentiles are "best" for net abatement). Thus, Scenario 640 could achieve an abatement target on about one-third fewer hectares than Scenario 565, but at the cost of substantially higher total emissions. To a large degree, this reflected the tradeoff between

collecting stover, which increased areal energy yield (Scenario 640), versus leaving it on the field where its organic C can be sequestered (Scenario 565) and operational emissions can be avoided. The second important difference between these scenarios was their N application rates, which were 10 and 15 g N m^{-2} for scenarios 565 and 640, respectively. While this was a relatively small difference in the context of the full range of N application rates, it corresponded to a general inflection point in terms of the simulated yield response curve. The decreasing marginal yield response lead to N uptake ratios (NUR, calculated as N taken up by plant as a fraction of total N application) of 1.12 and 0.97 for scenarios 565 and 640, respectively, and N_2O emissions of 38.3 and 72.4 g CO_2e m^{-2}.

The color coding of panels A-D in Figure 3.2 illustrates several management trends. The roughly linear clustering of points according to their residue removal level (panel A) shows a tradeoff between emissions intensity and net abatement. To shift to a higher level of residue removal in Figure 3.2A tends to cause an increase in net abatement (y-axis), due to the greater EtOH yield achieved, but also increases the emissions per unit energy (x-axis).

The high-level patterns in response to manure N fraction (panel B) are not as clear. In part this arises from the fact that the manure adjustment procedure scales back C sequestration savings at high manure input rates to reflect the declining proportion of cropland area needed to absorb the manure supply. For N application rates and manure N fractions that call for total manure inputs greater than about 5.7 g N m^{-2} (42% of all scenarios), the adjustment procedure reduced the DayCent-simulated C sequestration credit. Therefore, for high manure input rates, the trends in Figure 3.2B deviate somewhat from the raw sequestration dose-response simulated by DayCent.

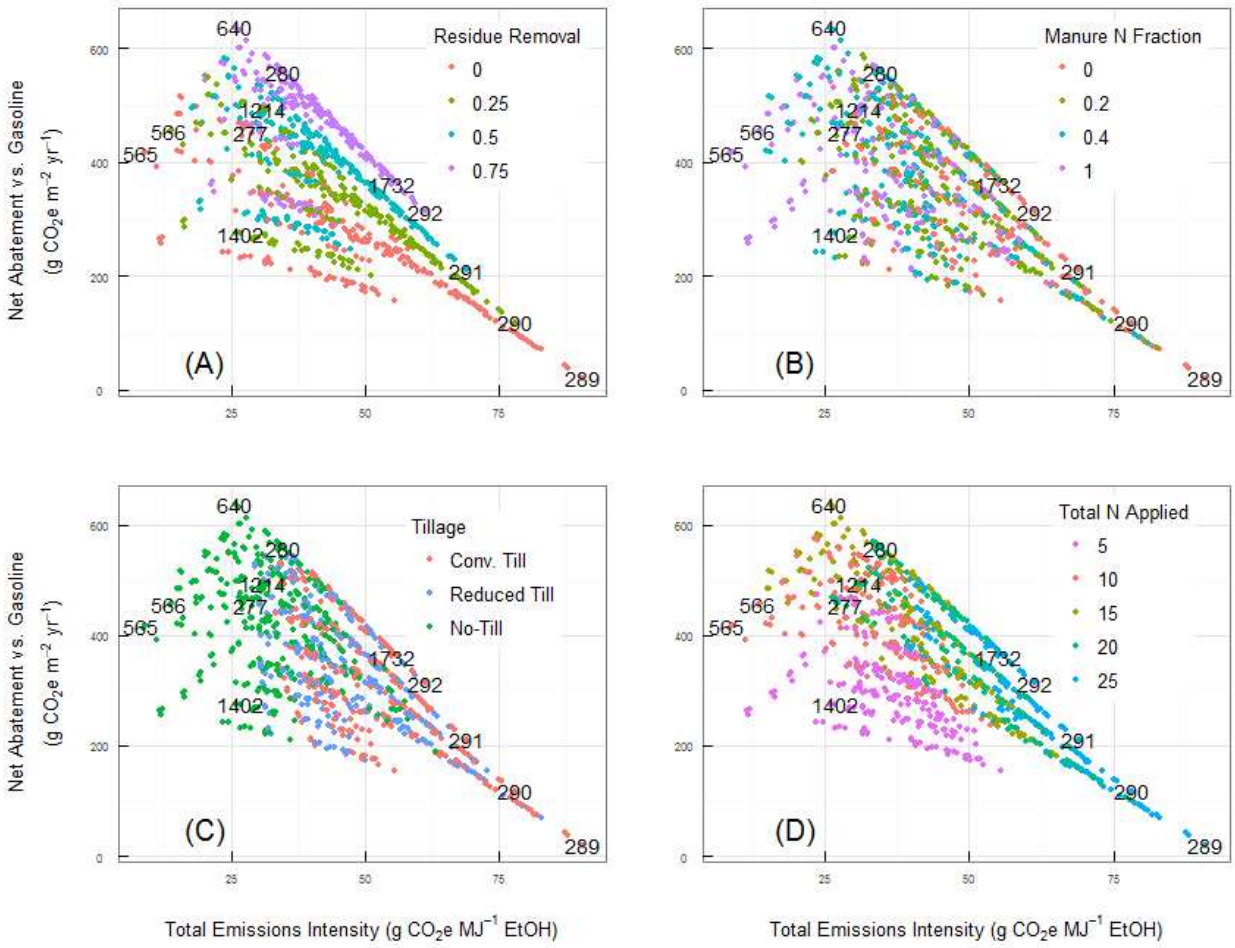

Figure 3.2. Total emissions intensity vs. net GHG abatement achieved for each management scenario, with color mapped to residue removal fraction (A), fraction of N from manure (B), tillage intensity (C), and total N application rate (D). Emissions intensities and net abatement were calculated from the total emissions and combined EtOH energy yield (grain and stover) per unit area of cropland. Scenario ID numbers from selected scenarios are displayed in their approximate position to facilitate comparison with other figures and Table 3.4 and Table 3.5.

Table 3.4. Management levels for best- and worst-performing scenarios based on several emissions metrics. Values in parentheses indicate the rank percentile (0 = lowest through 100 = highest) achieved by the scenario for the given metric. Green shading indicates "best" quintile of scenarios for a given outcome, while red shading indicates "worst" quintile.

Scenario ID	N Inhibitor	Rotation/ N Timing	Total N (kg ha^{-1})	N Manure Fraction	Tillage	Residue Removal	Total Emissions Intensity ($gCO_2e\ MJ^{-1}$)	Net GHG Abatement ($gCO_2e\ m^{-2}$)	Profit ($\$\ m^{-2}$)	Farm-Gate Emissions ($g\ CO_2e\ m^{-2}$)
565	Yes	CC/Plant N	10	1	No-Till	0	8 (0)	416 (66)	-0.044 (21)	-112 (0)
640	Yes	CC/Plant N	15	0.4	No-Till	0.75	26 (7)	639 (100)	-0.016 (91)	66 (24)
1402	No	CC/Split N	5	0.4	No-Till	0.25	27 (9)	275 (26)	-0.083 (0)	5 (9)
277	Yes	CC/Fall N	20	1	No-Till	0	29 (11)	454 (76)	0.003 (100)	-19 (5)
292	No	CC/Fall N	25	0	Conv. Till	0.75	61 (90)	313 (36)	-0.032 (49)	408 (100)
289	No	CC/Fall N	25	0	Conv. Till	0	91 (100)	20 (0)	-0.043 (23)	375 (99)

Table 3.5. DayCent C dynamics from best- and worst-performing scenarios (same scenarios as in Table 3.4). Values in parentheses indicate the rank percentile (0 = lowest through 100 = highest) achieved by the scenario for the given metric.

Scenario ID	N Inhibitor	Rotation/N Timing	Total N	N Manure Fraction	Tillage	Residue Removal	Grain Yield ($gC\ m^{-2}$)	Stover Harvested ($gC\ m^{-2}$)	Manure C Input ($gC\ m^{-2}$)	SOC Change Emissions ($gCO_2e\ m^{-2}$)
565	Yes	CC/Plant N	10	1	No-Till	0	535 (19)	0 (13)	102 (84)	-226 (3)
640	Yes	CC/Plant N	15	0.4	No-Till	0.75	654 (44)	201 (90)	61 (71)	-121 (18)
1402	No	CC/Split N	5	0.4	No-Till	0.25	379 (3)	39 (26)	20 (37)	-88 (33)
277	Yes	CC/Fall N	20	1	No-Till	0	766 (99)	0 (13)	205 (97)	-285 (0)
292	No	CC/Fall N	25	0	Conv. Till	0.75	669 (64)	206 (99)	0 (16)	0 (96)
289	No	CC/Fall N	25	0	Conv. Till	0	696 (87)	0 (13)	0 (16)	-59 (51)

The role of tillage, as shown in Figure 3.2C, is unambiguous: all of the high-performing scenarios for emissions intensity and the very best-performing scenarios for net abatement utilized no-till management. By comparison, the best emissions intensities for scenarios using reduced till and conventional till management were 29 and 32 g CO_2e MJ^{-1} EtOH.

Finally, Figure 3.2D shows that N application rate has a tradeoff dynamic similar to that observed for residue removal. Increasing N application – particularly up to the 15 g N m^{-2} level – increases crop growth and EtOH yields. This came at the cost of increasing marginal N_2O emissions, however, driving greater emissions intensity.

Best- and worst-performing scenarios

Figure 3.3 shows the itemized emissions budgets for the best- and worst-performing scenarios detailed in Table 3.4 and Table 3.5, as well as six randomly-selected scenarios. The scenarios here are sorted by their total emissions intensities (indicated by black dots), and range from a low intensity of 8 g CO_2e MJ^{-1} EtOH to a high of 91 g CO_2e MJ^{-1} EtOH. Perhaps most notable from this perspective is the large emissions credit achieved by four of the five best-performing scenarios for net soil C sequestration. The second major theme is that emissions due to N application, including direct N_2O and embodied emissions, are relatively modest for best-performing (left-most) scenarios but become major sources in the worst-performing (right-most) scenarios. The FFG emissions intensity (brown dots) generally track with the FTW emissions intensity, with most exceptions stemming from decreased residue collection rates. This shift improves farm-gate emissions intensity by sequestering more C, but entails a greater fraction of energy coming from grain, which has higher post-farm emissions intensity than stover largely due to land use change and differences in coproduct credits.

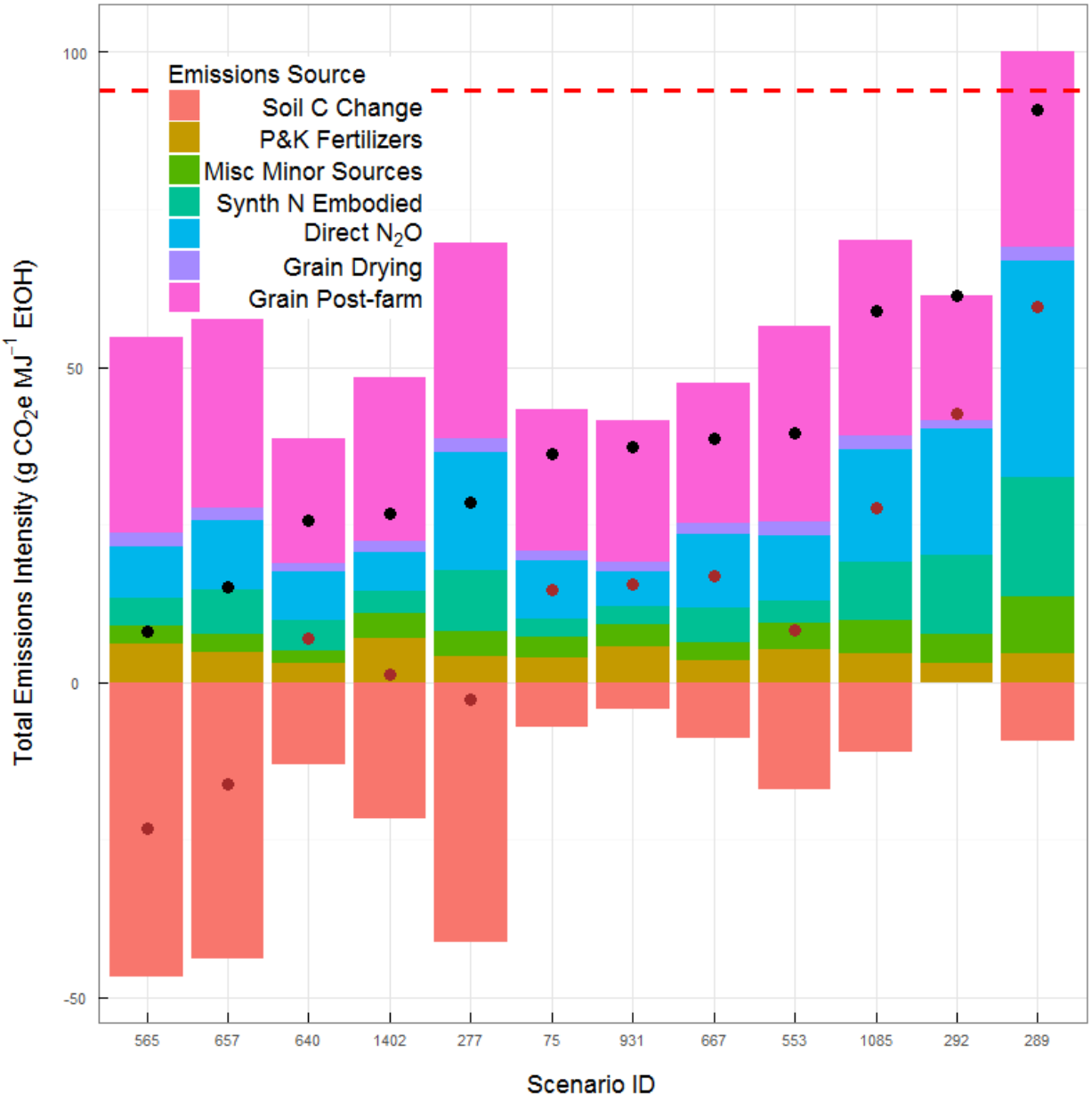

Figure 3.3. Full emissions budgets for the best- and worst-performing scenarios featured in Table 3.4 and Table 3.5 and six randomly-chosen scenarios. Since many budgets include negative emissions from soil C sequestration, FTW emissions intensities are given by black dots and FFG emissions intensities are given by brown dots. A dashed red line indicates the gasoline-equivalent emissions intensity. Note that several small emissions sources were consolidated into the "Misc. Minor Sources" category to aid in interpretation.

Biogenic emissions drivers

Figure 3.4 shows several important relationships driving the wide range of DayCent-simulated biogenic emissions. Panel A illustrates the dominant role of tillage intensity in determining the

rate of C sequestration for a given C input rate. Using the regression equations, we can make rough estimates of the "break-even" C input rates (x-intercepts) and sequestration rates (slopes) achieved by differing tillage intensities. The levels of C input required for SOC maintenance calculated from those models were 214, 180 and 130 g C m^{-2} for conventional, reduced and no-till respectively. The corresponding CO_2-equivalent sequestration rates for inputs above those levels would be 0.33, 0.45 and 0.72 g CO_2e m^{-2} g^{-1} additional C input for conventional, reduced and no-till respectively. These admittedly very rough estimates nonetheless underscore the overwhelming importance of C inputs and tillage intensity for explaining the range of FFG biogenic emissions budgets presented in this work.

Panels B and C of Figure 3.4 give closer looks at two management practices that largely determine – in conjunction with crop biomass productivity – the rates of C input to these soils. In Panel B, the y-axis shows the soil C change emissions for each scenario compared with a management-matched scenario with no stover removal. This is analogous to how the impact of stover removal on soil C would be determined in a field experimental setting: by comparing soil C change between otherwise identically-managed plots. The counter-intuitive result in Panel B is that stover removal from no-till fields constitutes a larger C loss relative to no removal, precisely because of the greater sequestration per unit of C input illustrated by Panel A. Thus, the slopes for the stover opportunity cost regressions (Panel B) are very similar in magnitude, but opposite in sign, to the sequestration rate regressions (Panel A).

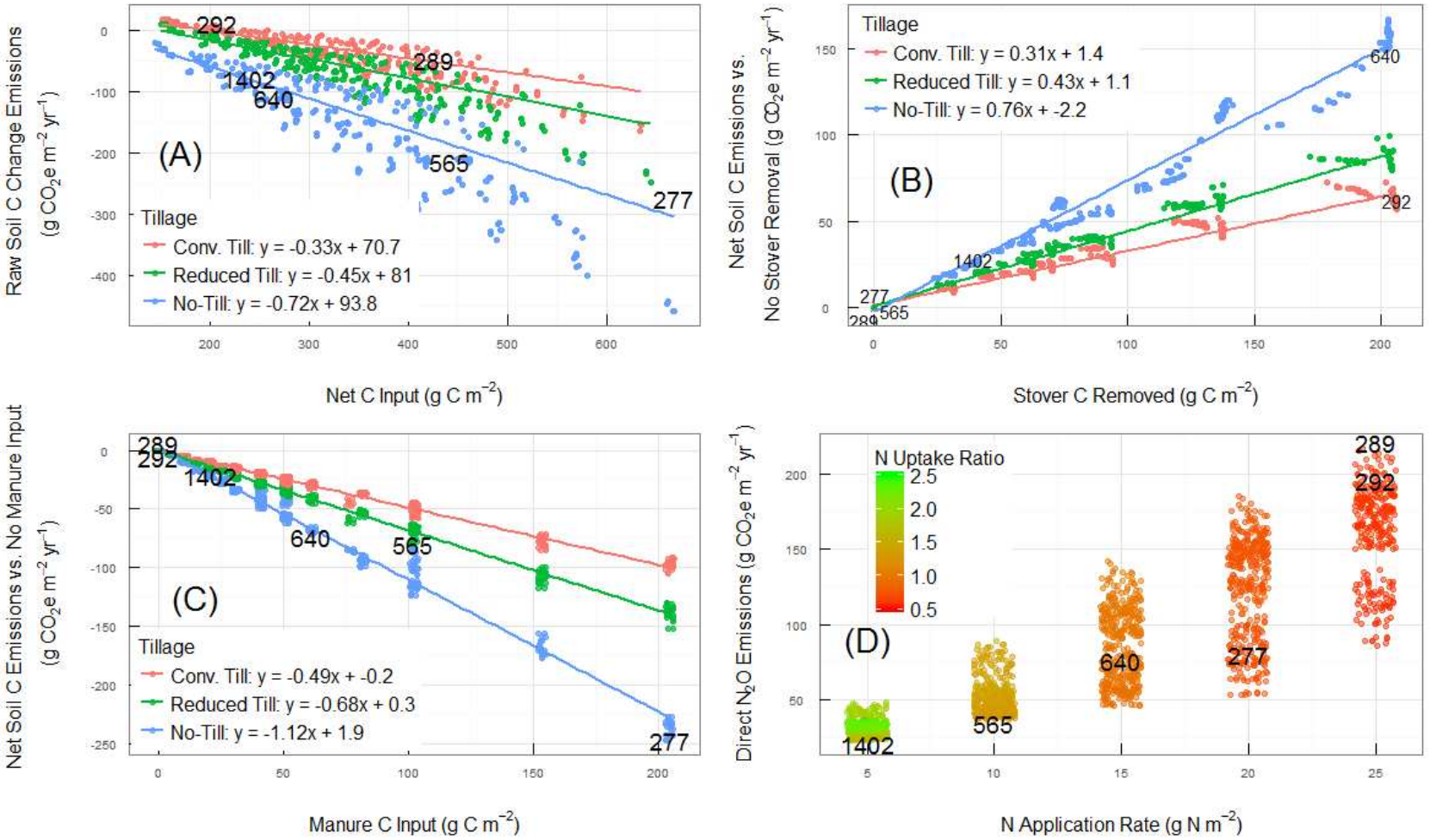

Figure 3.4. DayCent-simulated biogenic emissions as influenced by relevant management practices. Panel A shows the dominant role of tillage intensity and net C inputs in determining rates of soil C sequestration. Panel B shows the difference in C sequestration rate between simulations with stover removal and management-matched controls, and how this "opportunity cost" is actually higher under less-intensive tillage. Panel C shows the difference between simulations with manure additions and management-matched controls and the ability of no-till management to maximize the C sequestration benefits of manure inputs. Finally, panel D shows the increasing direct N_2O emissions that occur as N application rates increase and N uptake ratios decrease.

Panel C shows the DayCent-simulated emissions savings from manure-applied scenarios relative to management-matched no-manure scenarios. As with Panel B, each value was calculated by simple differencing of soil C change between corresponding scenario simulation results. The slopes give a rough approximation of the emissions dose-response to manure C input. By comparing the y-values of scenarios in Panels B and C we can get a sense for the levels of manure C input required to offset losses from stover removal. From the standpoint of an LCA, however, it should be noted that sequestration derived from manure C inputs does not necessarily represent a true emissions reduction. For this work, that fact was addressed by down-scaling the raw simulated soil C emissions credits shown in Figure 3.4C for application rates that would exceed the manure supply in the primary study area county (see Methods for details). This was based on the assumption that production scenarios should be credited for manure-derived sequestration only in proportion to the fraction of lands in the county that could actually receive manure at a given rate.

Finally, Figure 3.4D shows the direct N_2O emissions for each scenario as a function of its total N application rate (synthetic and manure N), with point color indicating the scenario's N uptake ratio. Direct N_2O emissions show an increasing trend with considerable spread as N application increases, while the N uptake ratio decreases as crop uptake saturates. Note that very high apparent N uptake ratios (>2) were achieved at low N application rates mostly by corn-soy scenarios. The N application rate and N uptake used in these calculations were taken from corn years only, so the N fixed and returned as residue by the soy crop was accounted as "free." In general, scenarios with N uptake ratios significantly above unity are likely not sustainable over long periods of time. Median direct N_2O emissions for a given N application rate were 15-40%

lower under corn-soy management as compared to any of the continuous corn scenario levels, except at the lowest N rate for which corn-soy emissions were slightly higher.

Dollar costs vs. emissions

The influences of major scenario management practices on costs and FTW emissions intensity are depicted in Figure 3.5. The relation of costs to stover removal (Panel A) is straightforward: as more stover is harvested, energy yield increases and thus costs per energy yield decrease. Additionally, stover collection costs themselves were modeled with economies of scale based on a cost curve presented by Graham *et al.* (2007), so unit costs decrease as collection rates increase. Panel B shows that the cost savings due to manure displacement of synthetic N are relatively small. In reality there may be significant savings related to improved soil quality impacts on crop production that may not be well-captured by the DayCent simulations. The costs associated with tillage intensity were relatively modest, as reflected by the lack of obvious vertical trends in Panel C. Conversely, the unambiguous emissions savings of no-till affirm tillage as a cost-effective measure for reducing emissions wherever agronomically appropriate. Total N application rate has a major role both in emissions and energy yield, and a more modest role in costs. The yield effect dominates in Figure 3.5D, with the highest cost-intensity scenarios all resulting from clearly suboptimal N application rates.

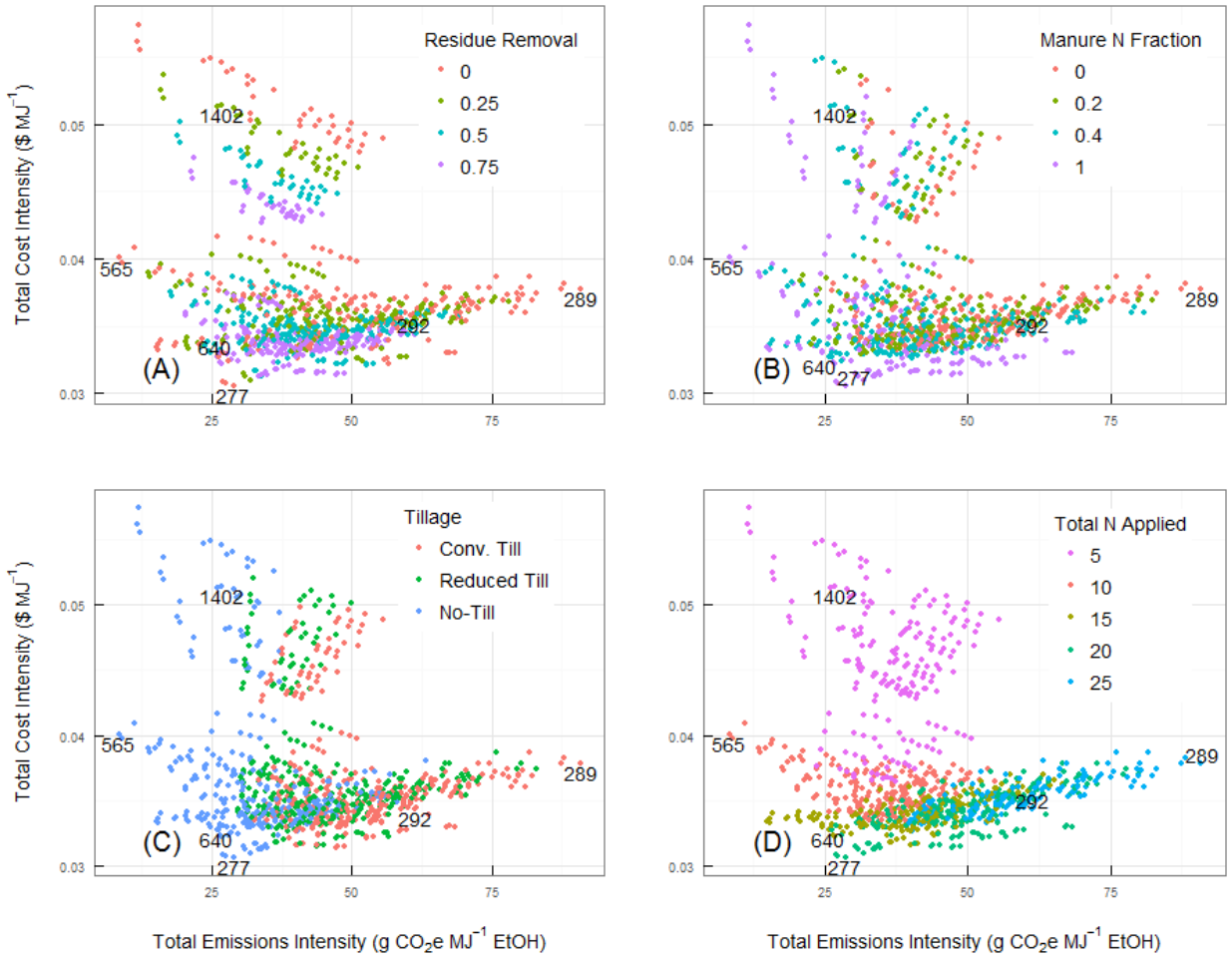

Figure 3.5. Total emissions intensity vs. cost intensity for each scenario, with color mapped to residue removal fraction (A), fraction of N from manure (B), tillage intensity (C), and total N application rate (D). Emissions and cost intensities were calculated from the total emissions/costs and combined EtOH energy yield (grain and stover) per unit area of cropland. Scenario ID numbers from selected scenarios are displayed in their approximate position to facilitate comparison with other figures and Table 3.4 and Table 3.5.

Carbon price impacts

We also calculated areal net profits for each scenario against a hypothetical EtOH price of \$2.50 gal^{-1} and several estimates for the social cost of carbon (SCC, underlying assumptions are detailed in Appendix). Figure 3.6 shows areal profits plus abatement premiums for each scenario under SCCs of \$0.00 (private profits only), \$12.37, \$43.20, and \$65.16 Mg^{-1} CO$_2$e for panels A-D, respectively. The non-zero SCCs given correspond to inflation-adjusted values given by

IAWG (2013) for discount rates of 5%, 3%, and 2.5% respectively. The increased profits shown on panels B-D may be thought of as "total profits," in the sense that they reflect the sum of private profits and dollar-valued social benefit (i.e., the abatement premium) derived from the EtOH yield produced under each scenario.

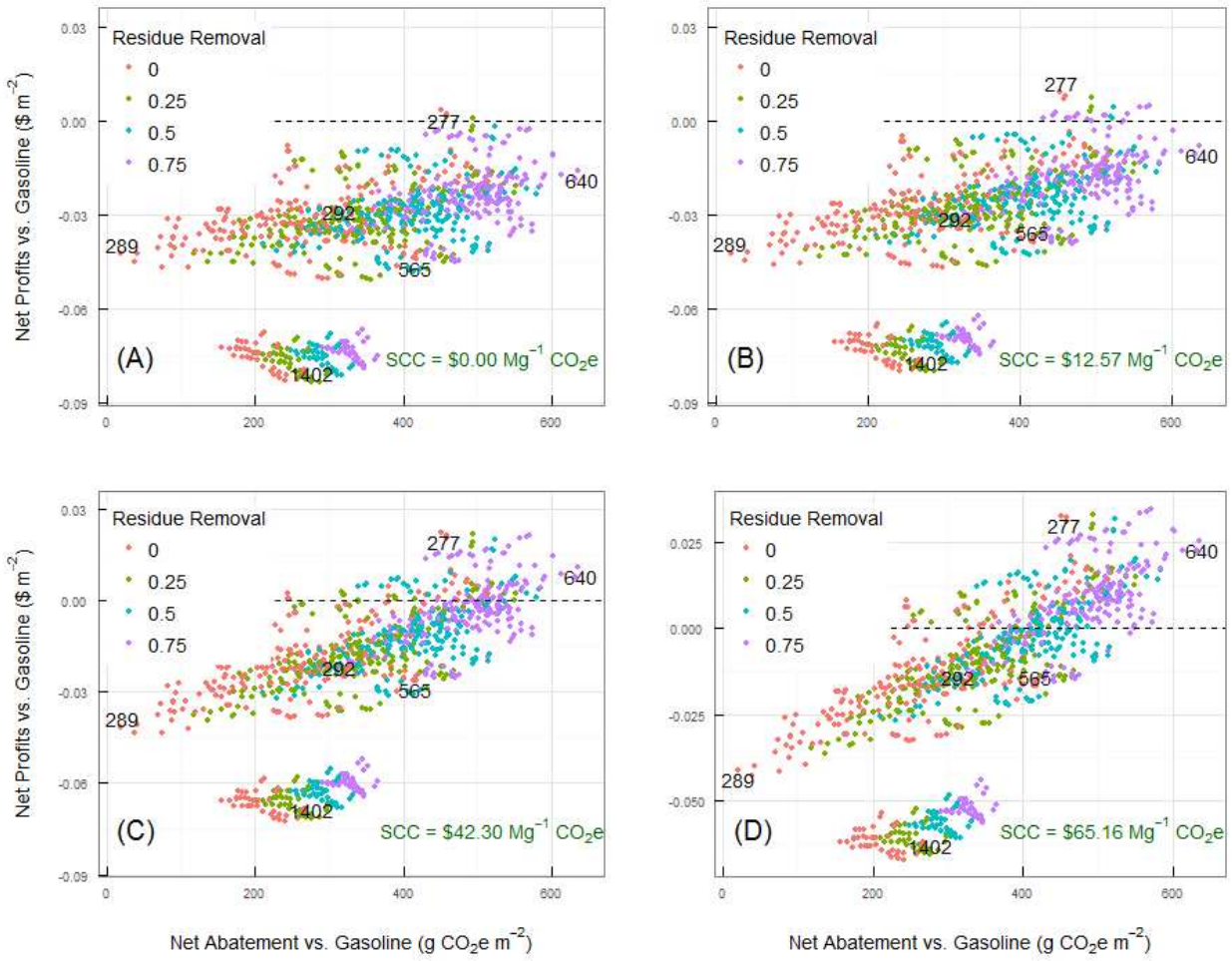

Figure 3.6. Profits vs. net emissions abatement for each scenario after accounting for EtOH cost savings against gasoline as a function of varying Social Cost of Carbon (SCC) estimates. The SCC estimates are inflation-adjusted values given by IAWG (2013) using discount rates of 5%, 3% and 2.5% for panels B, C, and D respectively. Scenario ID numbers from selected scenarios are displayed in their approximate position to facilitate comparison with other figures and Table 3.4 and Table 3.5.

In the case of a C tax or similar policy, the increased profits in panels B-D would be "internalized" and the abatement premium would represent a realized cost advantage between

each scenario and gasoline. Implicit in this accounting is that the market price for EtOH would increase the same amount as for gasoline (on an energy basis), so that the lower tax costs faced by EtOH would be a pure profit increase. In reality, the complex, economy-wide adjustments that would occur in response to a C price are well beyond the scope of this study. Thus, the profits shown in Figure 3.6 are intended to highlight qualitative trends in management profitability rather than make quantitative projections.

All panels in Figure 3.6 map color to the scenario residue removal rate to emphasize the disparate positive impact of increasing SCC on profitability for high levels of residue removal. Since the abatement premium is directly proportional to the net abatement achieved by a scenario, and high rates of stover removal tend to increase net abatement, these scenarios benefit most strongly from a high SCC. For example, the median net abatement rates were 249, 319, 397 and 471 g CO_2e m^{-2} for 0, 0.25, 0.5 and 0.75 removal rates, respectively. When these abatement rates were monetized using the highest SCC estimate of \$65.16 Mg^{-1} CO_2e, the resulting abatement premiums were 0.016, 0.021, 0.026, and 0.031 \$ m^{-2}, respectively. As can be seen by comparing Panels A and D in Figure 3.6, the slight profitability advantage of high residue removal scenarios with no SCC transforms to a substantial advantage with an SCC of \$65.16 Mg^{-1} CO_2e. Over that interval, the proportion of scenarios with residue removal rates of 0.75 being net profitable goes from 0% to 66%.

Discussion

Best practice scenarios

The results presented here support the contention that bioenergy life-cycle emissions are strongly influenced by farm management. The FTW emissions intensity of scenarios varied more than

10-fold, from a low of 8.0 to a high of 91 g CO_2e MJ^{-1} (see Table 3.4). At the same time, defining a single "best management" scenario is complicated by important tradeoffs. As shown by Figure 3.2 and Table 3.4, the lowest emissions intensity scenario (ID 565) used a low N application rate of 10 g N m^{-2}, resulting in grain yields in the 19th percentile of all scenarios. In contrast, the scenario that achieved the greatest net abatement vs. gasoline (ID 640) used 15 g N m^{-2} and removed 75% of corn residues, both of which served to increase EtOH energy yield. Perhaps the most practical drawback of scenarios such as ID 565 relates to the bottom line, however. As Figure 3.6 shows, scenario 565 is unprofitable even after accounting for the largest SCC estimate (panel D). By contrast, scenario 640 is moderately unprofitable without a C price (panel A) but at the two highest C prices is substantially profitable and among the best-performing scenarios.

Study design choices

Several important caveats pertain to the results presented here. The accounting method used to scale manure-derived emissions involved a number of simplifying assumptions. First, we assumed that feedlots would bear the burdens (costs and emissions) for transporting and applying manure to farm fields. While there are promising alternatives to direct land application, such as anaerobic digestion or composting, Ribaudo *et al.* (2003) indicate that direct land application remains the primary disposal method. We also assumed that farms would realize the benefits or costs from manure biogenic emissions following application. At the same time, we considered the "alternative fate" for manure application on a given farm to be land application to a nearby operation, resulting in equivalent emissions. This conceptual framework required a somewhat arbitrary boundary beyond which manure would not be transported. We chose the county within which most of the surveyed farms were located: Rock County, MN. Biogenic emissions from

manure were then scaled based on the fraction of Rock County cropping acres that would be manured at the scenario-specified rate to absorb the annual Rock County manure supply.

Most of these conceptual choices followed from our interest in summarizing the emissions associated with feedstock supplied to the Gevo, Inc. biorefinery. Scaling in this way reflects the aggregate impacts on those feedstock emissions that would occur if feedstock suppliers were a random sampling of Rock County producers. It underestimates the incentives that may be faced by individual farmers to accept manure application to their land if a C price were applied to agricultural C sequestration. It also fails to account for the marginal reduction in transport emissions achieved when a farmer accepts manure, against the alternative of the manure being transported to the next-most-distant farm. While such emissions are a part of the interlocking feedlot and cropping landscape, the competition among feedlots for croplands described by Ribaudo *et al.* (2003) indicates that feedlots presently bear these costs as a part of their business model.

The DayCent simulations used to model biogenic emissions and crop productivity did not explicitly replace N removed with stover. As a result, scenarios with stover removal generally suffered small productivity declines (around 5% of aboveground biomass) vs. management-matched no-removal simulations. Compared with studies that assume full N replacement, this has a few implications. First, the lower biomass yields reduce energy yield and thus increase emissions and cost intensity metrics. At the same time, removal scenarios were not charged for emissions and costs associated with replacing removed N. Also, since the management levels were simulated in a full factorial analysis up to a high N application level of 25 g N m^{-2}, removal scenarios with higher N input rates should be functionally equivalent to what would be achieved

with a lower specified input rate plus N replacement. For instance, the highest levels of N removal as residue were around 2.2 g N m^{-2}. Thus, as long as the equilibrium N input rate for a given scenario without removal was less than ~23 g N m^{-2}, the top N input rate scenario would be sufficient to replace residue N removals.

Crop rotation effects

The effects of continuous corn vs. corn-soy rotations were difficult to compare. With the sole exception of soil C change emissions, all emissions and costs for corn-soy rotations given here were from corn years only. Soy years were considered entirely separate to avoid complicated assumptions relating to the value of the soy crop in terms of emissions displacement and market value. While soybeans can be used as feedstock for biodiesel production, there was no indication that this was a significant pathway in the Luverne, MN supply area. Soil C change emissions were averaged across the 12-year period before removing soy year data points, so that corn years and soy years shared this component equally. This was done to avoid crediting corn with the very large, transitory increases in soil C that occur due to the much larger C input from corn residues vs. soy residues. A similar procedure was not used for soil N emissions, since it would have pushed significant fractions of the emissions from corn fertilization onto the more N-efficient soy crop.

Soil C dynamics

The soil C change dynamics were a major determinant of scenario performance in this work. Of the 1824 management scenarios considered, only 72 showed net soil C losses. All of those 72 included at least 0.5 residue removal and none employed no-till or derived 100% of N from manure. The only scenarios removing less than 75% of residues to lose soil C were fertilized at

the minimum rate of 5 g N m^{-2}. On the basis of the DayCent results, then, any reasonably productive management regime would be able to maintain or increase soil C stocks in these soils.

There are a variety of agronomic considerations that are not fully represented by DayCent, however. Wind and water erosion may be increased under residue removal. A sampling of work from sites around the U.S. Midwest summarized by Wilhelm *et al.* (2007) found that continuous corn sites under moldboard plow and conservation tillage required biomass cover of 3.11 and 0.65 Mg ha^{-1}, respectively, to control water erosion. Corresponding values for corn-soy cropping were 7.98 and 0.96 Mg ha^{-1}, respectively. All thresholds for wind erosion were lower than those for water erosion. No scenarios in this work were below the relevant thresholds for conservation tillage (even applying it to no-till scenarios), but 138 and 96 conventional-till scenarios fell short of the moldboard-plow thresholds for corn-soy and continuous corn rotations, respectively. While these constraints are not explicitly simulated by DayCent, the soil C advantages of no-till illustrated by Figure 3.4 strongly favor reductions in tillage intensity that, if adopted, would comfortably avoid problematic thresholds.

Changes in SOC for a given scenario would not continue indefinitely. Indeed, the net gains in SOC achievable in annual temperate cropping systems are typically the reversal of decades or even centuries of SOC decline caused by cultivation. Paustian *et al.* (1997) estimate that upland soils worldwide have lost approximately 43 billion Mg of SOC due to cultivation, and that roughly two-thirds of that amount could potentially be recovered through best management. Implicit in these estimates is the understanding that SOC stocks are the result of an equilibrium between C inputs (residues, exudates, organic amendments) and losses (harvest, decomposition, erosion). So in contrast to the "permanent" emissions reductions realized by displacing gasoline

or avoiding N_2O fluxes, the credits given for C sequestration are temporally limited and conditional on continued good management. Paustian *et al.* (1997) give a broad SOC stock estimate for undisturbed temperate grassland soils of 155 Mg C ha^{-1}. The median SOC stocks from all scenario simulations for this work was 63 Mg C ha^{-1}, implying historic losses on the order of 90 Mg C ha^{-1}. The median value for SOC change across scenarios was 0.18 Mg C ha^{-1} yr^{-1}. If we take the low-end estimate of Paustian *et al.* (1997) that one-half of historic losses (45 Mg C ha^{-1}) are recoverable through improved management, the median rate of C sequestration given would take more than 250 years to reach its "best management" plateau. At the highest simulated sequestration rate, 1.25 Mg C ha^{-1}, the plateau would be reached in about 36 years. Since this process is likely to be non-linear, the greatest gains from a given management change will occur in the first several years, with diminishing sequestration over decades to centuries.

Soil N dynamics

The crop productivity response to N generally leveled off at 15 g N m^{-2}, with small yield increases (~1-2%) between 15 and 20 g N m^{-2}. There was a notable exception among scenarios with high rates of manure N utilization and low tillage intensity. Among many such scenarios, the yield increase between N input rates of 15 and 20 g N m^{-2} was as high as 10-15%. Examining related DayCent outputs, these scenarios also showed relatively high levels of net N mineralization and low levels of mineral N stocks. This makes sense, since significant fractions of manure N are in organic forms unavailable to crops until mineralized, and low tillage intensity may lower mineralization rates and reduce the amount mineralized in time for crop uptake. Whatever the mechanism, these results suggest that use of no-till and manure N increase optimal N input rates closer to 20 g N m^{-2}, relative to more conventional management.

Direct N_2O fluxes simulated by DayCent, expressed as a percent of total applied N (emissions factor, EF) ranged from 0.54% to 1.9% with a median of 1.2%. These values generally agreed well with the IPCC Tier 1 estimate of 1% (de Klein *et al.*, 2006). In most contexts the lowest EFs were achieved at N application rates of 10 g N m^{-2}, although the combination of no-till and high manure N fractions yielded minimum EFs at higher N input rates. This may also be related to the gradual mineralization of manure N better matching mineral N supply with crop demand and reducing mineral N stocks available for N_2O production.

Cost budget considerations

The cost budgets presented here were built primarily with unit costs from Iowa State University extension farm budgets (Plastina, 2015). Many of these costs are highly variable in space and time, including some of the largest items such as land rent and capital costs. The literature estimates for the cost of feedstock conversion to EtOH are likewise subject to large changes attributable to technological progress and economies of scale. The effective market price for the final EtOH fuel is linked to the notoriously volatile market for transportation fuel and changing government subsidy policies. Finally, the SCC estimates used represent a consensus of three well-established Integrated Assessment Models (IAMs) but remain extremely sensitive to the choice of discount rate used for weighting future damages (IAWG, 2013). The cost and profit estimates given are therefore intended to qualitatively relate farm management with profitability, with an emphasis on *relative* trends within the management space.

Conclusions

Defining a clear best-practice management scenario for these farms is difficult, but this study makes clear several important trends. Perhaps the most consistently beneficial practice

considered was no-till management. No-till promoted soil C sequestration in virtually all scenarios, reduced embodied and fuel emissions, and has been shown elsewhere to reduce residue input requirements to control erosion (Wilhelm *et al.*, 2007). The potential complementarities between stover removal and manure inputs apparent in this modeling have been specifically corroborated by analogous field studies (Fronning *et al.*, 2008; Thelen *et al.*, 2010). In sum, these scenarios showed a large amount of swing potential, with plausible permutations of farm management driving FTW emissions intensities ranging from 10% to 100% those of gasoline (Figure 3.3). To realize this potential, future bioenergy feedstock classifications must consider not only crop species and end-product but also major farm management practices.

CHAPTER 4. CROP RESPONSE TO WARMING AND [CO_2]: WHAT DO WE KNOW AND HOW DO WE KNOW IT?

Agronomy, Scale and Climate Change

Projections of agricultural vulnerability to climate change rely heavily on process-based crop models (Parry *et al.*, 2004; Porter *et al.*, 2014; Elliott *et al.*, 2015). These models are calibrated to reproduce specific crop growth and yield formation processes in a dynamic way, making them capable of capturing impacts from conditions that exceed historical ranges. Two prominent features of climate change – elevated atmospheric [CO_2] (eCO_2) and extreme heat exposure – are of particular interest, as they are likely to have temporally-increasing, opposing impacts on yield in many locations. The responses of major crops to each of these factors have been well-studied in isolation and can be broadly reproduced by crop models. Their combined impacts, and interactions with other climatic and agronomic factors, are only beginning to be widely studied and tested in models. This paper summarizes current understanding of crop responses to eCO_2 and high temperatures and emphasizes areas of continuing uncertainty.

Agronomic studies of crop responses to environmental conditions span a range of spatial and temporal scales, from experiments with single plants over part of the growing season to global analyses of decades of yield data. Heat stress and [CO_2] have long been studied at relatively small scales (e.g., growth chamber and greenhouse environments) that facilitate a high degree of experimental control and mechanistic insight into the processes involved. Crop yield is strongly influenced by processes that are poorly represented at these scales, however, and so considerable effort has been devoted to developing systems for study of climate change factors in open fields (Hendrey *et al.*, 1993; Nijs & Kockelbergh, 1996; Kimball, 2005). However, even field

experiments may fail to account for yield variability arising from varying farm management, edaphic factors and low-frequency extreme weather events. Statistical analyses of historical yield and weather records encompass these factors and provide an important means of independently constraining effect estimates extrapolated from experimental results. Figure 4.1 depicts the relative strengths and weaknesses of field experiments and statistical analyses at a variety of spatial and temporal scales.

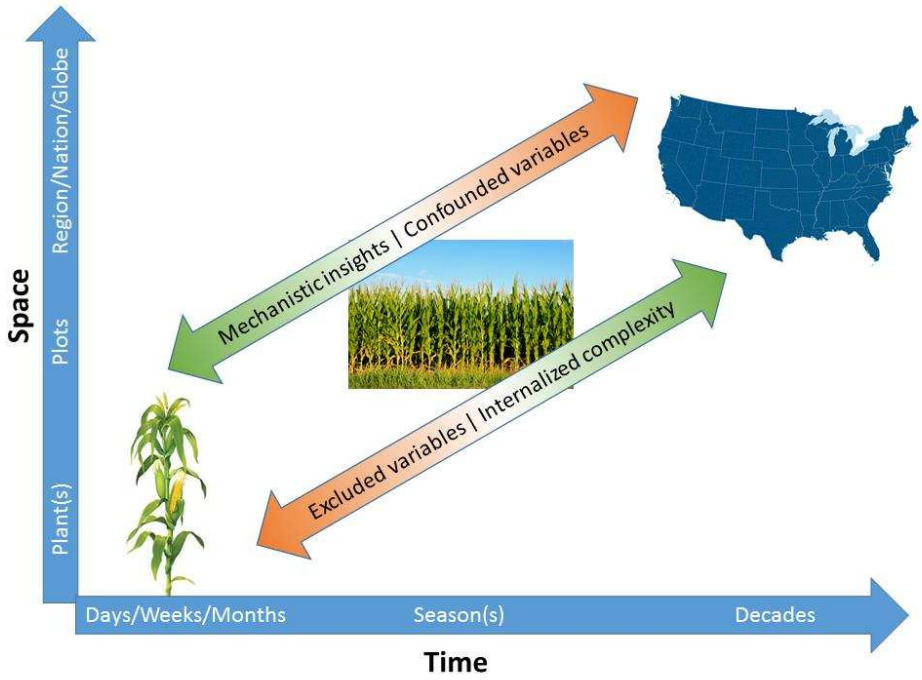

Figure 4.1. Complementary strengths (green, diagonal arrows) and weaknesses (red, diagonal arrows) of agronomic studies as a function of spatial and temporal scale. At the smallest scales, single plants are studied for a season or less under highly-controlled conditions, allowing for precise causal insights. Experiments with crops grown at plot-scale in open-air conditions are less controlled, but integrate important ecosystem processes. Finally, statistical analyses of large-scale yield and weather data incorporate the highest orders of complexity but are susceptible to spurious associations.

Crop models quantify and propagate agronomic understanding across scales. Hence, they are vital tools for integrated assessment modeling (IAM) exercises, which project crop yields under future climate change scenarios. Most of these models were formulated for specialized research

applications at a time before climate change impacts were commonly studied in open-field conditions and have been only sporadically updated to incorporate key findings (Rötter *et al.*, 2011).

The objectives of this paper are to survey the recent empirical literature on yield responses of three major crops (maize, soybean, wheat) to eCO_2 and elevated temperatures. In particular, it seeks to compare major findings from "bottom-up" experimental research with those derived from "top-down" statistical analyses of historic yield and climate data. The former are the foundation of the agronomic knowledge encapsulated in crop models, while the latter provide the only direct measures of yield response at the scales of interest to IAMs.

Field Experiments with [CO_2]

CO_2 enrichment methodologies

A number of experimental studies of the effects of eCO_2 on growth of agricultural crops were conducted in the 1960s and '70s, and were comprehensively reviewed by Kimball (1983). Most of these experiments were conducted in greenhouses and growth chambers and included 437 paired observations and 24 different species. After adjusting for the differing enrichment concentrations employed, Kimball (1983) found a yield enhancement of 33% for a doubling of [CO_2]. While he acknowledged the potential for differences in response between crops grown in growth chambers and those grown in open fields, he suggested for a variety of reasons that the greenhouse results included a "large conservative bias." Later reviews of the enclosure-based eCO_2 literature by Allen *et al.* (1987) and Cure & Acock (1986) found mean yield responses of 31% for soybean and 41% across 10 crop species, respectively.

The use of eCO_2 results from enclosure studies to make projections at field and larger scales is subject to various criticisms including the distorting effects of enclosures on temperature, light, wind, vapor pressure deficit, and pests and disease (Kimball *et al.*, 1997; Long *et al.*, 2006). The small scale of enclosure treatments also magnifies the influence of relatively small measurement errors and edge effects.

These concerns can be partially addressed through the use of fumigation within open-top chambers (OTCs), which allow plants to grow in open fields with unrestricted rooting and minimally-altered lighting (Rogers *et al.*, 1983). The cylindrical chamber barrier inevitably impedes airflow, alters vapor pressure deficit, and raises interior temperatures, however (Hendrey & Kimball, 1994).

In response to these and other limitations, free air CO_2 enrichment (FACE) systems were developed, with the first published results appearing in the early 1990s (Hendrey *et al.*, 1993). Thanks to their larger scale and lack of physical barriers, FACE systems better reproduce the aerodynamic coupling, light interception, rooting volumes, and exposure to biotic stressors experienced by field crops (Ainsworth & Long, 2005). Large FACE experiments have their own limitations compared with enclosure methods, however, including greater temporal fluctuations in $[CO_2]$, and practical constraints which limit the degree of $[CO_2]$ enrichment (Ziska & Bunce, 2007).

The results from FACE experiments align qualitatively with those from enclosure studies, although they debatably show responses of lower magnitude. Long *et al.* (2006) compared crop yield responses adjusted to 550 ppm from enclosure and FACE studies. They found an average

yield response of 13 and 0% for major C_3 and C_4 crops under FACE, respectively, vs. 31.5 and 18% under enclosure enrichment. Likewise, Long *et al.* (2005) found that model-based projections overestimated yield stimulation relative to FACE observations.

Tubiello *et al.* (2007) challenged the preceding interpretations in a way that illustrates several important considerations. They noted that many of the endpoints reported for FACE experiments are mechanistically linked (e.g., grain yield, aboveground biomass (AGB), photosynthesis), and so they should not be treated as independent observations in significance tests for a "true" difference in effect size between methods. When adjusting for this dependence, Tubiello found that the odds of the data presented by (Long *et al.*, 2006) occurring by chance in the absence of a "true" difference between methods were non-trivial ($P = 0.16$). Tubiello *et al.* (2007) also took issue with the procedure used to scale differences in reference and enriched [CO_2] between FACE and enclosure studies. Specifically, they found that by fitting a curve to disaggregated (rather than pooled, as used by Long *et al.*, 2006) enclosure observations the scaled enclosure results were considerably closer to FACE results. Other recent work has found statistical evidence of a publication bias in the primary FACE literature that may underlay a 20-40% exaggeration of crop responses to eCO_2 (Haworth *et al.*, 2016). These discrepancies underscore the sensitivity of inter-experiment comparisons to seemingly minor analytical choices, particularly in the relatively data-sparse and unsettled realm of FACE experiments.

An additional source of confusion stems from the fact that observations often considered together as "enclosure" results are in fact derived from several experimental paradigms. Ziska & Bunce (2007) sought to address this by analyzing non-FACE observations separately according to more specifically defined experimental approaches, including growth chambers, glasshouses,

soil-plant-atmosphere research (SPAR) units, temperature gradient tunnels (TGTs) and OTCs. After scaling results using a beta factor adjustment to reflect reference and enriched [CO_2] of 370 and 700 ppm, respectively, they found that results from all non-glasshouse enclosure types were not significantly different from FACE results for yields of rice, wheat or soybean.

Further difficulties in comparing results between FACE and enclosure studies include differences in ambient and enriched [CO_2] and the practice at some early FACE studies of fumigating only during daylight hours. The best way to avoid these complications would be to directly compare OTC with FACE plots in the same experiment. One such comparison studied cotton and wheat grown in OTC and FACE conditions in Maricopa, AZ. It found no significant difference between OTC and FACE for cotton in terms of the eCO_2 AGB response ratio (RR, quantity at eCO_2/quantity at aCO_2), but the absolute AGB was roughly 30% higher in the OTC versus the FACE plot. In contrast, the wheat crop showed similar absolute AGB and relative AGB response to eCO_2 across methods (Kimball *et al.*, 1997). The only other published side-by-side comparison between FACE and OTC grew wheat and soybean for two years using both enrichment methods. For soybean, the yield effect of eCO_2 was 49% under OTC versus only 27% under FACE. For wheat, the effect was 15-30% under OTC versus a non-significant effect under FACE. The reasons for the consistently higher eCO_2 effect under OTC were not clear, but may have resulted in part from the larger variability in [CO_2] within FACE plots (Bunce, 2016).

The following sections present major findings from FACE experiments with maize, soybean, and wheat. Since many of these findings have been well reviewed elsewhere (Leakey *et al.*, 2009; Vanuytrecht *et al.*, 2012; Bishop *et al.*, 2014; Kimball, 2016), the focus will be on concisely highlighting areas of consensus and uncertainty for each crop.

Maize

Theory predicts that photosynthesis of crops using the C_4 pathway should be insensitive to the direct effects of rising [CO_2], since rubisco activity in the bundle sheath cells is CO_2-saturated and rates of photorespiration are minimal (Leakey, 2009). Plant sensing of intercellular [CO_2] (c_i), however, has the potential to reduce stomatal conductance and thereby reduce soil water depletion and drought stress in response to eCO_2. This water-sparing effect has been observed using C_4 crops in both enclosure (reviewed in Leakey, 2009) and FACE (Ottman *et al.*, 2001; Leakey *et al.*, 2006; Manderscheid *et al.*, 2014) experiments. In most cases, FACE experiments showed substantial (30-40%) reductions in stomatal conductance for eCO_2-grown C_4 crops and smaller reductions in season-long evapotranspiration (ET; Conley *et al.*, 2001; Hussain *et al.*, 2013). As a result, C_4 crops (maize and sorghum) showed increases in photosynthesis, AGB, grain yield, and especially water-use efficiency (WUE) under eCO_2 when subjected to significant drought stress (Ottman *et al.*, 2001; Leakey *et al.*, 2006; Markelz *et al.*, 2011; Manderscheid *et al.*, 2014). Under well-watered conditions, stomatal conductance was still reduced but photosynthesis and grain yield were unaffected (Leakey *et al.*, 2009). Analysis of maize grain quality corroborated this trend, with drought stress quality impacts less severe for eCO_2-grown plants (Erbs *et al.*, 2015). The only FACE study to test the interaction between N supply and eCO_2 in maize found no significant N-by-[CO_2] interaction effect on yields (Markelz *et al.*, 2011). While FACE experiments with annual C_4 crops to date have convincingly demonstrated the impacts of eCO_2 on photosynthesis and water relations, impacts on other quantities such as belowground C allocation and whole plant N relations are unclear and should be investigated further under open-air conditions.

Soybean

As a C_3 crop, soybean yields would be expected to benefit directly from increased photosynthetic rates as well as indirectly from improved water relations. A substantial body of FACE research substantiates these theoretical predictions (Morgan *et al.*, 2005; Bernacchi *et al.*, 2007; Lam *et al.*, 2012a; Ruiz-Vera *et al.*, 2013; Bishop *et al.*, 2015; Bunce, 2016). A detailed analysis of soybean energy fluxes across four seasons found that ET was reduced on average by 12% in response to an eCO_2 of 550 ppm (Bernacchi *et al.*, 2007). ET reductions were somewhat smaller in percentage terms than reductions in g_s owing to a negative feedback, whereby reduced latent heat flux increased canopy temperature and relatively increased water loss. Soybean yield RRs based on 22 observation pairs and six publications at three FACE sites had an average of 1.14 and a standard deviation of 0.13 (Table 4.1).

Table 4.1. Average changes in yield, AGB and season evapotranspiration (ET) observed under FACE treatments relative to ambient controls.

Crop	Effect	% Change Under FACE	Standard Error	Paired FACE Observations	Sources
C4	Yield	4.1%	4.7%	9	(Conley *et al.*, 2001; Ottman *et al.*, 2001; Leakey *et al.*, 2006; Hussain *et al.*, 2013; Ruiz-Vera *et al.*, 2015)
	AGB	4.3%	2.3%	9	
	Season ET	-5.1%	2.4%	8	
Soybean	Yield	14%	4.4%	10	(Morgan *et al.*, 2005; Bernacchi *et al.*, 2007; Lam *et al.*, 2012a; Ruiz-Vera *et al.*, 2013)
	AGB	20%	3.1%	7	
	Season ET	-12%	1.8%	4	
Wheat	Yield	18%	2.5%	54	(Kimball *et al.*, 1995; Hunsaker *et al.*, 2000; Jamieson *et al.*, 2000; Weigel *et al.*, 2005; Norton *et al.*, 2008; Hoegy *et al.*, 2009; Lam *et al.*, 2012b, 2012c; Cai *et al.*, 2015; Nuttall *et al.*, 2015; Fitzgerald *et al.*, 2016; Houshmandfar *et al.*, 2016)
	AGB	21%	2.2%	38	
	Season ET	-1.3%	1.2%	8	

Recent research is beginning to shed light on the sources of variability in soybean response to eCO_2. Bishop et al. (2015) tested 18 soybean cultivars for two years, and a subset of nine cultivars for four years, at the soybean FACE facility in Champaign, IL. Across the full set of cultivars, RRs ranged from 1.00 to 1.20. Within the subset of cultivars grown for four years, yield RRs for a given cultivar were relatively consistent across years. This implies that some of the large variability in yield RRs across studies may be related to choice of cultivar. It also

provides the first evidence that within-species responsiveness to eCO_2 under FACE may be a heritable trait and thus subject to improvement through breeding. Analysis of cultivar physical traits showed that yield response to eCO_2 was negatively correlated with plant height ($R^2 = 0.66$) and positively correlated with the AGB response to eCO_2 ($R^2 = 0.69$; Bishop *et al.*, 2015).

Soybeans symbiotically fix N from the atmosphere, and so typically do not receive added N. Two studies of soybeans grown under FACE have reported N uptake and root nodule fixation responses to eCO_2. In the first (Lam *et al.*, 2012a), eCO_2 significantly increased aboveground N uptake of two cultivars, but had no effect on C:N ratio. Using isotope natural abundance, they found that N fixation by cultivar Zhonghuang 13 increased significantly under eCO_2, whereas fixation by cultivar Zhonghuang 35 was unchanged. Results from a second (Hao *et al.*, 2016) study with cultivar Zhonghuang 35 were largely the same, with total N uptake increasing sufficiently to maintain C:N ratios. That study also measured levels of ureides in expanding leaves, which are indicators of nodule N fixation. Since ureide concentrations were unchanged under eCO_2, the authors inferred that the additional N uptake required to maintain C:N ratios in these plants likely came from soil N stocks (Hao *et al.*, 2016). Thus, at least for certain cultivars, growth under higher future [CO_2] may increase soybean reliance on soil sources of N.

Wheat

A large number of FACE experiments have examined the response of wheat yield to eCO_2 (Kimball *et al.*, 1995; Jamieson *et al.*, 2000; Högy *et al.*, 2009; Lam *et al.*, 2012c; Weigel & Manderscheid, 2012; Cai *et al.*, 2015; Fitzgerald *et al.*, 2016; Houshmandfar *et al.*, 2016). Across these studies, the average yield RR was 1.18 based on 54 observational pairs (Table 4.1).

While most RRs from FACE studies fall under about 1.3, several observations from the Australian Grains FACE (AgFACE) facility suggest that relative yield responses can be much higher under certain circumstances (Fitzgerald *et al.*, 2016). That work imposed heat stress using a late sowing date, and also used two cultivars and irrigation levels. Of the 28 RRs comparing treatment-matched yields under eCO_2 to those under aCO_2, ten were at least 1.40 and four of these reached at least 1.70. These high-responding groups included both cultivars, normal and late times of sowing, and high- and low-irrigated plots, defying any obvious explanations. The absolute levels of water input at these sites were notably lower than those at other FACE study sites, however, leaving open the possibility for complex effects of eCO_2 under circumstances of more extreme drought stress. Further study of wheat response to eCO_2 under relatively severe stress regimes is needed to clarify these observations.

Fewer data are available regarding wheat water relations under eCO_2. Four years of irrigated wheat grown under FACE in Maricopa, AZ generally found reductions in season ET around 5%, but with substantial measurement uncertainties (Kimball *et al.*, 1999; Hunsaker *et al.*, 2000). Effects on g_s were greater, with reported reductions of 32% in Arizona (Wall *et al.*, 2000) and 18% for dryland wheat in Australia (Houshmandfar *et al.*, 2016).

Several authors have noted reductions in grain N concentrations for wheat grown under eCO_2 (Kimball *et al.*, 2001; Högy *et al.*, 2009; Myers *et al.*, 2014). Plausible explanations for this phenomenon include (1) simple dilution due to greater C productivity (Poorter *et al.*, 1997), (2) reductions in mass flow uptake from soil due to reduced transpiration (McGrath & Lobell, 2013), (3) reduced demand due to greater photosynthetic N use efficiency (PNUE; Leakey *et al.*, 2009), and (4) inhibition of plant nitrate assimilation due to reductions in photorespiration (Bloom *et al.*,

2014). While none of these explanations are mutually exclusive, a growing body of evidence from controlled experiments (Rachmilevitch *et al.*, 2004; Bloom *et al.*, 2010; Asensio *et al.*, 2015) and follow-up analyses of FACE observations (Cheng *et al.*, 2012; Bloom *et al.*, 2014; Myers *et al.*, 2014; Feng *et al.*, 2015) suggest that eCO_2 significantly impairs nitrate assimilation by C_3 crops (Figure 4.2). This phenomenon has been demonstrated repeatedly in enclosure studies of *Arabidopsis* and wheat, but has also been replicated in a range of other C_3 plants and contrasted with its absence in multiple C_4 and CAM plants (Bloom *et al.*, 2012). The experimental evidence for this inhibition includes increased accumulation of free nitrate in leaves, increased rates of CO_2 consumption relative to O_2 evolution (termed assimilatory quotient, AQ), and reduced growth rates of C_3 plants grown under NO_3^- nutrition with either eCO_2 or reduced O_2 atmospheres. These effects can be reversed by returning plants to NH_4^+ nutrition or ambient atmospheric conditions (Rachmilevitch *et al.*, 2004; Bloom *et al.*, 2010). The mechanistic dependence of shoot nitrate reduction on photorespiration is unclear, but may involve photorespiration's role in stimulating malate export from chloroplasts to cytoplasm, where it generates the NADH needed for the initial reduction of NO_3^- to NO_2^- (Bloom, 2015a).

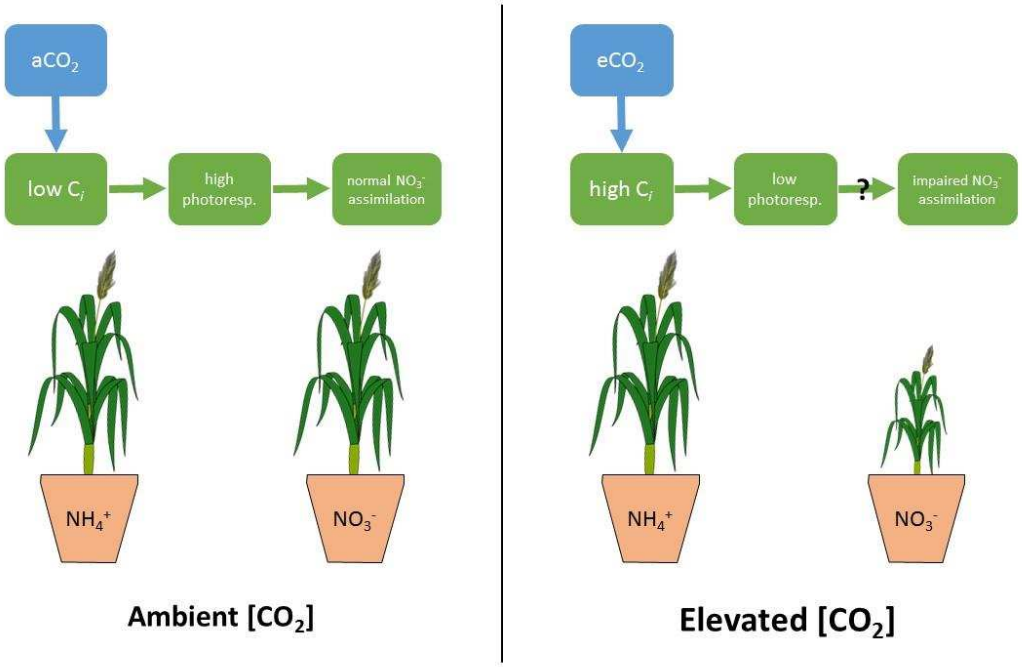

Figure 4.2. Schematic representation of the connections between atmospheric [CO_2], photorespiration, and nitrate assimilation in C_3 plants as postulated by (Bloom *et al.*, 2012). Elevated [CO_2] is known to reduce photorespiration in C_3 plants, and a body of experimental results (discussed in text) suggest that this impairs foliar NO_3^- reduction capacity, though the precise mechanism is poorly understood. C_i: leaf intercellular [CO_2].

Recent syntheses support the importance of this phenomenon for growth of C_3 crops under field conditions. Feng *et al.* (2015) examined the relationship between aboveground net primary productivity (ANPP) and AGB N concentration for FACE experiments with annual crops, grasslands, and forest ecosystems. They found that eCO_2 increased N uptake in absolute terms, but that many observations and the linear trend indicated a ~10% reduction in N uptake *for plants showing little to no ANPP response.* This negative intercept was significant for each ecosystem type analyzed separately, but was notably absent from experiments involving C_3 legumes and C_4 plants. These findings conflict with the hypothesis that reduced plant N under eCO_2 is primarily due to simple C dilution. Cheng *et al.* (2012) performed a meta-analysis of studies reporting plant N utilization and found that eCO_2 reduced plant nitrate use and increased reliance on ammonium. They also found in microcosm and field experiments that a C_3 grass

under eCO_2 increased C allocation to arbuscular mycorrhizal fungi (AMF) when grown in soil with normal nitrate levels, but not when grown in soil supplemented with a nitrification inhibitor to maintain stocks of reduced N (Cheng *et al.*, 2012). Finally, Bloom *et al.* (2014) tested wheat samples from the 1996 and 1997 growing seasons at the FACE facility in Maricopa, AZ and found that eCO_2-grown plants had higher proportions of total N as free nitrate and isotopic ^{15}N signatures consistent with reduced shoot nitrate assimilation.

As noted by two recent reviews (Bloom, 2015b; Walker *et al.*, 2016), photorespiration is a costly process, reducing CO_2 fixation by C_3 plants by 20-35%. The above findings provide a compelling case that its inhibition, whether by eCO_2 or through deliberate breeding or biotechnological manipulations, may have unexpected side effects on plant N relations. In real-world growing conditions, plants rely on a combination of nitrate and reduced N forms, and so prospective FACE experiments are urgently needed to elucidate the relevance of this phenomenon for crops under varying N availability regimes.

Statistical Measures of $[CO_2]$ Effect

It would be valuable to constrain experiment-derived projections with empirical estimates of CO_2 response from historic farm yield data. An initial effort to disentangle yield response to $[CO_2]$ from other time trends examined yield data for the top 20 national producers of wheat, rice and maize for the period 1958-2002 (Lobell & Field, 2008). Mean results from that analysis aligned with experimental estimates, but included wide confidence intervals due to the relatively small role of yearly $[CO_2]$ increment in inter-annual yield variability. A follow-up study used a different approach to estimate CO_2 fertilization effects for maize and soybean each under well-watered and water-stressed conditions (McGrath & Lobell, 2011). They estimated that the ~73

ppm increase in [CO_2] from 1960 to 2009 increased yields under water stress by 9% and 14% for maize and soybean, respectively, though estimates for individual states varied widely. Thus, attempts at independently corroborating eCO_2 experimental results using historic yield trends have had some success and, if refinements in methodology and data quality could further reduce background noise, this approach would provide much-needed quantification of yield responses integrated across large scales and varied stress regimes.

Field Experiments with Crop Warming

Compared with eCO_2, the effects of extreme heat exposure on crop yield are both more familiar and more variable on short timescales. Heat waves have afflicted crops throughout agricultural history, with impacts ranging from merely transitory growth reduction to outright failure. The disparity in outcomes is related to several factors, including the severity, duration, and phenological timing of heat stress events and interactions with other stressors, particularly water stress (Lobell & Gourdji, 2012). Controlled experiments offer mechanistic insights into these phenomena and can illustrate causal linkages. The extrapolation of experimental heat stress impacts to large spatial and temporal scales, however, involves large uncertainties related to how stress impacts interact and how heat exposures themselves will vary. Statistical analyses of historical yield data provide an independent approach to impact prediction that is complementary to experimental studies in many ways. The following sections explore heat stress impacts on crop yield as understood from these "bottom-up" and "top-down" perspectives.

Warming methodologies

Experimental studies of heat stress have overwhelmingly relied on enclosures for imposition of temperature treatments. In response to a set of concerns with enclosures similar to those that

prompted the development of FACE technology, including distorted micrometeorology, limited rooting volume, and edge effects, a growing number of experiments are using infrared heaters to raise canopy temperatures in open-air field environments in an analogous technique termed free-air temperature increase (FATI; Nijs & Kockelbergh, 1996) or, alternatively, temperature free-air controlled enhancement (T-FACE; Kimball, 2005).

Several micrometeorological details are important to the design and interpretation of open-air heating experiments. As described by Kimball (2011), the technique of heating crop canopies to a constant level of temperature rise using infrared heaters increases temperatures of the canopy itself and the soil surface by roughly the amounts expected under climate change physics. It does less to increase air temperatures above and within the canopy. Increased foliage temperatures without a concomitant increase in water vapor pressure of surrounding air reduces relative humidity faced by IR-warmed plants, whereas most climate change projections indicate roughly unchanged relative humidity (Amthor *et al.*, 2010). While this difference can be mitigated somewhat in irrigated crop systems by supplying additional water to the heated plots (Kimball, 2005), the associated increase in soil water depletion may be a significant confounding factor for experiments in rainfed systems.

It is also important to note that some experiments have used infrared heaters set to a constant heat flux rather than thermostatically controlled to achieve a constant temperature rise. Calculations by Kimball (2005) indicate that such a design will typically achieve much larger temperature increases at night than during daylight hours. Constant flux designs may thus be adequate for circumstances in which reduced diurnal temperature range (DTR) is anticipated, but recent analyses find little support for reduced DTR in most regions (Amthor *et al.*, 2010).

IR-driven constant temperature increases closely represent expected increases in mean growing season temperatures. However, if the inherent variability in temperature changes under climate change, then heat stress exposure may be under- or over-estimated by experiments for any given mean temperature increase. For instance, Orlowsky & Seneviratne (2012) analyzed global circulation model projections produced for the IPCC fourth assessment report. They found that in some regions and seasons, including Southern Europe, the Mediterranean, and the Central US, daily maximum temperatures (T_{max}) at the 90th percentile increased at twice the rate of those at the median (50th percentile). Likewise, Teng *et al.* (2016) found that Great Plains summer daily temperature anomalies would have an increase in standard deviation of roughly 20% by end of century compared with recent historical variability. This increase in extremes would cause significantly greater heat stress than that produced by constant temperature increase treatments against current weather conditions. Increases in critical temperature exposure under hypothetical uniform warming vs. increased variability are illustrated in Figure 4.3 using historical data from Urbana, IL. As can be seen from the expected exceedances given in each panel, changes in the distributional mean and standard deviation increase critical temperature exposures in a non-linear fashion, with variability playing a smaller but non-negligible role.

While extreme levels of temperature increase may be achievable using fully open-air IR heating (Kimball, 2011 suggests up to 10°C), in practice these conditions are produced using permanent enclosures or open-air plots with temporary enclosures in place during heat treatments only. Thus, heat stress experiments to-date have produced *either* the uniform increase in growing temperatures *or* the isolated episodes of extreme heat expected under climate change, but not both together. Attempts should be made to experimentally combine these distinct phenomena to determine whether their combined effects are more or less than simply additive.

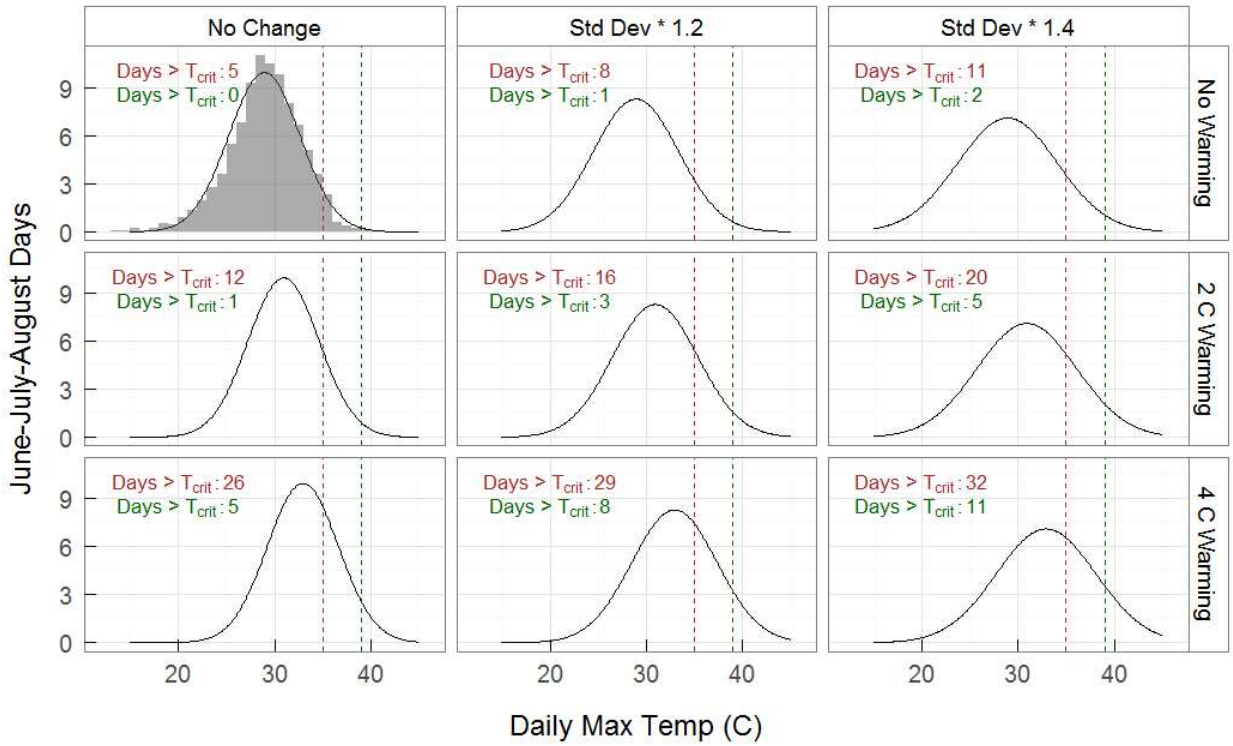

Figure 4.3. Summer daily maximum temperatures for Urbana, IL, averaged over the period 1990-2014 (top-left, bars), compared with a normal curve model of observed (top-left, line) and changing heat exposures under simple climate change scenarios. Intra-seasonal variability increases left-to-right across panels, while uniform warming is depicted top-to-bottom. Critical temperatures for corn (35°C; red) and soybean (39°C; green) are marked with vertical dashed lines, and expected summer days exceeding each threshold are given in the same color text.

Maize

Temperature thresholds at which heat stress begins vary depending on crop species, cultivar, growth phase, and other interacting stressors. Nevertheless, so-called cardinal temperatures have been identified for major species that show reasonable agreement across experiments where temperature is the only significant stressor. Hatfield *et al.* (2011) reviewed the agronomic literature and found that maize had optimal yield formation in the range 18-25°C, and experienced reproductive failure when subjected to temperatures in excess of 35°C. In a similar analysis, Sánchez *et al.* (2014) estimated optimal temperatures of 28, 31, and 26°C for vegetative growth, anthesis, and grain filling phases, respectively. They found corresponding maximum

temperatures (at which growth and/or yield formation effectively halt) of 39, 37, and 36 C, respectively.

Those cardinal temperatures were empirically determined by observing the response of yield and other long-term crop outcomes to temperature. A distinct approach was taken by Parent & Tardieu (2012), who performed a meta-analysis of measurements of underlying crop process rates and their responses to temperature. For eight diverse lines of maize, they found a consistent synchronization of normalized rates of growth processes including leaf elongation, cell division, shoot elongation, and leaf appearance rate for a range of temperatures. Rates of each process peaked at 30.8°C with little variation across maize lines and declined to reach half of their peak rates at 20.8 and 38.2°C. The lack of genetic differences in growth process responses to temperature between lines from temperate and tropical regions suggests that breeding for yield under hotter growing seasons will have to rely on other, more genetically-variable traits including plant maturity length, tolerance to extreme high temperatures, and water use efficiency.

Experimental work with maize delineates its vulnerabilities to late-season heat. Hatfield (2016) grew three hybrid maize cultivars in chambers maintained at ambient outdoor (Ames, IA, USA) temperature or ambient +4°C. Two of the three cultivars achieved greater vegetative AGB under the +4°C temperature regime, but grain yields were severely reduced, and two cultivar-years suffered complete yield failure. The author indicated that was caused by the effect of increased nighttime temperatures on leaf senescence rates and overall length of the grain-filling period. This work underscores the critical importance of understanding sensitivities of maize reproductive processes to extreme, but not implausible future temperature regimes.

Rattalino Edreira & Otegui (2012) studied the role of heat stress at three different reproductive growth phases in temperate and tropical maize cultivars. Maize was grown for two years in open-field conditions, with field-chamber heating treatments (33-40°C daytime temperature) applied for the 15 days preceding anthesis, 15 days starting at onset of silking, or the first 15 days of active grain filling. They found severe growth reductions during heating under all treatments, but only modest to moderate reductions in total AGB. The two earliest heating treatments reduced yield primarily through reductions in kernel set, leading to sink limitation. The latest treatment reduced yield – particularly in the temperate genotype – by reducing the length of grain-filling and radiation-use efficiency during grain-fill (Rattalino Edreira *et al.*, 2011; Rattalino Edreira & Otegui, 2012).

The interacting impacts of heating (2.7°C above ambient) and eCO_2 on maize grown under open-air conditions has only been reported once. As expected, there were no significant effects of eCO_2 on photosynthesis or yield when compared with aCO_2 plots subjected to the same temperature (i.e., ambient temperature or heated). Heating was found to reduce photosynthesis during the hotter, second half of the growing season, leading to reductions in grain yield but not total AGB (Ruiz-Vera *et al.*, 2015). This corroborates the findings of Hatfield (2016) and Rattalino Edreira & Otegui (2012) that heating seems to be primarily damaging to reproductive processes in maize.

Soybean

Hatfield *et al.* (2011) report soybean optimal temperature ranges of 25-37°C and 22-24°C for vegetative and reproductive growth, with yield failure at 39°C. Relatively few studies have examined soybean heat response under open-air conditions. Ruiz-Vera *et al.* (2013b) grew

soybeans for two seasons under factorial combinations of open-air heating (2.7°C above ambient) and eCO_2. Heating reduced photosynthesis relative to [CO_2]-matched plots in both seasons, with the reduction being significantly more pronounced in 2011 (ambient T_{avg}: 18.2°C) than in 2009 (ambient T_{avg}: 16.7°C). Seed yield showed a similar response, with no significant average change under heating in 2009 and a 33% reduction under heating in 2011. Interestingly, the heating and eCO_2 treatment had modestly lower yield than the heating-only treatment in 2011, possibly reflecting the effects of reduced stomatal conductance and a consequent 1°C increase in mid-day canopy temperatures in the eCO_2 plots (Ruiz-Vera *et al.*, 2013).

Another open-air experiment at the SoyFACE facility exposed soybeans to 3-day heat waves (6°C above ambient) at various reproductive phases during two seasons (Siebers *et al.*, 2015). All heat waves produced transient oxidative damage and reductions in photosynthesis and g_s, but yield reductions were only significant under heat waves timed during early pod development.

Wheat

Wheat has lower optimal temperature ranges than corn or soybean, estimated at 20-30°C for vegetative and 15°C for reproductive growth (Farooq *et al.*, 2011; Hatfield *et al.*, 2011). Its response to current and future temperature regimes is additionally complicated by the fact that winter varieties are at risk of damage from extreme low temperatures, which may be alleviated by the same trends that aggravate late-season heat stresses (Barlow *et al.*, 2015). A substantial number of open-air warming experiments have begun to delineate wheat response to heat stresses of varying timing, duration, and severity under field conditions.

When constant heating treatments are imposed on a background of optimal or above-optimal ambient temperature, yield losses result. Cai *et al.*(2015) grew wheat plants under FACE and infrared canopy temperature elevation (2°C above ambient, using infrared heaters) in Jiangsu, China. The effect of heat on yield was negative in all cases, with losses ranging from 17-21%.

Temperature elevation treatments also accelerate wheat phenological development, which may actually reduce exposure to damaging temperatures. Tian *et al.* (2012) grew wheat under open-air heating arrays for five seasons in Nanjing, China. Heating shortened the time to anthesis by an average of 10 days and increased yield by 16.3%. This gain was attributed to a combination of more favorable early spring temperatures for vegetative growth and reduced exposure to heat and drought stress due to the earlier timing of the reproductive phase.

As mentioned previously, infrared heating of canopies will inevitably also raise VPD and plant water stress under conditions of water scarcity. Fang *et al.* (2013) grew wheat in open-field conditions and applied several treatments, including infrared heating, heating and delayed sowing, or heating and increased irrigation. Yield was reduced relative to control by both heating only (9.0%) and delayed sowing with heating (21.2%), but was not significantly different when heating was accompanied by 20% increased irrigation.

Perhaps the most comprehensive implementation of constant temperature elevation combined uniform heating with 12 staggered sowing dates in Arizona, USA (Ottman et al., 2012). They found that grain yield decreased by 7.1% per 1°C above the post-anthesis average temperature of 21.9°C. The effect of infrared heating varied widely depending on planting date, however, with

no effect on yield of winter plantings, positive effect on yield of late fall plantings, and negative effect on yield of late spring plantings.

Constant temperature increase experiments provide vital information on crop responses to mean warming, but do not simulate the increasing incidence (due to larger variation around the mean) of extreme heat expected in some regions. Several open-air experiments have been conducted to isolate the effects of such extremes.

Liu et al. (2016) grew potted wheat plants in an open-air field except for specific time intervals of imposed heat stress within a phytotron. Treatments included most combinations of two cultivars, four growing seasons, two stress timings (anthesis and 10 days after anthesis), two stress durations (three or six days) and four stress levels (T_{min}/T_{max} of 17/27, 21/31, 25/35, 29/39°C). They found that every thermal unit above 30°C reduced yields by 1.5% when applied at anthesis and 1.15% when applied at grain filling.

Nuttall et al. (2015) grew two wheat cultivars under FACE conditions and used a mobile chamber to impose three-day heat stress (38°C daytime) either three days prior to anthesis or 15 days after anthesis. Heat applied before anthesis reduced yield by 0.22% per degree-hour above 32°C for cv. Scout, but had no impact on yield of cv. Yitpi. Stress applied after anthesis had no significant effect on yield in either cultivar.

Talukder et al. (2014) grew several cultivars over two years in field conditions and used a mobile chamber to impose a single 3-h heat stress (35°C) near flowering or during early grain set. Yield reductions across years, cultivars and stress timings ranged from 8% to 35%, with cv. Janz

showing the greatest yield losses. Stress-induced losses were significantly greater in 2009 (24%) vs. 2010 (12%), possibly due to the hotter and drier baseline conditions in 2009 causing increased canopy temperatures and damage to pollen and ovaries. Averaged across all cultivars, heat stress reduced post-heading duration by 11 days in 2009 and eight days in 2010, and post-heading duration was a strong predictor of grain yield.

Statistical Measures of Crop Warming Effect

The complex patterns of heat stress faced by field crops across large spatial and temporal scales cannot be fully represented within an experimental context. Fortunately, unlike [CO_2], the inherent variability of heat events – particularly across space (Lobell & Burke, 2010) – provides a relatively strong signal for quantification by empirical analyses of historical weather and yield data. These studies give an independent, and in many ways complementary, perspective on the role of heat in crop yield.

Maize

The role of high temperatures as a major driver of historic corn yield variability was highlighted by a 2009 study that used an unusual weather dataset to detect pronounced, nonlinear yield declines with exposure to high temperatures (Schlenker & Roberts, 2009). That work predicted yield in part based on cumulative season exposures to each 1°C temperature interval, and found that corn yields declined steeply with increasing exposure to temperatures above 29°C. A subsequent re-analysis, using an updated dataset, added VPD as a predictor and found it to be roughly as strong a negative predictor as the extreme temperature metric (Roberts *et al.*, 2012). Associated work using a dynamic crop model corroborated the importance of high-VPD

exposure as a driver of corn yield loss. Results suggested that a 2°C warming was roughly twice as damaging to yield as a 20% reduction in precipitation (Lobell *et al.*, 2013).

Other authors have noted strong yield impacts of coincident water scarcity and high temperatures. Anderson *et al.* (2015) used a process-based crop model (EPIC) to simulate historic soil water content for rainfed maize in the US Midwest from 1980-2012 and used estimated soil water as a predictor for their statistical model. Their analysis found that water status played a major role in determining heat stress impacts, with a 1°C temperature increase causing 6-10% yield losses under high water availability but 27-32.5% under low water availability. This work in the temperate, high-yielding US Midwest aligns with a similar analysis using data from maize yield trials in sub-Saharan Africa, which estimated each degree-day above 30°C caused 1% and 1.7% yield losses under well-watered and drought conditions, respectively (Lobell *et al.*, 2011).

The causal relationships between extreme heat, soil water depletion, and resulting yield loss in these types of studies are unclear. As noted by Basso & Ritchie (2014), hot days tend to co-occur with drought conditions due in part to a lack of evaporative cooling (Mueller & Seneviratne, 2012). Thus, measures of extreme degree-days may actually be signals for time spent under water scarcity, and season rainfall omits important drivers of soil water (runoff, drainage, early-season stored water) and so may obscure the primacy of water status for yields.

This problem was addressed by Urban *et al.* (2015), who included daily T_{max} as well as precipitation ("supply") and VPD ("demand") during a 30-day period representing reproductive growth in models of 1995-2012 maize yield in Iowa and Illinois. The interaction between supply

and demand was a significant, robust predictor of yields, with the effect of VPD becoming more pronounced in low-precipitation seasons.

Most empirical studies have either ignored crop growth phase or used relatively coarse approximations such as 30-day periods. Butler & Huybers (2015) included county-level USDA data on maize development along with various weather variables and found yield sensitivity to killing degree-days (KDD, degree-days above 29°C) was four times greater during early grain filling than during vegetative growth. While this difference is well-established from experimental work, its magnitude indicates that omission of growth phase information from statistical models may substantially reduce their explanatory value.

Existing adaptation of maize cultivars and management further complicates attempts to derive fixed heat-yield relationships. Butler & Huybers (2013) found that the sensitivity of US maize to KDD was much higher in low-KDD northern regions versus high-KDD southern regions. Likewise, they and others found that counties employing irrigation showed significantly lower sensitivity than neighboring rainfed counties.

A detailed analysis of irrigated maize contest yields by Carter (2015) found that VPD and precipitation were strongly inversely correlated, and that the highest yields were *positively* correlated with VPD and *negatively* correlated with precipitation. This appears to conflict with the previously-discussed findings of VPD as a negative predictor of maize yield (Fisher *et al.*, 2012; Lobell *et al.*, 2013), but it more likely reflects the altered correlation structure of intensively-managed, irrigated crop systems as compared to that of fields under "ordinary" management. For instance, two other strong positive predictors of yield were cumulative

radiation and long-season cultivars (Carter, 2015), both of which may increase exposure to drought stress under rainfed conditions. The broad mechanisms underlying relationships between VPD and water supply are depicted in Figure 4.4. Since large-scale yield analyses tend to include area under varying management intensities, sound interpretation of their results can be difficult and must consider these kinds of correlation structures.

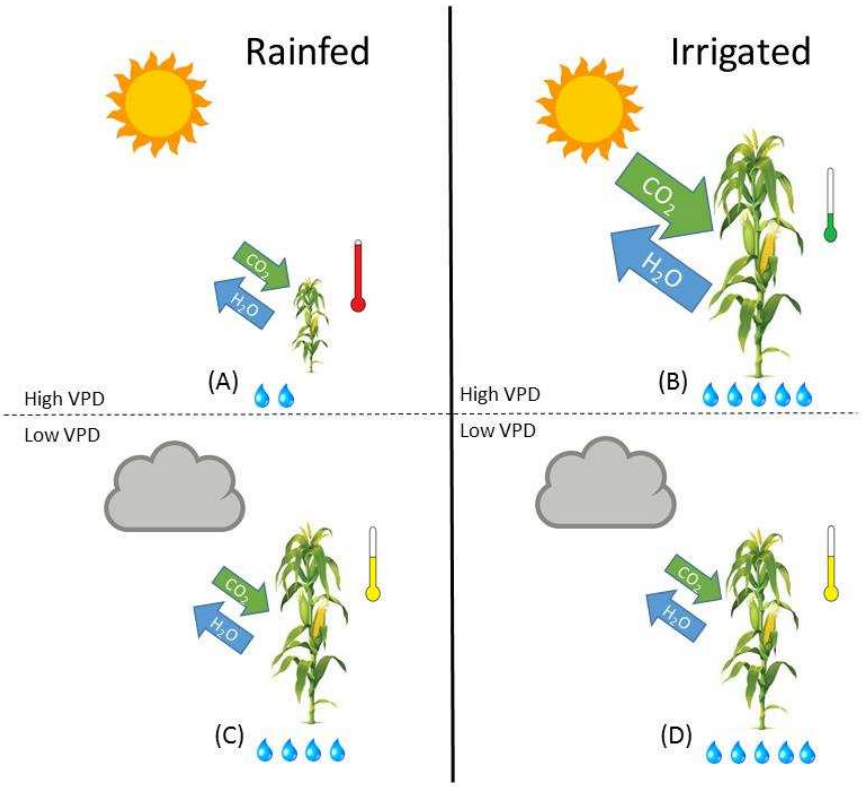

Figure 4.4. Conceptual diagram summarizing the interactions between irrigation status, VPD and maize yield important to interpretation of statistical climate-yield analyses (e.g., Roberts *et al.*, 2012; Anderson *et al.*, 2015; Carter, 2015). High VPD typically co-occurs with sunny days, which induce water- and heat-stresses in rainfed plants (A) but support maximal C-fixation and transpirational cooling when water is not limiting (B). Cloudy, low-VPD conditions cause light limited photosynthetic rates while also limiting transpirational cooling under rainfed (C) or irrigated (D) conditions. Thermometers indicate canopy temperature relative to air temperature. Water droplets indicate soil water supply.

Soybean

An early analysis of US corn-soy acreage found that Midwestern yields increased in cooler years, while Northern Plains yields increased in warmer years (Lobell & Asner, 2003), underscoring the importance of baseline climate for anticipating trends in crop temperature response. A useful high-level perspective on global crop distributions was provided by Lobell & Gourdji (2012). Their analysis combined major producing countries of six crops with their average growing season temperatures and presented them relative to the crop-specific optima estimated by Hatfield *et al.* (2011). Maize production in the US was grown at an average temperature of 19.5°C, modestly above the optimum of 18°C. Soybeans in the US, by contrast, were grown at a slightly higher season average temperature of 21°C, modestly below the optimum of 22°C. A later study found that soybean had the lowest historical (1980-2011) exposure to critical high temperatures (above 39°C) among maize, soybean, wheat and rice (Gourdji *et al.*, 2013). This resulted primarily from the impressive heat tolerance of soybean, with a critical temperature of 39°C versus 35°C for maize (again based on Hatfield *et al.*, 2011). These analyses indicate that soybean yields are under less immediate threat of losses to extreme heat than maize.

Lobell & Field (2007) estimated the effect of historic climate change on soybean yield. When considering the 1981-2002 time-frame, the effect of the warming trend on yields was non-significantly positive. However, when the effect was estimated separately for each decade from 1961-2002, a pattern emerged from the second (1971-1980) through fourth (1991-2001) decades of increasingly negative climate effects. A similar pattern was found for maize, but with more severe losses (~20%) in the latest decade as compared with soybean (~5%).

Similar effects have been discerned even in relatively cool growing regions. Kucharik & Serbin (2008) studied county corn and soybean yields in Wisconsin, on the northern edge of the US Corn Belt. They found that historic yields of both crops were maximized during cooler, wetter years, with warming likely reducing yield trends by 5-10% from 1976-2006. Taken together, these results suggest that soybean may have fared better than maize under climate change to-date, but that both crops are likely to sustain greater losses as warming accelerates.

Wheat

A key consideration for wheat response to climate warming concerns the opposing effects of reduced exposure to cold in the autumn and earlier spring development versus earlier and more severe summer heat waves. Tack *et al.* (2015) studied the impact of temperature on yields of rainfed winter wheat as reported from the Kansas Performance Test trials. They found a substantial beneficial effect of fall warming on yield due to the reduced incidence of frost damage and increased time for growth before onset of dormancy. However, this benefit was outweighed by the negative effect of spring warming under most uniform seasonal warming scenarios. In addition, they concluded that the longer grain-filling periods of recent, high-yielding varieties were more vulnerable to heat-induced losses than older, lower-yielding varieties. A later analysis of these data confirmed this tradeoff as a feature related to genetic clusters of wheat varieties (Tack *et al.*, 2015b). On the other hand, Rezaei *et al.* (2015) found strong trends of increasing spring and summer temperatures in Germany from 1951-2009 had shifted wheat heading dates forward by an average of 14 days and that this offset the potential increases in heat stress exposure around anthesis. Lobell *et al.* (2012) studied the relations of ordinary and extreme (>34°C) thermal time to growing season length of Indian wheat using satellite observations. Their calculations indicated that a 2°C temperature rise would accelerate

senescence by an average of nine days and reduce yields by 15-20%. While adoption of cultivars with shorter phenological durations and/or use of earlier sowing dates may reduce wheat exposure to extreme heat in temperate climates, growing regions with weaker seasonality (i.e., tropical regions) will have even smaller scope for adaptation through these kinds of changes.

Gourdji et al. (2012) examined a large set of climate and yield data from mostly-irrigated wheat yield trials at 349 locations worldwide. They found that reproductive stage temperatures above 12°C reduced yields, and yield responded negatively to increased temperature during the grain-filling period, throughout the dataset, with particularly steep declines when accompanied by low VPD conditions. This last point aligns with the previously-mentioned findings in maize (Butler & Huybers, 2015; Carter, 2015) that irrigation tends to mitigate yield loss at high temperatures and shifts VPD from a negative to a positive predictor of yield. One likely mechanism for this shift involves the role of soil water in supporting transpirational cooling of crop canopies. For example, (Siebert *et al.*, 2014) compared air temperature and canopy temperatures for rainfed and irrigated rye in Germany. They found canopy temperatures ranged from 6°C below to 8°C above air temperatures, with sandy rainfed fields usually above air temperature, and loamy irrigated fields usually below.

CO_2, Heat and Process Models

Process-based models are the primary tools used in most large-scale projections of climate change impacts on crop yield, including the IPCC AR5 (Porter *et al.*, 2014). In principle, these models are able to capture complex interactions between eCO_2 and heat, but the algorithms used

to simulate underlying phenomena vary widely (reviewed by Tubiello & Ewert, 2002; Eyshi Rezaei *et al.*, 2014).

CO_2 and heat stress in current crop models

As touched on previously, major crop models account for direct eCO_2 effects on yield through one of two mechanisms. The more mechanistic algorithms simulate photosynthetic biochemistry as given by Farquhar *et al*. (1980, 1982) and therefore include atmospheric [CO_2] as an input to their systems of equations. The more empirical algorithms employ an experimentally-derived CO_2 fertilization multiplier on daily photosynthesis or growth (reviewed by Tubiello & Ewert, 2002).

A similar divide exists for the simulation of eCO_2 effects on water use. Mechanistic approaches calculate leaf energy balance on sub-daily time-steps and adjust stomatal conductance to optimize C fixation (Ball *et al.*, 1987; Collatz *et al.*, 1991). Empirical approaches utilize an experiment-based multiplier on daily transpiration or transpiration efficiency (TE).

Heat stress algorithms are more varied. In part this results from the broader array of plant processes that are directly dependent on temperature as compared to [CO_2]. Most crop models use the thermal time concept to scale phenological development based on temperature, for example. By reducing the calendar duration of the grain-filling phase (under high temperatures) without a proportional increase in grain-filling rate, these systems can indirectly capture a major impact of heat on yield (e.g., CERES-maize: López-Cedrón *et al.*, 2005; CERES-wheat: Boote *et al.*, 2011). Likewise, models that explicitly estimate maintenance respiration may capture heat-induced yield reductions via temperature-dependent respiratory C losses (e.g., GAEZ model:

Leemans & Solomon, 1993; LPJ models: Bondeau *et al.*, 2007). For models that use radiation use efficiency (RUE) for simulating photosynthesis, a composite limitation factor commonly stands in for the temperature sensitivities of several underlying physiological processes including photosynthesis, photorespiration, maintenance respiration, and possibly also heat stress per se (EPIC models: Sharpley & Williams, 1990; DayCent: Parton *et al.*, 1998).

Several models use algorithms explicitly designed to account for heat stress effects, mostly focused on flowering and grain-filling dynamics. One approach is to have cultivar-specific cardinal temperatures for specific yield formation processes and phases (CERES-Wheat: Alderman *et al.*, 2013b). Heat-induced reductions in grain number are difficult to simulate but could account for sink limitations to yield that may be missed by source-oriented algorithms (APSIM-maize: Jin *et al.*, 2016). A less explicit way of approximating reproductive heat damage is to reduce harvest index as a function of near-anthesis critical heat exposure (CropSyst: Stockle *et al.*, 2003; PEGASUS: Deryng *et al.*, 2014). The methods for simulating extreme heat and CO_2 fertilization in several major crop models are described in Table 4.2.

Table 4.2. Summary of simulation approaches accounting for effects of [CO_2] and heat stress employed by models participating in the Global Gridded Crop Model Intercomparison (GGCMI; Rosenzweig *et al.*, 2014) and selected others. RUE: empirically derived multiplier on crop radiation use efficiency; TE: empirically derived multiplier to reduce crop transpiration; PS: [CO_2] enters directly into equations describing photosynthetic biochemistry; g_s: [CO_2] enters directly into equations describing regulation of stomatal conductance; Respiration: C losses to respiration increase non-linearly with temperature.

Model	CO_2: Production	CO_2: Transpiration	Heat Stress	Model Type	Reference
EPIC & GEPIC	RUE	TE	Temp limits RUE-based biomass gain	Site-based	(Sharpley & Williams, 1990; Kiniry *et al.*, 1992; Liu *et al.*, 2007)
IMAGE-GAEZ	RUE	--	Respiration	Agro-ecological zone	(Leemans & Solomon, 1993)
LPJ-GUESS & LPJmL	PS	g_s	Respiration	DGVM	(Smith *et al.*, 2001; Bondeau *et al.*, 2007)
DSSAT (CERES-maize, CERES-wheat, CropGro-soybean	RUE; soy: PS	TE; soy: g_s	Differential temp response curves for reproductive processes and development rates; grain number reduction	Site-based	(Jones *et al.*, 2003; López-Cedrón *et al.*, 2005; Boote *et al.*, 2011; Alderman *et al.*, 2013)
PEGASUS	RUE	TE	Near-anthesis heat exposure reduces yield	DGVM	(Deryng *et al.*, 2014)
CropSyst	RUE	TE	Heat during flowering reduces harvest index	Site-based	(Stockle *et al.*, 2003)
DayCent	RUE	TE	Temp limits RUE-based biomass gain	Site-based	(Parton *et al.*, 1998)
APSIM	RUE	TE	Temp limits RUE-based biomass gain, grain fill rate, and grain number	Site-based	(Keating *et al.*, 2003; Jin *et al.*, 2016)

There is an increasing emphasis on testing and comparison of process models, with particular focus on their ability to capture crop responses to well-studied climate change factors (Asseng, 2013; Bassu *et al.*, 2014; O'Leary *et al.*, 2015; Deryng *et al.*, 2016; Jin *et al.*, 2016). Some of these studies include experiments expressly designed to generate the kinds of well-controlled, dose-response relationships that can readily inform specific model processes (Asseng *et al.*, 2014; Cai *et al.*, 2015; Liu *et al.*, 2016a, 2016b). These efforts are vitally important for evaluating and improving the accuracy of process models and underlying algorithms for projection of climate change impacts.

Emerging themes for crop model improvement

As open-air experiments and empirical studies of climate change become increasingly sophisticated, their focus is shifting from quantifying first-order effects of single factors (e.g., growth stimulation by eCO_2; yield impact of hot seasons) to elucidating complex interactions between these and other factors. The results of these studies are beginning to identify important ways in which climate change factors interact with one another and with other agronomic factors. Process-based crop model development should continue to explore ways of simulating these second-order climate change effects.

The reduced transpiration under eCO_2 reduces latent heat flux and increases canopy temperatures. This effect caused an average warming of 0.7°C in FACE crop canopies versus controls in the experiments reviewed by Kimball (2016). Significant efforts have already been made to develop and compare algorithms for estimating canopy temperature itself, including empirical versus energy-balance methods (Webber *et al.*, 2015) as well as testing the utility of simulated canopy temperature versus air temperature for estimating heat stress and final yield

(Gabaldon-Leal *et al.*, 2016; Webber *et al.*, 2016). Wheat canopy temperature goodness of fit was similar between empirical algorithms and energy balance methods with correction for atmospheric stability conditions, though use of canopy temperature to drive heat stress only modestly improved yield prediction (Webber *et al.*, 2015). Similar work with a single maize model using an energy balance approach found that canopy temperature substantially improved final yield prediction relative to air temperature, though similar improvement could be achieved using air temperature together with a higher stress threshold temperature (Gabaldon-Leal *et al.*, 2016). While canopy temperature simulation is a substantial challenge, the increasing incidence of hot, dry conditions and reduced latent heat flux from eCO_2 crops justify continued effort to account for this important variable (Boote *et al.*, 2011; Siebert *et al.*, 2014).

The interactions of eCO_2 and heat with crop N dynamics are unclear. The phenomenon of photosynthetic acclimation has been frequently observed in diverse plants grown under eCO_2 (Ainsworth & Rogers, 2007). One mechanism underlying acclimation may be sink limitation, in which excess non-structural carbohydrates accumulate due to accelerated C fixation and downregulate Rubisco levels. Sink limitation has been found to worsen under conditions of low N supply (Ainsworth & Long, 2005). For wheat and other non-leguminous C_3 crops, the compromising effect of eCO_2 on leaf nitrate reduction (Bloom *et al.*, 2012) could conceivably exacerbate sink limitation by creating effective N shortages even where soil nitrate is ample. The relative contributions of these mechanisms must be clarified for accurate model processes to be developed. At present, most models that make any adjustment of N relations under eCO_2 lower the amount of N required for growth. This reflects a general interpretation of reduced foliar N concentrations as resulting from increased N use efficiency. However, if plants under eCO_2 have impaired NO_3^- assimilation ability, as discussed earlier, such processes will

overestimate yields of N-limited crops, particularly for situations where reduced N forms are scarce. In that case, models would need to account for the chemical form of N fertilizer (as stressed by Bloom, 2015a) as well as soil N transformations. Further research is urgently needed to determine whether acclimation of photosynthesis results from sink limitation, impaired nitrate assimilation, or some combination of these and other factors.

The reduction in stomatal conductance and resulting increases in canopy temperatures under eCO_2 are well-established in theory and experimental observation of well-watered crops. Under conditions of drought, eCO_2 crops would be expected to maintain adequate soil water and full transpiration longer than aCO_2 crops and thus avoid some stress exposure. In keeping with this understanding, most FACE studies (Kimball *et al.*, 1995; Conley *et al.*, 2001; Leakey *et al.*, 2006) and at least one meta-analysis (Bishop *et al.*, 2014) have found that eCO_2 effects on yield are equal or greater among water-limited treatments versus well-watered controls.

Recent work with soybean in Illinois has complicated understanding of this water-sparing effect, however. Using FACE in combination with rainfall exclusion structures over three years, Gray *et al.* (2016) found that eCO_2 treatments did not have greater soil water than aCO_2 treatments when subjected to reduced precipitation. In general, eCO_2 plants showed greater LAI development and reduced water use during vegetative growth, but then used as much or more water as aCO_2 plants in the hotter, drier conditions prevalent during reproductive growth (summarized in Figure 4.5). While much of this late-season water use was driven by the greater LAI of eCO_2 plants, Gray *et al.* (2016) also found that eCO_2 plants responded more strongly to drought-induced abscisic acid signaling, resulting in more g_s reduction than aCO_2 plants. FACE-

treated plants also had greater proportions of N-fixing root nodules in shallow, dry soil layers, apparently compromising N fixing activity.

These results underscore the considerable challenges faced by modelers attempting to predict crop yield responses to climate change factors. The findings of Gray *et al.* (2016) demonstrate that the near-universal positive effect of eCO_2 on yield of C_3 crops can vary dramatically (yield RR range: 0.95-1.32) based on complex interactions between vegetative development, timing of heat and precipitation, and root depth distribution. Importantly, the trend they observed of *declining* eCO_2 fertilization with increasing water limitation is contrary to conventional understanding and the results of several previous FACE studies (Kimball *et al.*, 1995; Conley *et al.*, 2001; Leakey *et al.*, 2006).

While existing modeling approaches, such as scalars on daily production and transpiration or RUE declines at high temperature, are reasonable for capturing broad average responses, future development should focus on explaining and replicating these temporally-sensitive, multi-factorial interactions.

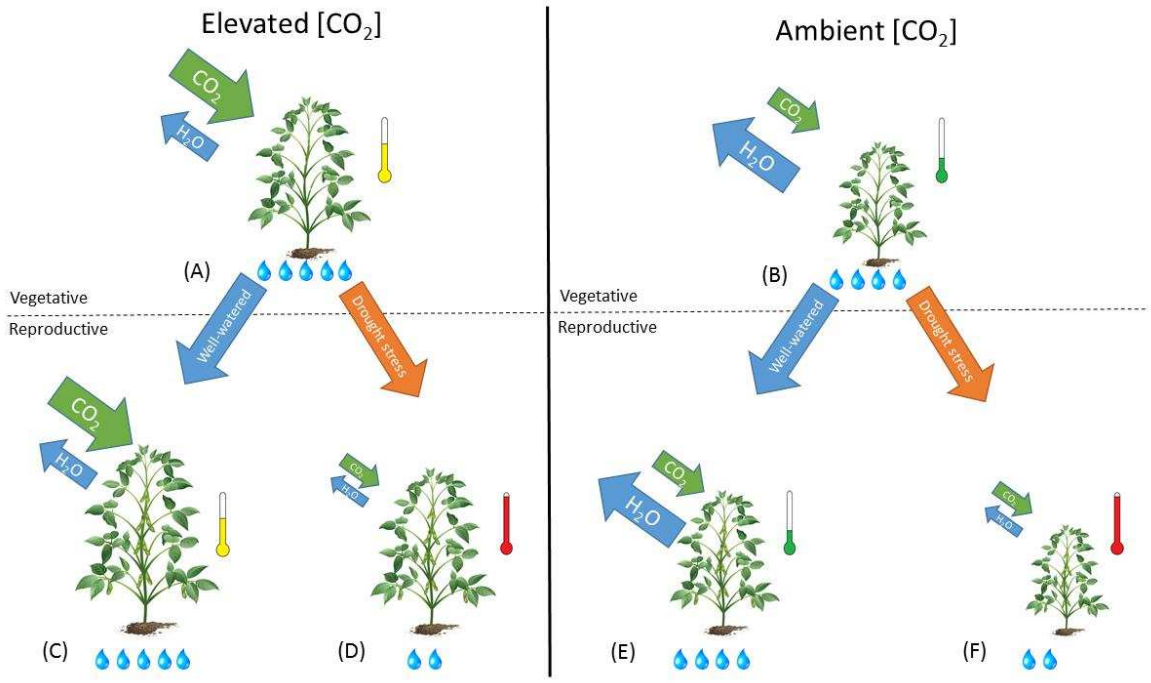

Figure 4.5. Conceptual diagram of interacting climate factors based on the results of Gray *et al.*, (2016) for soybean grown under FACE using rain-exclusion treatments. Elevated CO_2-grown plants (A) have enhanced C-fixation and LAI development during vegetative growth, accompanied by modestly reduced water losses and increased canopy temperatures (relative to ambient [CO_2], B). Under well-watered conditions, elevated [CO_2] continues to sustain greater C fixation and yields are enhanced (C relative to E). Under drought conditions, the greater LAI of the eCO_2-grown plants depletes soil water supplies and, combined with other factors (see text), reduces or abolishes any yield enhancement (D relative to F). Thermometers indicate canopy temperature relative to air temperature. Water droplets indicate soil water supply.

Conclusions

Crop breeding efforts and model-based climate impact assessments depend on reliable, empirical understanding of crop responses to heat and eCO_2. Whenever possible, these responses should be verified independently through both field experimentation and careful analysis of historical data. Experiments are necessary to tease out subtle mechanistic details, but are unable to capture the full range of real-world management, climate and edaphic features that integrate across space and time to determine large-scale yields. Statistical approaches face the complementary challenge, beginning with data that include these emergent trends but demanding thorough

understanding of mechanistic linkages to separate and correctly interpret signals. The recent convergence of statistical and experimental findings on crop responses to concurrent heat and drought is encouraging in this regard. Notwithstanding a few early efforts (Lobell & Field, 2008; McGrath & Lobell, 2011), knowledge of eCO_2 effects is mostly limited to experiments, but as atmospheric [CO_2] continues to rise and statistical methods are further refined, this approach may eventually constrain experimental estimates of eCO_2 effects in a similar way.

Most widely-used crop models incorporate CO_2 fertilization and heat stress-related processes that account for climate impacts in broad outline. Two recent analyses found that yield projections from crop modeling studies and statistical studies of historical yields show substantial agreement (Liu *et al.*, 2016c; Lobell & Asseng, 2017). The greater complexity revealed by recent experimental work, however, provides a basis for development and testing of more granular algorithms. These more mechanistic representations are of particular importance for temporal ranges (such as the late 21st century) and locations (such as the tropics) where regimes of interacting stressors may frequently exceed normal historical ranges. Process models exist to apply knowledge gained from experimental research, and they are our best tools for quantifying the implications of these new results for agricultural productivity under the unprecedented conditions crops will face in coming decades.

CHAPTER 5. MODELING CROP RESPONSE TO INCREASING ATMOSPHERIC [CO_2]

Introduction

Crops face unprecedented levels of atmospheric [CO_2]

Atmospheric carbon dioxide (CO_2) concentrations have increased from approximately 278 ppm at the start of the Industrial Revolution to greater than 400 ppm at present (Meinshausen *et al.*, 2011). According to the Representative Concentration Pathways (RCPs) used in the Intergovernmental Panel on Climate Change's (IPCC) 5th Assessment report (AR5; Hartmann *et al.*, 2013), atmospheric [CO_2] is likely to range between 443 and 541 ppm by 2050, and between 421 and 936 ppm by 2100 (Meinshausen *et al.*, 2011). Recent analysis of emissions trends suggests near-term [CO_2] have tracked toward the upper end of the RCP ranges (Friedlingstein *et al.*, 2014). Thus, in the foreseeable future, the [CO_2] encountered by terrestrial plants will be higher than at any time since the late Tertiary – more than two million years ago (Pearson & Palmer, 2000). Since CO_2 is an essential – and often rate-limiting – input to photosynthesis for all plants, this change has major implications for agricultural production in the 21st century.

Early CO_2 enrichment experiments

It was widely realized in the 1960s that greenhouse plants could be made more productive by increasing the [CO_2] within the greenhouse. Thus, the earliest large review of plant responses to eCO_2 (Kimball, 1983) included a wide range of specialty and commodity crops grown in small, tightly regulated enclosures. It found an average yield enhancement of 33% for a doubling of [CO_2]. Subsequent reviews found similar responses for soybean (31%; Allen *et al.*, 1987) and 10 major crop species (41%; Cure & Acock, 1986).

Crop model [CO_2]-response processes

The CO_2 response algorithms in major crop models, including the EPIC (Stockle *et al.*, 1992) and DSSAT (Peart *et al.*, 1989) families of models, were originally calibrated using growth and yield responses derived from enclosure studies. The reviews by Cure & Acock (1986) and Kimball (1983) were also cited by Metherell (1992) in his development of a CO_2 response process for the monthly Century biogeochemical model. Specifically, for a doubling of [CO_2], his process used multiplicative scalars to increase both monthly biomass production and maximum carbon-to-nitrogen (C:N) ratio of new biomass by a factor of 1.3 for C_3 crops, while reducing monthly transpiration by a factor of 0.77 for both C_3 and C_4 crops. This process was maintained when Parton *et al.* (1998) created the daily time-step version of Century known as DayCent.

Ainsworth *et al.* (2008) considered simulations by five dynamic crop models (mC-Wheat, Demeter, LINTUL, AFRC and Sirius) recreating the 1992-94 Maricopa wheat FACE experiments. They found the average modeled vs. observed responses to be 1.18 vs. 1.08 under well-watered conditions and 1.28 vs. 1.18 under water-stressed conditions, respectively, leading them to conclude that models parameterized against enclosure results overestimate [CO_2] responses observed under FACE. Others have contested this view, however, pointing out various difficulties in comparing enclosures with FACE experiments (Tubiello *et al.*, 2007). For instance, the broad category of "enclosure" experiments conceals several experimental paradigms, including growth chambers, glasshouses, soil-plant-atmosphere research (SPAR) units, temperature gradient tunnels (TGTs) and open-top field chambers (OTCs; Ziska & Bunce, 2007). In addition, the level of "elevated" [CO_2] employed by enclosure experiments (often double the ambient level, or about 700 ppm) has tended to be higher than that employed by

FACE experiments (often 550 ppm), necessitating a relatively arbitrary choice of mathematical scaling for effect size comparisons (Ainsworth *et al.*, 2008a).

Additional crop responses to eCO_2

After increases in aboveground biomass (AGB) and yield, the most widely-reported impact of eCO_2 on crops is a decrease in stomatal conductance (g_s) and, to a lesser extent, season evapotranspiration (ET) (Cure & Acock, 1986; Drake *et al.*, 1997; Kimball & Bernacchi, 2006; Leakey *et al.*, 2009). The smaller relative decreases in ET result from negative feedbacks, whereby reductions in g_s lead to reduced latent heat flux, raising canopy temperatures and thus marginally increasing the transpiration rate. At the same time, to the extent that eCO_2 accelerates AGB growth, the increase in total leaf area may feed back to increase total transpiration. Bernacchi *et al.* (2007) found that soybean grown under eCO_2 over four years averaged 10% lower g_s, 0.5°C higher midday canopy temperature, and 8.6% lower ET than the control. Maize grown at the same facility displayed (3-year averages) 9% lower season ET and 0.5°C increased canopy temperature when grown under eCO_2. The Maricopa wheat FACE experiment likewise reported a 0.6°C increase in canopy temperatures for the eCO_2 vs. ambient treatment (Kimball *et al.*, 1995). Despite the potential for negative feedbacks, Vanuytrecht *et al.* (2012) found that water productivity of FACE crops showed significant increases of 23 and 27% with respect to AGB and yield, respectively.

Several enclosure and FACE studies have reported an effect of eCO_2 on crop nitrogen (N) concentration or acquisition. In their review of the FACE literature, Kimball *et al.* (2002) found an average reduction of 16% in the nitrogen (N) concentration of AGB for C_3 grain crops. However, when expressed as a total amount of N, the reduction was 0.4%, not significantly

different from 0. A large review of results from 75 enclosure studies found that tissue N concentrations for eCO_2 treatments were reduced by 14% under eCO_2 compared with ambient treatments (Cotrufo *et al.*, 1998). A recent analysis by Feng *et al.* (2015) analyzed N concentration and N acquisition responses to FACE for grassland, cropland, and forest ecosystems as a function of their aboveground net primary production (ANPP) response. They found a mean reduction of 8% for N concentration in crop studies that persisted even among crops with little to no stimulation in ANPP.

The largest review of eCO_2 effects on belowground C allocation in crops found mixed results (Rogers *et al.*, 1996). Out of 264 observations from enclosure experiments, that work found a mean increase in root-to-shoot ratio (R:S ratio) of 11%. However, this effect was highly variable, with 59.5% of observations showing an increase, 3% showing no change, and 37.5% showing a decrease in belowground allocation (Rogers *et al.*, 1996). A recent review of FACE experiments with several major crops divided experiments into ranges by enrichment level. It found significant mean increases in root-to-shoot ratio of 14% and 35% for experiments with eCO_2 of 541-580 and 581-620 ppm, respectively (Vanuytrecht *et al.*, 2012).

Study rationale

This work investigated the hypothesis that the existing DayCent crop CO_2 response process and parameter values are inconsistent with the 20 years of experimental results that have been produced since its initial parameterization by Metherell (1992). The specific modeling undertaken toward this end was limited to results from five FACE sites because they provided the most straightforward test of model performance at replicating crop eCO_2 responses in long-running, open-air experimental conditions.

Methods

Experimental sites

Maricopa, AZ, USA: Four of the seven years of wheat, and both seasons of sorghum, modeled for this site were grown at the University of Arizona Agricultural Centre, Maricopa, AZ (33°4'N, 111°59'W, 358 m elevation). FACE experiments (aCO_2: 360 ppm, eCO_2: 550-560 ppm) were conducted at this facility from 1989-1999 using cotton (*Gossypium hirsutum* L.; 1989-1991 plantings), spring wheat (*Triticum aestivum* L. cv. Yecora Rojo; 1992, 1993, 1995 and 1996 plantings), and grain sorghum (*Sorghum bicolor* L.; 1998 and 1999 plantings). The soil at this site is described as a Trix clay loam [fine-loamy, mixed (calcareous) hyperthermic Typic Torrifluvents] (Soil Survey Staff, 2015). The FACE apparatus consisted of 25-m diameter rings into which CO_2-enriched air was blown day and night. Further details of the FACE apparatus can be found in Kimball (2006).

The first two wheat plantings were designed to test eCO_2-by-water interactions using two levels of [CO_2] and two levels of irrigation, with each treatment replicated four times. The second set of wheat plantings tested eCO_2-by-N supply interactions using two levels of [CO_2] and two levels of N fertilization. Table A7 and Table A8 present key agronomic and meteorological details from the four wheat and two sorghum seasons, respectively.

Champaign, IL, USA: Seven of the nine years of soybean and three years of corn modeled for this site were grown at the SoyFACE facility, which is part of the Experimental Research Station of the University of Illinois, Champaign, IL (40°02' N, 88°14'W, 228 m elevation). FACE experiments (aCO_2: 370-402 ppm, eCO_2: 550-590 ppm) were conducted at this facility using corn (*Zea mays* L., Pioneer cv 34B43) in rotation with soybean (*Glycine max* L. Merr. cv Pana

for 2001; thereafter Pioneer cv 93B15). The crops were rotated between opposite halves of a tile drained field that has been in continuous cultivation to arable crops for more than 100 years. The soil at this facility is a deep (>1 m) Flanagan/Drummer series fine-silty, mixed, mesic Typic Endoaquoll (Soil Survey Staff, 2015). The FACE apparatus was constructed in 20-m diameter octagonal plots with 4 replicates. All crops were rainfed, and fertilization was typical of regional practice, with no N applied to soybean and 202 kg N ha^{-1} applied to maize, plus an estimated residual 45 kg N ha^{-1} from the previous soybean crop.

This work modeled soybean FACE experiments from 2001, 2002, 2003, 2004, 2005, 2009 and 2011, and maize from 2004, 2006, 2008 and 2010. For soybean in 2009 and 2011, and maize in 2010, an infrared heating apparatus was used to warm crop canopies in a factorial design with FACE treatment, resulting in four replicated observations for those crop-years (further details in Ruiz-Vera *et al.*, 2013, 2015). Agronomic and meteorological details from the soybean and maize seasons simulated are presented in Table A9 and Table A10, respectively (sources as noted).

Horsham, Victoria, Australia: Three years of wheat modeled for this site were grown at the Australian Grains FACE experiment (aCO_2: 380-390 ppm, eCO_2: 550 ppm) in Horsham, Victoria, Australia (36°45'S, 142°07'E, 128 m elevation). The FACE apparatus consisted of 16, 12-m diameter rings and is described in detail by Mollah *et al.* (2009). Wheat (cv. Yitpi) was sown on six dates across three years: normal sowing (NS) and late sowing (LS) dates in 2007-2009. The late sowing dates were designed to expose crops to warmer, drier conditions and were combined in a factorial design with two levels of supplemental irrigation for each date (Fitzgerald *et al.*, 2016). The experimental site had been irrigated with sewage for more than 20

years prior to the experiment and so contained very high concentrations of mineral N. Thus, while N application treatments were performed, they had no discernible impact on crop growth or yield and so published results were pooled across nitrogen treatments (O'Leary *et al.*, 2015). Crop cultural information for these experiments is shown in Table A11.

Shizukuishi, Iwate, Japan: The seven years of rice (*Oryza sativa* L.) modeled for this site were grown in paddy fields in Shizukuishi township, Iwate prefecture on northern Honshu island, Japan (39°38'N, 140°57'E, 200 m elevation). Rice cultivar Akitakomachi was grown at this facility in 1998, 1999, 2000, 2003 and 2004. The 2007 and 2008 seasons compared cultivars Akitokomachi, Akita 63, Koshihikari and Takanari for their responses to eCO_2 (aCO_2: 365-379 ppm, eCO_2: 548-662 ppm). The soils on these farms were Andosol paddy soils and were flooded throughout the rice growing seasons. More site and FACE technical details can be found in Okada *et al.* (2001) and Kobayashi *et al.*, (2006), and agronomic details are given in Table A12.

Changping, Beijing, China: Three years of wheat and two years of soybean modeled for this site were grown at the China Mini-FACE facility managed by the Chinese Academy of Agricultural Sciences in Changping, Beijing, China (40°10'N, 116°14'E). Winter wheat (cv. Zhongmai 175) was grown in the 2007-2008, 2008-2009, and 2009-2010 growing seasons at two levels of N application and ambient (415 ppm) and enriched (550 ppm) [CO_2]. Soybean cultivar Zhonghuang 35 was grown in 2009 and 2011 and cultivar Zhonghuang 13 was grown in 2009. These FACE experiments (aCO_2: 415 ppm, eCO_2: 550 ppm) were conducted in the context of an ongoing winter wheat-soybean crop rotation in a semi-arid climate, in a clay loam soil with minimal irrigation. Further description of the FACE apparatus, site properties and crop

management practices can be found in Hao *et al.* (2012). Important crop cultural details for these experiments are given in Table A13.

DayCent inputs

The input data for these simulations were obtained from a variety of sources. In all cases, site and weather information contained or referred to within published articles was used when available. Data from weather stations located on or near experimental sites were available for the experiments in Maricopa, Arizona (Arizona Meteorological Network, Maricopa Station: http://ag.arizona.edu/azmet/), Champaign, Illinois (Midwestern Regional Climate Center, Urbana Station: http://mrcc.isws.illinois.edu/CLIMATE/) and Horsham, Australia (Australian Government Bureau of Meteorology, Polkemmet Road Station: http://www.bom.gov.au/climate/data/stations/). Weather for the experiments in Shizukuishi, Japan and Changping, China was obtained from the gridded NASA Prediction of Worldwide Energy Resource (POWER) database, version 1.0.2 (Stackhouse *et al.*, 2015).

Soil properties were collected from publications, which generally supplied key properties such as texture, pH, and organic matter content. Soil properties not given in publications were estimated from texture using the relationships derived by Saxton *et al.* (1986), and all soil inputs used in DayCent simulations are shown in Tables A14 through Table A18. Crop management practices such as planting date, N application and irrigation rates, and crop rotations were described in the publications for each site (described in Tables A7 through A13).

DayCent [CO_2]-response process

The primary objective of this work was to assess the ability of the existing DayCent crop CO_2 response algorithms and parameter values to reproduce crop responses to CO_2 enrichment under FACE conditions and, where needed, to adjust parameter values. The algorithm is summarized conceptually in Figure 5.1, using actual parameter names for clarity.

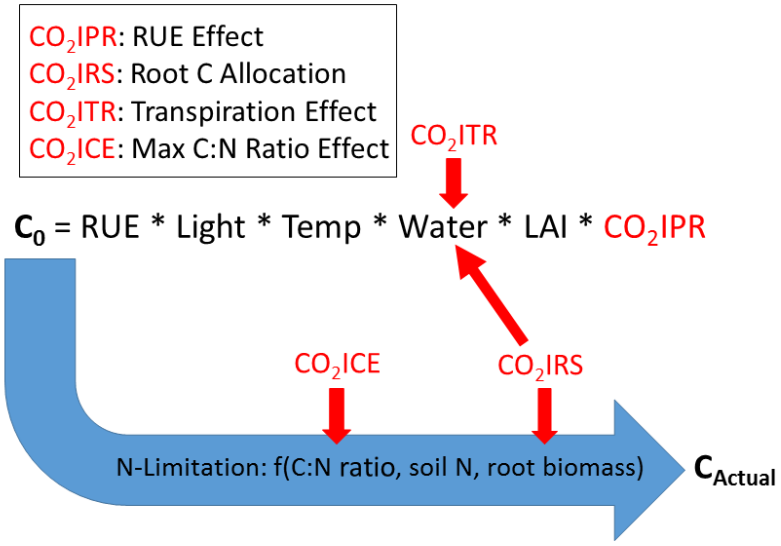

Figure 5.1. Conceptual diagram of the DayCent crop [CO_2] response algorithm. C_0 is the daily C production before N limitation. CO_2 effects are represented by the names of the actual crop-specific parameters involved. While the RUE effect (CO_2IPR) acts directly in determining the potential daily C production (C_0), the other three effects scale various quantities that then constrain productivity to varying degrees. The C:N ratio effect (CO_2ICE), for instance, reduces the amount of N required to sustain full C production (C_0) under eCO_2, and so will impact crops most in circumstances of N scarcity.

The multiplier active at a given [CO_2] is calculated from crop parameters that represent the response ratio (RR) expected for a doubling from the reference [CO_2] of 350 ppm to 700 ppm according to the following equation:

$$y = 1 + (Par - 1) / \log_{10}(2) * \log_{10}([CO_2]/350)$$

Where y is the scaled daily process multiplier, Par is the relevant parameter value (in practice, the RR expected at 700 ppm relative to 350 ppm), and [CO_2] is the current atmospheric CO_2 in the simulation. The default parameter values (black dots), process multipliers active at 550 ppm [CO_2] (black triangles), and underlying logarithmic curves for C_3 crops are illustrated in Figure 5.2.

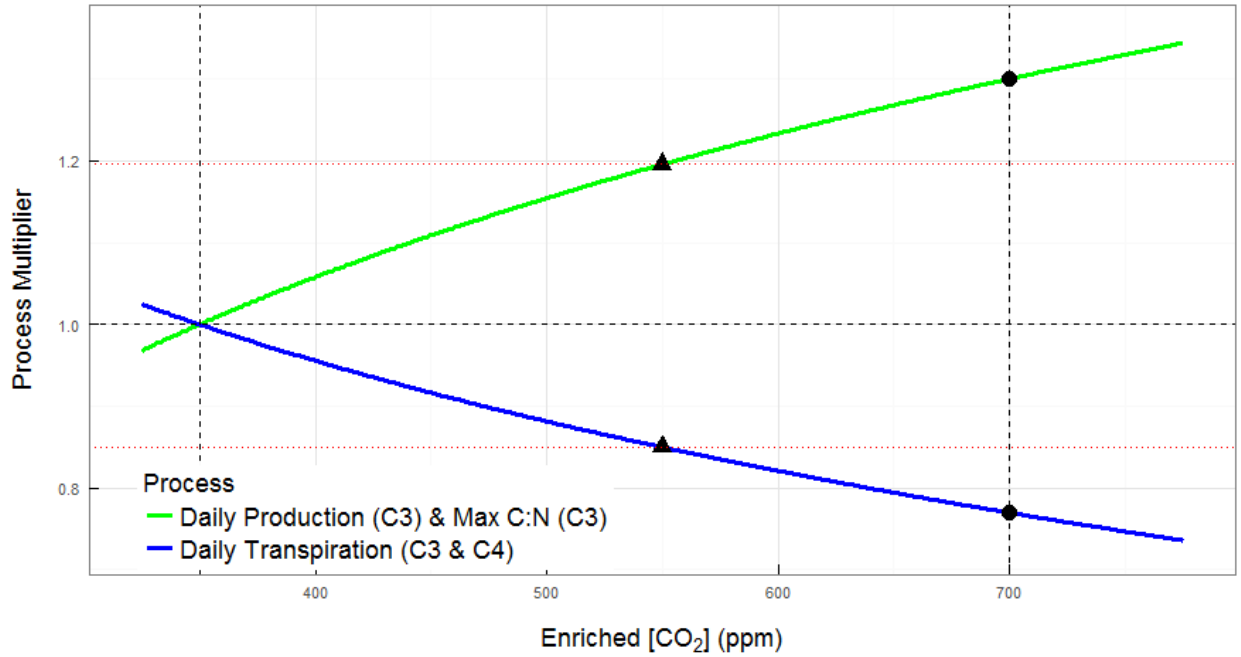

Figure 5.2. Depiction of the logarithmic curves used by DayCent to calculate crop process multipliers as a function of atmospheric [CO_2]. The algorithm assumes a reference ambient [CO_2] of 350 ppm at which multipliers are at 1.0 (left vertical line). At [CO_2] above 350 ppm, multipliers increase toward parameter values (black dots) defined as the process multiplier active under a [CO_2] doubling to 700 ppm (right vertical line). The actual process multipliers active at 550 ppm under default parameterization are shown as black triangles, with particular processes mapped to line color.

Initial calibration

A number of considerations informed the calibration process. First, calibration of non-CO_2 crop parameters was necessary to reproduce observed growth (yield, AGB, C:N ratio of AGB, R:S ratio) as well as possible under the least-limiting, ambient [CO_2] (aCO_2) treatments (eg., high N

application, high irrigation, etc.). For crops with multiple sites, it was occasionally necessary to use different crop parameter values at different sites, reflecting the realities of substantially different cultivar traits, growing season lengths and water and temperature regimes. The modeled vs. measured yields from this exercise are shown in Figure A6. Note that the Maricopa sorghum crop was damaged by a hailstorm about a month prior to harvest in 1999 (Ottman et al., 2001), which likely explains much of the yield loss not captured by DayCent in Figure A6D.

CO_2 response calibration

Since the goal of this work was to arrive at a single set of best-estimate values for crop species responses to eCO_2, CO_2 response parameters were calibrated across sites. After calibrating general growth parameters to relatively non-stressed, aCO_2 conditions, the four CO_2 response parameters were adjusted to match the percent responses to eCO_2 observed in the corresponding treatment-years. The final, calibrated set of crop parameters (including both CO_2 response and general growth parameters) for each crop at each site are given in the Appendix.

FACE training observations

The training observations used to test and re-calibrate the DayCent CO_2-response algorithm were gathered from a number of published articles. Many values were given numerically in the article text or tables. Where values were only given graphically, they were converted to numerical values using the Engauge Digitizer software v. 4.1 (Mitchell, 2002). Because DayCent tracks primarily C rather than biomass per se, observations reported as AGB dry matter were compared to simulated C mass by assuming a dry matter C content of 40%. Due to the scarcity of FACE studies using C_4 crops, we analyzed the data from corn grown in Champaign and sorghum grown in Maricopa together as a single C_4 crop class.

Broader literature comparisons

The experiments simulated for this work represent a subset of the growing agricultural FACE literature, which itself is only a part of the large body of work examining the impacts of eCO_2 on crops. For crop-outcome combinations with few or ambiguous results among the testing observations, results from the broader FACE and enclosure literature were considered for re-calibrating the relevant parameters. Sources for these comparison values are described in Table 5.1. Note that a large review of the FACE literature by Kimball *et al.* (2002) was not included as an outside source for comparison because its source experiments were almost entirely included within the training data modeled explicitly in this work.

Table 5.1. Summary of literature sources used to add context for DayCent performance evaluation and parameter recalibration.

Citation	Enrichment Methods Included	Mean Reported eCO_2	Secondary Treatment Handling
(Bishop *et al.*, 2014)	FACE, OTC, reported separately	FACE: 560 ppm OTC: 691 ppm	Non-stressed treatments only
(Ziska & Bunce, 2007)	FACE, various non-FACE methods reported separately	All methods scaled to 700 ppm using β factor	Pooled across
(Long *et al.*, 2006)	FACE, enclosures	All methods scaled to 550 ppm using non-rectangular hyperbola	Pooled across
(Cure & Acock, 1986)	Enclosures	Linear/Quadratic best-fit models: scaled to 680 ppm	Pooled across
(Kimball, 1983)	Enclosures	Pooled: eCO_2 500-1200 ppm	Pooled across

Results

Default CO_2 parameter values and performance

A major goal of this work was to test whether the existing DayCent CO_2 response algorithm, which was developed and calibrated by Metherell (1992) based on results from enclosure studies, could correctly predict crop CO_2 responses observed under FACE conditions. This algorithm includes daily multipliers of 1.3, 1.3 and 0.77 on daily growth, maximum C:N ratio of new biomass, and daily transpiration, respectively, for C_3 crops and a doubling of [CO_2]. For C_4 crops the only effect of CO_2 is a multiplier of 0.77 on daily transpiration. At lower eCO_2 levels, these multipliers are interpolated using a logarithmic curve. For the eCO_2 level of 550 ppm frequently used in FACE studies, these multipliers scale to 1.2, 1.2 and 0.85 for growth, max C:N ratio, and transpiration, respectively. The parameter values and corresponding scalars at 550 ppm [CO_2] are given in Table 5.2.

Table 5.2. DayCent crop CO_2 response parameter values based on the work of (Metherell, 1992). Each parameter represents a crop-specific multiplier on the corresponding daily process for a doubling of [CO_2] from 350 to 700 ppm. Values in parentheses are the actual daily process scalars active at 550 ppm, interpolated using the logarithmic curve employed by DayCent.

Crop	C_4	Rice	Soybean	Wheat
Growth	1.00 (1.00)	1.30 (1.20)	1.30 (1.20)	1.30 (1.20)
Transpiration	0.77 (0.85)	0.77 (0.85)	0.77 (0.85)	0.77 (0.85)
Max C:N	1.00 (1.00)	1.30 (1.20)	1.30 (1.20)	1.30 (1.20)
Root Allocation	1.00 (1.00)	1.00 (1.00)	1.00 (1.00)	1.00 (1.00)

The RRs for all four crops and five outcome variables assessed in this study are summarized in Figure 5.3. Note that "C_4" refers to pooled results from both corn and sorghum FACE experiments, since very few FACE experiments have been conducted with C_4 crops. It is important to reiterate that DayCent was calibrated to minimize bias relative to observed

outcomes (yield, AGB, C:N ratio, R:S ratio, season ET) for aCO_2, un-stressed treatments only. All simulations of stressed and/or eCO_2 treatments used crop parameter values from that calibration process, with no change of CO_2 response parameters from the values developed by (Metherell, 1992).

As shown in Figure 5.3, the existing CO_2 response algorithm accurately predicted the average RRs of grain yield, AGB, and season ET for the pooled C_4 crops. There were too few data regarding C:N ratio and R:S ratio responses from the simulated C_4 experiments to test these outcomes directly. Under default parameters for C_4 crops, only daily transpiration was affected by $[CO_2]$ (reduced by a factor of 0.85 in these simulations), so all impacts on outcomes other than season ET occurred indirectly. The slight increases in C:N ratio for some simulations likely reflect simple "growth dilution" of available N. The small reductions in R:S ratio under eCO_2 likely resulted from reduced water stress, which in DayCent can lead to reductions in belowground biomass allocation. At the same time, part of the decrease in R:S ratio results arithmetically from the increase in AGB. The complexity of these and other dynamic interactions underscores the importance of testing model CO_2 response algorithms against experiments rather than assuming roughly linear, independent season-long responses to daily process multipliers.

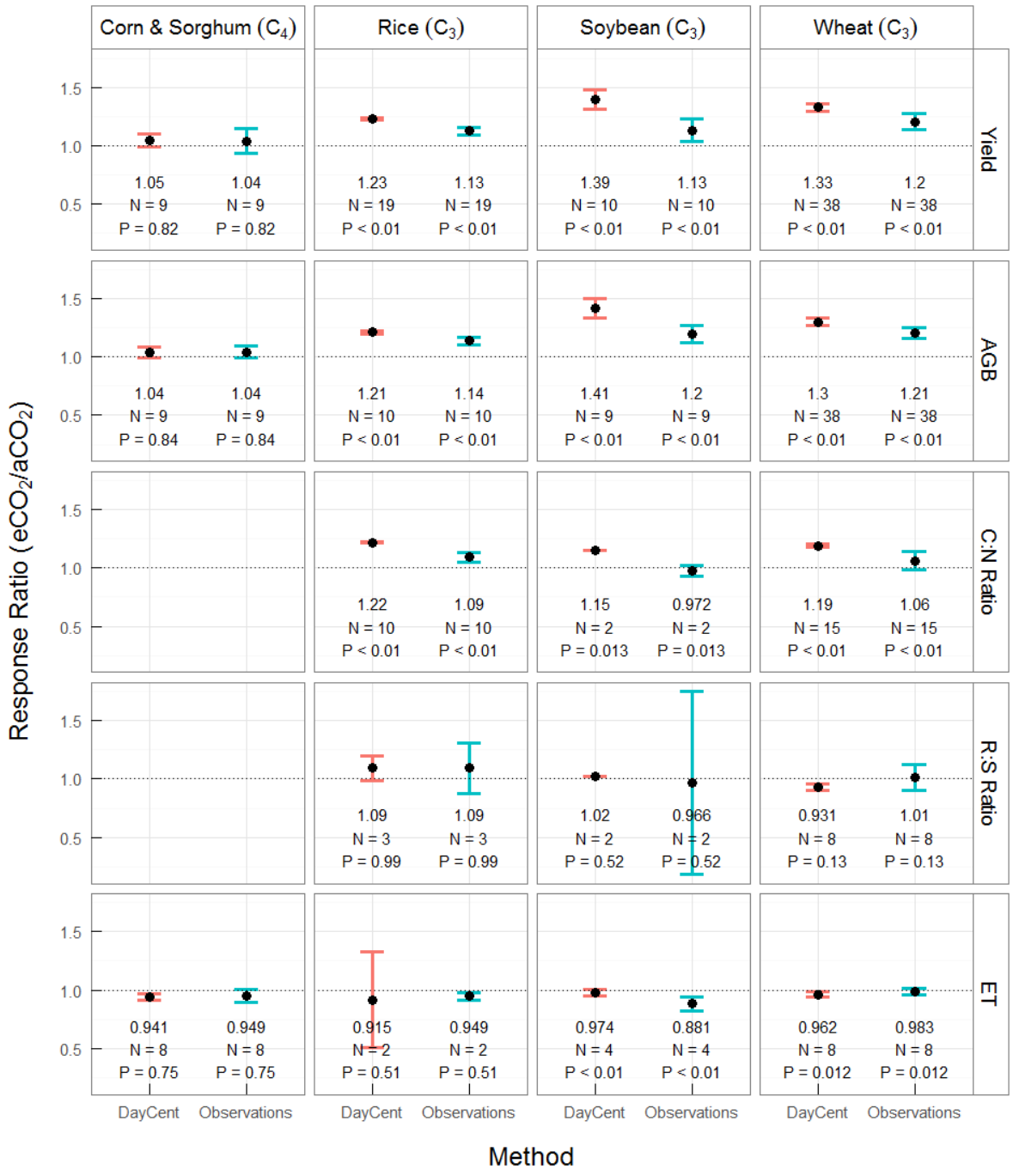

Figure 5.3. Observed and un-calibrated DayCent crop responses to eCO_2 for C_4 (corn and sorghum), rice, soybean and wheat, expressed as RRs. Black dots indicate the mean of all RRs for each crop-outcome-method combination, while error bars give the 95% confidence interval. Text below bars gives the mean value (top line), number of simulation-observation pairs (N), and p-values based on a Welch's two-sample paired t-test (P). N- and P- values are given for both bars within each panel for clarity, even though they are identical by definition. Blank panels had too few observations for statistical analysis.

The major takeaway from Figure 5.3 for C_3 crops is that DayCent's default parameter values overestimate crop growth responses to eCO_2, compared to a range of FACE experiments. The simulated vs. observed RRs for grain yield and AGB showed highly significant ($p < 0.01$) differences for all C_3 crops tested. With the exception of soybean AGB ($N = 9$), each of these differences was based on at least 10 simulation-observation pairs. Likewise, simulated C:N response exceeded the observed value for all three C_3 crops ($p < 0.05$), although for soybean this difference rested on only two simulation-observation pairs. Data for R:S ratio response to eCO_2 were relatively sparse and inconsistent. No crops showed a significant effect of eCO_2 on R:S ratio, or a significant difference between observed and simulated R:S ratio RRs. Thus, the available data from these experiments do not support a significant impact of eCO_2 on R:S ratio for rice, soybean or wheat. Finally, there was a significant difference between simulated and observed season ET RR only for soybean. Interestingly, the simulated season transpiration actually increased under eCO_2 for soybean (mean increase of 0.8 cm, compensated by a 1.6 cm decrease in evaporation), despite the daily transpiration multiplier of 0.85. This was due to the large increases in simulated canopy cover under eCO_2, which increased absolute crop water use even as the daily scalar reduced use on a relative basis.

Calibrated CO_2 parameter values and performance

Figure 5.4 summarizes RRs obtained after calibrating the CO_2 response parameters to reproduce the observed RRs shown in Figure 5.3. For C_4 crops, the daily multiplier on crop transpiration was increased slightly (i.e., closer to unity). The daily growth and maximum C:N ratio multipliers were reduced for each of the C_3 crops. The multiplier on belowground allocation was left at unity for all crops, as the observed RRs for R:S ratio were not significantly different from unity (no effect). The newly calibrated DayCent CO_2 response parameter values are given in

Table 5.3, along with the process scalars that would obtain for each given a simulation [CO_2] of 550 ppm.

Table 5.3. DayCent crop CO_2 response parameter values after calibration to match observed RRs. Each parameter represents a crop-specific multiplier on the corresponding daily process for a doubling of [CO_2] from 350 to 700 ppm. Values following parameters are the change from default value (n.c.: no change), while those in parentheses are the actual daily scalars active at 550 ppm, interpolated using the logarithmic curve employed by DayCent.

Crop →	C_4	Rice	Soybean	Wheat
Growth	1.00, n.c. (1.00)	1.21, -0.09 (1.14)	1.12, -0.18 (1.08)	1.22, -0.08 (1.14)
Transpiration	0.82, +0.05 (0.88)	0.75, -0.02 (0.84)	0.58, -0.19 (0.73)	0.88, +0.11 (0.92)
Max C:N	1.00, n.c. (1.00)	1.05, -0.25 (1.03)	1.00, -0.30 (1.00)	1.08, -0.22 (1.05)
Root Allocation	1.00, n.c. (1.00)	1.00, n.c. (1.00)	1.00, n.c. (1.00)	1.00, n.c (1.00)

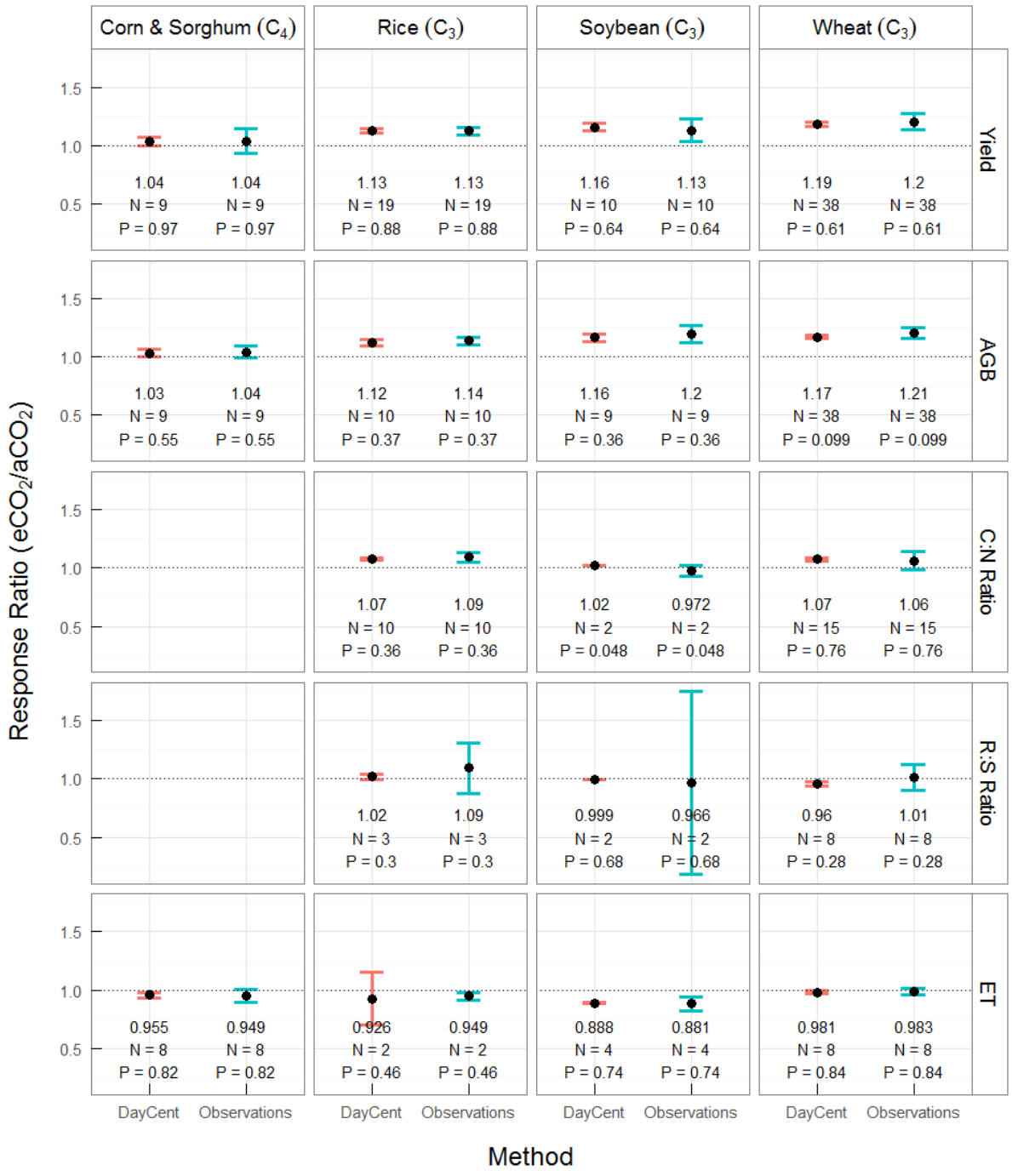

Figure 5.4. Observed and FACE-calibrated DayCent crop responses to eCO_2 for C_4 (corn and sorghum), rice, soybean and wheat, expressed as RRs. Black dots indicate the mean of all RRs for each crop-outcome-method combination, while error bars give the 95% confidence interval. Text below bars gives the mean value (top line), number of simulation-observation confidence interval. Text below bars gives the mean value (top line), number of simulation-observation pairs (N), and p-values based on a Welch's two-sample paired t-test (P). N- and P-values are given for both methods within each panel for clarity, even though they are identical by definition. Blank panels had too few observations for statistical analysis.

Calibrated CO_2 parameter stress performance

A major complicating factor in projecting crop response to [CO_2] concerns its interactions with abiotic and biotic stresses. Several of the FACE experiments included treatments with stress covariates designed to explore these interactions. In order to assess DayCent's ability to predict the role of abiotic stressors in the CO_2 responses, the data underlying Figure 5.3 and Figure 5.4 were pooled across C_3 crops (ie., rice, soybean and wheat) and grouped according to experimental stress treatments. Specifically, FACE observations were categorized as Unstressed, Water Stress, N Stress, or Heat Stress according to the experimenter's original designations. Any treatments that explicitly involved multiple stressors were excluded from this analysis.

The RRs obtained for simulated and observed outcomes grouped according to stress treatment are shown in Figure 5.5. Note that the results in Figure 5.5 exclude C_4 crops, which are typically analyzed separately due to their theoretical (and experimentally apparent) photosynthetic insensitivity to [CO_2].

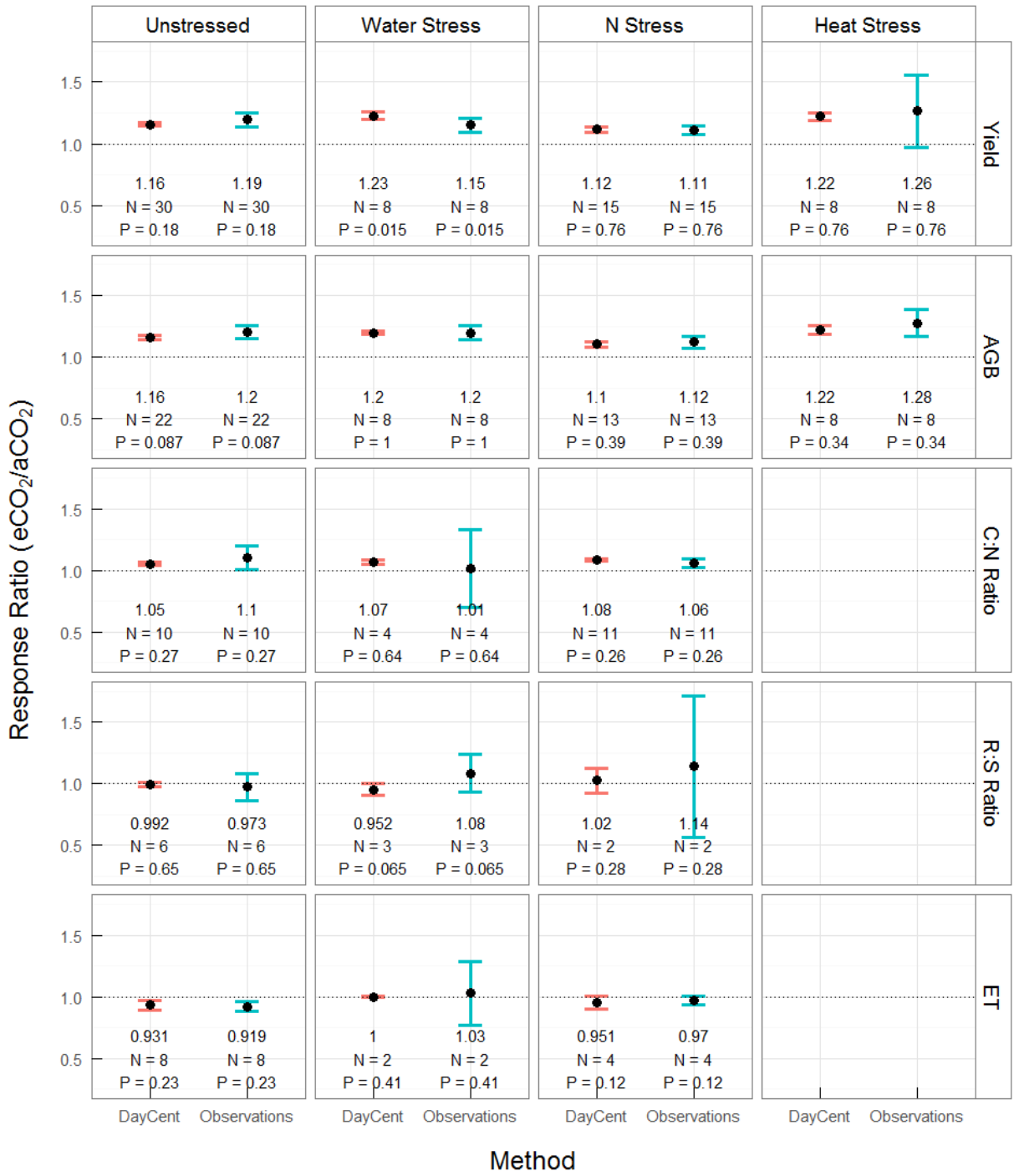

Figure 5.5. Observed and FACE-calibrated DayCent crop responses to eCO_2 for Unstressed, Water Stressed, N Stressed and Heat Stressed C_3 crops, expressed as RRs. Black dots indicate the mean of all RRs for each stress-outcome-method combination, while error bars give the 95% confidence interval. Text below bars gives the mean value (top line), number of simulation-observation pairs (N), and p-values based on a Welch's two-sample paired t-test (P). N- and P-values are given for both methods within each panel for clarity, even though they are identical by definition. Blank panels had too few observations for statistical analysis.

It is difficult to draw firm conclusions from Figure 5.5 about modeled or measured interactions between crop [CO_2] response and specific stressors because, even after pooling across C_3 crops, the observational evidence is sparse. The results in Figure 5.5 demonstrate DayCent's ability to reproduce some broad expected and/or observed effects of stress on crop responses to [CO_2]. The simulated RRs for water stress treatments were significantly greater than those for unstressed treatments for yield and AGB. This agrees directionally (though not statistically) with the corresponding observed RRs, as well as with some theory and evidence that growth responses to eCO_2 will be greater in the context of water stress (see, for example, Ainsworth *et al.*, 2008b). In an extreme instance, Lam *et al.*, (2012c) found a 60% increase in rainfed wheat yield and AGB in 2009, versus only 4% for the irrigated treatment.

Interestingly, both observed and simulated water stressed treatments in Figure 5.5 showed higher (i.e., closer to unity) RRs for season ET than unstressed equivalents. This is intuitively reasonable, as sufficiently water-stressed plants under eCO_2 may be expected to use all available water (as will unstressed plants), whereas if water is sufficient for aCO_2 plants then it will likely exceed the demand of eCO_2 plants and reduce season ET (discussed by Kimball & Bernacchi, 2006).

Both modeled and measured results showed decreased yield and AGB responses to eCO_2 for N stressed vs. unstressed treatments (both significant differences for modeled but nonsignificant for measured values). This directional trend aligns with the finding of a recent meta-analysis of FACE results, which showed that crop response to [CO_2] is significantly reduced in the context of N stress (Vanuytrecht *et al.*, 2012). N stress had a small but significant impact on simulated

but not measured C:N ratio response to [CO_2]. None of the remaining outcome metrics showed significant modeled or measured differences due to N stress.

Three experiments simulated for this work explicitly attempted to study the role of heat stress. Two of those experiments were conducted in Champaign, IL and used infrared heating elements to raise canopy temperatures of corn (1 season; Ruiz-Vera *et al.*, 2015b) and soybean (2 seasons; Ruiz-Vera *et al.*, 2013). The third experiment was conducted with spring wheat in Horsham, Australia, and used a later-than-usual time of sowing combined with supplemental irrigation to reduce the confounding influence of differing rainfall totals (Norton *et al.*, 2008; Lam *et al.*, 2012c; Fitzgerald *et al.*, 2016). The Heat Stress column of Figure 5.5 excludes results from C_4 crops, however, and so sample sizes are small. Simulated RRs for yield and AGB were significantly increased under heat stress, however, measured results were highly variable. In the infrared heating experiments with soybean, the observed yield response to eCO_2 for heated treatments was 1.26 in 2009 and 0.84 in 2011. Among a range of factors, the authors attributed a significant amount of this difference to the warmer temperatures during the 2011 growing season (Ruiz-Vera *et al.*, 2013). This underscores the fact that crop growth occurs relative to crop-, cultivar- and growth phase-specific optima (see, for example, Hatfield *et al.*, 2011), and a systematic increase in temperature may move crops closer to this optimum or beyond it, depending on baseline conditions.

Discussion

DayCent CO_2 process history

As mentioned previously, the DayCent crop [CO_2] response algorithms and default parameter values were originally developed for monthly Century by Metherell (1992) prior to the

availability of results from large-scale, replicated FACE experiments. Those defaults implemented scalars of 1.3 on monthly growth and maximum C:N ratios for C_3 crops, and a scalar of 0.77 on monthly transpiration for C_3 and C_4 crops, with logarithmic down-scaling from the benchmark eCO_2 of 700 ppm. The original Century algorithm was tested in a series of long-term simulations of four Colorado sites under various climate change weather scenarios, and several rotations involving corn, sorghum, millet and wheat. Yield RRs from growth at 700 ppm [CO_2] averaged over 72 simulation years were 1.62, 1.08, 1.04, and 0.97 for wheat, corn, millet and sorghum, respectively. The dramatic increase in yield for wheat was beyond the consensus estimates of any broad literature surveys, including the reviews of Kimball (1983) and Cure & Acock (1986) cited as major sources for the parameterization of Metherell (1992). By contrast, the results from C_4 crops corn, millet and sorghum align well with observations from enclosures and FACE experiments.

When daily DayCent was developed from the Century code base, it inherited the foregoing algorithm and parameter values from Century. The RRs presented in Figure 5.3 reflect the first test of this algorithm and parameter set against results from FACE experiments. For each of the C_3 crops considered, the simulated RRs for yield were significantly higher than measurements. For C_4 crops (here pooling data from corn and sorghum), however, the default parameterization was remarkably accurate versus an admittedly small set of measurements for yield, AGB, and season ET. This general overestimation of C_3 crop responses hardly stands as a conclusive test for "true" methodological differences between enclosures and FACE experiments. However, it does support the contention of Ainsworth *et al.* (2008b) that crop model [CO_2] response algorithms parameterized using enclosure results overestimate RRs when compared with FACE results.

DayCent simulated responses vs. literature reviews

The yield enhancement factors simulated by DayCent using its default parameter values and the new, FACE-calibrated values, were compared with several literature sources (Figure 5.6). Results from DayCent modeling using enclosure-calibrated CO_2 response factors appear as green bars with black outlines. Results obtained following calibration to the FACE training observations are shown as orange bars with black outlines. Mean RRs reported by literature reviews of enclosure and FACE experiments are depicted by green and orange bars without outlines, respectively. Note that literature estimates derived from experiments using high (>600 ppm) enriched [CO_2] were been down-scaled to 550 ppm using a logarithmic curve for interpolation.

The goal of Figure 5.6 is to give broad context for DayCent's CO_2 response performance before and after calibration. The literature sources overlapped considerably in terms of their underlying experimental data, and so these values cannot support quantitative inferences about differences between enclosure and FACE experimental methods. DayCent performance at simulating C_4 crop response to CO_2 was substantially below the early estimate of Cure & Acock (1986) and closely aligned with the training observations used in this study. This is relatively unsurprising, since Metherell (1992) conservatively chose to align the C_4 crop parameterization with theory by setting C_4 the direct growth scalar to unity. While the FACE literature on CO_2 response of annual C_4 crops remains limited, the results are consistently low, with most authors finding negligible yield enhancement except in times of water stress (Ottman *et al.*, 2001; Wall *et al.*, 2001; Leakey *et al.*, 2006; Hussain *et al.*, 2013).

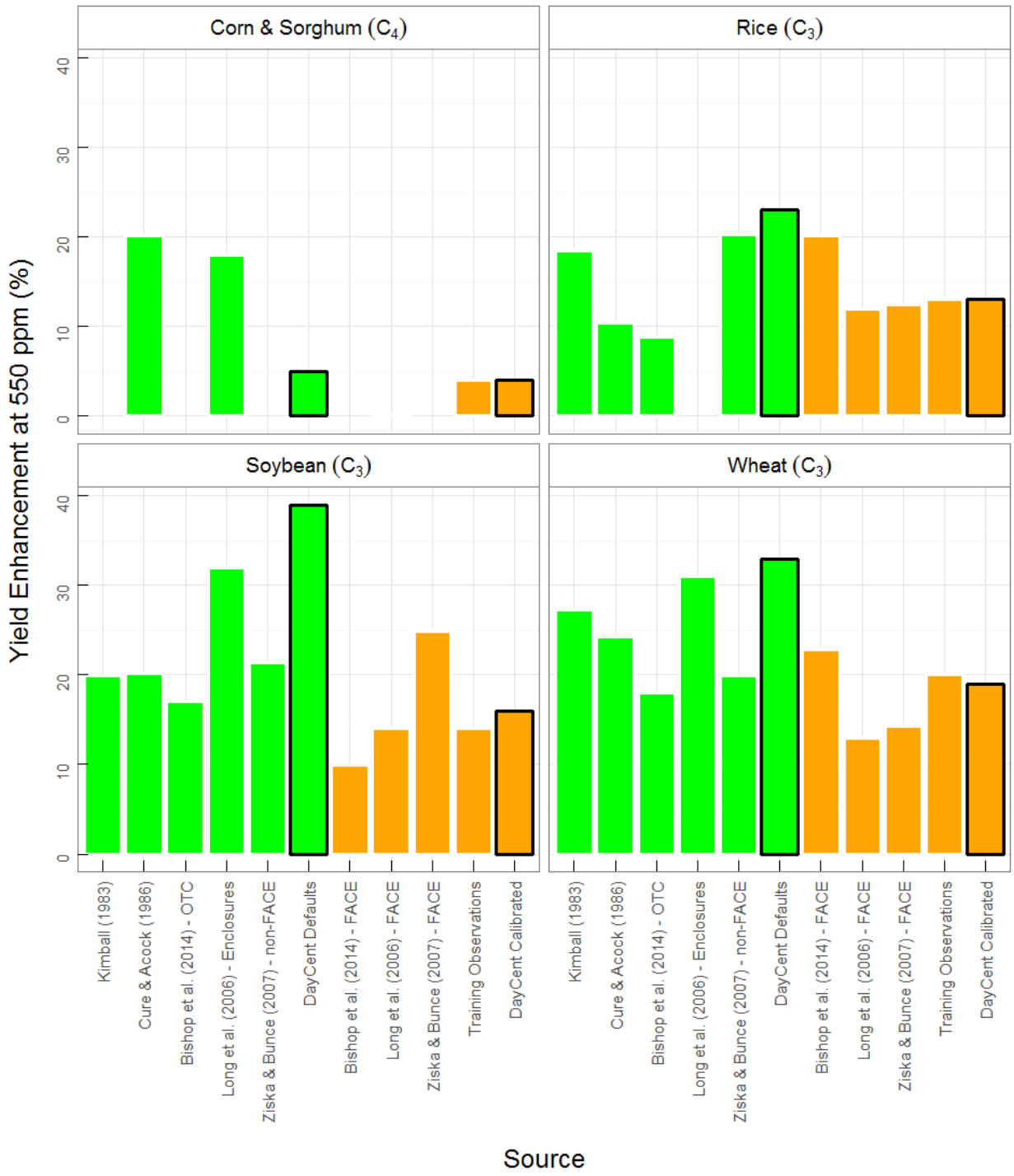

Figure 5.6. Yield enhancement factors simulated by DayCent (black outlines) using default [CO_2] response parameter values and FACE-calibrated parameter values, compared with various literature sources (no outlines). Green bars indicate observations from enclosure methodologies (and simulations of FACE experiments using enclosure-derived default parameter values), while orange bars indicate observations from FACE experiments (and FACE-calibrated simulations). Kimball (1983) and Cure & Acock (1986) were the primary sources for the DayCent Defaults

parameterization by Metherell (1992). Where literature sources reported results corresponding to eCO_2 levels above 600 ppm, enhancement factors were scaled to 550 ppm using a logarithmic curve for interpolation. Results from Ziska & Bunce (2007) for "Non-FACE" methods represent an observation-weighted average across the specific enclosure categories given in their data tables. Also note that the analysis of Bishop et al. (2014) included only observations from the least-stressed treatment in each study.

DayCent un-calibrated performance with C_3 crops was mixed, but yield responses were generally over-estimated relative to FACE results. Perhaps most notable is that DayCent default parameter results equaled or exceeded the highest literature estimates for C_3 crops regardless of experimental methodology. For rice, the literature sources shown in Figure 5.6 show large variability within enclosure and FACE methodologies. In particular, the analysis of (Bishop *et al.*, 2014) found a mean rice yield enhancement under FACE (~20%) that was actually *higher* than the enhancement under open-top chambers (OTC) (~8%), after adjusting for the higher mean eCO_2 level of OTC studies. That FACE result differs from the mean enhancement of the FACE training observations used for calibration here (13%). Part of this divergence may relate to the selection criterion of (Bishop *et al.*, 2014) to exclude treatments with stress covariates. For example, the experiments at Shizukuishi used here for model training were also a part of the Bishop dataset, but several observations involved N limitation and so would have been excluded. At the same time, the Bishop analysis included two sites in China and one site in Japan that were not simulated for our analysis. Such differences in underlying data, combined with analytical choices such as curve fitting for adjustment of differing aCO_2/eCO_2 levels, likely account for much of the inter-study variation visible in Figure 5.6.

The literature results for soybean also show substantial variability. In this case, (Ziska & Bunce, 2007) reported FACE results that are greater than an observation-weighted average of non-FACE results (25% vs 21% after adjusting to 550 ppm eCO_2). As they noted, however, this FACE

estimate was based on only four observations, one of which reported an 85% yield enhancement from an eCO_2 of 685 ppm using potted plants and a natural CO_2 spring (Miglietta *et al.*, 1993). While these are hardly disqualifying circumstances, the adjusted 54% result was much higher than the highest observed yield enhancement in the training observations used here (34%, from 10 observations).

The DayCent default results for soybean were much higher than any of the literature estimates, and nearly 3-fold greater than the training observations (39% vs 14% yield enhancement). Note that each of the DayCent Defaults bars for C_3 crops in Figure 5.6 resulted from the same set of CO_2 response parameters (given in Table 5.2). As part of investigating this phenomenon, we created a DayCent soybean crop lacking the ability to fix nitrogen and ran the exact same set of FACE simulations. The resulting mean yield enhancement was 22%, indicating that DayCent-simulated soybean responsiveness was facilitated by its ability to fix N. A similar difference was observed by (Ainsworth *et al.*, 2002), who found in a meta-analysis of the soybean eCO_2 literature that nodulated varieties showed 3-fold higher photosynthetic stimulation than non-nodulated varieties. This difference emerges in DayCent from a simplified representation of plant N limitation and photosynthesis, but is nonetheless an interesting correspondence with observed trends. Ainsworth *et al.* (2002) also found a significant reduction in harvest index (~8%) for soybean crops under eCO_2. This was reflected in the training observations for this work, with mean enhancements of 20% and 14% for AGB and yield, respectively, translating to a 30% reduction in harvest index. DayCent lacks a mechanism for modifying harvest index in response to $[CO_2]$ so parameter values were calibrated to split the difference between the observed AGB and yield stimulation rates. If future experimental work corroborates a reduction in harvest index, addition of a parameter to replicate this finding may be warranted.

Among the wheat literature estimates in Figure 5.6, Bishop *et al.* (2014) again reported a FACE value that was higher than their [CO_2]-adjusted result from OTCs. Wheat also had the highest yield RR based on the training observations (1.20) out of all crops studied here. A closer look at the underlying studies shows that the results presented by Fitzgerald *et al.* (2016) from Horsham, Australia had a major influence on this value. That work tested two wheat cultivars over three years at two water levels and two sowing dates (used as a proxy for heat stress), giving a total of 24 eCO_2/aCO_2 RRs. Out of that, three RRs exceeded 1.70 (all from wet treatments), eight were at least 1.35, and two were less than 0.90, though all AGB RRs were greater than 1.0. The reasons for these unusual RRs were not obvious, and several hypotheses were offered by Fitzgerald *et al.* (2016). It is notable that the wheat crops at Horsham were subject to more severe water limitation and produced lower yields than wheat from the other two sites simulated for our analysis (Figure A6). The large RRs observed at Horsham may represent a highly-stressed CO_2-response space not previously explored under FACE conditions.

CO_2-by-stress interactions

DayCent showed a qualitative ability to reproduce the increased [CO_2] fertilization effect that has been predicted and observed in crops subject to drought stress (eg., Kimball *et al.*, 1995; Ottman *et al.*, 2001; Leakey *et al.*, 2006). The meta-analysis of Bishop *et al.* (2014) found significantly decreasing yield (but not AGB) responses to eCO_2 with increasing growing season water input. On the other hand, recent rain-exclusion FACE experiments in Illinois indicate that moderate to severe drought stress *reduces or eliminates* eCO_2 fertilization due to a combination of greater early-season LAI development, elevated canopy temperatures, and greater plant responsiveness to abscisic acid signaling among eCO_2-grown plants (Gray *et al.*, 2016).

The training observations showed a modest reduction in yield response for N-stress treatments (Figure 5.5) vs. unstressed treatments that is also apparent in the simulated responses. The few yield and AGB observations from controlled heat stress treatments simulated for this work showed very large variability in their response to eCO_2. In contrast, the DayCent-simulated values showed greater responsiveness to eCO_2 in the heated treatments. This may reflect problems with the high-temperature region of DayCent's temperature-response curve, or differential timing of high absolute temperatures (from which heat treatments were a constant amount of increase) relative to sensitive periods of crop growth. Since DayCent uses a constant temperature-response curve throughout the season, it does not represent the disproportionate effects of heat stress at critical times such as flowering and grain filling.

Other outcomes

The data for outcomes other than yield and ABG among the training observations was limited but did permit some calibration of the transpiration, max C:N ratio, and belowground C allocation parameters. Measurements of season ET from FACE experiments showed consistent reductions in water use among eCO_2-grown crops (Hunsaker *et al.*, 2000; Conley *et al.*, 2001; Hussain *et al.*, 2013; Bernacchi & VanLoocke, 2014), though various feedbacks complicate the relationship between season-long ET and daily canopy transpiration (the quantity modified by the relevant DayCent parameter).

Observations of shoot or grain C:N concentration were more limited and highly variable. The largest review of eCO_2 literature focused on this outcome found mean increases in C:N ratio of 13, 28, 6 and 19% for corn, rice, soybean and wheat (Cotrufo *et al.*, 1998). Most of the underlying experiments for that study were conducted at eCO_2 levels well above the 550 ppm

used in many FACE sites, however, and only the effect for wheat was statistically significant (Cotrufo *et al.*, 1998). Theory would suggest that C_4 crops would show less change in C:N ratio (because of their smaller AGB response) under eCO_2, while soybean should be insulated by its ability to fix N from the atmosphere (at the cost of biomass C, cf. Leakey *et al.*, 2009). A recent review of N content of FACE-grown crops supported those predictions (Myers *et al.*, 2014). Thus, the calibration adopted here left the max C:N effect parameters at unity for corn and soy, while setting values that achieved relatively modest 7% increases for rice and wheat (Figure 5.4). More data are needed to understand the effect of eCO_2 on N content of major grain crops other than wheat, particularly corn and rice.

The most variable outcome by far in the training observations was for the $[CO_2]$ effect on R:S ratio. None of the crops had more than six RR values among the training observations used here, and none of the mean RRs were significantly different from unity (no effect). In a large review of the eCO_2 enclosure literature, Rogers *et al.* (1996) found that 59.5% of R:S ratios responses were positive and 37.5% were negative. In a recent review of the FACE literature, Vanuytrecht *et al.* (2012) found a significant positive response of R:S ratio to eCO_2. The analysis pooled responses across several crops not considered for this work, however, including root crops (potato, sugar beet) and perennials (perennial ryegrass, white clover) that may be expected to respond differently from the annual crops considered here. In view of the continued uncertainty among R:S ratio responses to eCO_2 regardless of methodology, we opted to leave the DayCent belowground C allocation parameters at unity.

Conclusions

This study tested the default DayCent CO_2 response parameters against FACE experimental observations across four major crops and five crop processes. In general, the default parameters overestimated yield and AGB responses for C_3 crops, while closely matching the few available data points from C_4 crops. Parameter values were calibrated to reproduce the observed RRs from FACE experiments where a consistent effect was discernible, while parameters controlling effects with weak observational support were conservatively left at unity. Now that FACE experiments have established a solid consensus on the effect ranges of yield, AGB and ET under open-air eCO_2 conditions, work should be targeted at clarifying the effect sizes and mechanisms underlying changes in AGB N content and C allocation.

BIBLIOGRAPHY

Abdalla M, Osborne B, Lanigan G, Forristal D, Williams M, Smith P, Jones MB (2013) Conservation tillage systems: A review of its consequences for greenhouse gas emissions. *Soil Use and Management*, **29**, 199–209.

Adler PR, Del Grosso SJ, Parton WJ (2004) Modeling Greenhouse Gas Emissions from Bioenergy Cropping Systems in Pennsylvania Using DAYCENT. In: *ASA-CSSA-SSSA Annual Meeting Abstracts*, p. Paper No. 5886.

Adler PR, Del Grosso SJ, Parton WJ (2007) Life-cycle assessment of net greenhouse-gas flux for bioenergy cropping systems. *Ecological Applications*, **17**, 675–691.

Ainsworth E, Long S (2005) What have we learned from 15 years of free-air CO_2 enrichment (FACE)? A meta-analytic review of the responses of photosynthesis, canopy properties and plant production to rising CO_2. *New Phytologist*, **165**, 351–71.

Ainsworth E, Rogers A (2007) The response of photosynthesis and stomatal conductance to rising [CO_2]: mechanisms and environmental interactions. *Plant Cell and Environment*, **30**, 258–270.

Ainsworth EA, Davey PA, Bernacchi CJ et al. (2002) A meta-analysis of elevated [CO_2] effects on soybean (Glycine max) physiology, growth and yield. *Global Change Biology*, **8**, 695–709.

Ainsworth E, Leakey A, Ort D, Long S (2008a) FACE-ing the facts: inconsistencies and interdependence among field, chamber and modeling studies. *New Phytologist*, **179**, 1–3.

Ainsworth EA, Beier C, Calfapietra C et al. (2008b) Next generation of elevated [CO_2] experiments with crops: a critical investment for feeding the future world. *Plant Cell and*

Environment, **31**, 1317–1324.

Alderman P, Quilligan E, Asseng S, Ewert F, Reynolds M (2013) Modeling wheat response to high temperature. In: *Modeling wheat response to high temperature*, p. 142. CIMMYT, El Batan, Mexico.

Allen L, Boote K, Jones J (1987) Response of vegetation to rising carbon dioxide: photosynthesis, biomass, and seed yield of soybean. *Global Biogeochemical Cycles*, **1**, 1–14.

Allmaras R, Schomberg H, Douglas Jr. C, Dao T (2000) Soil organic carbon sequestration potential of adopting conservation tillage in U.S. croplands. *Journal of Soil and Water Conservation*, **55**, 365–373.

Amthor JS, Hanson PJ, Norby RJ, Wullschleger SD (2010) A comment on "Appropriate experimental ecosystem warming methods by ecosystem, objective, and practicality" by Aronson and McNulty. *Agricultural and Forest Meteorology*, **150**, 497–498.

Anderson CJ, Babcock BA, Peng Y, Gassman PW, Campbell TD (2015) Placing bounds on extreme temperature response of maize. *Environmental Research Letters*, **10**, 1–8.

Asensio JSR, Rachmilevitch S, Bloom AJ (2015) Responses of Arabidopsis and wheat to rising CO_2 depend on nitrogen source and nighttime CO_2 levels. *Plant physiology*, **168**, 156–63.

Asseng S (2013) Uncertainty in simulating wheat yields under climate change. *Nature Climate Change*, **3**, 627–632.

Asseng S, Ewert F, Martre P et al. (2014) Rising temperatures reduce global wheat production. *Nature Climate Change*, **5**, 143–147.

Baker JM, Ochsner TE, Venterea RT, Griffis TJ (2007) Tillage and soil carbon sequestration—What do we really know? *Agriculture, Ecosystems & Environment*, **118**, 1–5.

Ball JT, Woodrow IE, Berry JA (1987) A Model Predicting Stomatal Conductance and its Contribution to the Control of Photosynthesis under Different Environmental Conditions. In: *Prog. Photosynth. Res.*, pp. 221–224. Springer Science+Business Media, Dordrecht.

Barlow KM, Christy BP, O'Leary GJ, Riffkin PA, Nuttall JG (2015) Simulating the impact of extreme heat and frost events on wheat crop production: A review. *Field Crops Research*, **171**, 109–119.

Basso B, Ritchie J (2014) Temperature and drought effects on maize yield. *Nature Climate Change*, **4**, 233.

Basso B, Gargiulo O, Paustian K, Robertson GP, Porter C, Grace PR, Jones JW (2011) Procedures for Initializing Soil Organic Carbon Pools in the DSSAT-CENTURY Model for Agricultural Systems. *Soil Science Society of America Journal*, **75**, 69.

Bassu S, Brisson N, Durand J-L et al. (2014) How do various maize crop models vary in their responses to climate change factors? *Global Change Biology*, **20**, 2301–2320.

Bernacchi CJ, VanLoocke A (2014) Terrestrial Ecosystems in a Changing Environment: A Dominant Role for Water. *Annual Review of Plant Biology*, **66**, 599–622.

Bernacchi CJ, Kimball BA, Quarles DR, Long SP, Ort DR (2007) Decreases in stomatal conductance of soybean under open-air elevation of [CO_2] are closely coupled with decreases in ecosystem evapotranspiration. *Plant physiology*, **143**, 134–144.

Bishop K, Leakey A, Ainsworth E (2014) How seasonal temperature or water inputs affect the relative response of C3 crops to elevated [CO_2]: a global analysis of open top chamber and free air CO_2 enrichment studies. *Food and Energy Security*, **3**, 33–45.

Bishop KA, Betzelberger AM, Long SP, Ainsworth EA (2015) Is there potential to adapt soybean (Glycine max Merr.) to future [CO_2]? An analysis of the yield response of 18

genotypes in free-air CO_2 enrichment. *Plant, Cell and Environment*, **38**, 1765–1774.

Blanchet K, Schmitt M (2007) Manure Management in Minnesota. , pp. 1–12. University of Minnesota Extension, St. Paul, MN.

Blanco-Canqui H, Lal R (2009) Corn Stover Removal for Expanded Uses Reduces Soil Fertility and Structural Stability. *Soil Science Society of America Journal*, **73**, 418.

Bloom AJ (2015a) The increasing importance of distinguishing among plant nitrogen sources. *Current Opinion in Plant Biology*, **25**, 10–16.

Bloom AJ (2015b) Photorespiration and nitrate assimilation: A major intersection between plant carbon and nitrogen. *Photosynthesis Research*, **123**, 117–128.

Bloom A, Burger M, Rubio Asensio J, Cousins A (2010) Carbon dioxide enrichment inhibits nitrate assimilation in wheat and Arabidopsis. *Science*, **328**, 899–904.

Bloom AJ, Rubio Asensio JS, Randall L, Rachmilevitch S, Cousins AB, Carlisle E a. (2012) CO_2 enrichment inhibits shoot nitrate assimilation in C3 but not C4 plants and slows growth under nitrate in C3 plants. *Ecology*, **93**, 355–367.

Bloom A, Burger M, Kimball B, PJ P (2014) Nitrate assimilation is inhibited by elevated CO_2 in field-grown wheat. *Nature Climate Change*, **4**, 477–180.

Bondeau A, Smith PC, Zaehle S et al. (2007) Modelling the role of agriculture for the 20th century global terrestrial carbon balance. *Global Change Biology*, **13**, 679–706.

Boote KJ, Allen LH, Prasad PV V, Jones JW (2011) Testing effects of climate change in crop models. In: *Handbook of Climate Change and Agroecosystems* (eds Hillel D, Rosenzweig C), pp. 109–129. Imperial College Press.

Bunce JA (2012) Responses of cotton and wheat photosynthesis and growth to cyclic variation in carbon dioxide concentration. *Photosynthetica*, **50**, 395–400.

Bunce JA (2016) Responses of soybeans and wheat to elevated CO_2 in free-air and open top chamber systems. *Field Crops Research*, **186**, 78–85.

Bureau of Labor Statistics: Inflation Calculator (2015) *US Bureau of Labor Statistics*, http://www.bls.gov/data/inflation_calculator.htm.

Butler EE, Huybers P (2013) Adaptation of US maize to temperature variations. *Nature Climate Change*, **3**, 68–72.

Butler EE, Huybers P (2015) Variations in the sensitivity of US maize yield to extreme temperatures by region and growth phase. *Environmental Research Letters*, **10**, 1–8.

Buyanovsky G a., Wagner GH (1998) Carbon cycling in cultivated land and its global significance. *Global Change Biology*, **4**, 131–141.

Cai C, Yin X, He S et al. (2015) Responses of wheat and rice to factorial combinations of ambient and elevated CO 2 and temperature in FACE experiments. *Global Change Biology*, **86**, 856–874.

Camargo GGT, Ryan MR, Richard TL (2013) Energy Use and Greenhouse Gas Emissions from Crop Production Using the Farm Energy Analysis Tool. *BioScience*, **63**, 263–273.

Carter EK (2015) *Heat stress in irrigated maize*. Cornell University, 1-107 pp.

Chamberlain JF, Miller SA, Frederick JR (2011) Using DAYCENT to quantify on-farm GHG emissions and N dynamics of land use conversion to N-managed switchgrass in the Southern US. *Agriculture, Ecosystems & Environment*, **141**, 332–341.

Chang K-H, Warland J, Voroney P, Bartlett P, Wagner-Riddle C (2013) Using DayCENT to Simulate Carbon Dynamics in Conventional and No-Till Agriculture. *Soil Science Society of America Journal*, **77**, 941–950.

Cheng L, Booker FL, Tu C et al. (2012) Arbuscular Mycorrhizal Fungi Increase Organic Carbon

Decomposition Under Elevated CO_2. *Science*, **337**, 1084–1087.

Clay DE, Chang J, Clay S a. et al. (2012) Corn yields and no-tillage affects carbon sequestration and carbon footprints. *Agronomy Journal*, **104**, 763–770.

Collatz GJ, Ball JT, Grivet C, Berry JA (1991) Physiological and Environmental-Regulation of Stomatal Conductance, Photosynthesis and Transpiration - a Model That Includes a Laminar Boundary-Layer. *Agricultural and Forest Meteorology*, **54**, 107–136.

Collins M, Knutti R, Arblaster J et al. (2013) Long-term Climate Change: Projections, Commitments and Irreversibility. In: *Climate Change 2013: The Physical Science Basis. Contribution of Working Group I to the Fifth Assessment Report of the Intergovernmental Panel on Climate Change* (eds Stocker T, Qin D, Plattner G-K, Tignor M, Allen S, Boschung J, Nauels A, Xia Y, Bex V, Midgley P), pp. 1029–1136. Cambridge University Press, Cambridge, UK.

Conant RT, Ogle SM, Paul EA, Paustian K (2011) Measuring and monitoring soil organic carbon stocks in agricultural lands for climate mitigation. *Frontiers in Ecology and the Environment*, **9**, 169–173.

Conley MM, Kimball BA, Brooks TJ et al. (2001) CO_2 enrichment increases water-use efficiency in sorghum. *New Phytologist*, **151**, 407–412.

Cotrufo MF, Ineson P, Scott A (1998) Elevated CO_2 reduces the nitrogen concentration of plant tissues. *Global Change Biology*, **4**, 43–54.

Cure J, Acock B (1986) Crop responses to carbon dioxide doubling: a literature survey. *Agricultural and Forest Meteorology*, **38**, 127–145.

Davis SC, Boddey RM, Alves BJR et al. (2013) Management swing potential for bioenergy crops. *GCB Bioenergy*, **5**, 623–638.

Deryng D, Conway D, Ramankutty N, Price J, Warren R (2014) Global crop yield response to extreme heat stress under multiple climate change futures. *Environmental Research Letters*, **9**, 34011.

Deryng D, Elliott J, Folberth C et al. (2016) Regional disparities in the beneficial effects of rising CO_2 concentrations on crop water productivity. *Nature Climate Change*, 1–5.

Drake BG, Gonzalez-Meler MA, Long SP (1997) MORE EFFICIENT PLANTS: A Consequence of Rising Atmospheric CO_2? *Annual review of plant physiology and plant molecular biology*, **48**, 609–639.

Elliott J, Müller C, Deryng D et al. (2015) The Global Gridded Crop Model Intercomparison: Data and modeling protocols for Phase 1 (v1.0). *Geoscientific Model Development*, **8**, 261–277.

Emery IR (2013) *Direct and Indirect Greenhouse Gas Emissions from Biomass Storage : Implications for Life Cycle Assessment of Biofuels*. Purdue University, Open Access Dissertations, Paper 177.

EPA (2015) *Inventory of U . S . Greenhouse Gas Emissions and Sinks : 1990-2013*. Washington, DC, 1-564 pp.

Erbs M, Manderscheid R, Huther L, Schenderlein A, Wieser H, Danicke S, Weigel H-J (2015) Free-air CO_2 enrichment modifies maize quality only under drought stress. *Agronomy for Sustainable Development*, **35**, 203–212.

Eyshi Rezaei E, Webber H, Gaiser T et al. (2014) Heat stress in cereals : Mechanisms and modelling. *European Journal of Agronomy*, **64**, 98–113.

Fang S, Su H, Liu W, Tan K, Ren S (2013) Infrared Warming Reduced Winter Wheat Yields and Some Physiological Parameters, Which Were Mitigated by Irrigation and Worsened by

Delayed Sowing. *PLoS ONE*, **8**, 19–22.

Fargione JE, Plevin RJ, Hill JD (2010) The ecological impact of biofuels. *Annual Review of Ecology, Evolution, and Systematics*, **41**, 351–377.

Farooq M, Bramley H, Palta JA, Siddique KHM (2011) Heat Stress in Wheat during Reproductive and Grain-Filling Phases. *Critical Reviews in Plant Sciences*, **30**, 491–507.

Farquhar GD, von Caemmerer S (1982) Modelling of Photosynthetic Response to Environmental Conditions. In: *Physiological Plant Ecology II*, pp. 549–587. Springer Berlin Heidelberg, Berlin, Heidelberg.

Farquhar GD, Von Caemmerer S, Berry JA (1980) A Biochemical Model of Photosynthetic Assimilation in Leaves of C_3 Species. *Planta*, **90**, 78–90.

Feng Z, Rütting T, Pleijel H et al. (2015) Constraints to Nitrogen Acquisition of Terrestrial Plants under Elevated CO_2. *Global Change Biology*, 1–17.

Fisher BAC, Hanemann WM, Roberts MJ, Schlenker W (2012) The Economic Impacts of Climate Change: Evidence from Agricultural Output and Random Fluctuations in Weather: Comment. *The American Economic Review*, **102**, 3749–3760.

Fitzgerald G, Tausz M, O'Leary G et al. (2016) Elevated atmospheric [CO_2] can dramatically increase wheat yields in semi-arid environments and buffer against heat waves. *Global Change Biology*, **22**, 2269–2284.

Friedlingstein P, Andrew RM, Rogelj J et al. (2014) Persistent growth of CO_2 emissions and implications for reaching climate targets. *Nature Geoscience*, **7**, 709–715.

Fronning BE, Thelen KD, Min DH (2008) Use of manure, compost, and cover crops to supplant crop residue carbon in corn stover removed cropping systems. *Agronomy Journal*, **100**, 1703–1710.

Gabaldon-Leal C, Webber H, Otegui ME et al. (2016) Modelling the impact of heat stress on maize yield formation. *Field Crops Research*, **198**, 226–237.

Gourdji SM, Sibley AM, Lobell DB (2013) Global crop exposure to critical high temperatures in the reproductive period: historical trends and future projections. *Environmental Research Letters*, **8**, 24041.

Graham RL, Nelson R, Sheehan J, Perlack RD, Wright LL (2007) Current and Potential U.S. Corn Stover Supplies. *Agronomy Journal*, **99**, 1–11.

Gray SB, Dermody O, Klein SP et al. (2016) Intensifying drought eliminates the expected benefits of elevated carbon dioxide for soybean. *Nature Plants*, **2**, 16132.

Del Grosso SJ, Parton WJ, Mosier AR et al. (2000) General CH 4 oxidation model and comparisons of CH4 oxidation in natural and managed systems biological limitation when water Optimum soil volumetric water content model performed well with the data used for model development values for Wop t , Wmi. *Global Biogeochemical Cycles*, **14**, 999–1019.

Del Grosso S, Ojima D, Parton W, Mosier A, Peterson G, Schimel D (2002) Simulated effects of dryland cropping intensification on soil organic matter and greenhouse gas exchanges using the DAYCENT ecosystem model. *Environmental Pollution*, **116**, S75–S83.

Del Grosso SJ, Mosier AR, Parton WJ, Ojima DS (2005) DAYCENT model analysis of past and contemporary soil N2O and net greenhouse gas flux for major crops in the USA. *Soil and Tillage Research*, **83**, 9–24.

Del Grosso SJ, Parton WJ, Mosier AR et al. (2006) DAYCENT national-scale simulations of nitrous oxide emissions from cropped soils in the United States. *Journal of environmental quality*, **35**, 1451–1460.

Del Grosso SJ, Halvorson AD, Parton WJ (2008) Testing DAYCENT model simulations of corn

yields and nitrous oxide emissions in irrigated tillage systems in Colorado. *Journal of environmental quality*, **37**, 1383–1389.

Del Grosso SJ, Ojima DS, Parton WJ, Stehfest E, Heistemann M, DeAngelo B, Rose S (2009) Global scale DAYCENT model analysis of greenhouse gas emissions and mitigation strategies for cropped soils. *Global and Planetary Change*, **67**, 44–50.

Del Grosso SJ, Ogle SM, Parton WJ, Breidt FJ (2010) Estimating uncertainty in N2O emissions from U.S. cropland soils. *Global Biogeochemical Cycles*, **24**.

Han X, Hao X, Lam SK et al. (2015) Yield and nitrogen accumulation and partitioning in winter wheat under elevated CO_2: A 3-year free-air CO_2 enrichment experiment. *Agriculture, Ecosystems & Environment*, **209**, 132–137.

Hao XY, Han X, Lam SK et al. (2012) Effects of fully open-air [CO_2] elevation on leaf ultrastructure, photosynthesis, and yield of two soybean cultivars. *Photosynthetica*, **50**, 362–370.

Hao X, Gao J, Han X et al. (2014) Effects of open-air elevated atmospheric CO_2 concentration on yield quality of soybean (Glycine max (L.) Merr). *Agriculture, Ecosystems & Environment*, **192**, 80–84.

Hao X, Li P, Han X et al. (2016) Effects of free-air CO_2 enrichment (FACE) on N, P, and K uptake of soybean in northern China. *Agricultural and Forest Meteorology*, **218**, 261–266.

Hartmann DL, Tank AMGK, Rusticucci M (2013) IPCC Fifth Assessment Report, Climate Change 2013: The Physical Science Basis. *IPCC*, **AR5**, 31–39.

Hasegawa T, Sakai H, Tokida T et al. (2013) Rice cultivar responses to elevated CO_2 at two free-air CO 2 enrichment (FACE) sites in Japan. *Functional Plant Biology*, **40**, 148–159.

Hatfield JL (2016) Increased Temperatures Have Dramatic Effects on Growth and Grain Yield

of Three Maize Hybrids. *Agricultural and Environmental Letters*, **1**, 1–5.

Hatfield JL, Boote KJ, Kimball BA et al. (2011) Climate impacts on agriculture: Implications for crop production. *Agronomy Journal*, **103**, 351–370.

Haworth M, Hoshika Y, Killi D (2016) Has the Impact of Rising CO 2 on Plants been Exaggerated by Meta-Analysis of Free Air CO 2 Enrichment Studies? *Frontiers in Plant Science*, **7**, 1–4.

Hendrey GR, Kimball BA (1994) The FACE program. *Agricultural and Forest Meteorology*, **70**, 3–14.

Hendrey GR, Lewin KF, Nagy J (1993) Free Air Carbon Dioxide Enrichment: Development, Progress, Results. *Vegetatio*, **104**, 16–31.

Hettinga WG, Junginger HM, Dekker SC, Hoogwijk M, McAloon AJ, Hicks KB (2009) Understanding the reductions in US corn ethanol production costs: An experience curve approach. *Energy Policy*, **37**, 109–203.

Hoegy P, Wieser H, Koehler P et al. (2009) Effects of elevated CO_2 on grain yield and quality of wheat: Results from a 3-year free-air CO_2 enrichment experiment. *Plant Biology*, **11**, 60–69.

Högy P, Wieser H, Köhler P et al. (2009) Effects of elevated CO_2 on grain yield and quality of wheat: results from a 3-year free-air CO_2 enrichment experiment. *Plant biology*, **11 Suppl 1**, 60–69.

Houshmandfar A, Fitzgerald GJ, Macabuhay AA, Armstrong R, Tausz-Posch S, Löw M, Tausz M (2016) Trade-offs between water-use related traits, yield components and mineral nutrition of wheat under Free-Air CO_2 Enrichment (FACE). *European Journal of Agronomy*, **76**, 66–74.

Hunsaker DJ, Kimball BA, Pinter PJ et al. (2000) CO_2 enrichment and soil nitrogen effects on

wheat evapotranspiration and water use efficiency. *Agricultural and Forest Meteorology*, **104**, 85–105.

Hussain MZ, Vanloocke A, Siebers MH et al. (2013) Future carbon dioxide concentration decreases canopy evapotranspiration and soil water depletion by field-grown maize. *Global Change Biology*, **19**, 1572–1584.

IAWG (2013) *Technical Update of the Social Cost of Carbon for Regulatory Impact Analysis*. Washington, DC, 1-22 pp.

Jacinthe PA, Dick WA, Lal R, Shrestha RK, Bilen S (2014) Effects of no-till duration on the methane oxidation capacity of Alfisols. *Biology and Fertility of Soils*, **50**, 477–486.

Jamieson PD, Berntsen J, Ewert F et al. (2000) Modelling CO_2 effects on wheat with varying nitrogen supplies. *Agricuture Ecosystems & Environment*, **82**, 27–37.

Jin Z, Zhuang Q, Tan Z, Dukes JS, Zheng B, Melillo JM (2016) Do maize models capture the impacts of heat and drought stresses on yield? Using algorithm ensembles to identify successful approaches. *Global Change Biology*, **22**, 3112–3126.

Jones JW, Hoogenboom G, Porter CH et al. (2003) DSSAT Cropping System Model. *European Journal of Agronomy*, **18**, 235–265.

Keating BA, Carberry PS, Hammer GL et al. (2003) An overview of APSIM, a model designed for farming systems simulation. *European Journal of Agronomy*, **18**, 267–288.

Kendall A, Chang B (2009) Estimating life cycle greenhouse gas emissions from corn–ethanol: a critical review of current U.S. practices. *Journal of Cleaner Production*, **17**, 1175–1182.

Kim S, Dale BE (2005) Life cycle assessment of various cropping systems utilized for producing biofuels: Bioethanol and biodiesel. *Biomass and Bioenergy*, **29**, 426–439.

Kim HY, Lieffering M, Kobayashi K, Okada M, Mitchell MW, Gumpertz M (2003a) Effects of

free-air CO_2 enrichment and nitrogen supply on the yield of temperate paddy rice crops. *Field Crops Research*, **83**, 261–270.

Kim HY, Lieffering M, Kobayashi K, Okada M, Miura S (2003b) Seasonal changes in the effects of elevated CO_2 on rice at three levels of nitrogen supply: a free air CO_2 enrichment (FACE) experiment. *Global Change Biology*, **9**, 826–837.

Kimball B (1983) Carbon Dioxide and Agricultural Yield: An Assemblage and Analysis of 430 Prior Observations. *Agronomy Journal*, **75**, 779–788.

Kimball BA (2005) Theory and performance of an infrared heater for ecosystem warming. *Global Change Biology*, **11**, 2041–2056.

Kimball B (2006) The effects of free-air enrichment of cotton, wheat, and sorghum. In: *Managed ecosystems and* CO_2 (eds Nosberger J, Long S, Norby R, Stitt M, Hendrey G, Blum H), pp. 47–67. Springer-Verlag, Berlin Heidelberg.

Kimball BA (2011) Comment on the comment by Amthor et al. on "Appropriate experimental ecosystem warming methods" by Aronson and McNulty. *Agricultural and Forest Meteorology*, **151**, 420–424.

Kimball BA (2016) Crop responses to elevated CO_2 and interactions with H2O, N, and temperature. *Current Opinion in Plant Biology*, **31**, 36–43.

Kimball BA, Bernacchi CJ (2006) Evapotranspiration, Canopy Temperature, and Plant Water Relations. In: *Managed Ecosystems and* CO_2 (eds Nosberger J, Long S, Norby R, Stitt M, Hendrey G, Blum H), pp. 311–324. Springer-Verlag, Berlin Heidelberg.

Kimball BA, Pinter PJ, Garcia RL et al. (1995) Productivity and water use of wheat under free-air CO_2 enrichment. *Global Change Biology*, **1**, 429–442.

Kimball BA, Pinter PJ, Wall GW et al. (1997) *Comparisons of Responses of Vegetation to*

Elevated Carbon Dioxide in Free-Air and Open Top Chamber Facilities. Madison, WI, 113-130 pp.

Kimball B, LaMorte RLR, Pinter PJ et al. (1999) Free-air CO_2 enrichment and soil nitrogen effects on energy balance and evapotranspiration of wheat. *Water Resources Research*, **35**, 1179–1190.

Kimball BA, Morris CF, Pinter PJ et al. (2001) Elevated CO_2, drought and soil nitrogen effects on wheat grain quality. *New Phytologist*, **150**, 295–303.

Kimball BA, Kobayashi K, Bindi M (2002) Responses of agricultural crops to free-air CO_2 enrichment. In: *Advances in Agronomy*, Vol. 77, pp. 293–368. Elsevier Science.

Kiniry JR, Blanchet R, Williams JR, Texier V, Jones CA, Cabelguenne M (1992) Sunflower simulation using the EPIC and ALMANAC models. *Field Crops Research*, **30**, 403–423.

Kirtman B, Power SB, Adedoyin J a. et al. (2013) Near-term Climate Change: Projections and Predictability. In: *Climate Change 2013: The Physical Science Basis. Contribution of Working Group I to the Fifth Assessment Report of the Intergovernmental Panel on Climate Change*, pp. 953–1028. Cambridge University Press, Cambridge, UK.

de Klein C, Novoa R, Ogle S et al. (2006) N2O Emissions From Managed Soils, and CO_2 Emissions From Lime and Urea Application. In: *IPCC Guidelines for National Greenhouse Gas Inventories. Volume 4: Agriculture, Forestry and Other Land Use*, pp. 1–54.

Kobayashi K, Okada M, Kim H (2006) Paddy rice responses to free-air [CO_2] enrichment. In: *Managed Ecosystems and* CO_2 (eds Nosberger J, Long S, Norby R, Stitt M, Hendrey G, Blum H), pp. 87–103. Springer-Verlag, Berlin Heidelberg.

Kucharik CJ, Serbin SP (2008) Impacts of recent climate change on Wisconsin corn and soybean yield trends. *Environmental Research Letters*, **3**, 34003.

Lal R (2004a) Soil carbon sequestration to mitigate climate change. *Geoderma*, **123**, 1–22.

Lal R (2004b) Carbon emission from farm operations. *Environment International*, **30**, 981–990.

Lam SK, Hao X, Lin E et al. (2012a) Effect of elevated carbon dioxide on growth and nitrogen fixation of two soybean cultivars in northern China. *Biology and Fertility of Soils*, **48**, 603–606.

Lam SK, Han X, Lin E, Norton R, Chen D (2012b) Does elevated atmospheric carbon dioxide concentration increase wheat nitrogen demand and recovery of nitrogen applied at stem elongation? *Agriculture, Ecosystems and Environment*, **155**, 142–146.

Lam SK, Chen D, Norton R, Armstrong R (2012c) Nitrogen demand and the recovery of 15N-labelled fertilizer in wheat grown under elevated carbon dioxide in southern Australia. *Nutrient Cycling in Agroecosystems*, **92**, 133–144.

Leakey ADB (2009) Rising atmospheric carbon dioxide concentration and the future of C4 crops for food and fuel. *Proceedings of the Royal Society B: Biological Sciences*, **276**, 2333–2343.

Leakey ADB, Uribelarrea M, Ainsworth EA, Naidu SL, Rogers A, Ort DR, Long SP (2006) Photosynthesis, productivity, and yield of maize are not affected by open-air elevation of CO_2 concentration in the absence of drought. *Plant Physiology*, **140**, 779–790.

Leakey A, Ainsworth EA, Bernacchi CJ, Rogers A, Long SP, Ort DR (2009) Elevated CO_2 effects on plant carbon, nitrogen, and water relations: six important lessons from FACE. *Journal of Experimental Botany*, **60**, 2859–2876.

Leemans R, Solomon AM (1993) Modeling the potential change in yield and distribution of the earth's crops under a warmed climate. *Climate Research*, **3**, 79–96.

Li X, Meixner T, Sickman JO, Miller AE, Schimel JP, Melack JM (2006) Decadal-scale

dynamics of water, carbon and nitrogen in a California chaparral ecosystem: DAYCENT modeling results. *Biogeochemistry*, **77**, 217–245.

Liska AJ, Yang HS, Bremer VR, Klopfenstein TJ, Walters DT, Erickson GE, Cassman KG (2009) Improvements in life cycle energy efficiency and greenhouse gas emissions of corn-ethanol. *Journal of Industrial Ecology*, **13**, 58–74.

Liu J, Williams JR, Zehnder AJB, Yang H (2007) GEPIC - modelling wheat yield and crop water productivity with high resolution on a global scale. *Agricultural Systems*, **94**, 478–493.

Liu B, Liu L, Asseng S, Zou X, Li J, Cao W, Zhu Y (2016a) Modelling the effects of heat stress on post-heading durations in wheat: A comparison of temperature response routines. *Agricultural and Forest Meteorology*, **222**, 45–58.

Liu B, Asseng S, Liu L, Tang L, Cao W, Zhu Y (2016b) Testing the responses of four wheat crop models to heat stress at anthesis and grain filling. *Global Change Biology*, **22**, 1890–1903.

Liu B, Asseng S, Müller C et al. (2016c) Similar estimates of temperature impacts on global wheat yield by three independent methods. *Nature Climate Change*, **1**, 1130–1136.

Lobell DB, Asner GP (2003) Climate and Management in U. S. Agricultural Yields. *Science*, **299**, 1032.

Lobell D, Asseng S (2017) Comparing estimates of climate change impacts from process-based and statistical crop models. *Environmental Research Letters*, **12**, 1–12.

Lobell DB, Burke MB (2010) On the use of statistical models to predict crop yield responses to climate change. *Agricultural and Forest Meteorology*, **150**, 1443–1452.

Lobell DB, Field CB (2007) Global scale climate–crop yield relationships and the impacts of

recent warming. *Environmental Research Letters*, **2**, 14002.

Lobell DB, Field CB (2008) Estimation of the carbon dioxide (CO_2) fertilization effect using growth rate anomalies of CO_2 and crop yields since 1961. *Global Change Biology*, **14**, 39–45.

Lobell DB, Gourdji SM (2012) The Influence of Climate Change on Global Crop Productivity. *Plant Physiology*, **160**, 1686–1697.

Lobell DB, Bänziger M, Magorokosho C, Vivek B (2011) Nonlinear heat effects on African maize as evidenced by historical yield trials. *Nature Climate Change*, **1**, 42–45.

Lobell DB, Sibley A, Ivan Ortiz-Monasterio J (2012) Extreme heat effects on wheat senescence in India. *Nature Climate Change*, **2**, 186–189.

Lobell DB, Hammer GL, McLean G, Messina C, Roberts MJ, Schlenker W (2013) The critical role of extreme heat for maize production in the United States. *Nature Climate Change*, **3**, 497–501.

Lokupitiya E, Paustian K (2006) Agricultural Soil Greenhouse Gas Emissions: A Review of National Inventory Methods. *Journal of Environment Quality*, **35**, 1413–1427.

Long SP, Ainsworth EA, Leakey ADB, Morgan PB (2005) Global food insecurity: Treatment of major food crops with elevated carbon dioxide or ozone under large-scale fully open-air conditions suggests recent models may have overestimated future yields. *Philosophical Transactions of the Royal Society B-Biological Sciences*, **360**, 2011–2020.

Long SP, Ainsworth EA, Leakey ADB, Nosberger J, Ort DR (2006) Food for thought: Lower-than-expected crop yield stimulation with rising CO_2 concentrations. *Science*, **312**, 1918–1921.

López-Cedrón FX, Boote KJ, Ruíz-Nogueira B, Sau F (2005) Testing CERES-Maize versions to

estimate maize production in a cool environment. *European Journal of Agronomy*, **23**, 89–102.

Manderscheid R, Erbs M, Weigel H-J (2014) Interactive effects of free-air CO_2 enrichment and drought stress on maize growth. *European Journal of Agronomy*, **52**, 11–21.

Mann L, Tolbert V, Cushman J (2002) Potential environmental effects of corn (Zea mays L.) stover removal with emphasis on soil organic matter and erosion. *Agriculture, Ecosystems and Environment*, **89**, 149–166.

Markelz RJC, Strellner RS, Leakey ADB (2011) Impairment of C4 photosynthesis by drought is exacerbated by limiting nitrogen and ameliorated by elevated [CO_2] in maize. *Journal of experimental botany*, **62**, 3235–46.

McGrath JM, Lobell DB (2011) An independent method of deriving the carbon dioxide fertilization effect in dry conditions using historical yield data from wet and dry years. *Global Change Biology*, **17**, 2689–2696.

McGrath JM, Lobell DB (2013) Reduction of transpiration and altered nutrient allocation contribute to nutrient decline of crops grown in elevated CO_2 concentrations. *Plant Cell and Environment*, **36**, 697–705.

Meinshausen M, Smith SJ, Calvin K et al. (2011) The RCP greenhouse gas concentrations and their extensions from 1765 to 2300. *Climatic Change*, **109**, 213–241.

Mesinger F, DiMego G, Kalnay E et al. (2006) North American regional reanalysis. *Bulletin of the American Meteorological Society*, **87**, 343–360.

Metherell A (1992) *Simulation of Soil Organic Matter Dynamics an Nutrient Cycling in Agroecosystems*. Colorado State University.

Miglietta F, Raschi A, Resti P, Badiani M (1993) Growth and onto-morphogenesis of soybean

(Glycine max Merril) in an open, naturally CO_2-enriched environment. *Plant Cell and Environment*, **16**, 909–918.

Mitchell M (2002) Engauge Digitizer. http://digitizer.sourceforge.net/.

Mollah M, Norton R, Huzzey J (2009) Australian grains free-air carbon dioxide enrichment (AGFACE) facility: Design and performance. *Crop and Pasture Science*, **60**, 697–707.

Morgan PB, Bollero GA, Nelson RL, Dohleman FG, Long SP (2005) Smaller than predicted increase in aboveground net primary production and yield of field-grown soybean under fully open-air [CO_2] elevation. *Global Change Biology*, **11**, 1856–1865.

Mosier A, Schimel D, Valentine D, Bronson K, Parton W (1991) Methane and nitrous oxide fluxes in native, fertilized and cultivated grasslands. *Nature*, **350**, 330–332.

Mueller B, Seneviratne SI (2012) Hot days induced by precipitation deficits at the global scale. *Proc Natl Acad Sci U S A*, **109**, 12398–12403.

Myers SS, Zanobetti A, Kloog I et al. (2014) Increasing CO_2 threatens human nutrition. *Nature*, **510**, 139–142.

Nijs I, Kockelbergh F (1996) Free air temperature increase (FATI): a new tool to study global warming effects on plants in the field. *Plant Cell and Environment*, **19**, 495–502.

Norton R, Fitzgerald G, Korte C (2008) The effect of elevated carbon dioxide on the growth and yield of wheat in the Australian Grains Free Air Carbon dioxide Enrichment (AGFACE) experiment. In: *Proceedings of the 14th Australian Agronomy Conference*. Adelaide, SA, Australia.

NRCS (2004) State Soil Geographic Database (SSURGO). *United States Department of Agriculture*, http://www.nrcs.usda.gov/wps/portal/nrcs/main/soil.

Nuttall J, Barlow K, Christy B, Leary GO, Fitzgerald GJ (2015) Heat shock response in wheat

under Free Air CO_2 Enrichment. In: *Proceedings of the 17th ASA Conference*, pp. 15–18. Hobart, Australia.

O'Leary GJ, Christy B, Nuttall J et al. (2015) Response of wheat growth, grain yield and water use to elevated CO_2 under a Free-Air CO_2 Enrichment (FACE) experiment and modelling in a semi-arid environment. *Global Change Biology*, **21**, 2670–2686.

Ogle SM, Breidt FJ, Easter M, Williams S, Killian K, Paustian K (2010) Scale and uncertainty in modeled soil organic carbon stock changes for US croplands using a process-based model. *Global Change Biology*, **16**, 810–822.

Ogle S, Adler P, Breidt F et al. (2014) Chapter 3: Quantifying greenhouse gas sources and sinks in cropland and grazing systems. In: *Quantifying Greenhouse Gas Fluxes in Agriculture and Forestry : Methods for Entity-Scale Inventory*. U.S. Department of Agriculture, Office of the Chief Economist, Washington, DC.

Okada M, Lieffering M, Nakamura H, Yoshimoto M, Kim HY, Kobayashi K (2001) Free-air CO_2 enrichment (FACE) using pure CO_2 injection: system description. *New Phytologist*, **150**, 251–260.

Orlowsky B, Seneviratne SI (2012) Global changes in extreme events: Regional and seasonal dimension. *Climatic Change*, **110**, 669–696.

Ottman MJ, Kimball BA, Pinter PJ et al. (2001) Elevated CO_2 increases sorghum biomass under drought conditions. *New Phytologist*, **150**, 261–273.

Ottman MJ, Kimball BA, White JW, Wall GW (2012) Wheat growth response to increased temperature from varied planting dates and supplemental infrared heating. *Agronomy Journal*, **104**, 7–16.

Parent B, Tardieu F (2012) Temperature Responses of Developmental Processes Have not Been

Affected By Breeding in Different Ecological Areas for 17 Crop Species. *New Phytologist*, **194**, 760–774.

Parry ML, Rosenzweig C, Iglesias A, Livermore M, Fischer G (2004) Effects of climate change on global food production under SRES emissions and socio-economic scenarios. *Global Environmental Change*, **14**, 53–67.

Parton WJ, Hartman M, Ojima D, Schimel D (1998) DAYCENT and its land surface submodel: description and testing. *Global and planetary Change*, **19**, 35–48.

Paustian K, Andrén O, Janzen HH et al. (1997) Agricultural soils as a sink to mitigate CO_2 emissions. *Soil Use and Management*, **13**, 230–244.

Paustian K, Cole CV, Sauerbeck D, Sampson N (1998) CO_2 Mitigation by Agriculture: An Overview. *Climatic Change*, **40**, 135–162.

Pearson PPN, Palmer MMR (2000) Estimating Paleogene atmospheric pCO_2 using boron isotope analysis of foraminifera. *GFF*, **122**, 127–128.

Peart R, Jones J, Curry R (1989) Impact of climate change on crop yield in the southeastern USA: a simulation study. In: *The Potential Effects of Global Climate Change on the United States, Report to Congress.* (eds Smith J, Tirpak D). EPA-230-05-89-050, Washington, DC, Appendix C.

Pepper DA, Del Grosso SJ, McMurtrie RE, Parton WJ (2005) Simulated carbon sink response of shortgrass steppe, tallgrass prairie and forest ecosystems to rising [CO_2], temperature and nitrogen input. *Global Biogeochemical Cycles*, **19**, 1–20.

Perlack RRD, Stokes BBJ, Eaton LM, Turnhollow AF (2011) *U.S. Billion Ton Update: Biomass Supply for a Bioenergy and Bioproducts Industry*. Oak Ridge National Laboratory, Oak Ridge, TN, 1-227 pp.

Plastina A (2015) Estimated Costs of Crop Production in Iowa - 2015. *Iowa State University Extension*, https://www.extension.iastate.edu/agdm/crops/html/.

Poorter H, Van Berkel Y, Baxter R et al. (1997) The effect of elevated CO_2 on the chemical composition and construction costs of leaves of 27 C3 species. *Plant Cell and Environment*, **20**, 472–482.

Porter JR, Xie L, Challinor AJ et al. (2014) Food security and food production systems. In: *Climate Change 2014: Impacts, Adaptation, and Vulnerability. Part A: Global and Sectoral Aspects. Contribution of Working Group II to the Fifth Assessment Report of the Intergovernmental Panel on Climate Change*, pp. 485–533. Cambridge University Press, Cambridge, UK.

Pre Consultants (2012) SimaPro Life Cycle Assessment software and database.

Qin Z, Canter C, Dunn J et al. (2015) *Incorporating Agricultural Management Practices into the Assessment of Soil Carbon Change and Life-Cycle Greenhouse Gas Emissions of Corn Stover Ethanol Production*. Office of Scientific and Technical Information, Department of Energy, Argonne, IL.

Rachmilevitch S, Cousins AB, Bloom AJ (2004) Nitrate assimilation in plant shoots depends on photorespiration. *Proceedings of the National Academy of Sciences of the United States of America*, **101**, 11506–11510.

Rattalino Edreira JI, Otegui ME (2012) Heat stress in temperate and tropical maize hybrids: Differences in crop growth, biomass partitioning and reserves use. *Field Crops Research*, **130**, 87–98.

Rattalino Edreira JI, Budakli Carpici E, Sammarro D, Otegui ME (2011) Heat stress effects around flowering on kernel set of temperate and tropical maize hybrids. *Field Crops*

Research, **123**, 62–73.

Rezaei EE, Webber H, Gaiser T, Naab J, Ewert F (2014) Heat stress in cereals : Mechanisms and modelling. *European Journal of Agronomy*.

Rezaei EE, Siebert S, Ewert F (2015) Intensity of heat stress in winter wheat—phenology compensates for the adverse effect of global warming. *Environmental Research Letters*, **10**, 24012.

Ribaudo M, Gollehon N, Aillery M et al. (2003) *Manure Management for Water Quality : Costs to Animal Feeding Operations of Applying Manure. Agricultural Economic Report Number 824*. Economic Research Service, United Stated Department of Agriculture, Washington, DC.

Risse L, Cabrera L, Franzluebbers A et al. (2006) *Land Application of Manure for Beneficial Reuse*, Vol. 65. Lincoln, NE, 283-316 pp.

Roberts MJ, Schlenker W, Eyer J (2012) Agronomic weather measures in econometric models of crop yield with implications for climate change. *American Journal of Agricultural Economics*, **95**, 236–243.

Robertson GP, Vitousek PM (2009) Nitrogen in Agriculture: Balancing the Cost of an Essential Resource. *Annual Review of Environment and Resources*, **34**, 97–125.

Rogers HH, Heck WW, Heagle a. S (1983) A Field Technique for the Study of Plant Responses to Elevated Carbon Dioxide Concentrations. *Journal of the Air Pollution Control Association*, **33**, 42–44.

Rogers H, Prior S, Runion G, Mitchell R (1996) Root to shoot ratio and CO_2. *Plant and Soil*, **187**, 229–248.

Rosenzweig C, Elliott J, Deryng D et al. (2014) Assessing agricultural risks of climate change in

the 21st century in a global gridded crop model intercomparison. *Proceedings of the National Academy of Sciences of the United States of America*, **111**, 3268–73.

Rötter RP, Carter TR, Olesen JE, Porter JR (2011) Crop-climate models need an overhaul. *Nature Climate Change*, **1**, 175–177.

Ruiz-Vera UM, Siebers M, Gray SB et al. (2013) Global Warming Can Negate the Expected CO_2 Stimulation in Photosynthesis and Productivity for Soybean Grown in the Midwestern United States. *Plant Physiology*, **162**, 410–423.

Ruiz-Vera UM, Siebers MH, Drag DW, Ort DR, Bernacchi CJ (2015) Canopy warming caused photosynthetic acclimation and reduced seed yield in maize grown at ambient and elevated [CO_2]. *Global Change Biology*, **21**, 4237–4249.

Sánchez B, Rasmussen A, Porter JR (2014) Temperatures and the growth and development of maize and rice: A review. *Global Change Biology*, **20**, 408–417.

Saxton KEE, Rawls WJJ, Romberger JSS, Papendick RII (1986) Estimating generalized soil-water characteristics from texture. *Soil Science Society of America Journal*, **50**, 1031–1036.

Schlenker W, Roberts MJ (2009) Nonlinear temperature effects indicate severe damages to U.S. crop yields under climate change. *Proceedings of the National Academy of Sciences of the United States of America*, **106**, 15594–15598.

Schnepf R, Yacobucci BD (2011) *Renewable Fuel Standard (RFS): Overview and Issues*, Vol. R40155. Congressional Research Service, Washington, DC.

Searchinger T, Heimlich R, Houghton RA et al. (2008) Use of U.S. Croplands for Biofuels Increases Greenhouse Gases Through Emissions from Land-Use Change. *Science*, **319**, 1238–1240.

Sharpley AN, Williams JR (1990) EPIC: The erosion-productivity impact calculator. *U.S.*

Department of Agriculture Technical Bulletin, 235.

Sheehan J, Aden A, Paustian K, Killian K, Brenner J, Walsh M, Nelson R (2003) Energy and Environmental Aspects of Using Corn Stover for Fuel Ethanol. *Journal of Industrial Ecology*, **7**, 117–146.

Shimono H, Okada M, Yamakawa Y, Nakamura H, Kobayashi K, Hasegawa T (2008) Rice yield enhancement by elevated CO_2 is reduced in cool weather. *Global Change Biology*, **14**, 276–284.

Siebers MH, Yendrek CR, Drag D et al. (2015) Heat waves imposed during early pod development in soybean (Glycine max) cause significant yield loss despite a rapid recovery from oxidative stress. *Global change biology*, 1–13.

Siebert S, Ewert F, Eyshi Rezaei E, Kage H, Graß R (2014) Impact of heat stress on crop yield—on the importance of considering canopy temperature. *Environmental Research Letters*, **9**, 44012.

Sims AL, Schepers JS, Olson RA, Power JF (1998) Irrigated corn yield and nitrogen accumulation response in a comparison of no-till and conventional till: Tillage and surface-residue variables. *Agronomy Journal*, **90**, 630–637.

Six J, Conant RT, Paul EA, Paustian K (2002) Stabilization mechanisms of soil organic matter: Implications for C-saturation of soils. *Plant and Soil*, **241**, 155–176.

Smith B, Prentice IC, Sykes MT (2001) Representation of vegetation dynamics in modelling of European ecosystems: comparison of two contrasting approaches within European climate space. *Global Ecology and Biogeography*, **10**, 621–637.

Smith P, Martino D, Cai Z et al. (2008) Greenhouse gas mitigation in agriculture. *Philosophical transactions of the Royal Society of London. Series B, Biological sciences*, **363**, 789–813.

Smith P, Bustamante M, Ahammad H et al. (2014) Agriculture, Forestry and Other Land Use (AFOLU). In: *Climate Change 2014: Mitigation of Climate Change. Contribution of Working Group III to the Fifth Assessment Report of the Intergovernmental Panel on Climate Change*, pp. 811–922. Cambridge University Press, Cambridge, UK.

Soil Survey Staff (2015) Web Soil Survey. https://websoilsurvey.sc.egov.usda.gov/. Accessed 07-01-2015.

Solomon BD, Barnes JR, Halvorsen KE (2007) Grain and cellulosic ethanol: History, economics, and energy policy. *Biomass and Bioenergy*, **31**, 416–425.

Sperling D, Yeh S (2007) *A Low-Carbon fuel standard for California, part 2: Policy analysis*. Davis, CA, 1-91 pp.

Stackhouse PW, Westberg D, Hoell JM, Chandler WS, Zhang T (2015) Prediction Of Worldwide Energy Resource (POWER) --- Agroclimatology Methodology --- (1.0 Latitude by 1.0 Longitude Spatial Resolution). 1–46.

Stewart CE, Paustian K, Conant RT, Plante AF, Six J (2009) Soil carbon saturation: Implications for measurable carbon pool dynamics in long-term incubations. *Soil Biology and Biochemistry*, **41**, 357–366.

Stockle CO, Williams JR, Rosenberg NJ, Jones CA (1992) A method for estimating the direct and climatic effects of rising atmospheric carbon dioxide on growth and yield of crops: Part I—Modification of the EPIC model for climate change analysis. *Agricultural Systems*, **38**, 225–238.

Stockle CO, Donatelli M, Nelson R (2003) CropSyst, a cropping systems simulation model. *European Journal of Agronomy*, **18**, 289–307.

Syswerda SP, Corbin AT, Mokma DL, Kravchenko AN, Robertson GP (2011) Agricultural

Management and Soil Carbon Storage in Surface vs. Deep Layers. *Soil Science Society of America Journal*, **75**, 92–102.

Tack J, Barkley A, Nalley LL (2015a) Effect of warming temperatures on US wheat yields. *Proceedings of the National Academy of Sciences of the United States of America*, **112**, 6931–6.

Tack J, Barkley A, Rife TW, Poland JA, Nalley LL (2015b) Quantifying Variety-specific Heat Resistance and the Potential for Adaptation to Climate Change. *Global Change Biology*, 1–9.

Teng H, Branstator G, Meehl GA, Washington WM (2016) Projected intensification of subseasonal temperature variability and heat waves in the Great Plains. *Geophysical Research Letters*, **43**, 2165–2173.

Thelen KD, Fronning BE, Kravchenko A, Min DH, Robertson GP (2010) Integrating livestock manure with a corn-soybean bioenergy cropping system improves short-term carbon sequestration rates and net global warming potential. *Biomass and Bioenergy*, **34**, 960–966.

Tian Y, Chen J, Chen C et al. (2012) Warming impacts on winter wheat phenophase and grain yield under field conditions in Yangtze Delta Plain, China. *Field Crops Research*, **134**, 193–199.

Tubiello FN, Ewert F (2002) Simulating the effects of elevated CO_2 on crops: approaches and applications for climate change. *European Journal of Agronomy*, **18**, 57–74.

Tubiello FN, Amthor JS, Boote KJ et al. (2007) Crop response to elevated CO_2 and world food supply - A comment on “Food for Thought...” by Long et al., Science 312 : 1918-1921, 2006. *European Journal of Agronomy*, **26**, 215–223.

Turhollow A, Perlack R, Eaton L et al. (2014) The updated billion-ton resource assessment.

Biomass and Bioenergy, **70**, 149–164.

Urban DW, Sheffield J, Lobell DB (2015) The impacts of future climate and carbon dioxide changes on the average and variability of US maize yields under two emission scenarios. *Environmental Research Letters*, **10**, 45003.

Vanuytrecht E, Raes D, Willems P, Geerts S (2012) Quantifying field-scale effects of elevated carbon dioxide concentration on crops. *Climate Research*, **54**, 35–47.

Walker BJ, VanLoocke A, Bernacchi CJ, Ort DR (2016) The Costs of Photorespiration to Food Production Now and in the Future. *Annual Review of Plant Biology*, **67**, 107–129.

Wall GW, Adam NR, Brooks TJ et al. (2000) Acclimation response of spring wheat in a free-air CO(2) enrichment (FACE) atmosphere with variable soil nitrogen regimes. 2. Net assimilation and stomatal conductance of leaves. *Photosynthesis research*, **66**, 79–95.

Wall G, Brooks T, Adam N (2001) Elevated atmospheric CO_2 improved Sorghum plant water status by ameliorating the adverse effects of drought. *New Phytologist*, **152**, 231–248.

Wang M, Han J, Dunn JB, Cai H, Elgowainy A (2012) Well-to-wheels energy use and greenhouse gas emissions of ethanol from corn, sugarcane and cellulosic biomass for US use. *Environmental Research Letters*, **7**, 1–13.

Wang Z, Dunn J, Han J, Wang M (2013) *Material and Energy Flows in the Production of Cellulosic Feedstocks for Biofuels for the GREET ^{TM} Model*. Energy Systems Division, Argonne National Laboratory, Argonne, IL.

Webber H, Martre P, Asseng S et al. (2015) Canopy temperature for simulation of heat stress in irrigated wheat in a semi-arid environment: A multi-model comparison. *Field Crops Research*, **202**, 21–35.

Webber H, Ewert F, Kimball BA et al. (2016) Simulating canopy temperature for modelling heat

stress in cereals. *Environmental Modelling and Software*, **77**, 143–155.

Weigel H-J, Manderscheid R (2012) Crop growth responses to free air CO_2 enrichment and nitrogen fertilization: Rotating barley, ryegrass, sugar beet and wheat. *European Journal of Agronomy*, **43**, 97–107.

Weigel HJ, Pacholski A, Burkart S et al. (2005) Carbon turnover in a crop rotation under free air CO_2 enrichment (FACE). *PEDOSPHERE*, **15**, 728–738.

West TO, Post WM (2002) Soil organic carbon sequestration rates by tillage and crop rotation: A global data analysis. *Soil Science Society of America Journal*, **66**, 1930–46.

Wilhelm WW, Doran JW, Power JF (1986) Corn and Soybean Yield Response to Crop Residue Management Under No-Tillage Production Systems. *Agronomy Journal*, **189**, 184–189.

Wilhelm WW, Johnson JMF, Hatfield JL, Voorhees WB, Linden DR (2004) Crop and Soil Productivity Response to Corn Residue Removal: A Literature Review. *Agronomy Journal*, **96**, 1–17.

Wilhelm WW, Johnson JMF, Karlen DL, Lightle DT (2007) Corn Stover to Sustain Soil Organic Carbon Further Constrains Biomass Supply. *Agronomy Journal*, **99**, 1665.

Zhang Y (2016) *Simulating canopy dynamics, productivity and water balance of annual crops from field to regional scales*. Colorado State University, 1-165 pp.

Zhao X, Liu SL, Pu C et al. (2016) Methane and nitrous oxide emissions under no-till farming in China: A meta-analysis. *Global Change Biology*, **22**, 1372–1384.

Ziska LH, Bunce JA (2007) Predicting the impact of changing CO_2 on crop yields: some thoughts on food. *New Phytologist*, **175**, 607–617.

APPENDIX

Chapter 2 Supporting Information

Additional on-farm inputs

Fuel consumption was calculated using reference values together with survey responses reporting equipment used for tillage and other field operations, total grain yield, and road distance to the biorefinery. Table A1 summarizes herbicide and pesticide usage as reported by farms, on an area-weighted basis.

Surveyed farms reported liming fields at an average rate of 95 lb per acre, which was just over half the USDA average rates for Minnesota. Since fields are only limed at several-year intervals, our three-year survey period may have failed to capture a representative sample of these events. Therefore, we chose to use the Minnesota state average application rate of 169 lb lime $acre^{-1}$ $year^{-1}$ in calculating liming-related emissions.

Table A1. Area-weighted average herbicide and pesticide usage

Ag chemical	Application rate (kg per hectare)
Glyphosate kg per ha	0.7878
Glufosinate ammonium kg per ha	0.0108
Sulfonyl urea compounds kg per ha	0.0002
Phenoxy 2 4 D kg per ha	0.0042
Atrazine compounds kg per ha	0.1760
Acetochlor kg per ha	0.5174
Metolachlor kg per ha	0.0282
Dicamba kg per ha	0.0004
Clopyralid kg per ha	0.0088
Pesticides unspecified kg per ha	0.0298
Other herbicides kg per ha	0.0201
Isoxaflutole kg per ha	0.0010
Mesotrione kg per ha	0.0161
Diflufenzopyr kg per ha	0.0001
Flumetsulam kg per ha	0.0028

Table A2. Adjusted rate of application and assumed nutrient content for manure as fertilizer

Manure type	Units per acre	Adjusted rate of application	Nitrogen (lb N per unit applied)	Phosphate (lb P_2O_5 per unit applied)	Potassium (lb K_2O per unit applied)
Beef	tons/acre	1.58	7	4	7
Chicken	tons/acre	0.08	60	46	31
Dairy (dry)	tons/acre	0.02	10	3	6
Dairy (liquid)	gal/acre	84.26	0.031	0.015	0.019
Swine (liquid)	gal/acre	594.27	0.03	0.025	0.024

Table A3. Equipment and energy requirements for various tilling, harvesting and planting activities

Operation	Implement Assumed	Diesel (gal/ac)
Min till Planting	16 Row-30 40 ft	0.53
Harvesting	Combine Corn Hd 8 Row-30 20 ft	1.88
Grain Cart	Grain Cart 30 ft	1.44

Lime, urea broadcast, urea dry, urea spreader, urea floater, other dry fert, DAP spinner	Spreading dry fertilizer, bulk cart	0.15
Herbicide - liquid or dry, fungicide - headline	Boom sprayer 50 ft	0.1
Stalk shredding	Stalk shredder 20 ft	0.17
SEEDBED prep	---	---
Ground roller used for soybean	---	---
Anhy tilling, anhy incorporate, anhy knife, anhy bar	Anhydrous ammonia (30-inch spacing)	0.55
Urea strip till	---	---
Corn residue baled and removed.	---	---
Rake corn stalks	Hy Rake (Wheel, 2-16") 30 ft	0.07
Bale corn stalks	Round Baler 1500 lb, 20 ft	0.35
Moving bales off field	Hauling, field plus 1/2 mile = green forage	0.3
Field cultivator	Field cultivator, 47'	0.32
Disk	Tandem Disk H.D. 30 ft fold	0.79
In-line ripper	V-Ripper 30" O.C. 17'	0.99
Row cultivation	16 Row-30, 40 ft	0.44
Soil finisher	Field cultivator, 47'	0.32
Strip-till machine	V-Ripper 30" O.C. 17'	0.99
Manure incorporated/broadcast	Spreading dry fertilizer, bulk cart	0.15
Manure injected with sweeps or knives	Chisel plow 15'	0.6
No till drill	No till drill 30ft	0.81
Harvesting silage	Corn Head for SP Harvstr Base 8 Row, 20 Ft	2.35
Disc-chisel	16.3 foot and 21.3 foot "Chisel plow, front disk"	0.97
Disc-ripper	Comb Disk & V-Ripper 22.5 or 17.5Ft	1.47

Table A4. Assumptions for grain transport energy requirements

Transport type	Fuel economy mpg	Capacity (bushels per load)
Semi	8	950
Tractor + wagon	3	1300
Grain truck	8	625
Tractor+wagon/Grain	5.5	962.5
Grain truck/Semi	8	625

DayCent cultivation intensity scores

Cultivation events in DayCent cause increased rates of decomposition and transfers of organic C between model SOC pools. A set of four parameters for each type of cultivation event dictate the resulting decomposition rate increases for SOC pools. These parameters tend to increase with increasing depth and breadth of soil disruption, causing small SOC losses after use of a planter and much larger losses after use of a moldboard plow, for example. In order to assess the relative impacts of each farmer's cultivation practices on these soil processes and the resulting emissions, a numerical Tillage Decomposition Effect (TDE) was calculated by summing the four parameters that specify the magnitude of a cultivation event's impact on SOC decomposition rates for each event reported by the farmer. The resulting per-event impacts were summed for each separate cultivation event across the 2-year crop rotation period, resulting in a single value for each farm.

Details of alternate N_2O estimation methods

The USDA method for direct N_2O estimation started with a base emissions rate determined by crop, soil texture, and USDA Land Resource Region that represents estimated emissions under typical management. The base emissions rate was then adjusted based on various management practices including N fertilization rate, organic amendment amount and type, and binary tillage intensity (conventional or no-till). The IPCC Tier 1 method assumed that 1% of N from all

inputs (i.e. synthetic fertilizer, manure, and crop residue) would be emitted to the atmosphere directly as N_2O. Broader management and site factors such as tillage, weather, and soil texture were not considered.

Chapter 3 Supporting Information

Supply-adjustment procedure for manure emissions

In general, manure additions in DayCent have emissions reduction benefits when used to displace synthetic N because some fraction of the manure C is sequestered in soil C pools, thus providing an apparent negative emission. Unlike most of the inputs evaluated in this study, the manure applied to fields was a waste product produced without regard to farmer demand. Thus, it was important to consider the emissions that would have occurred under an alternative, "business-as-usual" handling of the manure. If, for instance, the norm for manure disposal in the study area were anaerobic digestion for power production, followed by land application of digestate, then direct land application may represent a net increase in emissions by comparison. There was also a question relating to whether the feedlot (which produced the manure) or the farm (which utilized it) should bear the burdens or benefits of emissions that occur after land application.

We chose a set of assumptions and estimates about the study area in order to address these issues. First of all, we assumed on the basis of literature discussions of manure management practices (see Ribaudo et al., 2003) that the most likely alternative to application on the modeled farm would be application to similar cropland located nearby. This was based on the recognition that feedlots have strong economic incentives to distribute manure on nearby land to minimize transport costs. The major determinants of these transport costs are the willingness of nearby

farmers to accept manure on their lands, and the acceptable maximum application rates in accordance with EPA rules (Ribaudo et al., 2003). We next assumed that feedlots would bear the emissions burdens of transporting manure to farm field and applying it, again because this aligns with the default economic arrangement (Ribaudo et al., 2003), but the farm would bear any emissions benefits or burdens from manure after application. Our third assumption was that we could define a maximum radius that, for the purposes of our study, would circumscribe the area of interest (AOI) within which manure could be applied. Since most (63%) of the Gevo survey respondent acreage was located in Rock County, MN, we chose to use it as our AOI for the purposes of estimating manure supply dynamics. Specifically, we obtained estimates for the annual manure N load produced by feedlots in Rock County (3473 Mg N yr^{-1}), cropland acreage available for application (60,730 ha in corn and/or soy), and the maximum acceptable application rates (15.7 and 20.2 g manure N m^{-2} for corn-soy and corn-corn acres, respectively) from the Assistant Director of the Soil & Water Conservation District (Douglas Bos, personal communication). We eliminated the 96 management permutations that involved manure N inputs above the regulatory maximum rates mentioned. We used the county manure and cropland figures to estimate the fraction of hectares within the AOI that would receive manure at each of the application rates described by the management scenarios.

Table A5. Sample biogenic emissions for varying levels of manure N input. Emissions values are medians of management permutations with the specified N input rate derived 100% from manure. Supply-adjusted emissions were linearly interpolated between simulated emissions from manured soils and non-manured management-matched soils based on the percent of cropland needed to absorb the manure supply at the given rate.

Manure Input Rate (g N m^{-2})	Percent of Manured Cropland	Median Simulated Biogenic Emissions (g CO_2e m^{-2})	Median No-manure Biogenic Emissions (g CO_2e m^{-2})	Median Supply-adjusted Biogenic Emissions (g CO_2e m^{-2})
5	100%	-22.0	12.6	-22.0
10	57.2%	-59.2	17.9	-28.8
15	38.1%	-56.6	62.2	18.5
20	28.6%	-42.5	103.7	60.3

We were then able to pair field emissions (SOC change, direct N_2O, indirect N_2O) for every management permutation with those from the management-matched no-manure simulation. For each field emissions component, the difference between each simulation and its management-matched no-manure control was considered the "manure effect" on emissions for that management permutation. The actual emissions assigned to each management permutation were calculated by interpolating between the actual (with manure) emissions and the management-matched no-manure control, based on the fraction of cropland hectares within the AOI that would be needed to absorb the manure supply produced within the AOI. For example, if the manure supply was sufficient to supply half of the AOI acreage at a given application rate, the biogenic emissions assigned to permutations with that application rate would be half-way between the with-manure and no-manure amounts. This approach scaled the manure effect on field emissions in proportion to the area within the AOI that would receive manure at the given rate, thus quantifying the average emissions impact of manure production across the AOI. Supply chain emissions embodied in synthetic N and P use were also scaled to reflect the fraction of synthetic nutrients that could be displaced by manure nutrients across the AOI

(manured and non-manured hectares), rather than the displacement implied by the manure use in the particular permutation.

Monetary farm budget methodology

Survey responses were used in conjunction with unit costs from Plastina (2015) to calculate per-farm costs for corn seed and non-N fertilizers and liming. Unit cost data for the wide range of specific herbicides and pesticides was not readily available and so the default cost per area from the Extension budgets was used for these inputs. Finally, a number of items were taken at their default values from the Extension budgets and combined under the heading "Financial and Other Costs". These included land rent, crop insurance, interest on preharvest costs, farm labor, and miscellaneous operational costs such as chemical spraying and grain harvest.

Management scenarios were used to calculate costs of related inputs. Tillage was estimated based on the specific implements and passes simulated within DayCent for a given level of tillage intensity, using per-operation costs from Plastina (2015). Costs for N fertilizer and application were calculated from scenario N application rates. Costs for grain drying were based on DayCent-simulated yields.

Costs for stover collection, baling, and stacking at the field edge were calculated using an exponential regression curve developed by (Graham et al., 2007). The curve expresses the cost per Mg of stover collected as a declining function of the collection rate, including savings provided by changing collection equipment at increasing collection rates. For this work, a new best-fit curve was derived by digitizing the data points given in Graham et al. (2007) Figure 4

and using non-linear least squares to solve for the best single curve of the form used by the authors ($y = ax^b$). That best-fit curve was:

$$\text{Stover Cost, \$ Mg}^{-1} = 46.15 * (\text{Collection Rate, Mg ha}^{-1})^{-0.363}$$

The costs calculated using that curve were then adjusted from 2002 dollars to 2015 dollars using the online calculator provided by the Bureau of Labor Statistics (2015).

FTW costs were then calculated using the estimated ethanol energy yields from each scenario and literature estimates of costs for feedstock conversion. Conversion cost for grain to ethanol was based on Hettinga et al., (2009), who gave a figure of \$0.13 l^{-1} grain ethanol in 2005 dollars, which amounted to \$0.16 l^{-1} in 2015 dollars. Conversion cost for cellulosic ethanol was based on Solomon et al., (2007), who gave a figure of \$0.39 l^{-1} ethanol in 2006 dollars, which amounted to \$0.46 l^{-1} in 2015 dollars. As discussed in both of the source studies, the costs for grain or cellulosic conversion are sensitive to a number of factors, including technological change, economies of scale, energy prices, interest rates, etc. Therefore, calculations based on these values should be regarded tentatively and is primarily valuable for identifying qualitative relationships between farm management and economic incentives.

Estimates of profit per unit area are based on FTW cost estimates. While it may seem awkward to compare farm management actions with profits that would be faced by the biorefinery selling ethanol, we felt that it was important to evaluate management economics in the context of the nearly 3-fold difference in downstream costs. This allowed us to compare the relative value of each feedstock net of their downstream conversion costs and avoid adding an additional layer of

assumptions by picking separate feedstock prices. Finally, profits were calculated against an ethanol price of \$2.50 gal^{-1}.

Table A6. Major input costs calculated in building farm budgets. Rates and unit costs of each input were derived from farm survey responses, scenario management input levels, Iowa State Extension farm budgets, and literature sources as detailed in text.

Input	Rate from:	Unit Cost	Unit cost source(s)
Corn seed	Survey	\$12.75 kg^{-1}	(Plastina, 2015)
Phosphorous fertilizer	Survey	\$1.06 kg^{-1}	
Potash fertilizer	Survey	\$0.90 kg^{-1}	
Lime	Extension	\$24.70 ha^{-1}	
Pesticides & herbicides	Extension	\$144.00 ha^{-1}	
Harvest operations	Extension	\$144.16 ha^{-1}	
Operator labor	Extension	\$91.51 ha^{-1}	
Land rent	Extension	\$674.31 ha^{-1}	
Crop insurance	Extension	\$33.59 ha^{-1}	
Preharvest interest	Extension	\$30.43 ha^{-1}	
Tillage, corn: Conventional Reduced No-till Tillage, soy: Conventional Reduced No-till	Scenario	 \$70 ha^{-1} \$66 ha^{-1} \$40 ha^{-1} \$54 ha^{-1} \$51 ha^{-1} \$40 ha^{-1}	
Synthetic N	Scenario	\$1.04 kg^{-1}	
Synth N application	Scenario	\$26 ha^{-1}	
Grain drying	Scenario	\$9.43 Mg^{-1}	
Stover collection & nutrient replacement	Scenario	Rate-dependent curve (see text)	(Graham et al., 2007)
Stover EtOH Conversion	Scenario	\$0.39 l^{-1}	(Solomon et al., 2007)
Grain EtOH Conversion	Scenario	\$0.16 l^{-1}	(Hettinga et al., 2009)
Ethanol Market Price	Scenario	\$2.50 USD gal^{-1}	

Farm supply chain emissions

Emissions from survey supply chain inputs averaged 57.7 g CO_2e m^{-2}, and ranged from 25.2 to 121.7 g CO_2e m^{-2}. The largest and most-variable farm supply chain emissions sources were phosphorous and potash fertilizers (mean: 27.9 g CO_2e m^{-2}) and non-field energy use (mean: 18.0 g CO_2e m^{-2}). Figure A1 shows the distribution of individual farms for 12-year total emissions related to survey supply chain management practices.

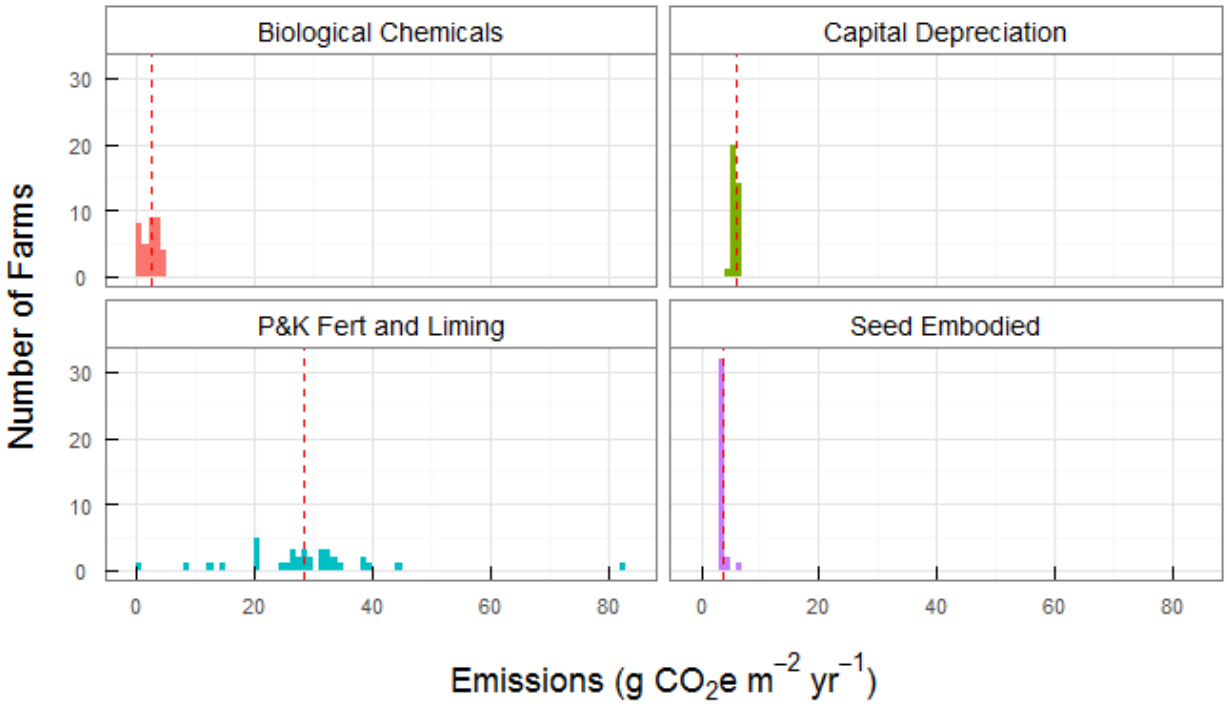

Figure A1. Distributions of emissions from survey supply chain inputs. These are the same farm inputs values given in previous work (Kent et al., in submission), but with scenario-related inputs removed. Each histogram encompasses a total of 35 farms, and bins have a width of 1 g CO_2e $m^{-2}yr^{-1}$.

Scenario supply chain inputs

For scenario-related management inputs not simulated by DayCent, emissions were assigned to scenarios based on their levels of different management variables. So, for instance, the equipment simulated in DayCent for No-till management is a single pass with a seed drill, so all

scenarios with No-till management were assigned a value from Lal (2004b) for the C-equivalent emissions from fuel and embodied equipment for this operation. A variety of sources were used to estimate the scenario-related supply chain emissions, and this process was described in the Methods. The mean scenario supply chain emissions were 31.9 g CO_2e m^{-2} and ranged from 3.7 to 81.5 g CO_2e m^{-2}. The distribution of scenario supply chain emissions is shown in Figure A2.

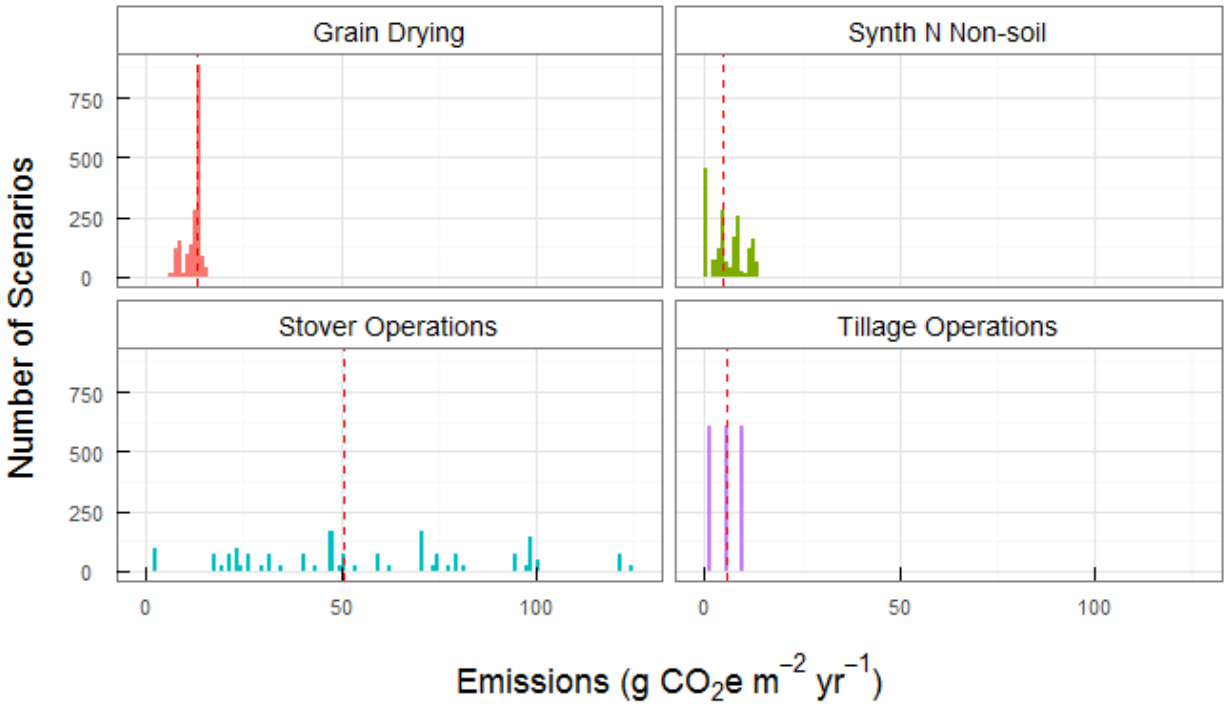

Figure A2. Distributions of emissions from scenario supply chain inputs. Each histogram encompasses a total of 1824 management scenarios, and bins have a width of 1 g CO_2e $m^{-2}yr^{-1}$.

DayCent biogenic emissions

The management levels shown in Table 3.1 were simulated in DayCent for every permutation of the six variables. The biogenic emissions from each scenario were unique results for that particular management permutation. Averaged across scenarios, the scenario biogenic emissions simulated by DayCent amounted to only 17 g CO_2e m^{-2}, which is less than the mean values for either survey supply chain or scenario supply chain emissions (Figure A3). However, the range

of biogenic emissions was very large, with a minimum of -212 g CO_2e m^{-2} and a maximum of 209 g CO_2e m^{-2}.

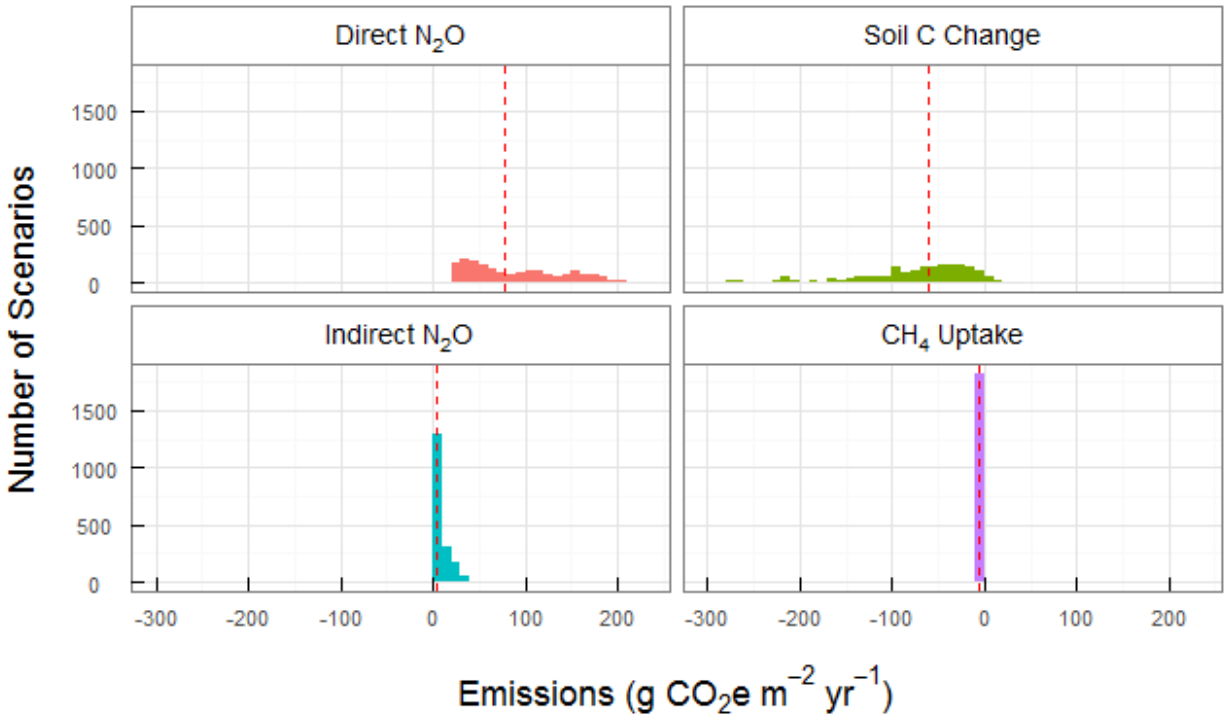

Figure A3. Distributions of study-area average biogenic emissions for all scenarios. Each histogram encompasses a total of 1824 management scenarios, vertical dashed lines indicate median values, and bins have a width of 10 g CO_2e $m^{-2}yr^{-1}$.

Mass vs. marginal allocation of emissions between grain and stover

The FFG emissions summarized in Figure 3.1 encompass DayCent simulation modeling of biogenic emissions combined with supply chain emissions budgets developed to account for all significant emissions embodied in farm inputs and activities. To facilitate comparison of these results with other work, which typically reports biofuel emissions on an energy basis and includes emissions related to biofuel conversion and distribution, we used EtOH yield and emissions values for post-farm activities given by Wang et al. (2012; see Table 4). We then

partitioned the total areal emissions from each management scenario between grain EtOH and stover EtOH using two different methods.

In the first, which we refer to as "marginal allocation", stover was assessed the supply chain emissions from collection, baling and stacking, replacement fertilizers, stover transport and stover post-farm activities, while all other farm inputs, grain transport and post-farm grain activities and were allocated to grain. In addition, stover was burdened with the difference in biogenic emissions between DayCent simulations that differed only in whether or not stover was removed. This approach makes sense from a status-quo perspective, in which corn is cropped primarily for grain harvest and the harvest of stover is a management change under consideration.

In the second allocation approach, dubbed "mass allocation", all supply chain and post-farm emissions directly relating to stover production and conversion were assessed as stover emissions. Likewise, grain was assessed for all grain-specific farm and post-farm activities such as grain harvest and drying, grain transport and grain post-farm emissions. However, all biogenic emissions and those supply chain emissions not clearly related to either feedstock (tillage, N fertilization, etc.) were allocated to each feedstock in proportion to the mass of C removed with each feedstock. This approach allots management burdens according to each feedstock's share of C removals from the system, and so it makes the most sense from a perspective where both grain and stover are viewed as important products of the feedstock cropping system.

The results of the marginal and mass allocation procedures for each scenario are shown in Figure A4 and Figure A5. Those figures also display dashed lines indicating the RFS2 emissions limits that apply to fuels derived from each feedstock. They also show the Scenario ID numbers corresponding to several best- and worst-performing management scenarios for several outcome metrics. The same set of ID numbers are detailed in Table 3.4 and appear on several plots in this study, allowing readers to compare the performance of specific scenarios across emissions metrics.

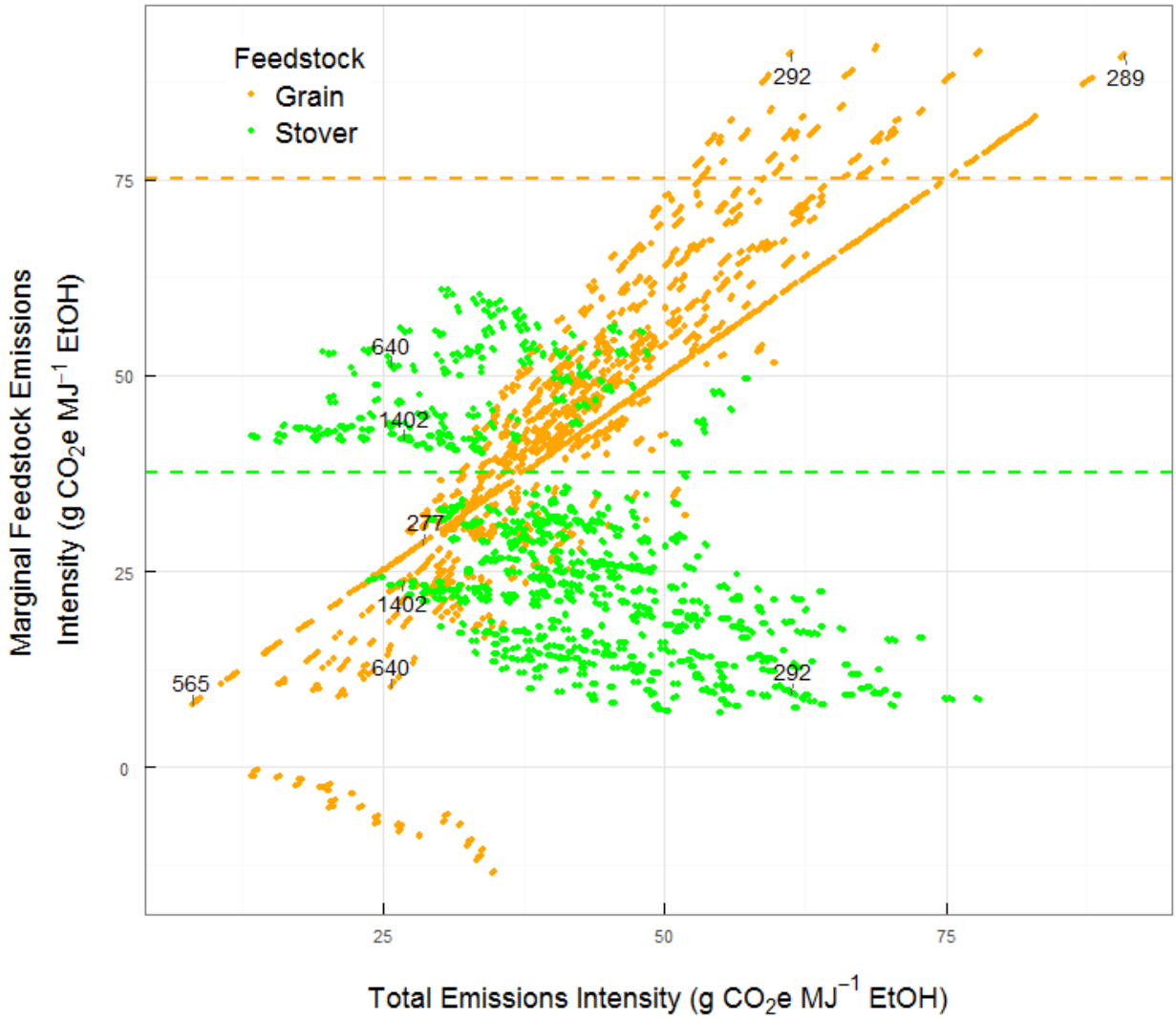

Figure A4. FTW emissions intensity for each management scenario, partitioned between grain and stover using marginal allocation (see Methods for details) and plotted against total emissions intensity. Dashed lines indicate the emissions upper limits defined in the US RFS2 for qualifying Renewable Fuels (orange line, applies to grain EtOH) and Cellulosic Fuels (green line, applies to corn stover EtOH). Scenario ID numbers from selected scenarios are displayed in their approximate positions to facilitate comparison with other figures and Table 3.4 and Table 3.5.

The marginal allocation method used to generate Figure A4 is useful for understanding the emissions attributable to stover EtOH relative to a baseline of identical management without residue collection. By penalizing stover for all foregone C sequestration, however, it generates counter-intuitive results. For instance, the management scenarios with the highest stover

emissions intensities are actually those with no-till management (for example, Scenario IDs 1214, 640 and 280), because under no-till a greater fraction of the lost stover C would have been sequestered as compared to conventional tillage. In other words, stover collection from no-till land represents a greater "opportunity cost" in terms of C sequestration. Of course, this is primarily useful as a descriptive metric rather than a prescriptive metric, since no-till would be expected to sequester more C in absolute terms, whether or not stover is harvested.

In contrast to the marginal allocation shown in Figure A4, the feedstock emissions intensities shown in Figure A5 were calculated by allocating most farm emissions based on the proportion of biomass C removed from the system with each feedstock. This caused feedstock emissions to track linearly with total emissions, with small differences primarily attributable to the fraction of residue being collected. As an illustration of the complexities involved when comparing partial and total emissions intensities, consider Scenario IDs 640 and 1214 in Figure A5. Scenario 640 had higher mass-allocated intensities than 1214 for both grain and stover, but had a lower total emissions intensity. Close examination of the specific values given for these Scenarios in Table 3.4 shows that this occurred because Scenario 640 collected a larger fraction of stover (0.75 vs. 0.25). This means that a larger fraction of its total EtOH energy came from the higher-intensity feedstock (grain), and this difference was more important than the small increases in individual feedstock intensities.

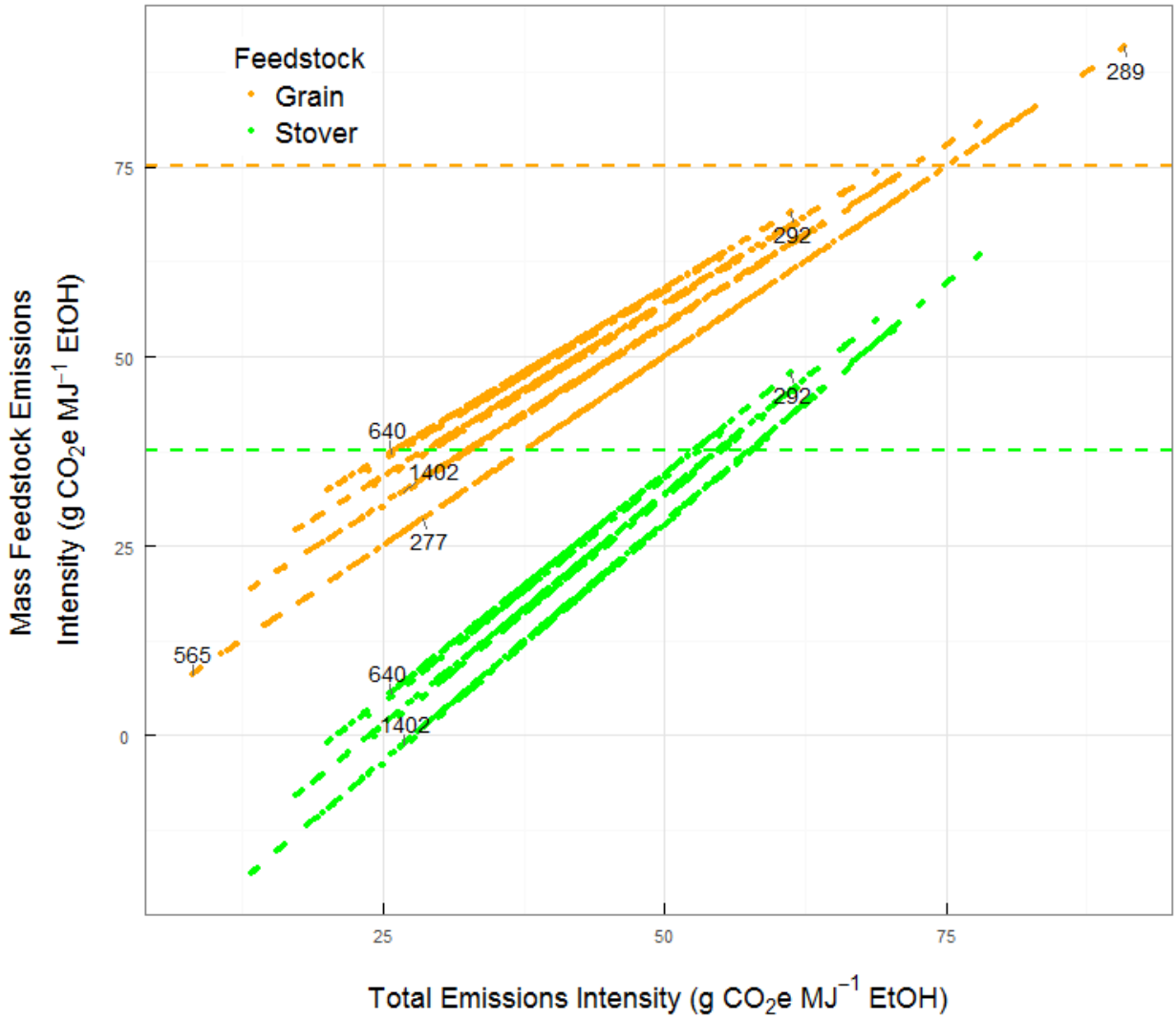

Figure A5. FTW emissions intensity for each management scenario, partitioned between grain and stover using mass allocation (see Methods for details). Dashed lines indicate the emissions upper limits defined in the US RFS2 for qualifying Renewable Fuels (orange line, applies to grain EtOH) and Cellulosic Fuels (green line, applies to corn stover EtOH). Scenario ID numbers from selected scenarios are displayed in their approximate position to facilitate comparison with other figures and Table 3.4 and Table 3.5.

Social cost of carbon methodology and assumptions

The SCC is an economic concept that attempts to quantify the monetary cost of climate change damages attributable to a marginal unit of CO_2-equivalent emissions. As one might imagine, there is very large uncertainty in the determination of this value. The estimates used in the present calculations correspond to multi-model averages reported for different assumed discount

rates as reported by the Interagency Working Group on the Social Cost of Carbon (IAWG, 2013).

Any actual price on emissions would raise costs for fossil fuels and biofuels. Thus, rather than presenting the increased scenario EtOH prices that would be expected after adding the embedded C tax to existing costs, we chose to calculate the difference in C tax that would apply to EtOH derived from each scenario relative to energy-equivalent gasoline. Scenarios were credited with dollar-valued reductions in costs as a function of the emissions (and thus C tax burden) they avoided relative to gasoline. We refer to this difference as an "abatement premium", and its value is specific to each scenario and hypothetical SCC. The abatement premium ($\$ m^{-2}$) expresses the net cost advantage against gasoline conferred by a given SCC for each scenario, and is simply the product of net abatement ($g\ CO_2e\ m^{-2}$) times SCC ($\$ (g\ CO_2e)^{-1}$).

Of course, the use of $\$2.50\ gal^{-1}$ as market price for EtOH was somewhat arbitrary. Prices for transportation fuel are notoriously volatile, and prices faced by EtOH producers are additionally subject to changing federal and state subsidies as well as rapid technological change and economies of scale. The first-order impact of changing EtOH prices is straightforward, with higher prices increasing profits for all scenarios on an absolute scale. However, since scenarios vary significantly in their total energy yield (hence revenue) per cropping area, profits from high-productivity scenarios were more sensitive to a given price change than those from low-productivity scenarios.

Chapter 5 Supporting Information

Crop cultural information from simulated FACE experiments

Table A7. Key details for the four seasons of wheat cropping at Maricopa, AZ, USA.

Experiment ID →	MCWht92	MCWht93	MCWht95	MCWht96
Planting Date	15-Dec-1992	08-Dec-1993	15-Dec-1995	15-Dec-1996
Harvest Date	24-May-1993	01-Jun-1994	29-May-1996	28-May-1997
FACE Start	01-Jan-1993	28-Dec-1993	01-Jan-1996	03-Jan-1997
FACE End	16-May-1993	18-May-1994	15-May-1996	12-May-1997
Irrigation + Rainfall (mm)	Wet: 676 Dry: 351	Wet: 681 Dry: 318	High N: 731 Low N: 670	High N: 650 Low N: 577
N Fertilization (kg N ha^{-1})	All: 271	All: 261	High N: 383 Low N: 100	High N: 383 Low N: 45
Ambient/Enriched [CO_2] (ppm)	360/550	360/550	360/560	360/560
Source(s)	(Kimball *et al.*, 1995; Kimball, 2006)		(Kimball *et al.*, 1999)	

Table A8. Key details for the two seasons of sorghum cropping at Maricopa, AZ, USA.

Experiment ID →	MCSor98	MCSor99
Planting Date	16-Jul-1998	15-Jun-1999
Harvest Date	21-Dec-1998	26-Oct-1999
FACE Start	31-Jul-1998	01-Jul-1999
FACE End	21-Dec-1998	26-Oct-1999
Irrigation + Rainfall (mm)	Wet: 1218 Dry: 474	Wet: 1047 Dry: 491
N Fertilization (kg N ha^{-1})	279	266
Ambient/Enriched [CO_2] (ppm)	396/579	402/585
Source(s)	(Ottman *et al.*, 2001; Kimball & Bernacchi, 2006)	

Table A9. Key details for the seven seasons of soybean cropping at Champaign, IL, USA.

Experiment ID →	SFSoy01	SFSoy02	SFSoy03	SFSoy04	SFSoy05	SFSoy09	SFSoy11
Planting Date	23-May-2001	01-Jun-2002	27-May-2003				
Harvest Date	20-Oct-2001	16-Oct-2002	11-Oct-2003				
Rainfall (mm)						643	610
Ambient/Enriched [CO_2] (ppm)	370/550	370/550	370/550	375/550	375/550	385/585	390/590
Source(s)	(Morgan *et al.*, 2005; Bernacchi *et al.*, 2007)					(Ruiz-Vera *et al.*, 2013)	

Table A10. Key details for the three seasons of corn cropping at Champaign, IL, USA.

Experiment ID →	SFCrn04	SFCrn06	SFCrn10
Planting Date	29-Apr-2004	28-Apr-2006	28-Apr-2008
Harvest Date	10-Sep-2004		
Rainfall (mm)	426	487	424
Ambient/Enriched [CO_2] (ppm)	376/550	382/550	390/550
Source(s)	(Leakey *et al.*, 2006; Hussain *et al.*, 2013; Ruiz-Vera *et al.*, 2015)		

Table A11. Key details for the five seasons of wheat cropping at Horsham, Victoria, AUS.

Experiment ID →	AGWht07 NS	AGWht07 LS	AGWht08 NS	AGWht08 LS	AGWht09 NS	AGWht09 LS
Planting Date	18-Jun-2007	23-Aug-2007	04-Jun-2008	05-Aug-2008	23-Jun-2009	19-Aug-2009
Harvest Date	12-Dec-2007	24-Dec-2007	08-Dec-2008	15-Dec-2008	08-Dec-2009	15-Dec-2009
N Applied + In Soil (kg N ha^{-1})			200	210	211	
Irrigation + Rainfall (mm)	Dry: 219 Wet: 267	Dry: 159 Wet: 207	Dry: 178 Wet: 208	Dry: 108 Wet: 164	Dry: 223 Wet: 293	Dry: 170 Wet: 230
Ambient/Enriched [CO_2] (ppm)	380/550	380/550	390/550	390/550	390/550	390/550
Source(s)	(Norton *et al.*, 2008; Lam *et al.*, 2012c; Fitzgerald *et al.*, 2016)					

Table A12. Key details for the seven seasons of rice cropping at Shizukuishi, Iwate, Japan.

Experiment ID →	JFRice98	JFRice99	JFRice00	JFRice03	JFRice04	JFRice07	JFRice08
Planting Date	07-May-1998	28-Apr-1999	29-Apr-2000	01-May-2003	01-May-2004	01-May-2007	01-May-2008
Harvest Date	29-Sep-1998	20-Sep-1999	19-Sep-1999				
N Fertilization (kg N ha^{-1})	Low: 40 Med: 80 High: 120	Low: 40 Med: 90 High: 150	Low: 40 Med: 90 High: 150	CRN: 80 Spl: 90	CRN: 80 Spl: 90	All: 90	All: 90
Ambient/Enriched [CO_2] (ppm)	368/662	369/640	365/586	366/570	365/548	379/570	376/576
Source(s)	(Kim *et al.*, 2003a, 2003b; Kobayashi *et al.*, 2006)			(Shimono *et al.*, 2008)		(Hasegawa *et al.*, 2013)	

Table A13. Key details for the three seasons of wheat and two seasons of soy cropping at Changping, Beijing, China.

Experiment ID →	CHWht07	CHWht08	CHWht09	CHSoy09	CHSoy11
Planting Date	07-Oct-2007	10-Oct-2008	10-Oct-2009	17-Jun-2009	24-Jun-2011
Harvest Date	07-Jun-2008	13-Jun-2009	27-Jun-2010	06-Oct-2009	04-Oct-2011
N Fertilization (kg N ha^{-1})	Low: 100 High: 170	Low: 100 High: 170	Low: 100 High: 170	4.8	4.8
Irrigation + Rainfall (mm)	459	319	323	420	647
Ambient/Enriched [CO_2] (ppm)	415/550	415/550	415/550	415/550	415/550
Source(s)	(Lam *et al.*, 2012b; Han *et al.*, 2015)			(Lam *et al.*, 2012a; Hao *et al.*, 2014)	

Soils input data from simulated FACE experiments

Table A14. Soils input data used for simulations of FACE experiments at the Maricopa, AZ, USA site.

Layer Upper Bound (cm)	Layer Lower Bound (cm)	Bulk Density (g/cm^3)	Field Capacity (v/v)	Wilting Point (v/v)	% Roots in layer	% Sand	% Clay	% Organic matter	Min soil water content (v/v)	Saturated hydraulic conductivity (cm/s)	pH
0	2	1.31	0.3	0.215	1%	35%	34%	1%	0.14508	0.00064	8.5
2	5	1.31	0.3	0.215	5%	35%	32%	1%	0.10881	0.00064	8.5
5	10	1.31	0.3	0.215	28%	35%	32%	1%	0.07254	0.00064	8.5
10	20	1.27	0.3	0.215	34%	35%	32%	1%	0.018135	0.00064	8.5
20	30	1.27	0.3	0.215	11%	35%	32%	1%	0	0.00064	8.6
30	45	1.3	0.29	0.205	6%	35%	30%	1%	0	0.00021	8.6
45	60	1.47	0.29	0.205	5%	35%	30%	0%	0	0.00021	8.6
60	75	1.57	0.23	0.205	3%	35%	30%	0%	0	0.00021	8.6
75	90	1.57	0.23	0.164	2%	45%	30%	0%	0	0.00047	8.6
90	105	1.57	0.23	0.164	1%	45%	30%	0%	0	0.00047	8.6
105	120	1.57	0.23	0.164	1%	50%	30%	0%	0	0.00047	8.6
120	150	1.57	0.23	0.164	1%	55%	30%	0%	0	0.00047	8.6
150	180	1.57	0.23	0.164	1%	60%	30%	0%	0	0.00047	8.6

Table A15. Soil input data used for simulations of FACE experiments at the Champaign, IL, USA site.

Layer Upper Bound (cm)	Layer Lower Bound (cm)	Bulk Density (g/cm^3)	Field Capacity (v/v)	Wilting Point (v/v)	% Roots in layer	% Sand	% Clay	% Organic matter	Min soil water content	Saturated hydraulic conductivity (cm/s)	pH
0	2	1.34	0.30917	0.1221	0.01124	0.06	0.2	0.02	0.09768	0.00038	6.8
2	5	1.34	0.30917	0.1221	0.04494	0.06	0.2	0.02	0.07326	0.00038	6.8
5	10	1.34	0.30917	0.1221	0.2809	0.06	0.2	0.02	0.04884	0.00038	6.8
10	20	1.34	0.30917	0.1221	0.33708	0.06	0.2	0.02	0.01221	0.00038	6.8
20	30	1.34	0.30917	0.1221	0.11236	0.06	0.2	0.02	0	0.00038	6.8
30	45	1.28	0.34333	0.16326	0.05618	0.06	0.3	0.02	0	0.00018	5.5
45	60	1.25	0.38276	0.20767	0.04494	0.03	0.37	0	0	0.00012	6
60	75	1.25	0.38276	0.20767	0.03371	0.03	0.37	0	0	0.00012	6
75	90	1.25	0.38276	0.20767	0.02247	0.03	0.37	0	0	0.00012	6
90	105	1.25	0.38276	0.20767	0.01124	0.03	0.37	0	0	0.00012	6
105	120	1.25	0.38276	0.20767	0.01124	0.03	0.37	0	0	0.00012	6
120	150	1.25	0.38276	0.20767	0.01124	0.03	0.37	0	0	0.00012	6
150	180	1.28	0.33963	0.15736	0.01124	0.02	0.28	0	0	0.00021	6.3
180	210	1.28	0.33963	0.15736	0.01124	0.02	0.28	0	0	0.00021	6.3

Table A16. Soil input data used for simulations of FACE experiments at the Horsham, Victoria, Australia site.

Layer Upper Bound (cm)	Layer Lower Bound (cm)	Bulk Density (g/cm^3)	Field Capacity (v/v)	Wilting Point (v/v)	% Roots in layer	% Sand	% Clay	% Organic matter	Min soil water content	Saturated hydraulic conductivity (cm/s)	pH
0	2	1.14	0.39	0.2	0.01	0.325	0.35	0.01248	0.08	0.00086	8.4
2	5	1.14	0.39	0.2	0.04	0.325	0.35	0.01248	0.06	0.00086	8.4
5	10	1.14	0.39	0.2	0.25	0.325	0.35	0.01248	0.04	0.00086	8.4
10	20	1.14	0.39	0.2	0.3	0.3	0.4	0.01248	0.01	0.00086	8.4
20	30	1.3	0.4	0.23	0.1	0.3	0.4	0.00708	0	0.00086	8.4
30	45	1.3	0.4	0.23	0.05	0.275	0.45	0.00708	0	0.00086	8.4
45	60	1.37	0.42	0.27	0.04	0.275	0.45	0.00354	0	0.00086	8.9
60	75	1.4	0.43	0.3	0.03	0.25	0.5	0.00177	0	0.00086	9
75	90	1.4	0.45	0.35	0.02	0.25	0.5	0.00044	0	0.00086	9
90	105	1.4	0.45	0.35	0.01	0.225	0.55	0.00044	0	0.00086	9
105	120	1.4	0.45	0.36	0	0.225	0.55	0.00022	0	0.00086	9
120	150	1.4	0.45	0.37	0	0.2	0.6	0.00011	0	0.00086	9.1
150	180	1.4	0.45	0.37	0	0.2	0.6	0.00011	0	0.00086	9.1

Table A17. Soil input data used for simulations of FACE experiments at the Shizukuishi, Iwate, Japan site.

Layer Upper Bound (cm)	Layer Lower Bound (cm)	Bulk Density (g/cm^3)	Field Capacity (v/v)	Wilting Point (v/v)	% Roots in layer	% Sand	% Clay	% Organic matter	Min soil water content	Saturated hydraulic conductivity (cm/s)	pH
0	2	0.73	0.32494	0.10263	0.01	0.43	0.26	0.0083	0.08	0.00086	5.6
2	5	0.73	0.32494	0.10263	0.04	0.43	0.26	0.0083	0.06	0.00086	5.6
5	10	0.73	0.32494	0.10263	0.25	0.43	0.26	0.0083	0.04	0.00086	5.6
10	20	0.73	0.32494	0.10263	0.3	0.43	0.26	0.0083	0.01	0.00086	5.6
20	30	0.73	0.32494	0.10263	0.1	0.43	0.26	0.0083	0	0.00086	5.6
30	45	0.73	0.32494	0.10263	0.05	0.43	0.26	0.0083	0	0.00086	5.6
45	60	0.73	0.32494	0.10263	0.04	0.43	0.26	0.0083	0	0.00086	5.6
60	75	0.73	0.32494	0.10263	0.03	0.43	0.26	0.0083	0	0.00086	5.6
75	90	0.73	0.32494	0.10263	0.02	0.43	0.26	0.0083	0	0.00086	5.6
90	105	0.73	0.32494	0.10263	0.01	0.43	0.26	0.0083	0	0.00086	5.6
105	120	0.73	0.32494	0.10263	0	0.43	0.26	0.0083	0	0.00086	5.6
120	150	0.73	0.32494	0.10263	0	0.43	0.26	0.0083	0	0.00086	5.6
150	180	0.73	0.32494	0.10263	0	0.43	0.26	0.0083	0	0.00086	5.6

Table A18. Soil input data used for simulations of FACE experiments at the Changping, Beijing, China site.

Layer Upper Bound (cm)	Layer Lower Bound (cm)	Bulk Density (g/cm^3)	Field Capacity (v/v)	Wilting Point (v/v)	% Roots in layer	% Sand	% Clay	% Organic matter	Min soil water content	Saturated hydraulic conductivity (cm/s)	pH
0	2	1.21	0.344	0.156	0.01	0.33	0.33	0.0106	0.08	0.000205	8.4
2	5	1.21	0.344	0.156	0.04	0.33	0.33	0.0106	0.06	0.000205	8.4
5	10	1.21	0.344	0.156	0.25	0.33	0.33	0.0106	0.04	0.000205	8.4
10	20	1.21	0.344	0.156	0.3	0.33	0.33	0.0106	0.01	0.000205	8.4
20	30	1.21	0.344	0.156	0.1	0.33	0.33	0.0106	0	0.000205	8.4
30	45	1.21	0.344	0.156	0.05	0.33	0.33	0.0106	0	0.000205	8.4
45	60	1.21	0.344	0.156	0.04	0.33	0.33	0.0106	0	0.000205	8.4
60	75	1.21	0.344	0.156	0.03	0.33	0.33	0.0106	0	0.000205	8.4
75	90	1.21	0.344	0.156	0.02	0.33	0.33	0.0106	0	0.000205	8.4
90	105	1.21	0.344	0.156	0.01	0.33	0.33	0.0106	0	0.000205	8.4
105	120	1.21	0.344	0.156	0	0.33	0.33	0.0106	0	0.000205	8.4
120	150	1.21	0.344	0.156	0	0.33	0.33	0.0106	0	0.000205	8.4
150	180	1.21	0.344	0.156	0	0.33	0.33	0.0106	0	0.000205	8.4

Initial DayCent calibration

This work made use of a recently updated version of DayCent that includes improved simulation of crop LAI and water use and crop growth based on thermal time accumulation (ie., growing degree days rather than calendar days). The rationale, testing and validation of these improvements is described in Zhang (2016).

The goal of the initial calibration process was to minimize systematic bias within DayCent results compared to important observational variables. In practice, the parameters controlling RUE and crop phenology were adjusted as little as possible from default values (which are not cultivar-specific) until the absolute value of relative bias was less than 10%. Modest adjustments to the water use, N limitation, and root allocation parameters were made to improve agreement between observed and simulated season ET, C:N and R:S ratios, respectively.

Crop thermal time parameters for each crop were adjusted to achieve agreement with observed crop anthesis and flowering dates. The resulting parameter values were not necessarily the same as those reported in papers, since methods of thermal time calculation were not always consistent with the one used by DayCent, and temperatures in weather input files were not identical to those measured by on-site weather stations.

In two cases this could not be achieved (Table A14): R:S ratio for wheat, and C:N ratio for rice. The discrepancy in R:S ratio for wheat was caused by a single DayCent simulation of irrigated wheat in Horsham, which was moderately water-stressed and thus increased belowground allocation and reached a R:S ratio of 0.094 versus an observed value of 0.054 (Lam *et al.*, 2012c). The simulated water input was close to the reported amount (34 cm simulated vs 30 cm

reported by Lam *et al.*, 2012c), but this was very low relative to the comparable totals reported for non-water stressed wheat treatments at Maricopa (greater than 60 cm from Kimball *et al.*, 1995 and Hunsaker *et al.*, 2000).

Table A19. DayCent modeled vs. measured performance statistics after calibration to observations from ambient, unstressed FACE treatments. Note that crop-outcome combinations with fewer than three observations were excluded.

Crop	Outcome	Intercept (SE)	Slope (SE)	R^2	N	P	Bias	RMSE
Soy	Yield (g C m^{-2})	38.3 (37.3)	0.602 (0.314)	0.38	8	0.103	6.57	27.1
C_4	Yield (g C m^{-2})	232 (153)	0.295 (0.398)	0.155	5	0.512	7.44	110
C_4	Season ET (mm)	3.59 (20.3)	0.795 (0.382)	0.521	6	0.106	13.57	11.5
Wheat	Yield (g C m^{-2})	82.2 (26.5)	0.614 (0.112)	0.734	13	0.000185	-1.37	63.6
Wheat	Season ET (mm)	58.8 (44.6)	0.0529 (0.75)	0.00248	4	0.95	-4.35	4.2
Wheat	C:N Ratio	-36.6 (48.1)	2.26 (1.77)	0.291	6	0.269	8.37	4.94
Wheat	R:S Ratio	-0.0202 (0.00238)	1.4 (0.0409)	0.999	3	0.0186	-4.02	0.00672
Rice	Yield (g C m^{-2})	12.7 (83.1)	0.897 (0.326)	0.407	13	0.019	5.32	37
Rice	C:N Ratio	179 (143)	-3.93 (4.22)	0.178	6	0.404	-35.2	15.5

The C:N ratio of several rice observations based on Shimono *et al.* (2008) was derived from reported N uptake and dry biomass figures, assuming a 40% C content of dry biomass. While these treatments included N application comparable with the medium N treatments of (Kim *et*

al., 2003b), the observed values averaged a C:N ratio of 52.1, which was substantially higher than corresponding values from the low N treatments of (Kim *et al.*, 2003b).

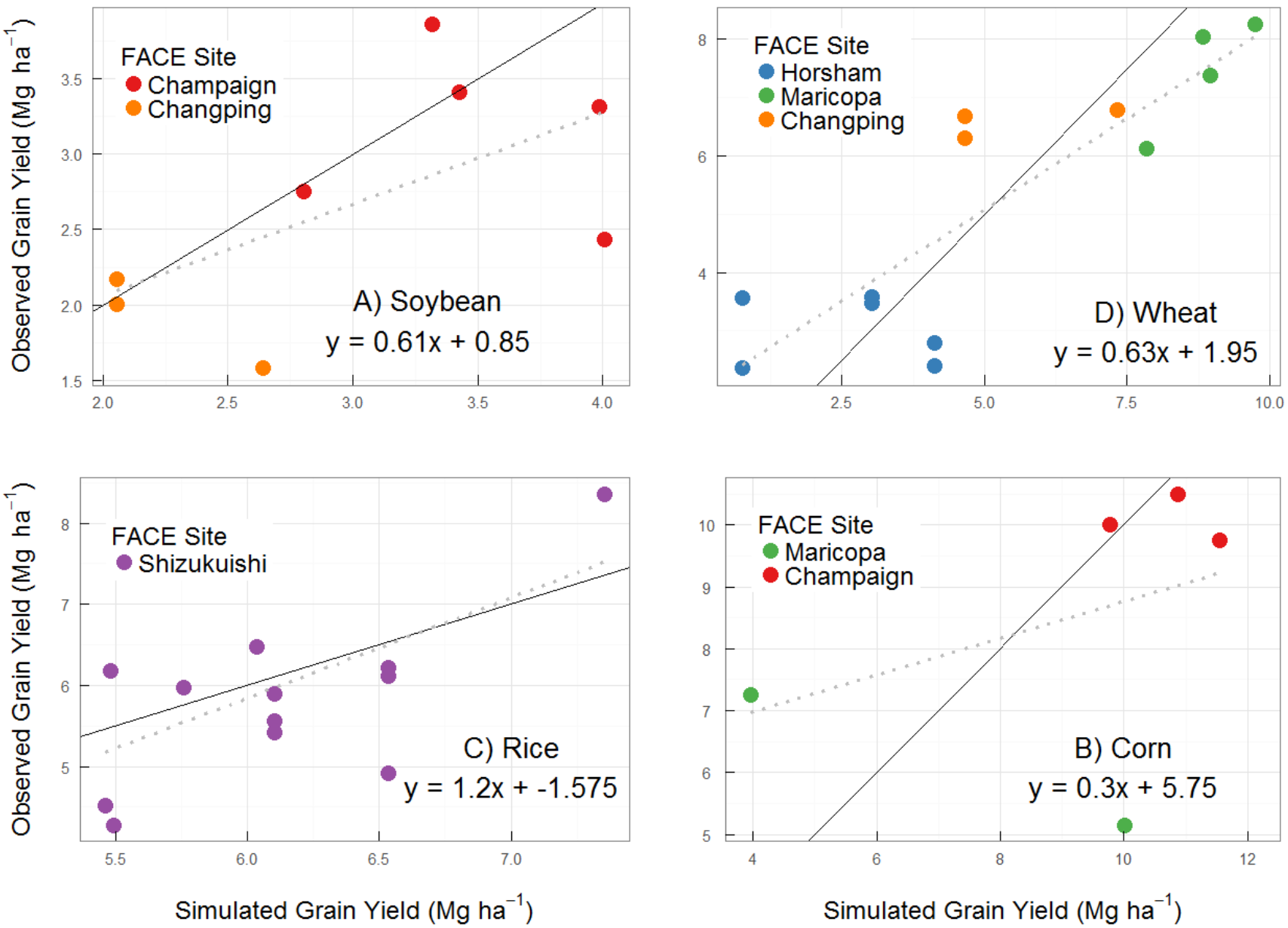
FACE Site
Champaign
Changping
A) Soybean
y = 0.61x + 0.85
FACE Site
Horsham
Maricopa
Changping
D) Wheat
y = 0.63x + 1.95
FACE Site
Shizukuishi
C) Rice
y = 1.2x + -1.575
FACE Site
Maricopa
Champaign
B) Corn
y = 0.3x + 5.75
Observed Grain Yield (Mg ha^{-1})
Simulated Grain Yield (Mg ha^{-1})

Figure A6. Observed vs. simulated grain yields for soybean, wheat, rice and C_4 crops (corn & sorghum) from ambient, unstressed treatments only. Solid black lines depict 1:1 lines, while dotted gray lines show linear regression of observed on simulated values. Simulated results shown here reflect DayCent performance after calibrating crop parameters unrelated to [CO_2] response, including radiation use efficiency (RUE), phenology, biomass N requirements, and C partitioning.

Calibrated DayCent crop.100 parameter files

The following are the specific calibrated crop parameter sets (contained in an input file known as a crop.100 file) used for each crop at each site. Note that parameter values for a given crop sometimes vary between different sites, but the CO_2 response parameters were calibrated to be the same for a given crop across sites. The actual files exist in a single column but have been converted to two-column format here for readability.

Champaign, Illinois, USA

Maize

C6 corn built on: C603 corn-c6 P31

```
0.185       'PRDX(1)'   6/15/10 SAW 1.2
30.0        'PPDF(1)'
45.0        'PPDF(2)'
1.0         'PPDF(3)'
2.5         'PPDF(4)'
0.0         'BIOFLG'
1800.0      'BIOK5'
0.9         'PLTMRF'
150.0       'FULCAN'
5           'FRTCINDX'
0.4         'FRTC(1)' 6/3/10 SAW .5
0.1         'FRTC(2)'
90.0        'FRTC(3)' days
0.1         'FRTC(4)'
0.1         'FRTC(5)'
0.3         'CFRTCN(1)'
0.25        'CFRTCN(2)'
0.5         'CFRTCW(1)'
0.1         'CFRTCW(2)'
700.0       'BIOMAX' 700
20.0        'PRAMN(1,1)' 15
150.0       'PRAMN(2,1)'
190.0       'PRAMN(3,1)'
62.5        'PRAMN(1,2)'
150.0       'PRAMN(2,2)'
150.0       'PRAMN(3,2)'
40.0        'PRAMX(1,1)'
230.0       'PRAMX(2,1)'
230.0       'PRAMX(3,1)'
125.0       'PRAMX(1,2)'
230.0       'PRAMX(2,2)'
230.0       'PRAMX(3,2)'
45.0        'PRBMN(1,1)'
390.0       'PRBMN(2,1)'
340.0       'PRBMN(3,1)'
0.0         'PRBMN(1,2)'
0.0         'PRBMN(2,2)'
0.0         'PRBMN(3,2)'
60.0        'PRBMX(1,1)'
420.0       'PRBMX(2,1)'
420.0       'PRBMX(3,1)'
0.0         'PRBMX(1,2)'
0.0         'PRBMX(2,2)'
0.0         'PRBMX(3,2)'
0.12        'FLIGNI(1,1)'
0.0         'FLIGNI(2,1)'
0.06        'FLIGNI(1,2)'
0.0         'FLIGNI(2,2)'
0.06        'FLIGNI(1,3)'
0.0         'FLIGNI(2,3)'
0.58        'HIMAX'   6/15/10 SAW 0.60
0.5         'HIWSF'
1.0         'HIMON(1)'
0.0         'HIMON(2)'
0.75        'EFRGRN(1)'
0.6         'EFRGRN(2)'
0.6         'EFRGRN(3)'
0.04        'VLOSSP'
0.0         'FSDETH(1)'
0.0         'FSDETH(2)'
0.0         'FSDETH(3)'
500.0       'FSDETH(4)'
0.1         'FALLRT'
0.05        'RDRJ'
0.05        'RDRM'
0.14        'RDSRFC'
2.0         'RTDTMP'
0.0         'CRPRTF(1)'
0.0         'CRPRTF(2)'
0.0         'CRPRTF(3)'
0.05        'MRTFRAC'
0.0         'SNFXMX(1)'
-15.0       'DEL13C'
1.0         'CO2IPR(1)'
0.82        'CO2ITR(1)'
```

1.0 'CO2ICE(1,1,1)'
1.0 'CO2ICE(1,1,2)'
1.0 'CO2ICE(1,1,3)'
1.0 'CO2ICE(1,2,1)'
1.0 'CO2ICE(1,2,2)'
1.0 'CO2ICE(1,2,3)'
1.0 'CO2IRS(1)'
0.10000 'CKMRSPMX(1)'
0.15000 'CKMRSPMX(2)'
0.05000 'CKMRSPMX(3)'
0.00000 'CMRSPNPP(1)'
0.00000 'CMRSPNPP(2)'
1.25000 'CMRSPNPP(3)'
1.00000 'CMRSPNPP(4)'
4.00000 'CMRSPNPP(5)'
1.50000 'CMRSPNPP(6)'
0.23000 'CGRESP(1)'
0.23000 'CGRESP(2)'
0.23000 'CGRESP(3)'
0.25000 'NO3PREF(1)'
7.00000 'CLAYPG'
0.50000 'CMIX'
-13.000 'TMPGERM'
730.00 'DDBASE'
-3.5 'TMPKILL'
10 'BASETEMP'
30 'BASETEMP(2)'
650 'MNDDHRV'
650 'MXDDHRV'
120.0 'CURGDYS'
0.5 'CLSGRES'
0.12 'CMXTURN'
1.0 'NPP2CS(1)'
2.0 'CAFUE'
1.40 'EMAX'
1.1 'KCET'
0.6 'KLIGHT'
0.02 'SLA'
0.9 'LEAFCL'
0.9 'LEAFEMERG'
0.3 'LEAFMX'
0.02 'LEAFPM'
103 'DDEMERG'
850 'DDLAIMX'

Soybean

SYBN soybeans built on: SY02 Soybeans Mead2
0.07 'PRDX(1)' 6/15/10 SAW 0.65
27.0 'PPDF(1)'
40.0 'PPDF(2)' 40 8/20/10 SAW
1.0 'PPDF(3)'
2.5 'PPDF(4)'
0.0 'BIOFLG'
1800.0 'BIOK5'
1.4 'PLTMRF'
150.0 'FULCAN'
5 'FRTCIN'
0.35 'FRTC(1)' 6/8/10 SAW 0.5 .4
0.05 'FRTC(2)' 0.1 8/13/10 SAW
60.0 'FRTC(3)' days
0.1 'FRTC(4)' 6/8/10 SAW 0.2
0.1 'FRTC(5)'
0.4 'CFRTCN(1)'
0.25 'CFRTCN(2)'
0.5 'CFRTCW(1)'
0.1 'CFRTCW(2)'
200.0 'BIOMAX'
5.0 'PRAMN(1,1)'
150.0 'PRAMN(2,1)'
100.0 'PRAMN(3,1)'
15.0 'PRAMN(1,2)'
150.0 'PRAMN(2,2)'
100.0 'PRAMN(3,2)'
15.0 'PRAMX(1,1)'
230.0 'PRAMX(2,1)'
100.0 'PRAMX(3,1)'
30.0 'PRAMX(1,2)'
230.0 'PRAMX(2,2)'

100.0 'PRAMX(3,2)'
24.0 'PRBMN(1,1)'
390.0 'PRBMN(2,1)'
100.0 'PRBMN(3,1)'
0.0 'PRBMN(1,2)'
0.0 'PRBMN(2,2)'
000.0 'PRBMN(3,2)'
32.0 'PRBMX(1,1)'
420.0 'PRBMX(2,1)'
100.0 'PRBMX(3,1)'
0.0 'PRBMX(1,2)'
0.0 'PRBMX(2,2)'
000.0 'PRBMX(3,2)'
0.12 'FLIGNI(1,1)'
0.0 'FLIGNI(2,1)'
0.06 'FLIGNI(1,2)'
0.0 'FLIGNI(2,2)'
0.06 'FLIGNI(1,3)'
0.0 'FLIGNI(2,3)'
0.55 'HIMAX' 6/8/10 SAW 0.31
0.5 'HIWSF' 0.25 8/13/10 SAW .5
1.0 'HIMON(1)' 6/18/10 SAW 2
0.0 'HIMON(2)' 6/18/10 SAW 1
0.70 'EFRGRN(1)' 6/16/10 SAW
0.57 .75
0.6 'EFRGRN(2)'
0.6 'EFRGRN(3)'
0.04 'VLOSSP'
0.0 'FSDETH(1)'
0.0 'FSDETH(2)'
0.0 'FSDETH(3)'
500.0 'FSDETH(4)'
0.1 'FALLRT'
0.5 'RDRJ'
0.15 'RDRM'
0.14 'RDSRFC'
2.0 'RTDTMP'
0.0 'CRPRTF(1)'
0.0 'CRPRTF(2)'
0.0 'CRPRTF(3)'
0.05 'MRTFRAC'
0.0600 'SNFXMX(1)'
-27.0 'DEL13C'
1.12 'CO2IPR(1)'
0.58 'CO2ITR(1)'
1.0 'CO2ICE(1,1,1)'
1.0 'CO2ICE(1,1,2)'
1.0 'CO2ICE(1,1,3)'
1.0 'CO2ICE(1,2,1)'
1.0 'CO2ICE(1,2,2)'
1.0 'CO2ICE(1,2,3)'
1.0 'CO2IRS(1)'
0.10000 'CKMRSPMX(1)'
0.15000 'CKMRSPMX(2)'
0.05000 'CKMRSPMX(3)'
0.00000 'CMRSPNPP(1)'
0.00000 'CMRSPNPP(2)'
1.25000 'CMRSPNPP(3)'
1.00000 'CMRSPNPP(4)'
4.00000 'CMRSPNPP(5)'
1.50000 'CMRSPNPP(6)'
0.23000 'CGRESP(1)'
0.23000 'CGRESP(2)'
0.23000 'CGRESP(3)'
0.50000 'NO3PREF(1)'
6.00000 'CLAYPG'
0.50000 'CMIX'
-17.0000 'TMPGERM'
500 'DDBASE'
-2.0 'TMPKILL'
10 'BASETEMP'
30 'BASETEMP(2)'
900 'MNDDHRV' 100
900 'MXDDHRV' 400
120.0 'CURGDYS'
0.5 'CLSGRES'
0.12 'CMXTURN'
1.0 'NPP2CS(1)'
2.0 'CAFUE'
0.90 'EMAX'

1.1 'KCET'
0.6 'KLIGHT'
0.025 'SLA'
0.7 'LEAFCL'
0.85 'LEAFEMERG'
0.30 'LEAFMX'
0.00 'LEAFPM'
103 'DDEMERG'
1000 'DDLAIMX'

Maricopa, Arizona, USA

Sorghum

SORG sorghum built from corn built on:
C603 corn-c6 P31
0.115 'PRDX(1)' 6/15/10 SAW 1.2
30.0 'PPDF(1)'
45.0 'PPDF(2)'
1.0 'PPDF(3)'
2.5 'PPDF(4)'
0.0 'BIOFLG'
1800.0 'BIOK5'
0.9 'PLTMRF'
150.0 'FULCAN'
5 'FRTCINDX'
0.4 'FRTC(1)' 6/3/10 SAW .5
0.1 'FRTC(2)'
90.0 'FRTC(3)' days
0.1 'FRTC(4)'
0.1 'FRTC(5)'
0.3 'CFRTCN(1)'
0.25 'CFRTCN(2)'
0.5 'CFRTCW(1)'
0.1 'CFRTCW(2)'
700.0 'BIOMAX' 700
20.0 'PRAMN(1,1)' 15
150.0 'PRAMN(2,1)'
190.0 'PRAMN(3,1)'
62.5 'PRAMN(1,2)'
150.0 'PRAMN(2,2)'
150.0 'PRAMN(3,2)'
40.0 'PRAMX(1,1)'
230.0 'PRAMX(2,1)'
230.0 'PRAMX(3,1)'
125.0 'PRAMX(1,2)'
230.0 'PRAMX(2,2)'
230.0 'PRAMX(3,2)'
45.0 'PRBMN(1,1)'
390.0 'PRBMN(2,1)'
340.0 'PRBMN(3,1)'
0.0 'PRBMN(1,2)'
0.0 'PRBMN(2,2)'
0.0 'PRBMN(3,2)'
60.0 'PRBMX(1,1)'
420.0 'PRBMX(2,1)'
420.0 'PRBMX(3,1)'
0.0 'PRBMX(1,2)'
0.0 'PRBMX(2,2)'
0.0 'PRBMX(3,2)'
0.12 'FLIGNI(1,1)'
0.0 'FLIGNI(2,1)'
0.06 'FLIGNI(1,2)'
0.0 'FLIGNI(2,2)'
0.06 'FLIGNI(1,3)'
0.0 'FLIGNI(2,3)'
0.55 'HIMAX' 6/15/10 SAW 0.60
0.5 'HIWSF'
1.0 'HIMON(1)'
0.0 'HIMON(2)'
0.75 'EFRGRN(1)'
0.6 'EFRGRN(2)'
0.6 'EFRGRN(3)'
0.04 'VLOSSP'
0.0 'FSDETH(1)'
0.0 'FSDETH(2)'
0.0 'FSDETH(3)'
500.0 'FSDETH(4)'
0.1 'FALLRT'
0.05 'RDRJ'

0.05 'RDRM'
0.14 'RDSRFC'
2.0 'RTDTMP'
0.0 'CRPRTF(1)'
0.0 'CRPRTF(2)'
0.0 'CRPRTF(3)'
0.05 'MRTFRAC'
0.0 'SNFXMX(1)'
-15.0 'DEL13C'
1.0 'CO2IPR(1)'
0.82 'CO2ITR(1)'
1.0 'CO2ICE(1,1,1)'
1.0 'CO2ICE(1,1,2)'
1.0 'CO2ICE(1,1,3)'
1.0 'CO2ICE(1,2,1)'
1.0 'CO2ICE(1,2,2)'
1.0 'CO2ICE(1,2,3)'
1.0 'CO2IRS(1)'
0.10000 'CKMRSPMX(1)'
0.15000 'CKMRSPMX(2)'
0.05000 'CKMRSPMX(3)'
0.00000 'CMRSPNPP(1)'
0.00000 'CMRSPNPP(2)'
1.25000 'CMRSPNPP(3)'
1.00000 'CMRSPNPP(4)'
4.00000 'CMRSPNPP(5)'
1.50000 'CMRSPNPP(6)'
0.23000 'CGRESP(1)'
0.23000 'CGRESP(2)'
0.23000 'CGRESP(3)'
0.25000 'NO3PREF(1)'
7.00000 'CLAYPG'
0.50000 'CMIX'
-13.000 'TMPGERM'
1000.00 'DDBASE'
-3.5 'TMPKILL'
10 'BASETEMP'
30 'BASETEMP(2)'
850 'MNDDHRV'
850 'MXDDHRV'
120.0 'CURGDYS'
0.5 'CLSGRES'
0.12 'CMXTURN'
1.0 'NPP2CS(1)'
2.0 'CAFUE'
1.40 'EMAX'
1.2 'KCET'
0.6 'KLIGHT'
0.02 'SLA'
0.9 'LEAFCL'
0.9 'LEAFEMERG'
0.3 'LEAFMX'
0.02 'LEAFPM'
103 'DDEMERG'
1000 'DDLAIMX'

Wheat

SW3 spring wheat build on: W3F5 Wheat, GDD, new LAI
0.105 'PRDX(1)'
0.105 'PRDX(1)'
20.0 'PPDF(1)'
40.0 'PPDF(2)'
0.7 'PPDF(3)'
5.0 'PPDF(4)'
0.0 'BIOFLG'
1800.0 'BIOK5'
40 'PLTMRF'
150.0 'FULCAN'
5.00000 'FRTCINDX'
0.4 'FRTC(1)'
0.03 'FRTC(2)'
60.0 'FRTC(3)' days
0.1 'FRTC(4)'
0.1 'FRTC(5)'
0.4 'CFRTCN(1)'
0.25 'CFRTCN(2)'
0.6 'CFRTCW(1)'
0.1 'CFRTCW(2)'

300.0	'BIOMAX'
14.0	'PRAMN(1,1)'
100.0	'PRAMN(2,1)'
100.0	'PRAMN(3,1)'
28.0	'PRAMN(1,2)'
160.0	'PRAMN(2,2)'
200.0	'PRAMN(3,2)'
40.0	'PRAMX(1,1)'
200.0	'PRAMX(2,1)'
230.0	'PRAMX(3,1)'
120.0	'PRAMX(1,2)'
260.0	'PRAMX(2,2)'
270.0	'PRAMX(3,2)'
45.0	'PRBMN(1,1)'
390.0	'PRBMN(2,1)'
340.0	'PRBMN(3,1)'
0.0	'PRBMN(1,2)'
0.0	'PRBMN(2,2)'
0.0	'PRBMN(3,2)'
60.0	'PRBMX(1,1)'
420.0	'PRBMX(2,1)'
420.0	'PRBMX(3,1)'
0.0	'PRBMX(1,2)'
0.0	'PRBMX(2,2)'
0.0	'PRBMX(3,2)'
0.15	'FLIGNI(1,1)'
0.0	'FLIGNI(2,1)'
0.06	'FLIGNI(1,2)'
0.0	'FLIGNI(2,2)'
0.06	'FLIGNI(1,3)'
0.0	'FLIGNI(2,3)'
0.45	'HIMAX'
0.5	'HIWSF'
1.0	'HIMON(1)'
0.0	'HIMON(2)'
0.65	'EFRGRN(1)'
0.6	'EFRGRN(2)'
0.6	'EFRGRN(3)'
0.04	'VLOSSP'
0.0	'FSDETH(1)'
0.0	'FSDETH(2)'
0.0	'FSDETH(3)'
200.0	'FSDETH(4)'
0.12	'FALLRT'
0.05	'RDRJ'
0.05	'RDRM'
0.14	'RDSRFC'
2.0	'RTDTMP'
0.0	'CRPRTF(1)'
0.0	'CRPRTF(2)'
0.0	'CRPRTF(3)'
0.05	'MRTFRAC'
0.0	'SNFXMX(1)'
-27.0	'DEL13C'
1.22	'CO2IPR(1)'
0.88	'CO2ITR(1)'
1.08	'CO2ICE(1,1,1)'
1.0	'CO2ICE(1,1,2)'
1.0	'CO2ICE(1,1,3)'
1.08	'CO2ICE(1,2,1)'
1.0	'CO2ICE(1,2,2)'
1.0	'CO2ICE(1,2,3)'
1.0	'CO2IRS(1)'
0.10000	'CKMRSPMX(1)'
0.15000	'CKMRSPMX(2)'
0.05000	'CKMRSPMX(3)'
0.00000	'CMRSPNPP(1)'
0.00000	'CMRSPNPP(2)'
1.25000	'CMRSPNPP(3)'
1.00000	'CMRSPNPP(4)'
4.00000	'CMRSPNPP(5)'
1.50000	'CMRSPNPP(6)'
0.23000	'CGRESP(1)'
0.23000	'CGRESP(2)'
0.23000	'CGRESP(3)'
0.25000	'NO3PREF(1)'
6.00000	'CLAYPG'
0.50000	'CMIX'
-10.0000	'TMPGERM'
1000.00	'DDBASE'

-20.0 'TMPKILL'
5 'BASETEMP'
26 'BASETEMP(2)'
500 'MNDDHRV'
500 'MXDDHRV'
120.0 'CURGDYS'
0.5 'CLSGRES'
0.12 'CMXTURN'
1.0 'NPP2CS(1)'
2.0 'CAFUE'
0.90 'EMAX'
1.2 'KCET'
0.85 'KLIGHT'
0.03 'SLA'
0.4 'LEAFCL'
0.7 'LEAFEMERG'
0.15 'LEAFMX'
0.0 'LEAFPM'
0.01 'DDEMERG'
1000 'DDLAIMX'

Horsham, Victoria, Australia

Wheat

SW3AU spring wheat build on: W3F5
Wheat, GDD, new LAI
0.16 'PRDX(1)'
20.0 'PPDF(1)'
40.0 'PPDF(2)'
0.7 'PPDF(3)'
5.0 'PPDF(4)'
0.0 'BIOFLG'
1800.0 'BIOK5'
40 'PLTMRF'
150.0 'FULCAN'
5.00000 'FRTCINDX'
0.4 'FRTC(1)'
0.03 'FRTC(2)'
60.0 'FRTC(3)' days
0.05 'FRTC(4)'
0.1 'FRTC(5)'
0.4 'CFRTCN(1)'
0.25 'CFRTCN(2)'
0.6 'CFRTCW(1)'
0.1 'CFRTCW(2)'
300.0 'BIOMAX'
14.0 'PRAMN(1,1)'
100.0 'PRAMN(2,1)'
100.0 'PRAMN(3,1)'
28.0 'PRAMN(1,2)'
160.0 'PRAMN(2,2)'
200.0 'PRAMN(3,2)'
40.0 'PRAMX(1,1)'
200.0 'PRAMX(2,1)'
230.0 'PRAMX(3,1)'
120.0 'PRAMX(1,2)'
260.0 'PRAMX(2,2)'
270.0 'PRAMX(3,2)'
45.0 'PRBMN(1,1)'
390.0 'PRBMN(2,1)'
340.0 'PRBMN(3,1)'
0.0 'PRBMN(1,2)'
0.0 'PRBMN(2,2)'
0.0 'PRBMN(3,2)'
60.0 'PRBMX(1,1)'
420.0 'PRBMX(2,1)'
420.0 'PRBMX(3,1)'
0.0 'PRBMX(1,2)'
0.0 'PRBMX(2,2)'
0.0 'PRBMX(3,2)'
0.15 'FLIGNI(1,1)'
0.0 'FLIGNI(2,1)'
0.06 'FLIGNI(1,2)'
0.0 'FLIGNI(2,2)'
0.06 'FLIGNI(1,3)'
0.0 'FLIGNI(2,3)'
0.52 'HIMAX'
0.50 'HIWSF'
1.0 'HIMON(1)'

0.0 'HIMON(2)'
0.65 'EFRGRN(1)'
0.6 'EFRGRN(2)'
0.6 'EFRGRN(3)'
0.04 'VLOSSP'
0.0 'FSDETH(1)'
0.0 'FSDETH(2)'
0.0 'FSDETH(3)'
200.0 'FSDETH(4)'
0.12 'FALLRT'
0.05 'RDRJ'
0.05 'RDRM'
0.14 'RDSRFC'
2.0 'RTDTMP'
0.0 'CRPRTF(1)'
0.0 'CRPRTF(2)'
0.0 'CRPRTF(3)'
0.05 'MRTFRAC'
0.0 'SNFXMX(1)'
-27.0 'DEL13C'
1.22 'CO2IPR(1)'
0.88 'CO2ITR(1)'
1.08 'CO2ICE(1,1,1)'
1.0 'CO2ICE(1,1,2)'
1.0 'CO2ICE(1,1,3)'
1.08 'CO2ICE(1,2,1)'
1.0 'CO2ICE(1,2,2)'
1.0 'CO2ICE(1,2,3)'
1.0 'CO2IRS(1)'
0.10000 'CKMRSPMX(1)'
0.15000 'CKMRSPMX(2)'
0.05000 'CKMRSPMX(3)'
0.00000 'CMRSPNPP(1)'
0.00000 'CMRSPNPP(2)'
1.25000 'CMRSPNPP(3)'
1.00000 'CMRSPNPP(4)'
4.00000 'CMRSPNPP(5)'
1.50000 'CMRSPNPP(6)'
0.23000 'CGRESP(1)'
0.23000 'CGRESP(2)'
0.23000 'CGRESP(3)'
0.25000 'NO3PREF(1)'
6.00000 'CLAYPG'
0.50000 'CMIX'
-10.0000 'TMPGERM'
900.00 'DDBASE'
-20.0 'TMPKILL'
5 'BASETEMP'
26 'BASETEMP(2)'
500 'MNDDHRV'
500 'MXDDHRV'
120.0 'CURGDYS'
0.5 'CLSGRES'
0.12 'CMXTURN'
1.0 'NPP2CS(1)'
2.0 'CAFUE'
0.90 'EMAX'
1.2 'KCET'
0.85 'KLIGHT'
0.03 'SLA'
0.4 'LEAFCL'
0.7 'LEAFEMERG'
0.15 'LEAFMX'
0.0 'LEAFPM'
0.01 'DDEMERG'
1000 'DDLAIMX'

Shizukuishi, Iwate, Japan

Rice

RICL spring wheat build on: W3F5
Wheat, GDD, new LAI
0.145 'PRDX(1)'
30.0 'PPDF(1)'
45.0 'PPDF(2)'
1.0 'PPDF(3)'
2.50 'PPDF(4)'
0.0 'BIOFLG'
1800.0 'BIOK5'

40 'PLTMRF'
150.0 'FULCAN'
5.0 'FRTCINDX'
0.4 'FRTC(1)'
0.03 'FRTC(2)'
60.0 'FRTC(3)' days
0.0001 'FRTC(4)'
0.0001 'FRTC(5)'
0.4 'CFRTCN(1)'
0.25 'CFRTCN(2)'
0.6 'CFRTCW(1)'
0.1 'CFRTCW(2)'
700.0 'BIOMAX'
20.0 'PRAMN(1,1)'
100.0 'PRAMN(2,1)'
100.0 'PRAMN(3,1)'
40.0 'PRAMN(1,2)'
160.0 'PRAMN(2,2)'
200.0 'PRAMN(3,2)'
40.0 'PRAMX(1,1)'
200.0 'PRAMX(2,1)'
230.0 'PRAMX(3,1)'
120.0 'PRAMX(1,2)'
260.0 'PRAMX(2,2)'
270.0 'PRAMX(3,2)'
45.0 'PRBMN(1,1)'
390.0 'PRBMN(2,1)'
340.0 'PRBMN(3,1)'
0.0 'PRBMN(1,2)'
0.0 'PRBMN(2,2)'
0.0 'PRBMN(3,2)'
60.0 'PRBMX(1,1)'
240.0 'PRBMX(2,1)'
240.0 'PRBMX(3,1)'
0.0 'PRBMX(1,2)'
0.0 'PRBMX(2,2)'
0.0 'PRBMX(3,2)'
0.15 'FLIGNI(1,1)'
0.0 'FLIGNI(2,1)'
0.06 'FLIGNI(1,2)'
0.0 'FLIGNI(2,2)'
0.06 'FLIGNI(1,3)'
0.0 'FLIGNI(2,3)'
0.45 'HIMAX'
0.5 'HIWSF'
1.0 'HIMON(1)'
0.0 'HIMON(2)'
0.65 'EFRGRN(1)'
0.6 'EFRGRN(2)'
0.6 'EFRGRN(3)'
0.04 'VLOSSP'
0.0 'FSDETH(1)'
0.0 'FSDETH(2)'
0.0 'FSDETH(3)'
200.0 'FSDETH(4)'
0.12 'FALLRT'
0.05 'RDRJ'
0.05 'RDRM'
0.14 'RDSRFC'
2.0 'RTDTMP'
0.0 'CRPRTF(1)'
0.0 'CRPRTF(2)'
0.0 'CRPRTF(3)'
0.05 'MRTFRAC'
0.0 'SNFXMX(1)'
-27.0 'DEL13C'
1.21 'CO2IPR(1)'
0.75 'CO2ITR(1)'
1.05 'CO2ICE(1,1,1)'
1.0 'CO2ICE(1,1,2)'
1.0 'CO2ICE(1,1,3)'
1.05 'CO2ICE(1,2,1)'
1.0 'CO2ICE(1,2,2)'
1.0 'CO2ICE(1,2,3)'
1.0 'CO2IRS(1)'
0.1 'CKMRSPMX(1)'
0.150 'CKMRSPMX(2)'
0.050 'CKMRSPMX(3)'
0.0 'CMRSPNPP(1)'
0.0 'CMRSPNPP(2)'

1.250 'CMRSPNPP(3)'
1.0 'CMRSPNPP(4)'
4.0 'CMRSPNPP(5)'
1.5 'CMRSPNPP(6)'
0.230 'CGRESP(1)'
0.230 'CGRESP(2)'
0.230 'CGRESP(3)'
0.250 'NO3PREF(1)'
6.0 'CLAYPG'
0.5 'CMIX'
-10.0000 'TMPGERM'
1200.00 'DDBASE'
-20.0 'TMPKILL'
5 'BASETEMP'
26 'BASETEMP(2)'
800 'MNDDHRV'
800 'MXDDHRV'
120.0 'CURGDYS'
0.5 'CLSGRES'
0.12 'CMXTURN'
1.0 'NPP2CS(1)'
2.0 'CAFUE'
0.9 'EMAX'
1.2 'KCET'
0.85 'KLIGHT'
0.03 'SLA'
0.4 'LEAFCL'
0.7 'LEAFEMERG'
0.15 'LEAFMX'
0.0 'LEAFPM'
0.01 'DDEMERG'
1200 'DDLAIMX'

Changping, Beijing, China

Soybean

SYBNCH soybeans built on: SY02
Soybeans Mead2
0.11 'PRDX(1)' 6/15/10 SAW 0.65
20.0 'PPDF(1)'
35.0 'PPDF(2)' 40 8/20/10 SAW
1.0 'PPDF(3)'
2.5 'PPDF(4)'
0.0 'BIOFLG'
1800.0 'BIOK5'
1.4 'PLTMRF'
150.0 'FULCAN'
5 'FRTCIN'
0.35 'FRTC(1)' 6/8/10 SAW 0.5 .4
0.05 'FRTC(2)' 0.1 8/13/10 SAW
60.0 'FRTC(3)' days
0.1 'FRTC(4)' 6/8/10 SAW 0.2
0.1 'FRTC(5)'
0.4 'CFRTCN(1)'
0.25 'CFRTCN(2)'
0.5 'CFRTCW(1)'
0.1 'CFRTCW(2)'
200.0 'BIOMAX'
5.0 'PRAMN(1,1)'
150.0 'PRAMN(2,1)'
100.0 'PRAMN(3,1)'
15.0 'PRAMN(1,2)'
150.0 'PRAMN(2,2)'
100.0 'PRAMN(3,2)'
15.0 'PRAMX(1,1)'
230.0 'PRAMX(2,1)'
100.0 'PRAMX(3,1)'
30.0 'PRAMX(1,2)'
230.0 'PRAMX(2,2)'
100.0 'PRAMX(3,2)'
24.0 'PRBMN(1,1)'
390.0 'PRBMN(2,1)'
100.0 'PRBMN(3,1)'
0.0 'PRBMN(1,2)'
0.0 'PRBMN(2,2)'
000.0 'PRBMN(3,2)'
32.0 'PRBMX(1,1)'
420.0 'PRBMX(2,1)'
100.0 'PRBMX(3,1)'

```
0.0          'PRBMX(1,2)'
0.0          'PRBMX(2,2)'
000.0         'PRBMX(3,2)'
0.12         'FLIGNI(1,1)'
0.0          'FLIGNI(2,1)'
0.06         'FLIGNI(1,2)'
0.0          'FLIGNI(2,2)'
0.06         'FLIGNI(1,3)'
0.0          'FLIGNI(2,3)'
0.28          'HIMAX'  6/8/10 SAW 0.31
0.5          'HIWSF' 0.25 8/13/10 SAW .5
1.0          'HIMON(1)' 6/18/10 SAW 2
0.0          'HIMON(2)' 6/18/10 SAW 1
0.70         'EFRGRN(1)' 6/16/10 SAW
0.57 .75
0.6          'EFRGRN(2)'
0.6          'EFRGRN(3)'
0.04         'VLOSSP'
0.0          'FSDETH(1)'
0.0          'FSDETH(2)'
0.0          'FSDETH(3)'
500.0         'FSDETH(4)'
0.1          'FALLRT'
0.5          'RDRJ'
0.15         'RDRM'
0.14         'RDSRFC'
2.0          'RTDTMP'
0.0          'CRPRTF(1)'
0.0          'CRPRTF(2)'
0.0          'CRPRTF(3)'
0.05         'MRTFRAC'
0.0600        'SNFXMX(1)'
-27.0        'DEL13C'
1.12         'CO2IPR(1)'
0.58         'CO2ITR(1)'
1.0          'CO2ICE(1,1,1)'
1.0          'CO2ICE(1,1,2)'
1.0          'CO2ICE(1,1,3)'
1.0          'CO2ICE(1,2,1)'
1.0          'CO2ICE(1,2,2)'
1.0          'CO2ICE(1,2,3)'
1.0          'CO2IRS(1)'
0.10000       'CKMRSPMX(1)'
0.15000       'CKMRSPMX(2)'
0.05000       'CKMRSPMX(3)'
0.00000       'CMRSPNPP(1)'
0.00000       'CMRSPNPP(2)'
1.25000       'CMRSPNPP(3)'
1.00000       'CMRSPNPP(4)'
4.00000       'CMRSPNPP(5)'
1.50000       'CMRSPNPP(6)'
0.23000       'CGRESP(1)'
0.23000       'CGRESP(2)'
0.23000       'CGRESP(3)'
0.50000       'NO3PREF(1)'
6.00000       'CLAYPG'
0.50000       'CMIX'
-17.0000       'TMPGERM'
500.0        'DDBASE'
-2.0         'TMPKILL'
10           'BASETEMP'
30           'BASETEMP(2)'
700          'MNDDHRV' 100
700          'MXDDHRV' 400
120.0         'CURGDYS'
0.5          'CLSGRES'
0.12         'CMXTURN'
1.0          'NPP2CS(1)'
2.0          'CAFUE'
0.90         'EMAX'
1.1          'KCET'
0.6          'KLIGHT'
0.025         'SLA'
0.7          'LEAFCL'
0.85          'LEAFEMERG'
0.30          'LEAFMX'
0.00         'LEAFPM'
103           'DDEMERG'
900          'DDLAIMX'
```

Wheat

W3 winter wheat build on: W3F5 Wheat, GDD, new LAI

0.23 'PRDX(1)'
20.0 'PPDF(1)'
40.0 'PPDF(2)'
0.7 'PPDF(3)'
5.0 'PPDF(4)'
0.0 'BIOFLG'
1800.0 'BIOK5'
40 'PLTMRF'
150.0 'FULCAN'
6.00000 'FRTCINDX'
0.4 'FRTC(1)'
0.03 'FRTC(2)'
60.0 'FRTC(3)' days
0.1 'FRTC(4)'
0.1 'FRTC(5)'
0.4 'CFRTCN(1)'
0.25 'CFRTCN(2)'
0.6 'CFRTCW(1)'
0.1 'CFRTCW(2)'
300.0 'BIOMAX'
14.0 'PRAMN(1,1)'
100.0 'PRAMN(2,1)'
100.0 'PRAMN(3,1)'
28.0 'PRAMN(1,2)'
160.0 'PRAMN(2,2)'
200.0 'PRAMN(3,2)'
40.0 'PRAMX(1,1)'
200.0 'PRAMX(2,1)'
230.0 'PRAMX(3,1)'
120.0 'PRAMX(1,2)'
260.0 'PRAMX(2,2)'
270.0 'PRAMX(3,2)'
45.0 'PRBMN(1,1)'
390.0 'PRBMN(2,1)'
340.0 'PRBMN(3,1)'
0.0 'PRBMN(1,2)'
0.0 'PRBMN(2,2)'
0.0 'PRBMN(3,2)'
60.0 'PRBMX(1,1)'
420.0 'PRBMX(2,1)'
420.0 'PRBMX(3,1)'
0.0 'PRBMX(1,2)'
0.0 'PRBMX(2,2)'
0.0 'PRBMX(3,2)'
0.15 'FLIGNI(1,1)'
0.0 'FLIGNI(2,1)'
0.06 'FLIGNI(1,2)'
0.0 'FLIGNI(2,2)'
0.06 'FLIGNI(1,3)'
0.0 'FLIGNI(2,3)'
0.5 'HIMAX'
0.50 'HIWSF'
1.0 'HIMON(1)'
0.0 'HIMON(2)'
0.65 'EFRGRN(1)'
0.6 'EFRGRN(2)'
0.6 'EFRGRN(3)'
0.04 'VLOSSP'
0.0 'FSDETH(1)'
0.0 'FSDETH(2)'
0.0 'FSDETH(3)'
200.0 'FSDETH(4)'
0.12 'FALLRT'
0.05 'RDRJ'
0.05 'RDRM'
0.14 'RDSRFC'
2.0 'RTDTMP'
0.0 'CRPRTF(1)'
0.0 'CRPRTF(2)'
0.0 'CRPRTF(3)'
0.05 'MRTFRAC'
0.0 'SNFXMX(1)'
-27.0 'DEL13C'
1.22 'CO2IPR(1)'
0.88 'CO2ITR(1)'
1.08 'CO2ICE(1,1,1)'

1.0	'CO2ICE(1,1,2)'	800.00	'DDBASE'
1.0	'CO2ICE(1,1,3)'	-20.0	'TMPKILL'
1.08	'CO2ICE(1,2,1)'	5	'BASETEMP'
1.0	'CO2ICE(1,2,2)'	26	'BASETEMP(2)'
1.0	'CO2ICE(1,2,3)'	200	'MNDDHRV'
1.0	'CO2IRS(1)'	200	'MXDDHRV'
0.10000	'CKMRSPMX(1)'	120.0	'CURGDYS'
0.15000	'CKMRSPMX(2)'	0.5	'CLSGRES'
0.05000	'CKMRSPMX(3)'	0.12	'CMXTURN'
0.00000	'CMRSPNPP(1)'	1.0	'NPP2CS(1)'
0.00000	'CMRSPNPP(2)'	2.0	'CAFUE'
1.25000	'CMRSPNPP(3)'	0.90	'EMAX'
1.00000	'CMRSPNPP(4)'	1.2	'KCET'
4.00000	'CMRSPNPP(5)'	0.85	'KLIGHT'
1.50000	'CMRSPNPP(6)'	0.06	'SLA'
0.23000	'CGRESP(1)'	0.4	'LEAFCL'
0.23000	'CGRESP(2)'	0.7	'LEAFEMERG'
0.23000	'CGRESP(3)'	0.15	'LEAFMX'
0.25000	'NO3PREF(1)'	0.0	'LEAFPM'
6.00000	'CLAYPG'	0.01	'DDEMERG'
0.50000	'CMIX'	800	'DDLAIMX'
-10.0000	'TMPGERM'		